

RA 505 Robot Sensing and Vision

Lecture 22

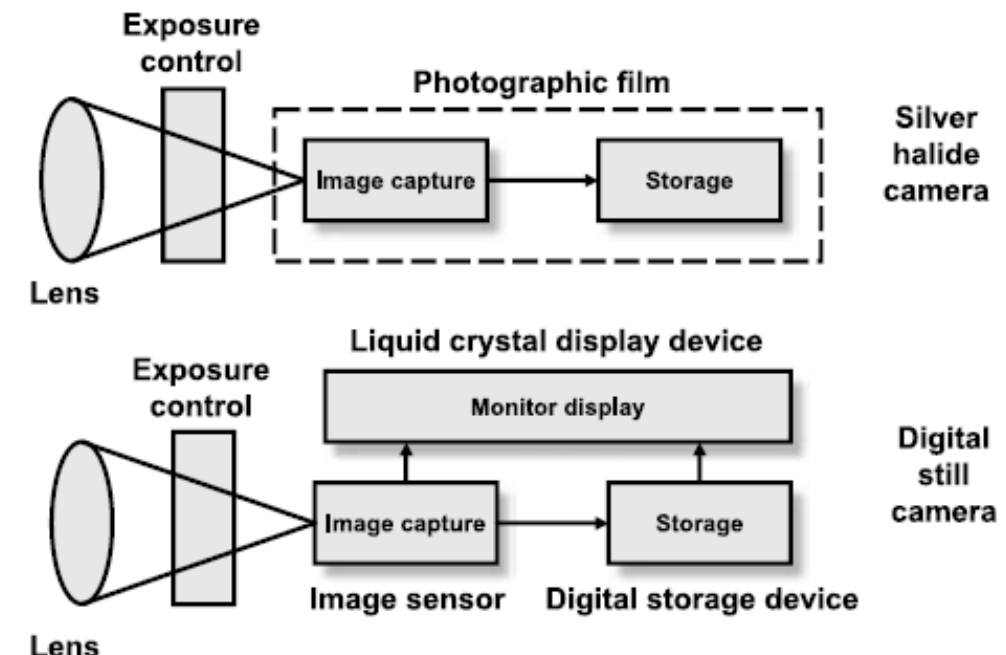
Dr. Rishikesh Kulkarni
Department of Electronics and Electrical Engineering
IIT Guwahati

Syllabus

- Binary, monochrome and RGB imaging sensors
- Velocity sensors,
- Accelerometers
- Tactile sensors.
- Ultrasound rangefinders
- Optical rangefinders - LASER scanner, static LED array
- Structured lighting, dynamic focusing
- Interfacing of vision sensors

DIGITAL CAMERA

- Difference between a silver halide photographic camera and an electronic still camera
- Conventional silver halide cameras
- Electronic still cameras
 - Analog storage
 - Digital storage
- Mavica (Magnetic video camera)
 - image signals captured by the semiconductor image sensor
 - stored on a magnetic floppy disk.
- Why did still video system fail?
 - Cost
 - Poor picture print quality (VGA quality (640×480 pixels))



DIGITAL CAMERA



Fuji digital still camera DS-1P (CCD+Static RAM)

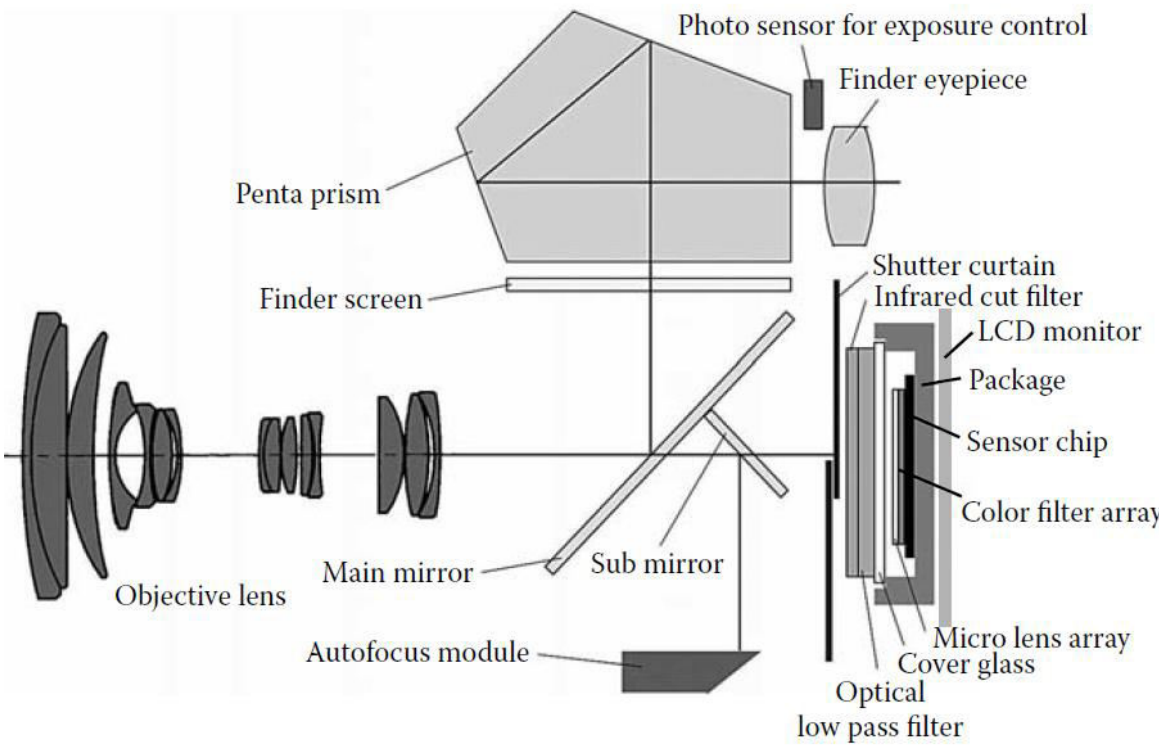


Kodak DCS-1

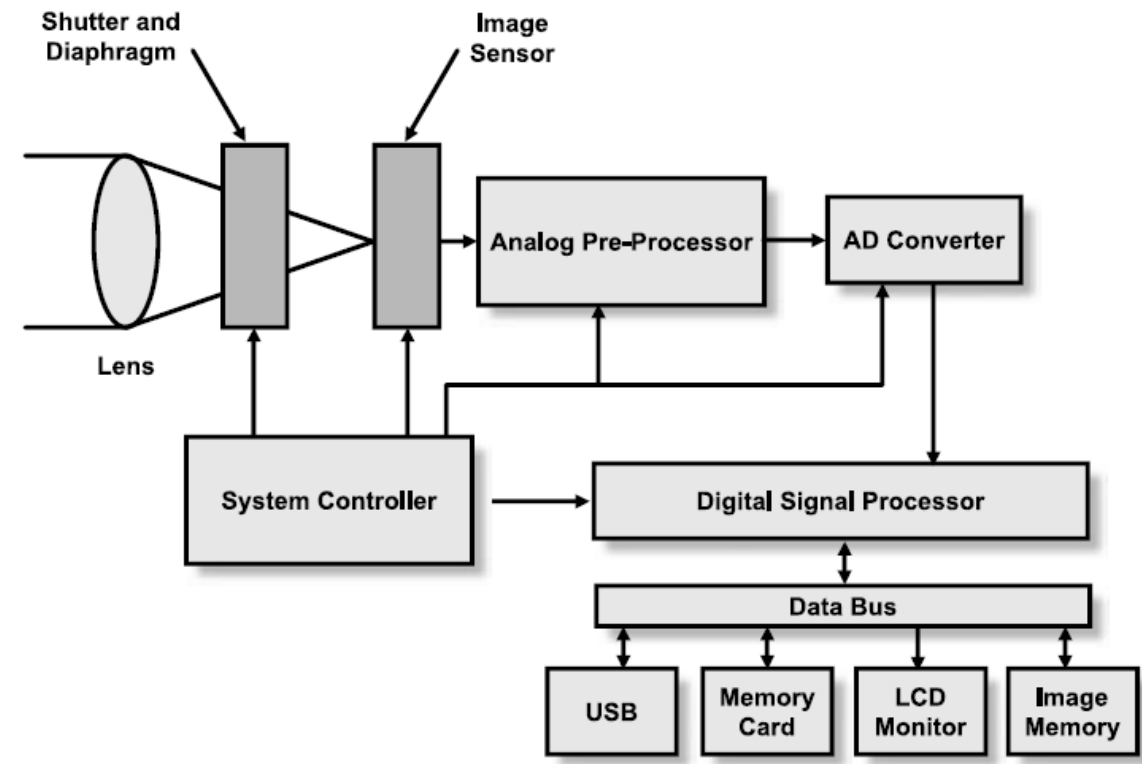


Casio QV-10 (LCD monitor display)

DIGITAL CAMERA



Typical arrangement of an SLR digital still camera



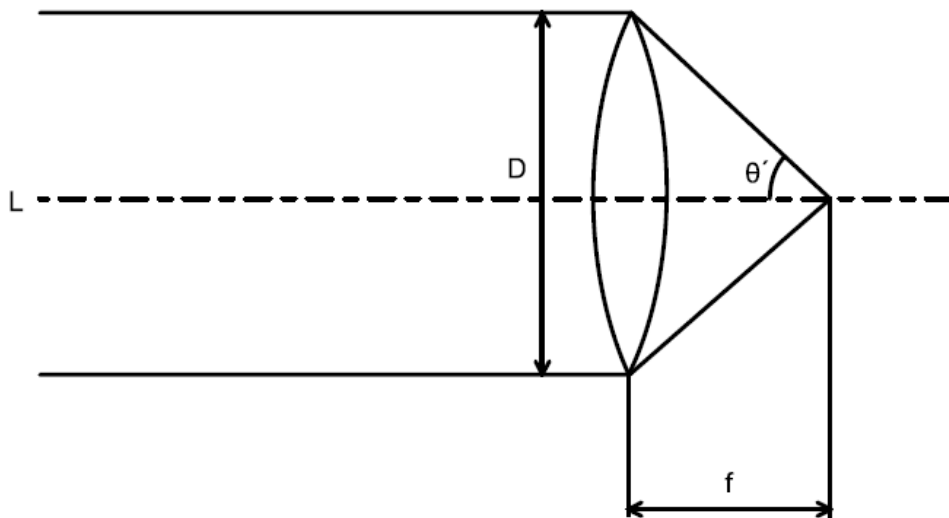
Typical block diagram of a digital still camera.
Additional optics (IR filter + Optical LPF)

DIGITAL CAMERA

- OPTICS
 - Objective lens, IR filter, optical low pass filer
- IMAGING DEVICES
 - CCD and CMOS sensors
- ANALOG CIRCUIT
 - Sample-and-hold, color separation, AGC (automatic gain control), level clamp, tone adjustment, ADC
- DIGITAL CIRCUIT
 - DSP; tone adjustment; RGB to YCC color conversion; white balance; image compression/decompression; exposure control, auto focus, and automatic white balance
- SYSTEM CONTROL
 - exposure control (AE), auto focus

DIGITAL STILL CAMERA

- Imaging optics, imaging elements, and image-processing technology



Schematic diagram of single lens

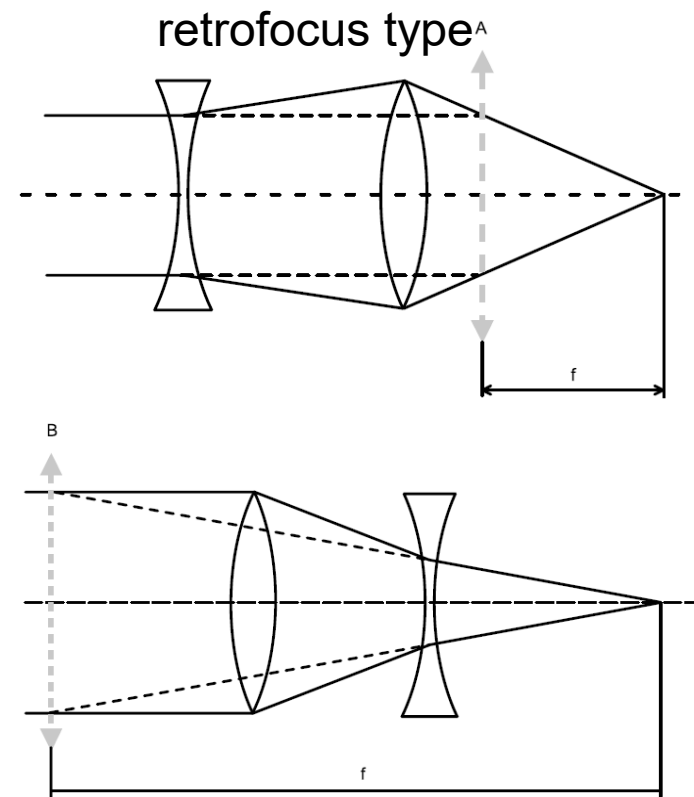
$$F = \frac{1}{2 \sin \theta'} \quad F = \frac{f}{D}$$

$$\frac{1}{f} = (n - 1) \cdot \left(\frac{1}{R_1} - \frac{1}{R_2} \right)$$

$$\frac{1}{f} = \frac{n - 1}{R_1} + \frac{1 - n}{R_2} + \frac{d(n - 1)^2}{nR_1R_2}$$

$$\frac{1}{f} = \frac{1}{f_1} + \frac{1}{f_2} - \frac{d}{f_1f_2}$$

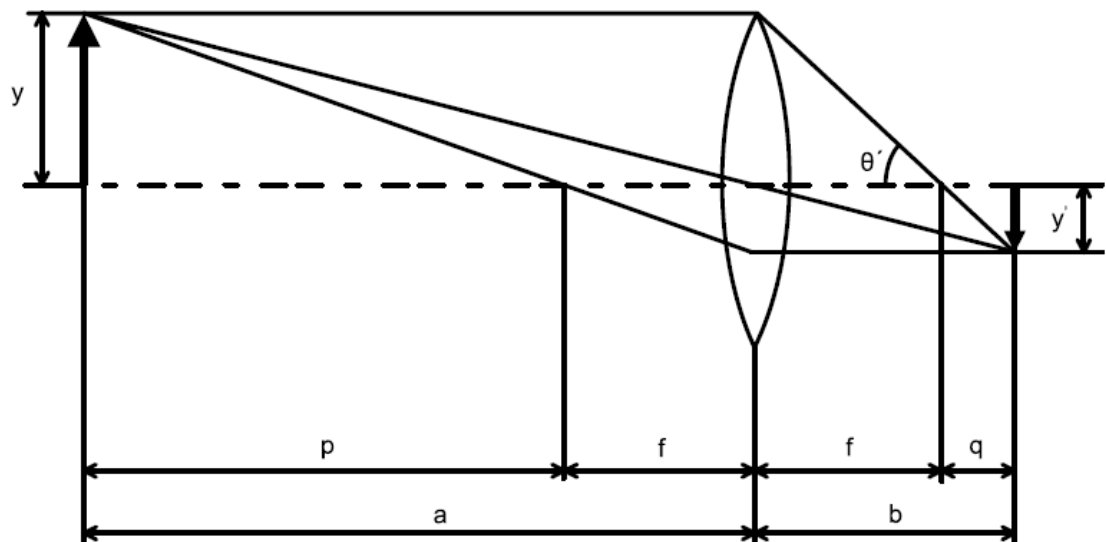
Refractive power/
power of lens = inverse
of the focal length



telephoto type

DIGITAL STILL CAMERA

brightness of the lens (the image plane brightness) $\propto 1/F^2$



$$m = \frac{y'}{y} = \frac{q}{f} = \frac{f}{p} = \frac{b}{a}$$
$$\frac{1}{f} = \frac{1}{a} + \frac{1}{b}$$

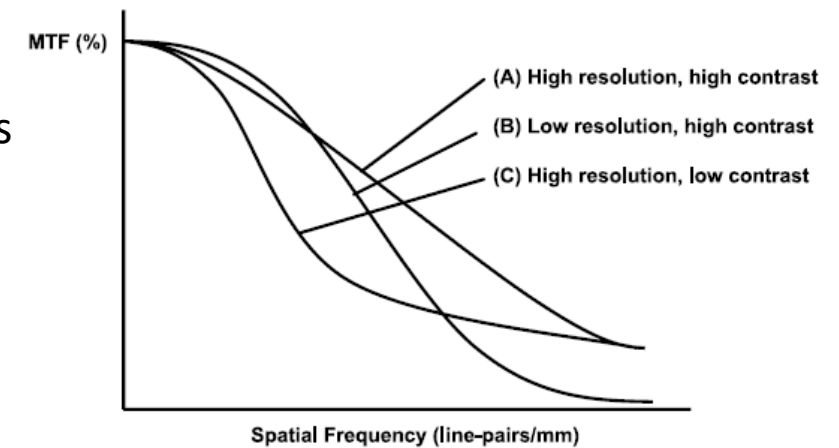
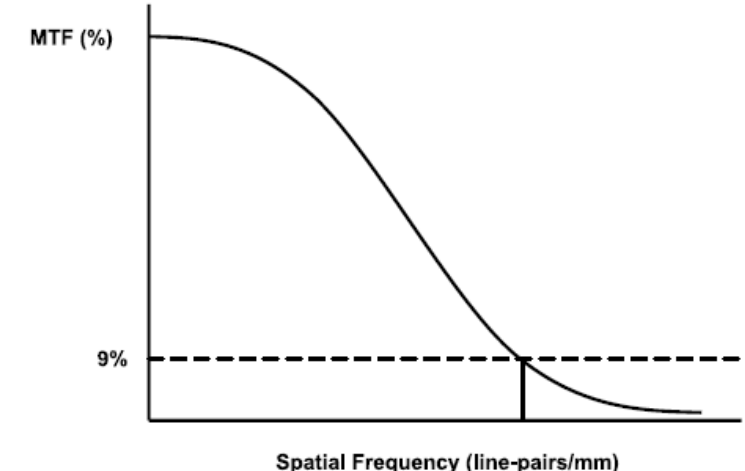
When the distance to the object is limited, the image is formed farther away from the lens than is the case for very far-off objects, so the brightness at the image plane (the surface of the imaging element) is lower.

effective F-number $F' = \frac{f + q}{D} = \left(1 + \frac{q}{f}\right) \cdot \frac{f}{D} = (1 + m)F$

DIGITAL STILL CAMERA

$$E_i = \frac{\pi}{4} E_o T \left(\frac{1}{(1+m)F} \right)^2$$

- This equation gives us the brightness at the centre of the image, but the brightness at the periphery of the image is generally lower than this.
- The cosine fourth law: theta is the angle diverging from the optical axis facing towards the photographed area on the object side (half the field of view).
- ‘Wide-angle lens’: field of view of 65 degree or more
- ‘Telephoto lens’: field of view of 25 degree or less
- Modulation transfer function (MTF) and resolution: Frequently used as a standard for evaluating the imaging performance of any lens
- Higher the frequency (the more detailed the object pattern), the greater the decline in object reproducibility.
- Resolution: measure for evaluating the level of detail that can be captured; line-pairs/mm



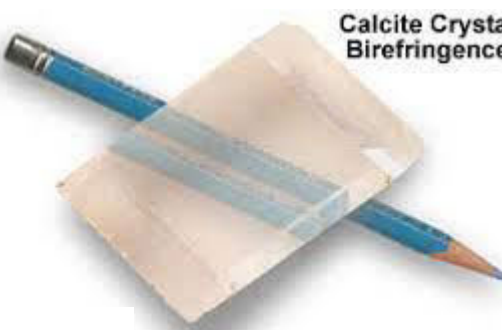
Depth of field and Depth of focus

- $\text{DOF} = 2u^2Fc/f^2$
 - u = distant to object
 - f = focal length
 - F = F-number
 - c = circle of least confusion
- Depth of focus = $2Fc$
- Circle of least confusion : 2 to 2.5 units of pixel pitch

$$S = t \cdot \frac{n_e^2 - n_o^2}{2n_e n_o}$$

Optical low-pass filter

- Thin, birefringent plates made from liquid crystal or lithium niobate
- Diffractive optical elements or special aspherical surfaces
 - different refractive indexes depending on the direction in which light is polarized
- Birefringent material is a single material with two refractive indexes.
- used to mitigate the moiré effect caused by the interaction of patterns in the object and the pattern on the imaging element caused by the arrangement of imaging element pixels at a fixed pitch

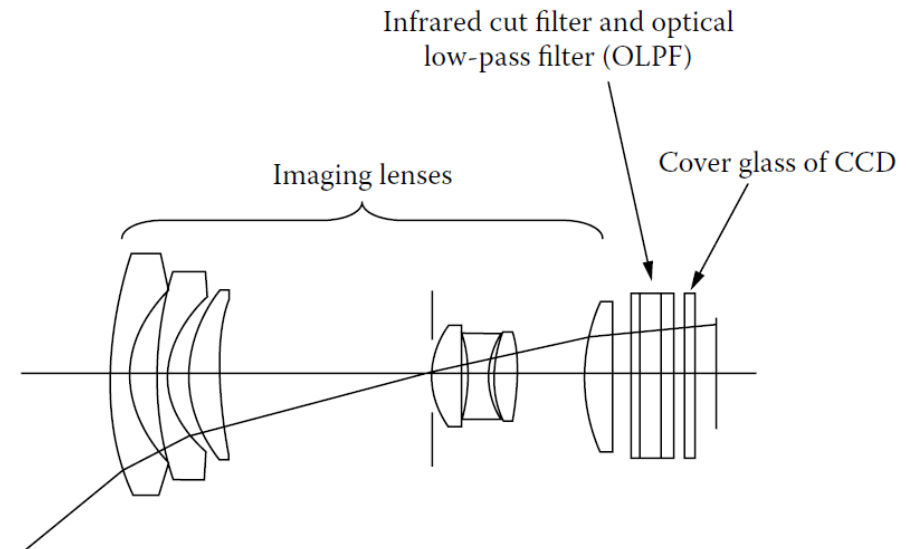


Aberration

- Spherical aberration
- Comatic
- Astigmatism
- Curvature of field
- Distortion
- Axial or longitudinal chromatic aberration

Imaging Optics

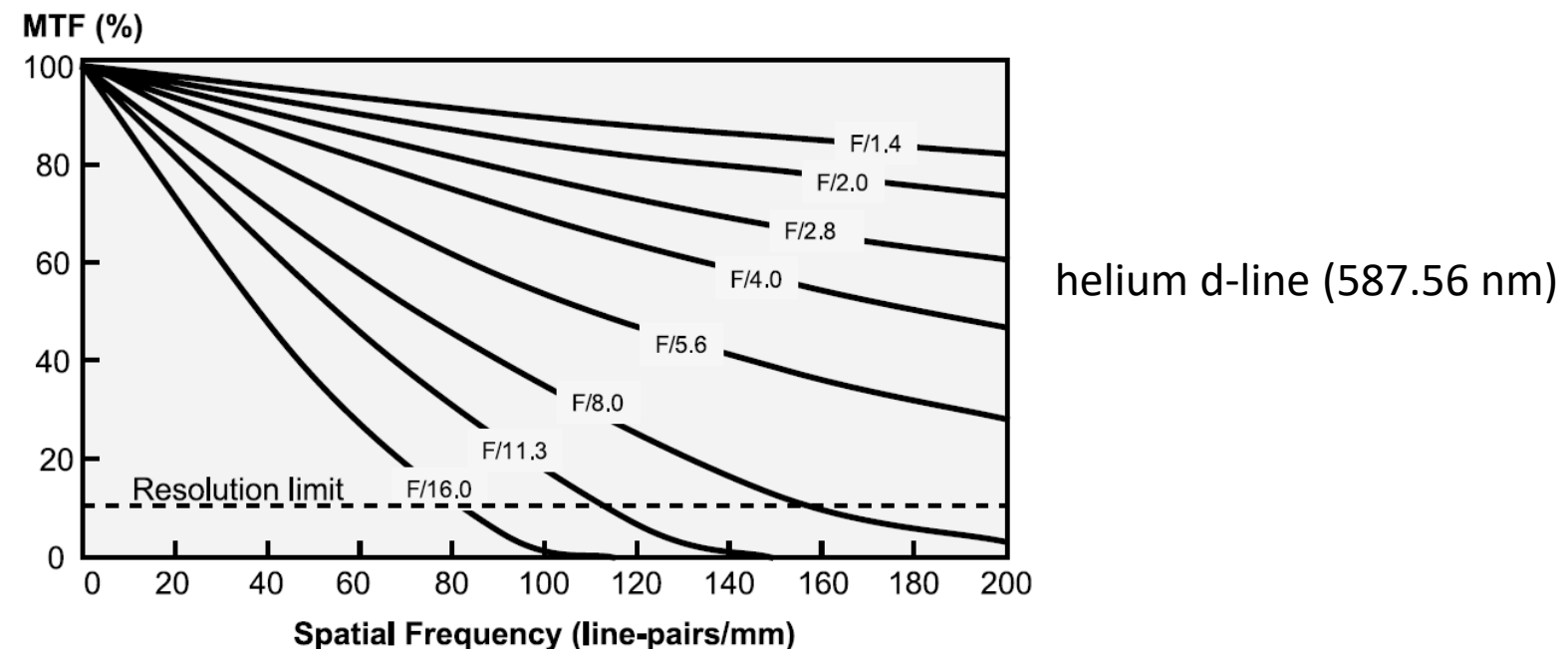
- Imaging lenses, an infrared cut filter, and an optical low-pass filter (OLPF)
- Imaging lenses: zoom lenses, combination of multiple lens
- Infrared cut filters: cut out unwanted infrared light; to avoid highly sensitive of imaging element to unwanted infrared light



Effect of diffraction

- Pixel pitch at the scale of wavelength
- Airy disc $r = 1.22\lambda F$

$$MTF(v) = \frac{2}{\pi} \cdot \left(\cos^{-1}(\lambda F v) - \lambda F v \sqrt{1 - (\lambda F v)^2} \right)$$



RA 505 Robot Sensing and Vision

Lecture 22

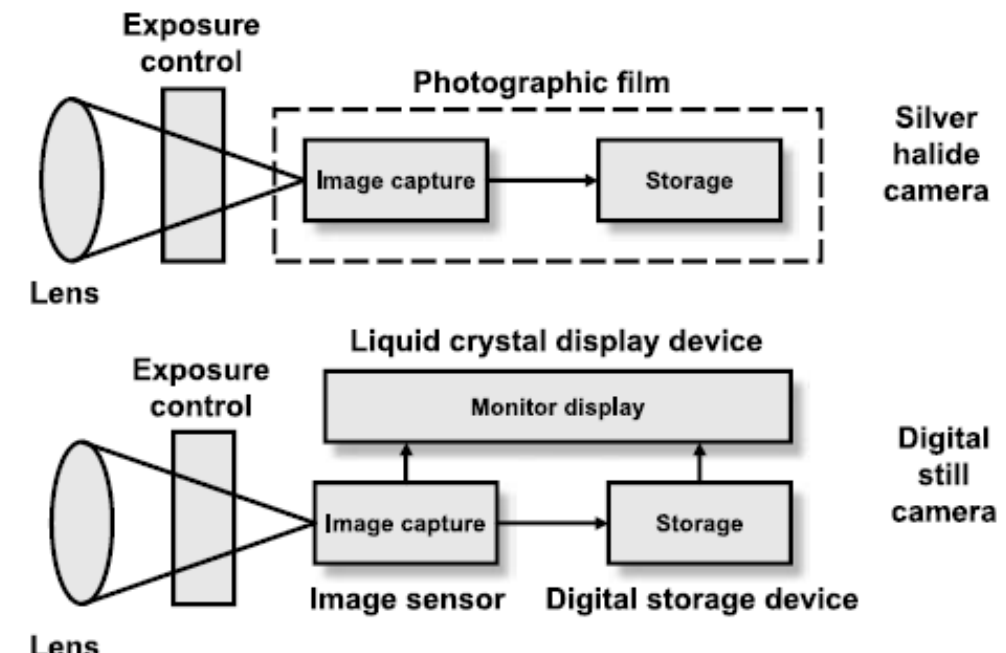
Dr. Rishikesh Kulkarni
Department of Electronics and Electrical Engineering
IIT Guwahati

Syllabus

- Binary, monochrome and RGB imaging sensors
- Velocity sensors,
- Accelerometers
- Tactile sensors.
- Ultrasound rangefinders
- Optical rangefinders - LASER scanner, static LED array
- Structured lighting, dynamic focusing
- Interfacing of vision sensors

DIGITAL CAMERA

- Difference between a silver halide photographic camera and an electronic still camera
- Conventional silver halide cameras
- Electronic still cameras
 - Analog storage
 - Digital storage
- Mavica (Magnetic video camera)
 - image signals captured by the semiconductor image sensor
 - stored on a magnetic floppy disk.
- Why did still video system fail?
 - Cost
 - Poor picture print quality (VGA quality (640×480 pixels))



DIGITAL CAMERA



Fuji digital still camera DS-1P (CCD+Static RAM)

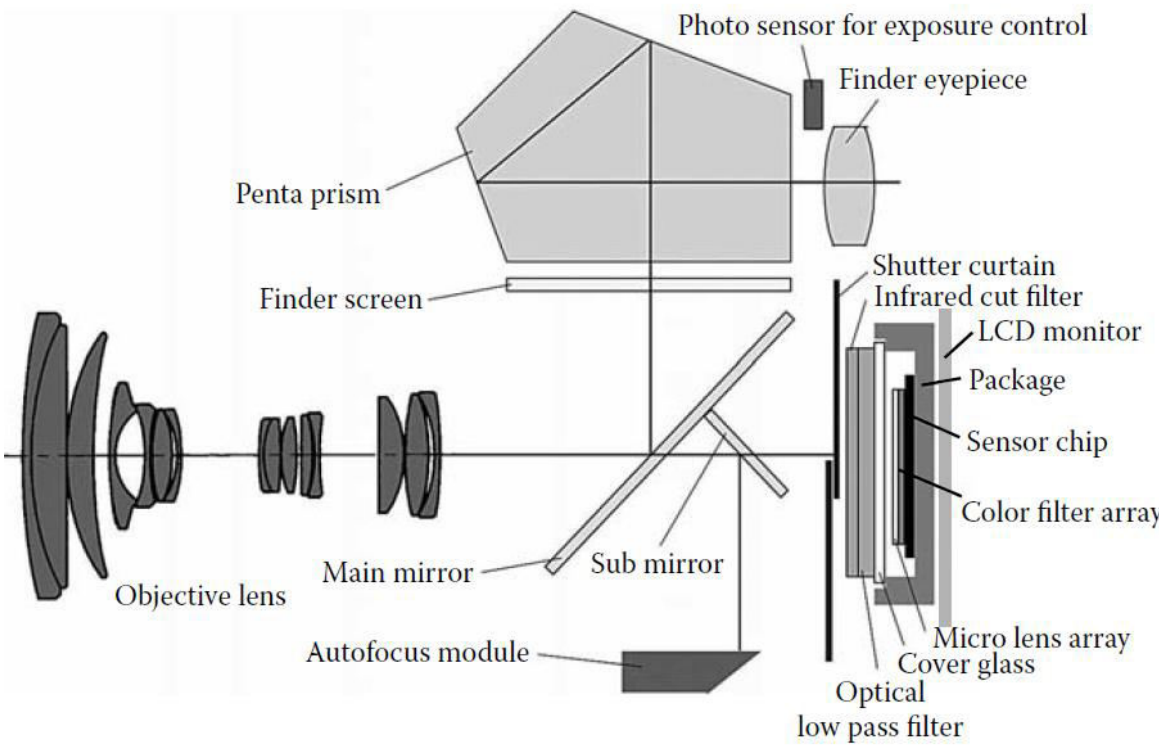


Kodak DCS-1

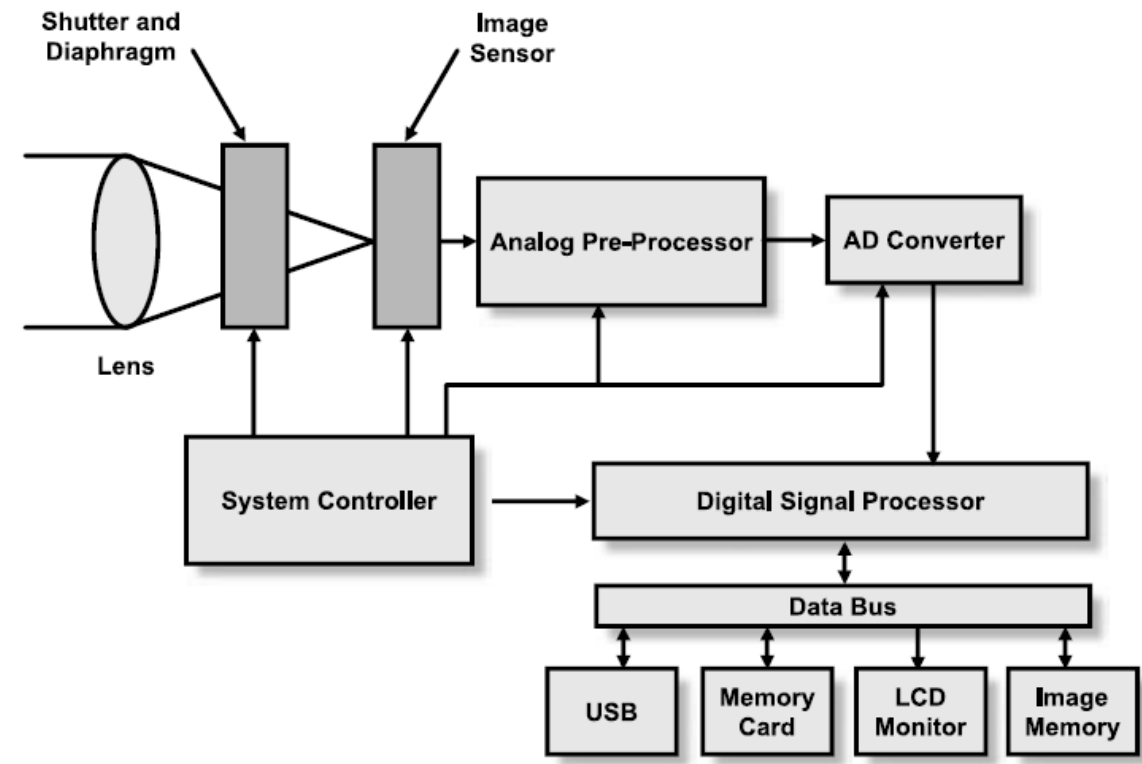


Casio QV-10 (LCD monitor display)

DIGITAL CAMERA



Typical arrangement of an SLR digital still camera



Typical block diagram of a digital still camera.
Additional optics (IR filter + Optical LPF)

DIGITAL CAMERA

- OPTICS
 - Objective lens, IR filter, optical low pass filter
- IMAGING DEVICES
 - CCD and CMOS sensors
- ANALOG CIRCUIT
 - Sample-and-hold, color separation, AGC (automatic gain control), level clamp, tone adjustment, ADC
- DIGITAL CIRCUIT
 - DSP; tone adjustment; RGB to YCC color conversion; white balance; image compression/decompression; exposure control, auto focus, and automatic white balance
- SYSTEM CONTROL
 - exposure control (AE), auto focus

References

- Image sensors and Signal Processing for Digital Still Cameras, Ed. Junichi Nakamura, Taylor & Francis Group, LLC, 2006.

RA 505 Robot Sensing and Vision

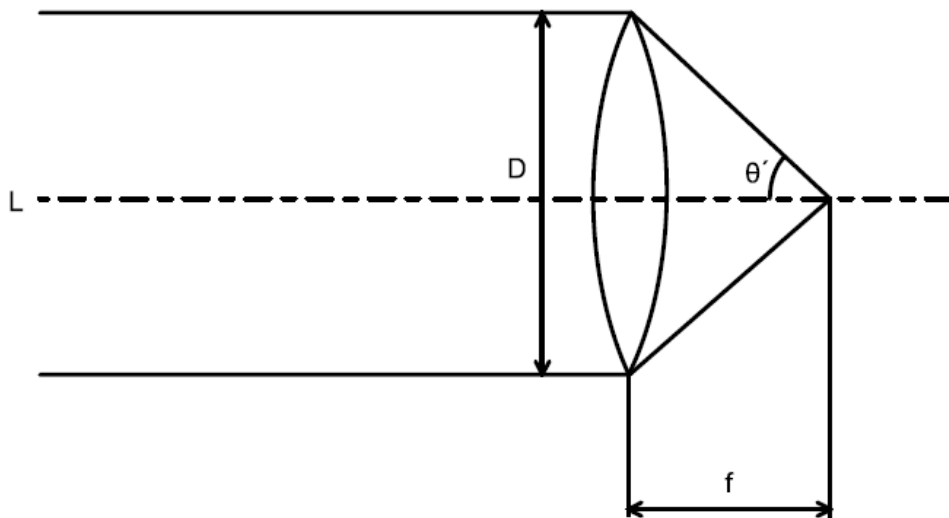
Lecture 24

Dr. Rishikesh Kulkarni
Department of Electronics and Electrical Engineering
IIT Guwahati

Fourier transform

DIGITAL STILL CAMERA

- Imaging optics, imaging elements, and image-processing technology



Schematic diagram of single lens

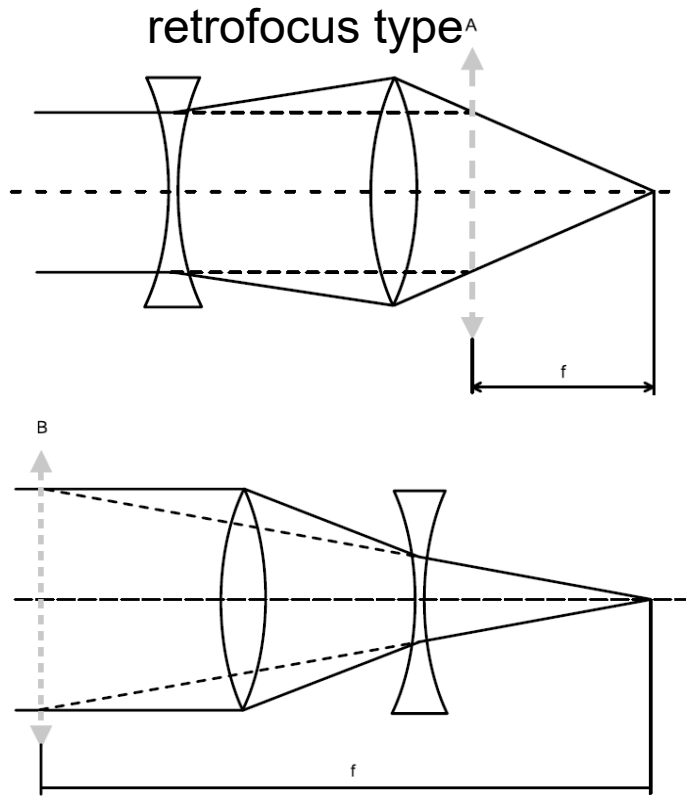
$$F = \frac{1}{2 \sin \theta'} \quad F = \frac{f}{D}$$

$$\frac{1}{f} = (n - 1) \cdot \left(\frac{1}{R_1} - \frac{1}{R_2} \right)$$

$$\frac{1}{f} = \frac{n - 1}{R_1} + \frac{1 - n}{R_2} + \frac{d(n - 1)^2}{n R_1 R_2}$$

$$\frac{1}{f} = \frac{1}{f_1} + \frac{1}{f_2} - \frac{d}{f_1 f_2}$$

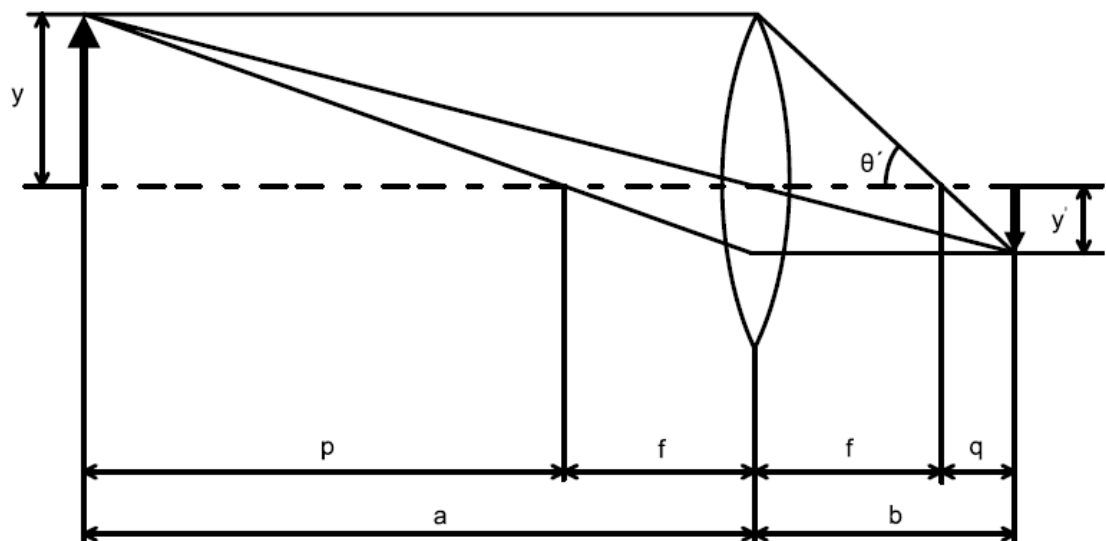
Refractive power/
power of lens = inverse
of the focal length



telephoto type

DIGITAL STILL CAMERA

brightness of the lens (the image plane brightness) $\propto 1/F^2$



$$m = \frac{y'}{y} = \frac{q}{f} = \frac{f}{p} = \frac{b}{a}$$
$$\frac{1}{f} = \frac{1}{a} + \frac{1}{b}$$

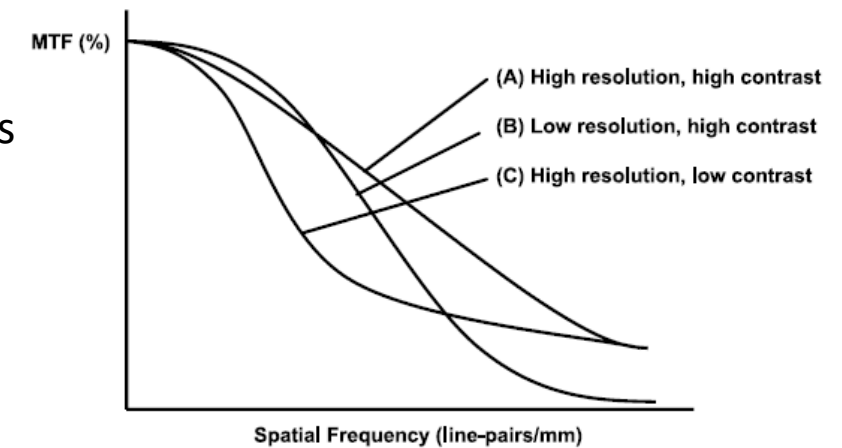
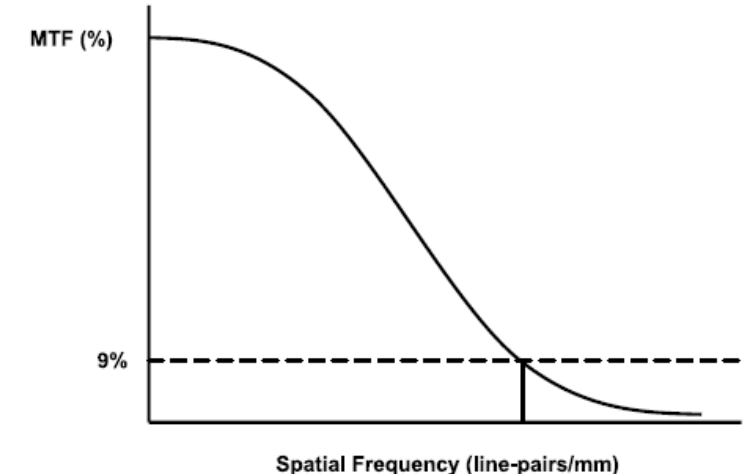
When the distance to the object is limited, the image is formed farther away from the lens than is the case for very far-off objects, so the brightness at the image plane (the surface of the imaging element) is lower.

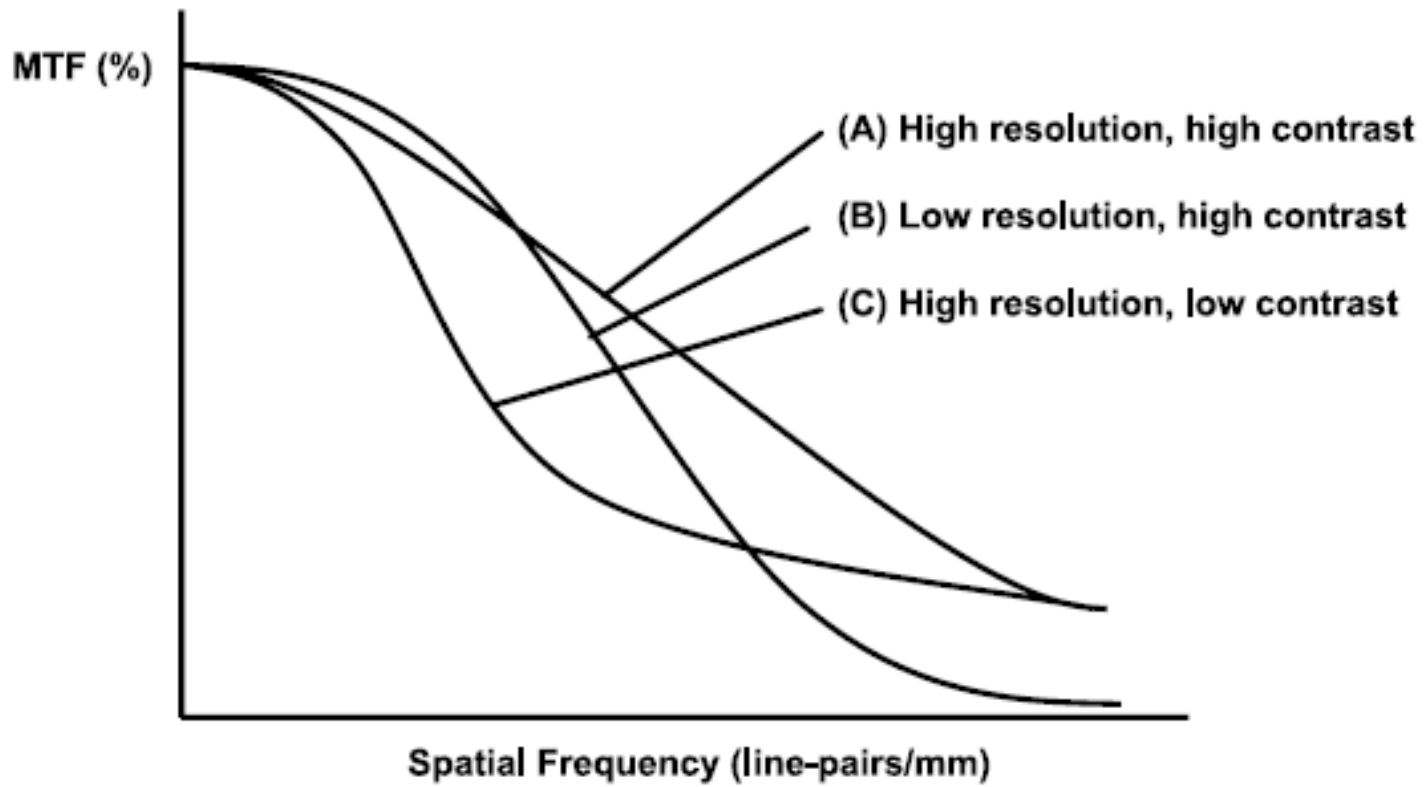
effective F-number $F' = \frac{f + q}{D} = \left(1 + \frac{q}{f}\right) \cdot \frac{f}{D} = (1 + m)F$

DIGITAL STILL CAMERA

$$E_i = \frac{\pi}{4} E_o T \left(\frac{1}{(1+m)F} \right)^2$$

- This equation gives us the brightness at the centre of the image, but the brightness at the periphery of the image is generally lower than this.
- The cosine fourth law: theta is the angle diverging from the optical axis facing towards the photographed area on the object side (half the field of view).
- ‘Wide-angle lens’: field of view of 65 degree or more
- ‘Telephoto lens’: field of view of 25 degree or less
- Modulation transfer function (MTF) and resolution: Frequently used as a standard for evaluating the imaging performance of any lens
- Higher the frequency (the more detailed the object pattern), the greater the decline in object reproducibility.
- Resolution: measure for evaluating the level of detail that can be captured; line-pairs/mm





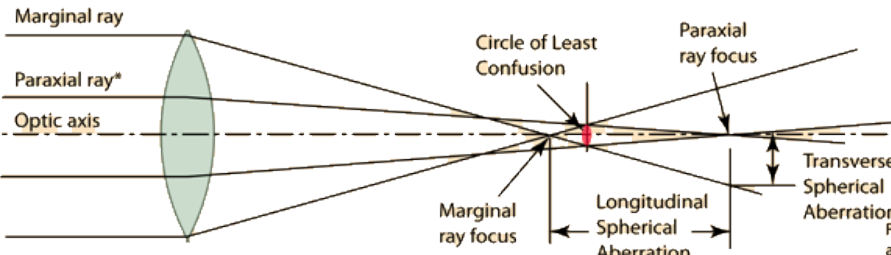
RA 505 Robot Sensing and Vision

Lecture 25

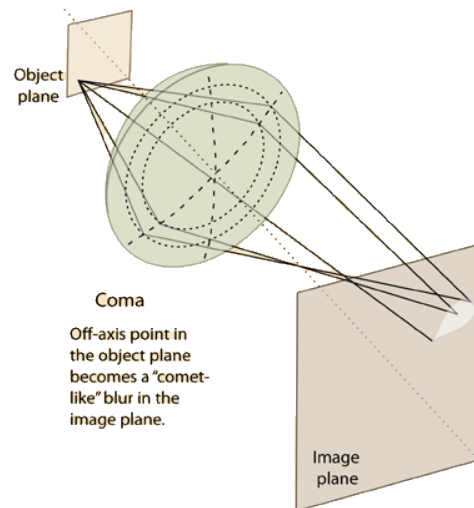
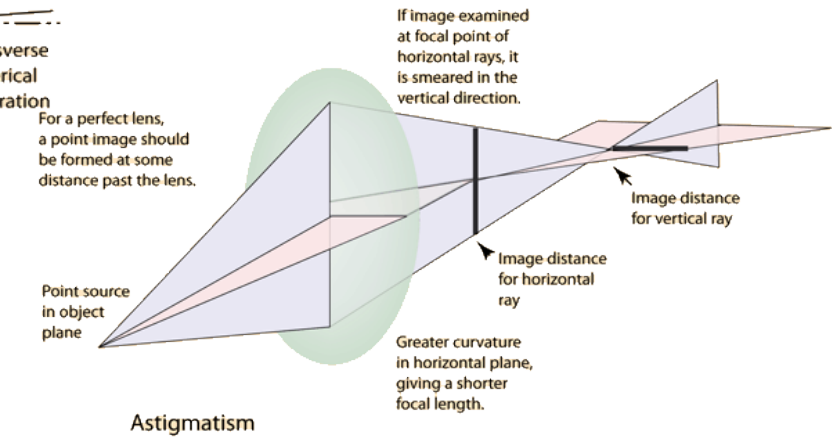
Dr. Rishikesh Kulkarni
Department of Electronics and Electrical Engineering
IIT Guwahati

Aberration

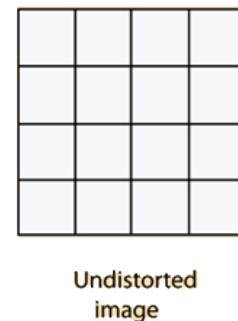
- Spherical aberration
- Comatic
- Astigmatism
- Curvature of field
- Distortion
- Axial or longitudinal chromatic aberration



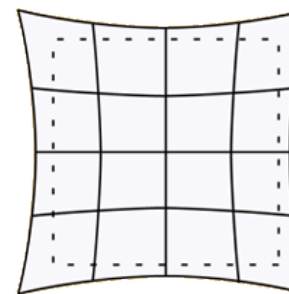
* Paraxial ray means a ray on the optic axis or very close to it, which the ray in the diagram is not. It is drawn further out to illustrate the idea of the circle of confusion.



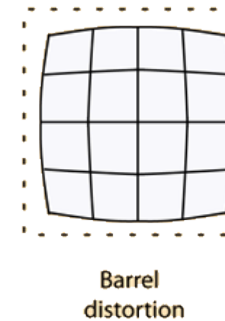
Coma
Off-axis point in the object plane becomes a "comet-like" blur in the image plane.



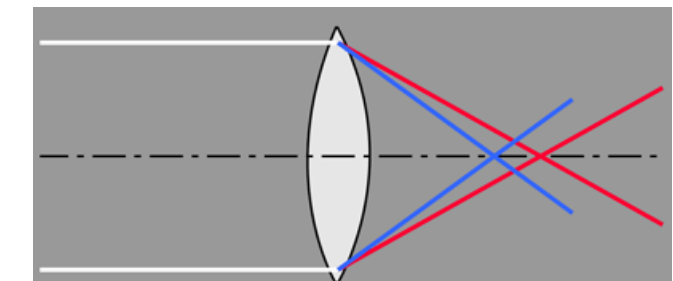
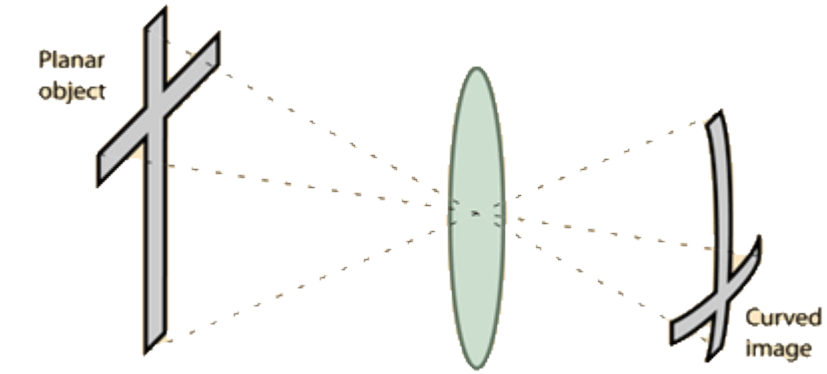
Undistorted image



Pincushion distortion



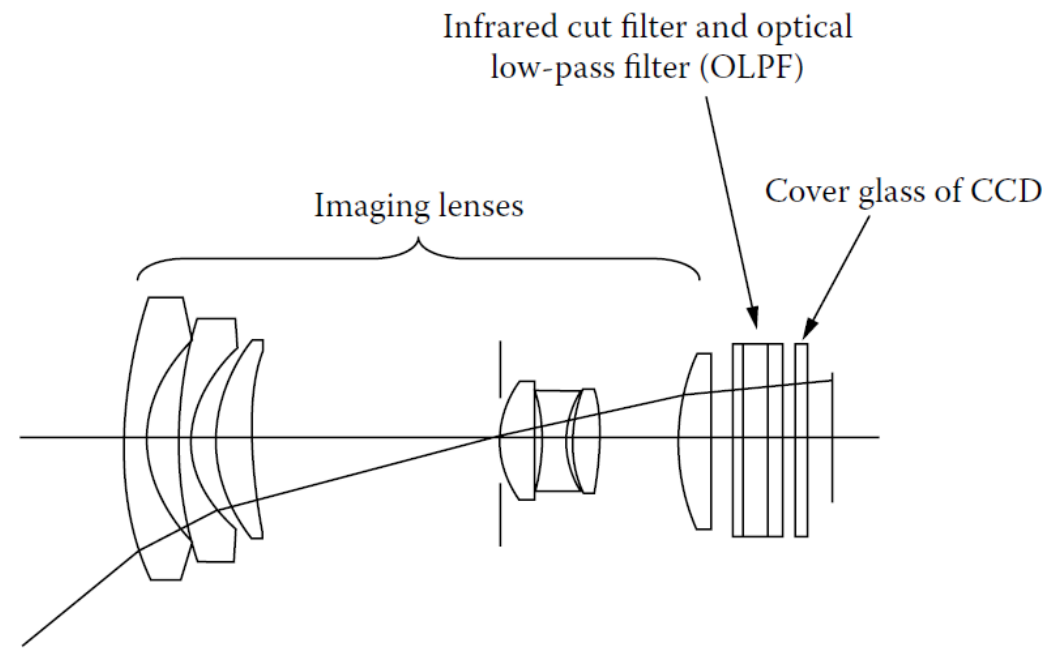
Barrel distortion





Imaging Optics

- Imaging lenses, an infrared cut filter, and an optical low-pass filter (OLPF)
- Imaging lenses: zoom lenses, combination of multiple lens
- Infrared cut filters: cut out unwanted infrared light; to avoid highly sensitive of imaging element to respond to unwanted infrared light



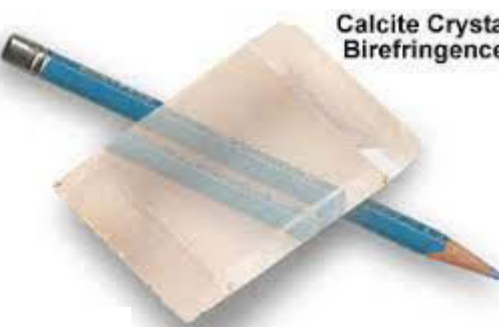
Depth of field and Depth of focus

- Depth of field = $2u^2Fc/f^2$
 - u= distant to object
 - f = focal length
 - F = F-number
 - c = circle of least confusion
- Depth of focus = $2Fc$
- Circle of least confusion : 2 to 2.5 units of pixel pitch

$$S = t \cdot \frac{n_e^2 - n_o^2}{2n_e n_o}$$

Optical low-pass filter

- Thin, birefringent plates made from liquid crystal or lithium niobate
- Diffractive optical elements or special aspherical surfaces
 - different refractive indexes depending on the direction in which light is polarized
- Birefringent material is a single material with two refractive indexes.
- used to mitigate the moiré effect caused by the interaction of patterns in the object and the pattern on the imaging element caused by the arrangement of imaging element pixels at a fixed pitch

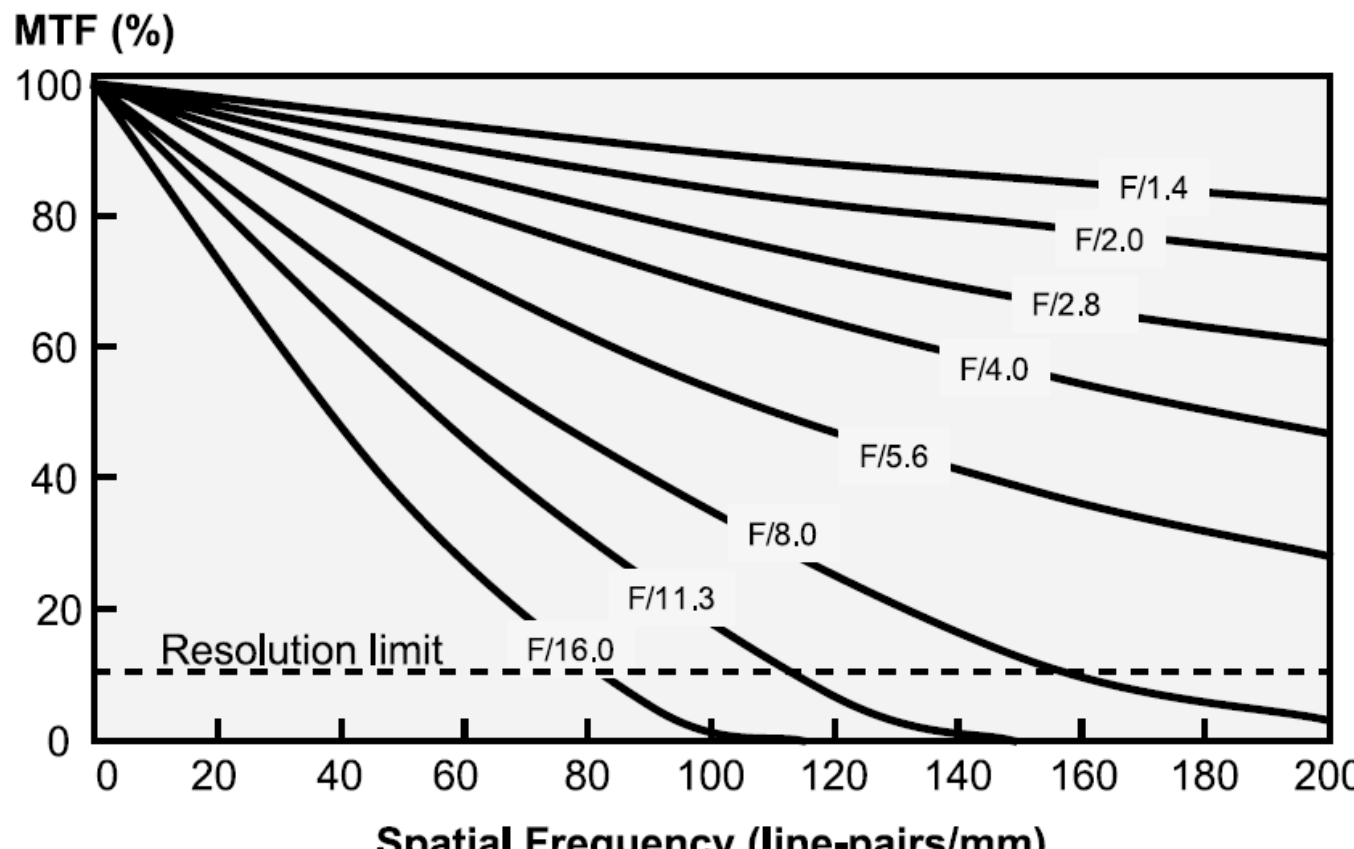


Effect of diffraction

$$MTF(v) = \frac{2}{\pi} \cdot \left(\cos^{-1}(\lambda F v) - \lambda F v \sqrt{1 - (\lambda F v)^2} \right)$$

587.56 nm

- Pixel pitch at the scale of wavelength
- Airy disc $r = 1.22\lambda F$



helium d-line (587.56 nm)

Basics of Image Sensors

- Imager: solid-state image sensor
- Wide spectral range; focus on visible range (380 nm – 780 nm)
- Silicon: suitable for visible image sensors
- Number of picture elements: Pixels; converts lights into holes/electrons
- Charged-coupled device (CCD) image sensor
- Complementary metal-oxide semiconductor (CMOS) image sensor
- High quality image: high resolution, high sensitivity, a wide dynamic range, good linearity for color processing, and very low noise

Functions of Image Sensors

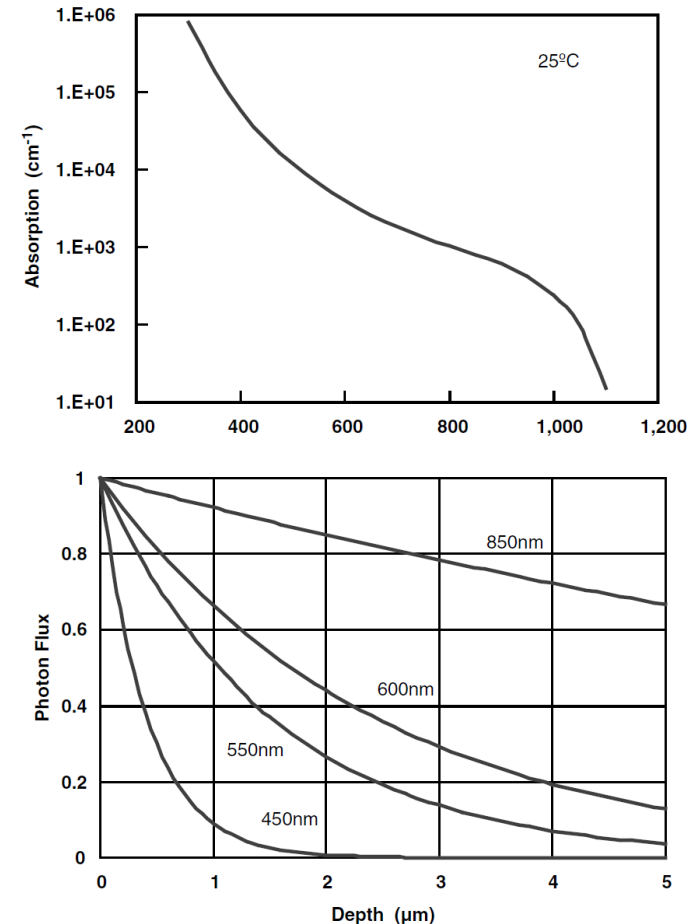
- Photoconversion

$$E_{\text{photon}} = h \cdot v = \frac{h \cdot c}{\lambda} \geq E_g$$

- Silicon band gap energy: 1.1 eV => wavelengths shorter than 1100 nm is absorbed and photon-to-signal charge conversion takes place
- Number of photons absorbed in a region with thickness dx is proportional to the intensity of the photon flux $\Phi(x)$; x : the distance from the semiconductor surface

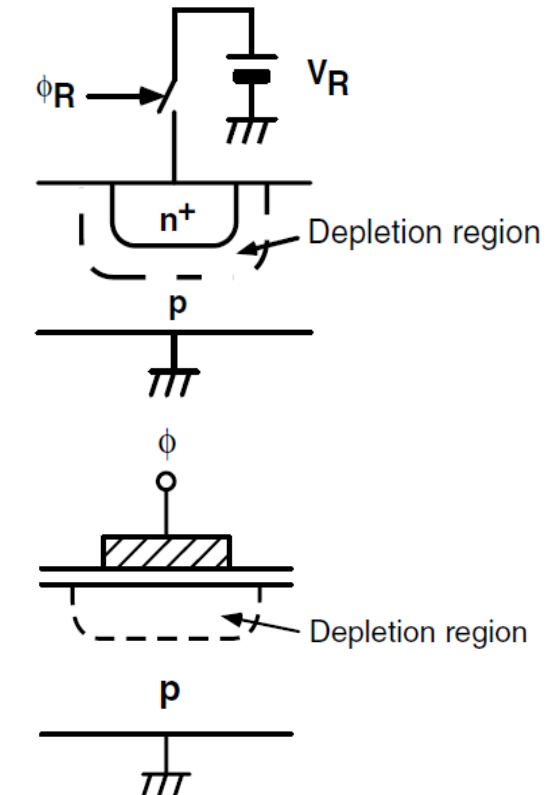
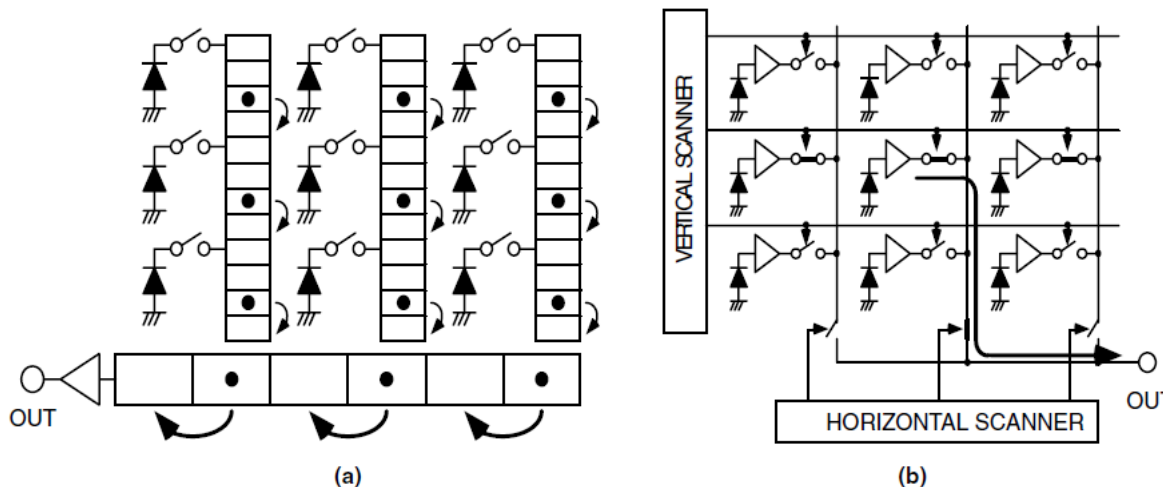
$$\Phi(x) = \Phi_0 \cdot \exp(-\alpha x)$$

- photon flux decays exponentially with the distance from the surface; penetration depth ($1/\alpha$)

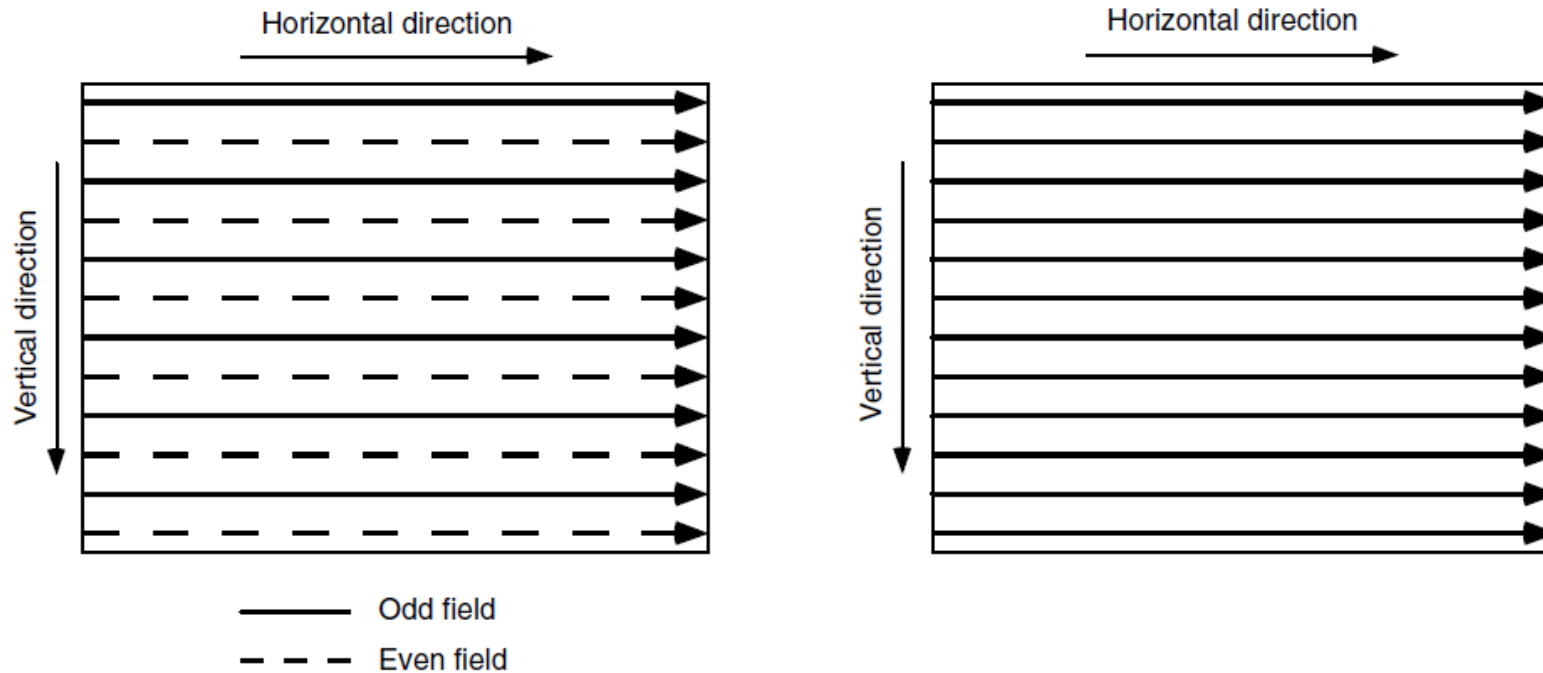


Charge collection and Accumulation

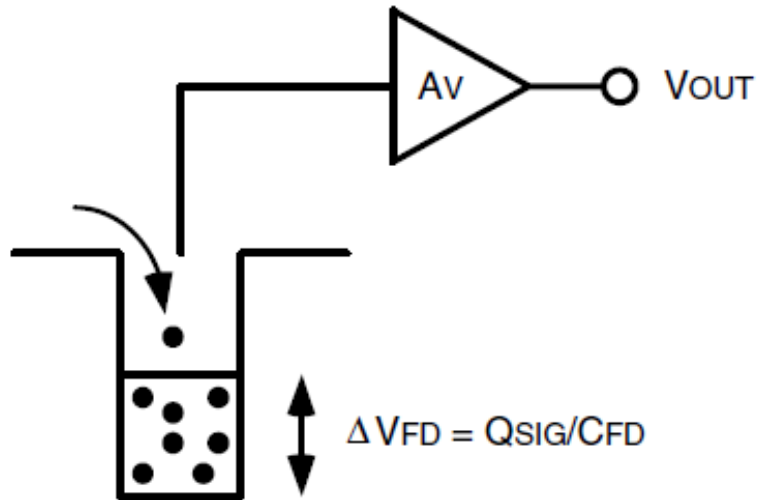
- Photodiode
- Metal-oxide semiconductor (MOS) diode
- Charge transfer
 - accumulated charge or the corresponding signal voltage or current must be read out from a pixel in an image sensor chip to the outside world
 - Scanning: two-dimensional signal transformation into time-sequenced signal (charge transfer, X-Y addressing)



Interlaced Scan and Progressive Scan



Charge Detection and conversion gain



$$\Delta V_{FD} = \frac{Q_{sig}}{C_{FD}}$$

$$\Delta V_{OUT} = A_V \cdot \Delta V_{FD}$$

- Potential well is monitored by the voltage buffer
- Capacitance C_{FD} acts as a charge-to-voltage conversion capacitance

- Conversion gain

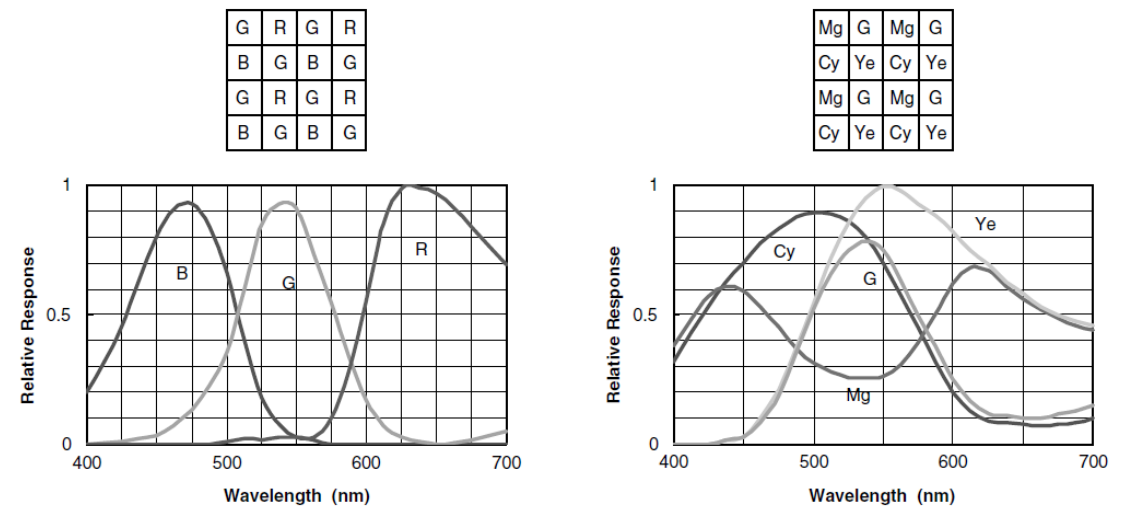
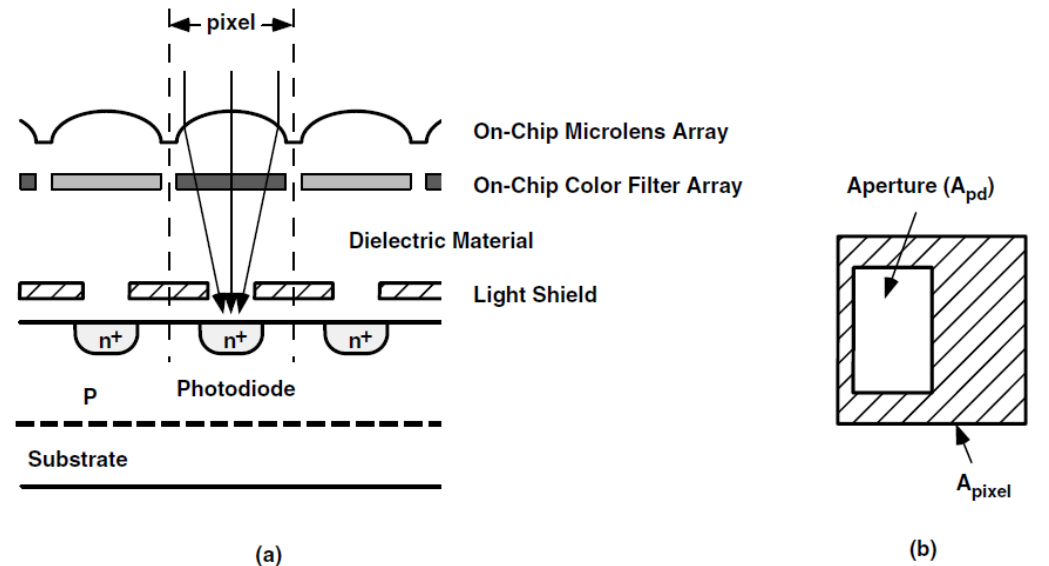
$$C.G. = \frac{q}{C_{FD}} \quad [\mu\text{V/electron}]$$

Change in voltage obtained by 1 electron at the charging node

$$C.G._{output_referred} = A_V \cdot \frac{q}{C_{FD}}$$

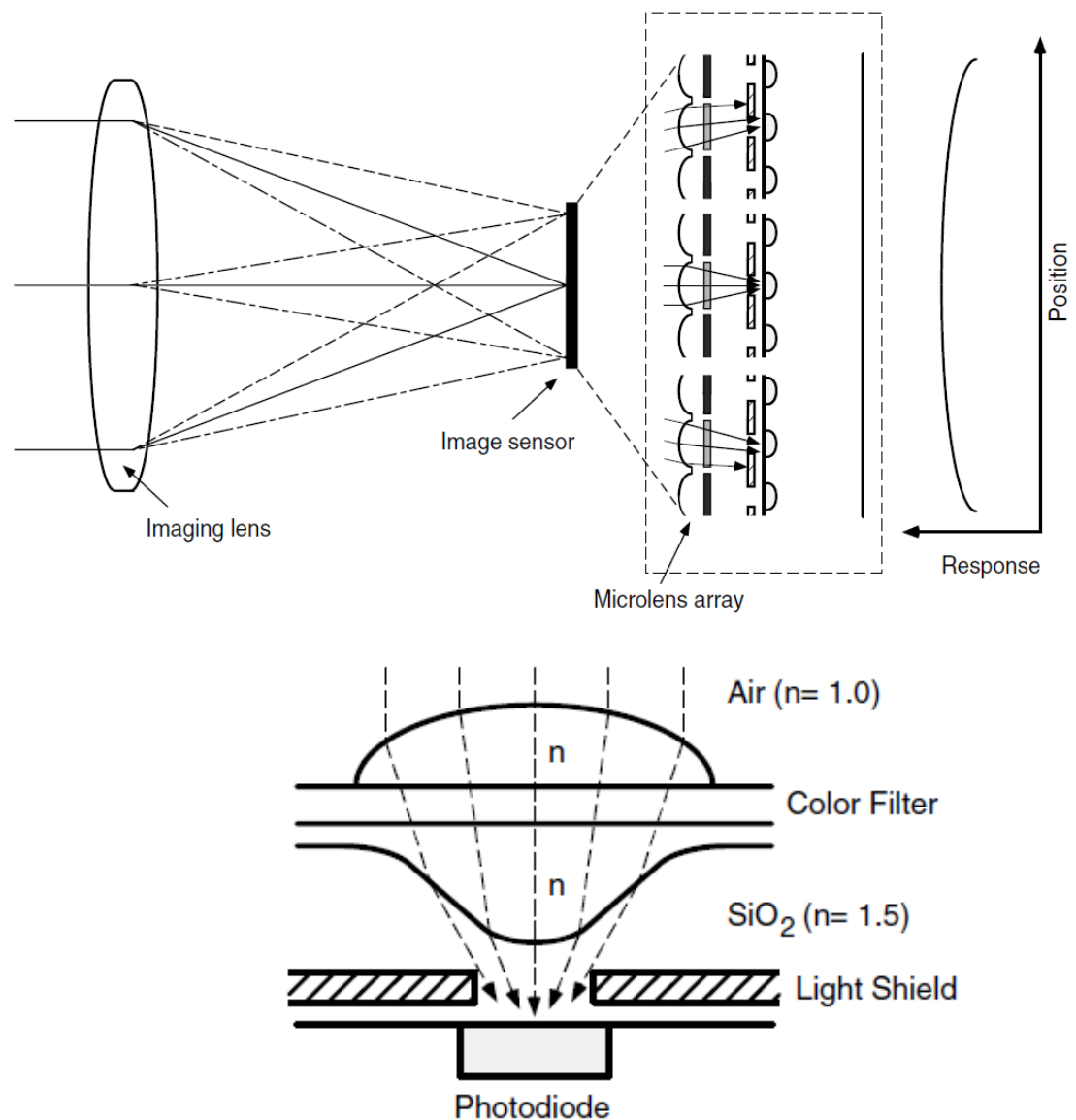
Photodetector in a pixel

- **Fill factor = $(A_{ps} / A_{pix}) \times 100\%$**
 - the portion of the pixel covered with the light shield includes the area that holds a transfer gate, a channel stop region that isolates pixels, and a V-CCD shift register
 - active-pixel CMOS image sensors: at least three transistors (a reset transistor, a source follower transistor, and a row select transistor) are covered by light shield
- **Color filter array**
 - on-chip color filter array (CFA)
 - RGB CFAs: superior color reproduction and higher color signal-to-noise ratio
 - luminance differences are associated with green whereas color perception is associated with red and blue
 - CMY CFAs: cyan, magenta, and yellow
 - Materials: pigment type and dye type



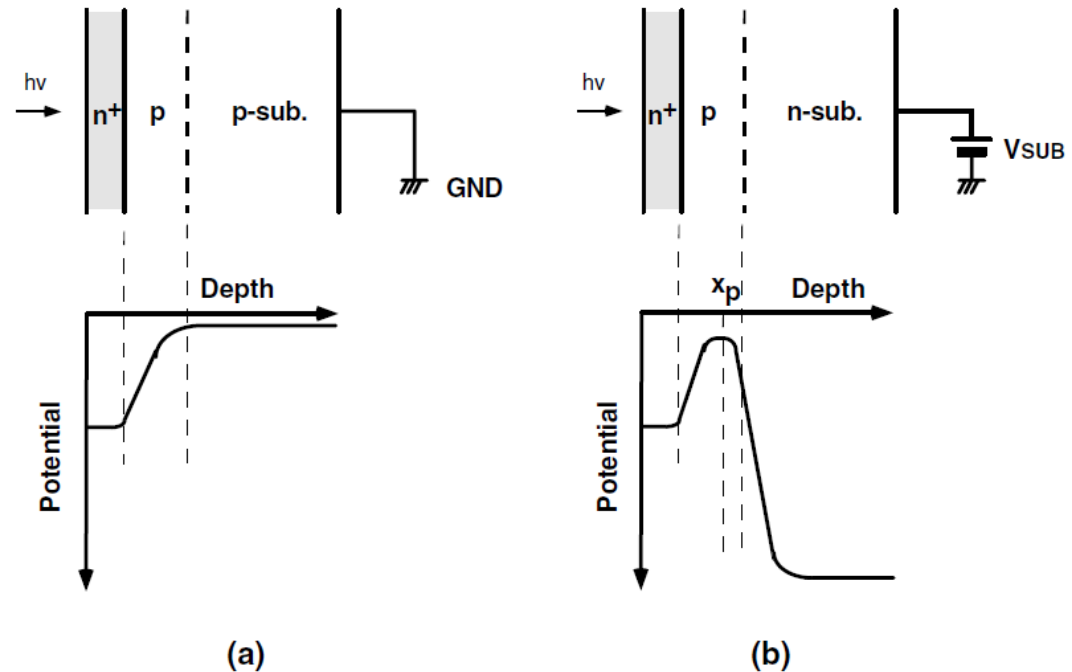
Photodetector in a pixel

- Microlens array
 - On-chip microlens array(OMA)
 - Collimates light to the photodiode
 - color filter layer-> transparent resin
 - photolithographic patterning
 - Increase in sensitivity
 - Shading effect
 - Reduce smear in CCD image sensors and crosstalk between pixels caused by minority carrier diffusion
- Reflection at SiO_2 and Si interface
 - Refractive index variation causes reflection
 - more than 20 to 30% of the incident light is reflected at the silicon surface in the visible light range
 - Anti-reflective films formed above the photodiode



Photodetector in a pixel

- Charge collection efficiency
 - $\eta(\lambda) = \frac{\text{signal charge}}{\text{photo-generated charge}}$
 - Depends on substrate type, impurity profile, minority carrier lifetime in the bulk and photodiode biasing
- Full-well capacity
 - photodiode operates in the charge-integrating mode
 - Limited charge handling capacity
 - Saturation charge
 - $N_{sat} = \frac{1}{q} \int_{V_{reset}}^{V_{max}} C_{PD}(V) dV$



RA 505 Robot Sensing and Vision

Lecture 25

Dr. Rishikesh Kulkarni
Department of Electronics and Electrical Engineering
IIT Guwahati

Basics of Image Sensors

- Imager: solid-state image sensor
- Wide spectral range; focus on visible range (380 nm – 780 nm)
- Silicon: suitable for visible image sensors
- Number of picture elements: Pixels; converts lights into holes/electrons
- Charged-coupled device (CCD) image sensor
- Complementary metal-oxide semiconductor (CMOS) image sensor
- High quality image: high resolution, high sensitivity, a wide dynamic range, good linearity for color processing, and very low noise

Functions of Image Sensors

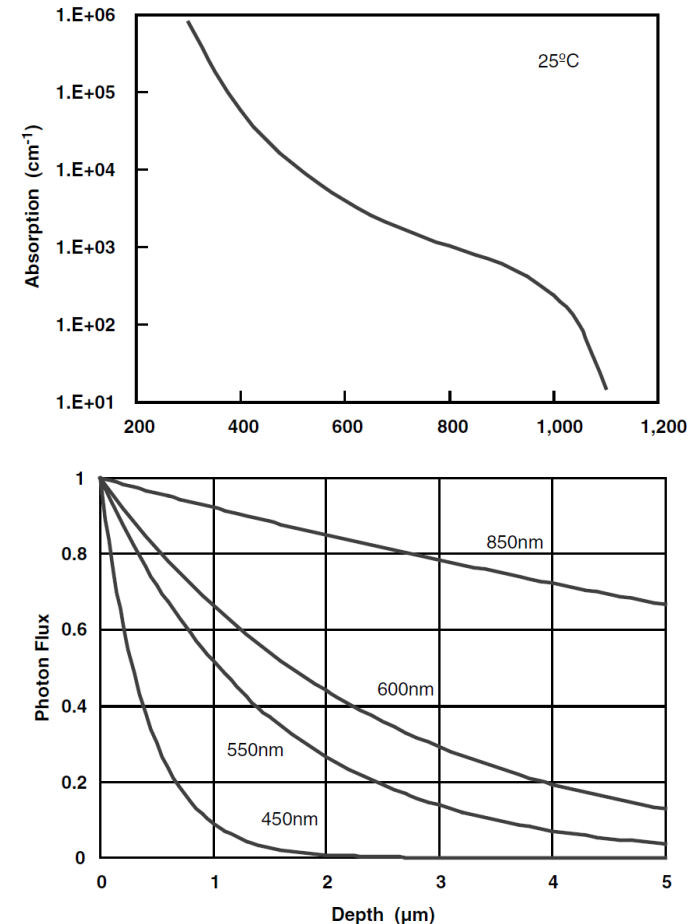
- Photoconversion

$$E_{\text{photon}} = h \cdot v = \frac{h \cdot c}{\lambda} \geq E_g$$

- Silicon band gap energy: 1.1 eV => wavelengths shorter than 1100 nm is absorbed and photon-to-signal charge conversion takes place
- Number of photons absorbed in a region with thickness dx is proportional to the intensity of the photon flux $\Phi(x)$; x : the distance from the semiconductor surface

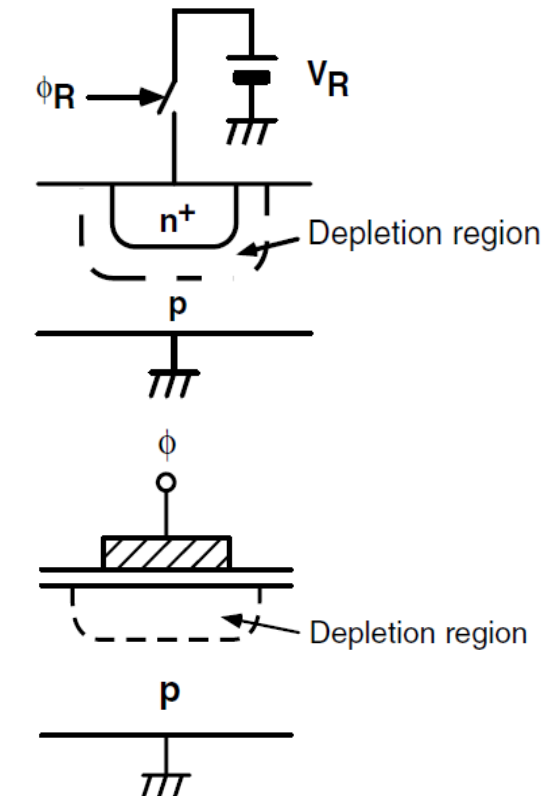
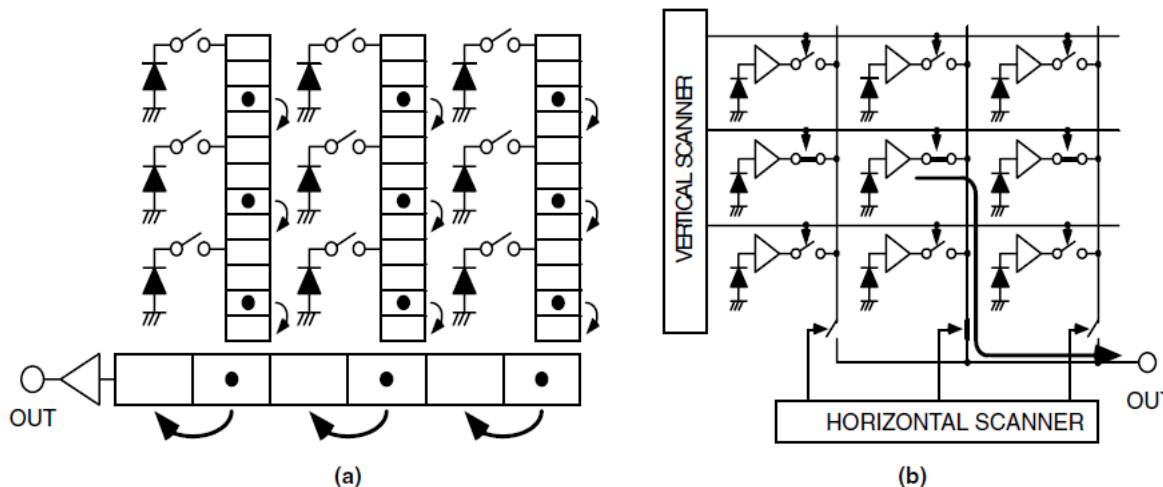
$$\Phi(x) = \Phi_0 \cdot \exp(-\alpha x)$$

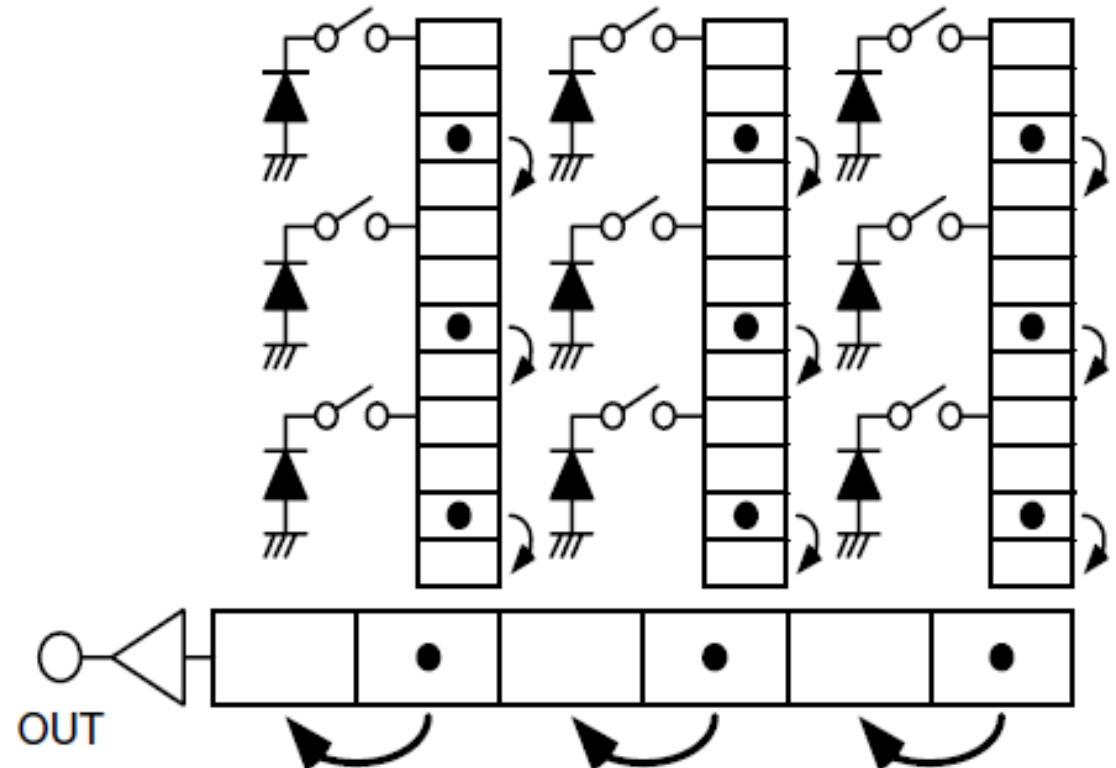
- photon flux decays exponentially with the distance from the surface; penetration depth ($1/\alpha$)



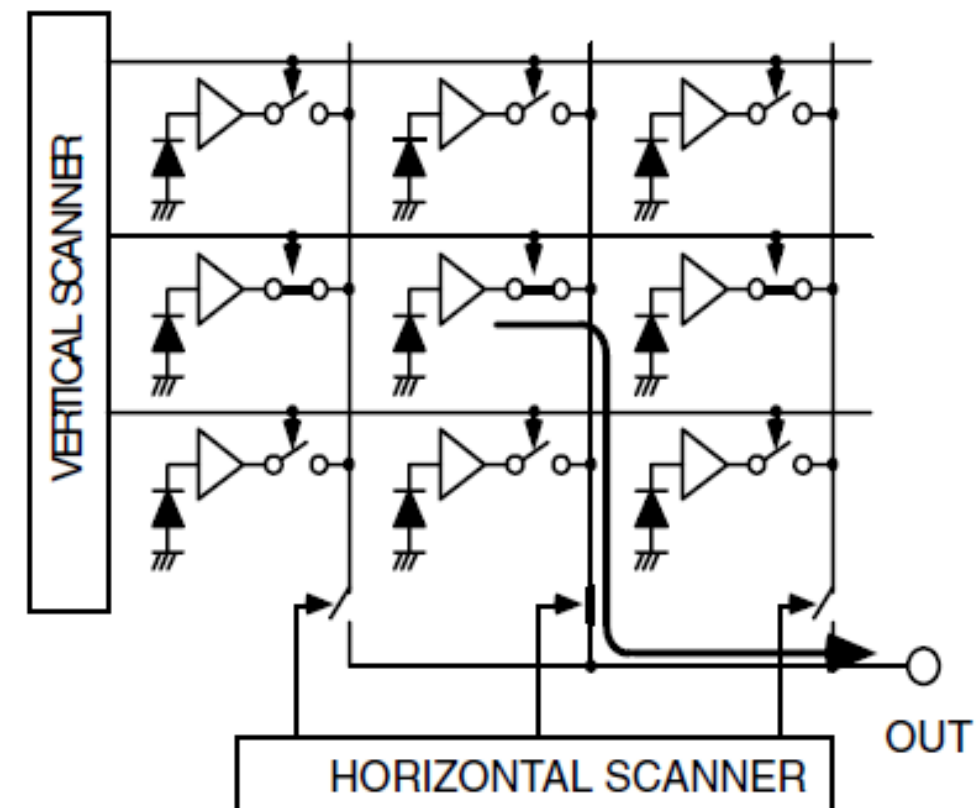
Charge collection and Accumulation

- Photodiode
- Metal-oxide semiconductor (MOS) diode
- Charge transfer
 - accumulated charge or the corresponding signal voltage or current must be read out from a pixel in an image sensor chip to the outside world
 - Scanning: two-dimensional signal transformation into time-sequenced signal (charge transfer, X-Y addressing)



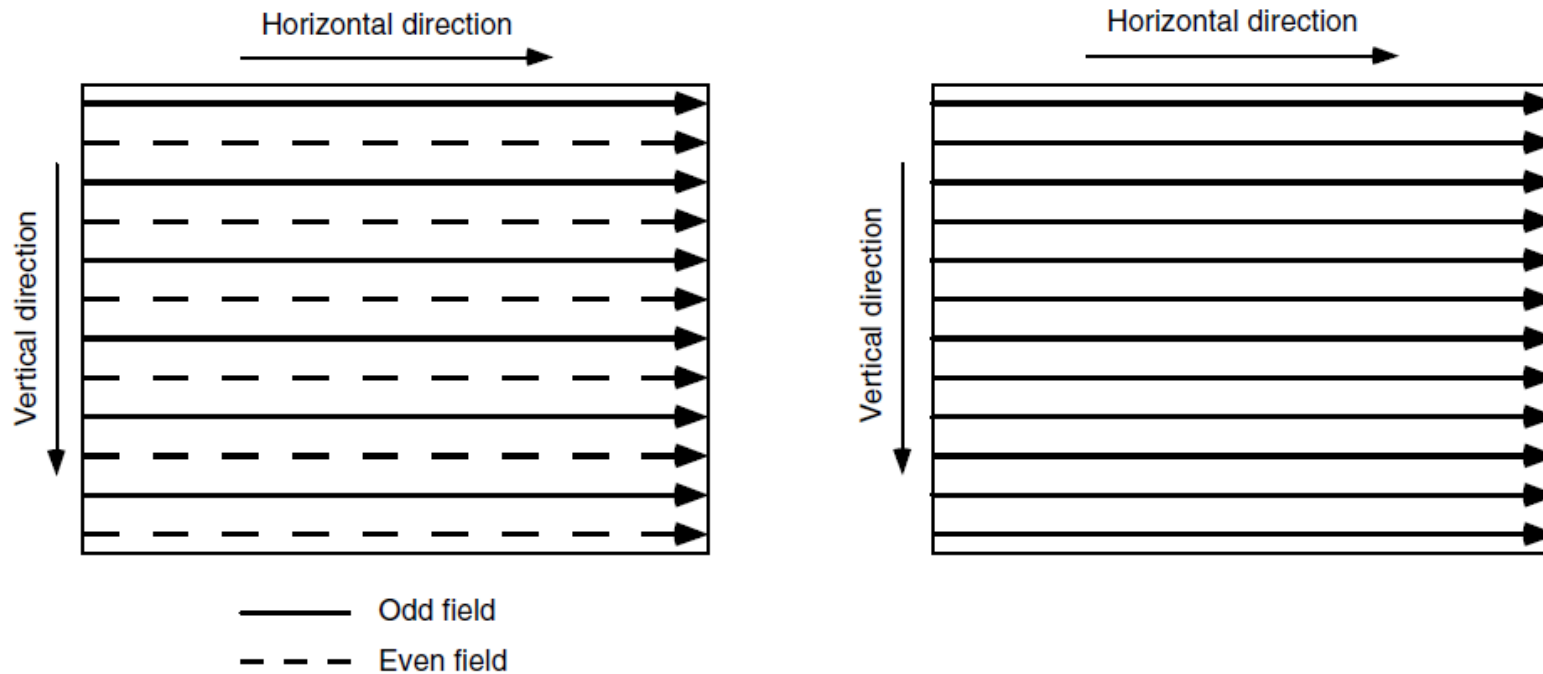


(a)

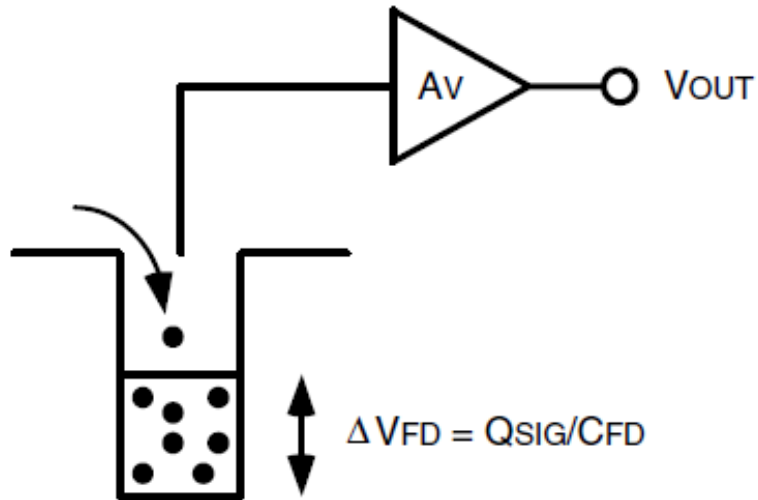


(b)

Interlaced Scan and Progressive Scan



Charge Detection and conversion gain



$$\Delta V_{FD} = \frac{Q_{sig}}{C_{FD}}$$

$$\Delta V_{OUT} = A_V \cdot \Delta V_{FD}$$

- Potential well is monitored by the voltage buffer
- Capacitance C_{FD} acts as a charge-to-voltage conversion capacitance

- Conversion gain

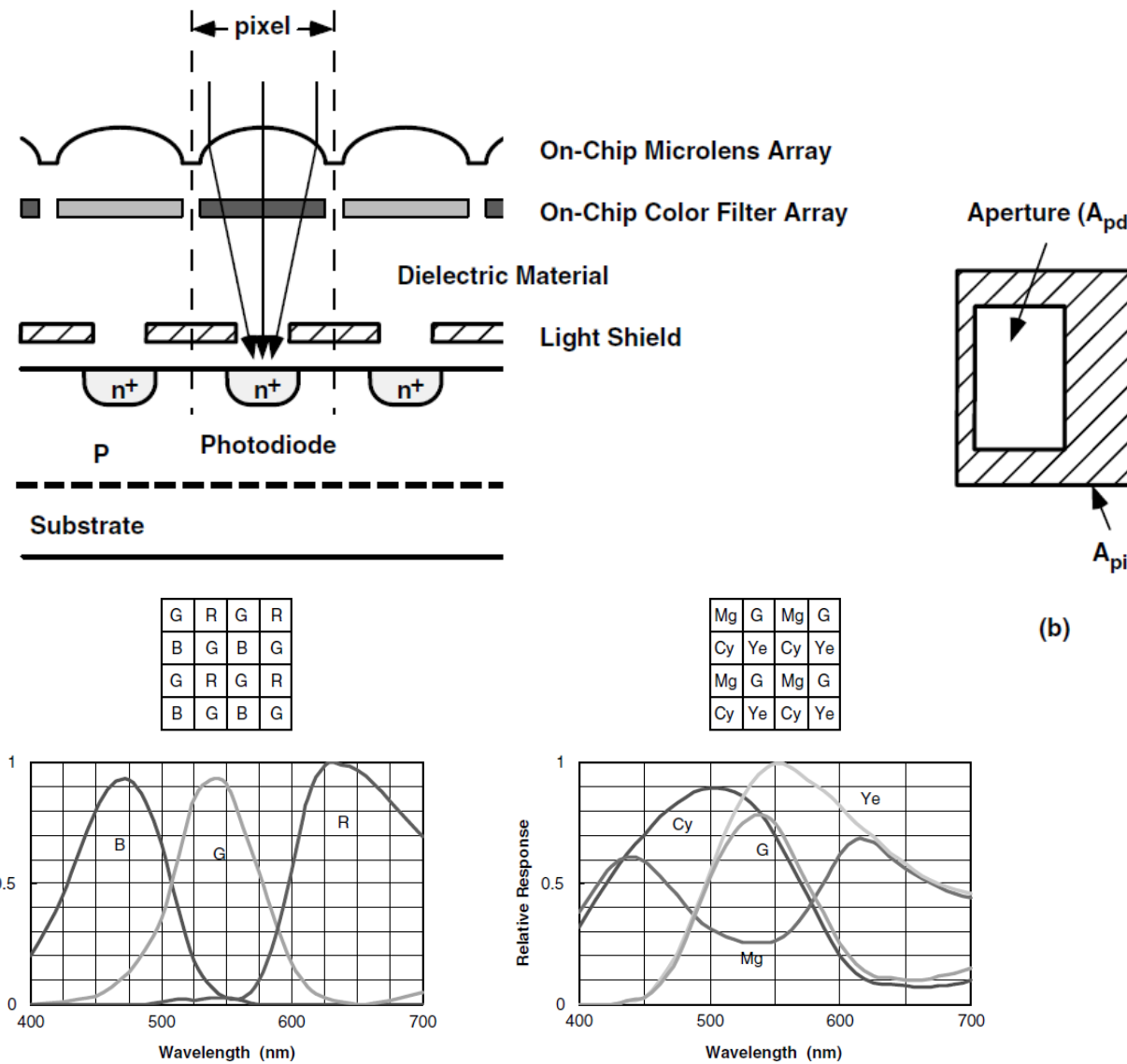
$$C.G. = \frac{q}{C_{FD}} \quad [\mu\text{V/electron}]$$

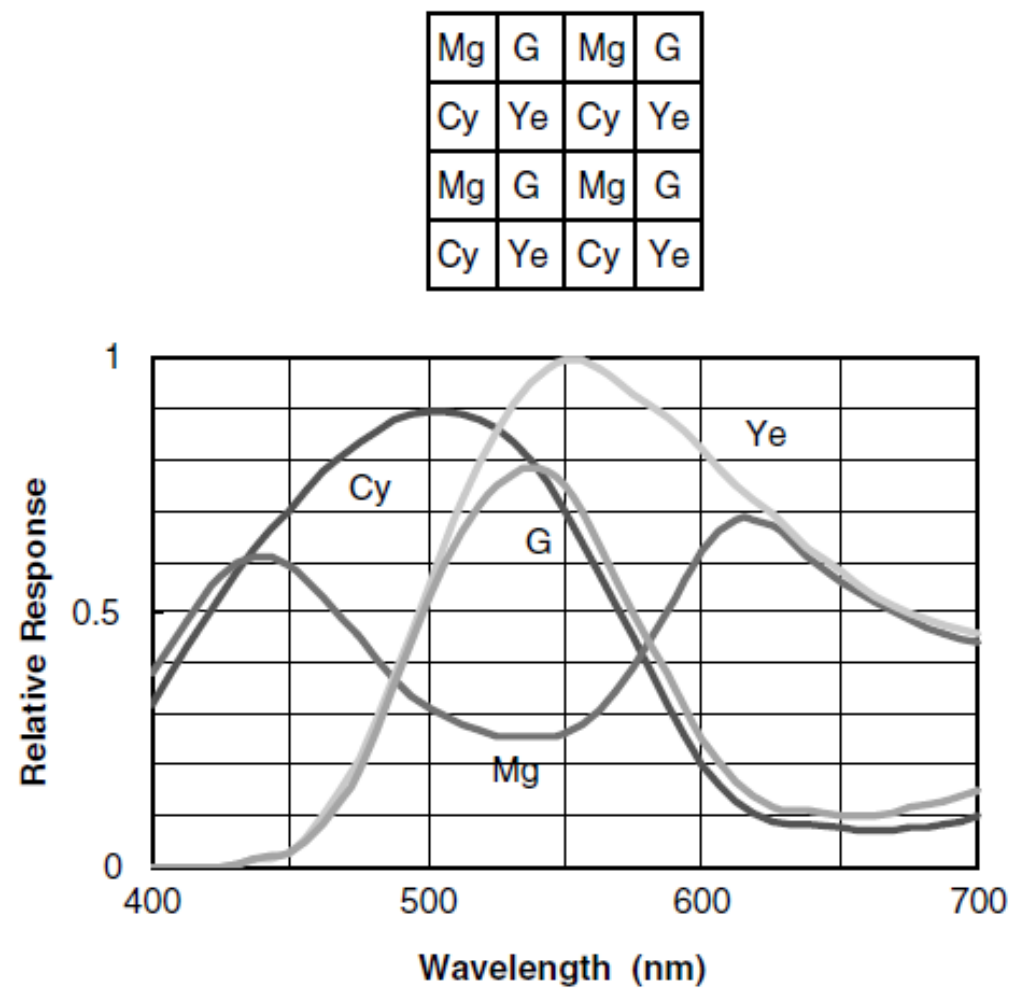
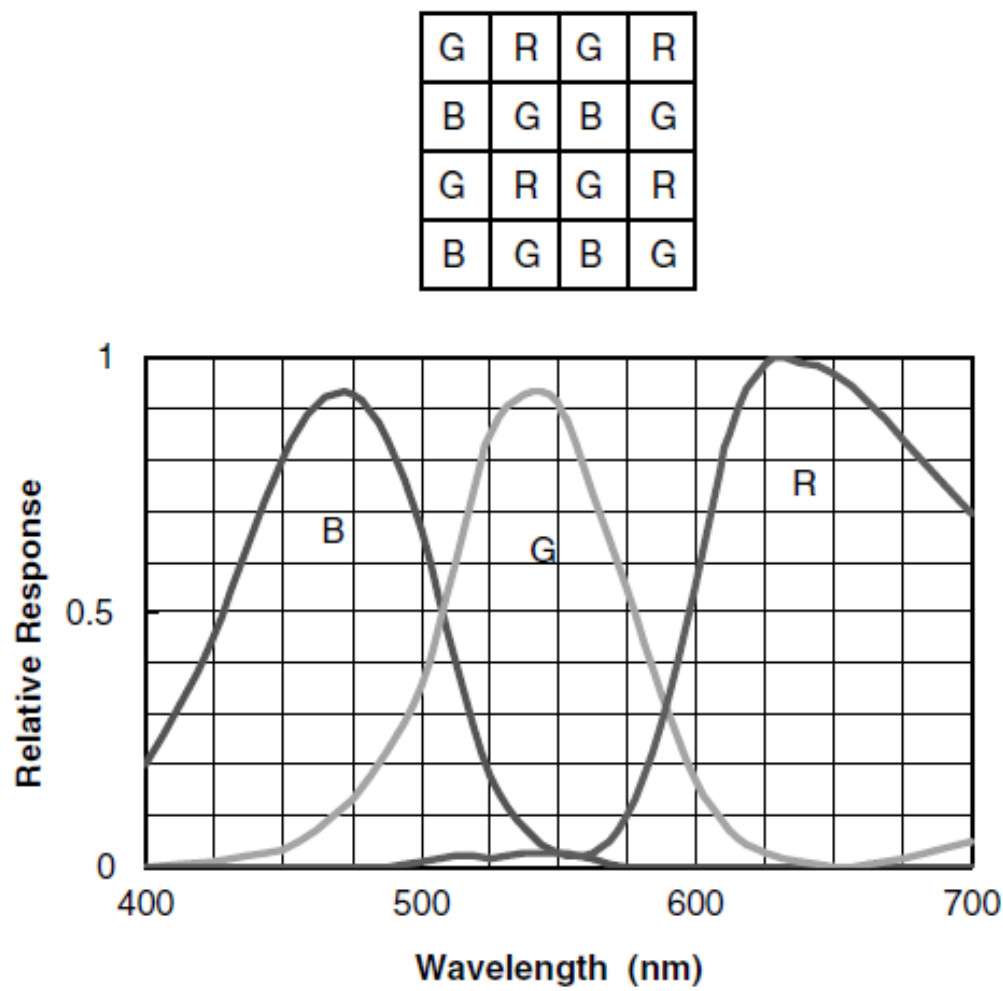
Change in voltage obtained by 1 electron at the charging node

$$C.G._{output_referred} = A_V \cdot \frac{q}{C_{FD}}$$

Photodetector in a pixel

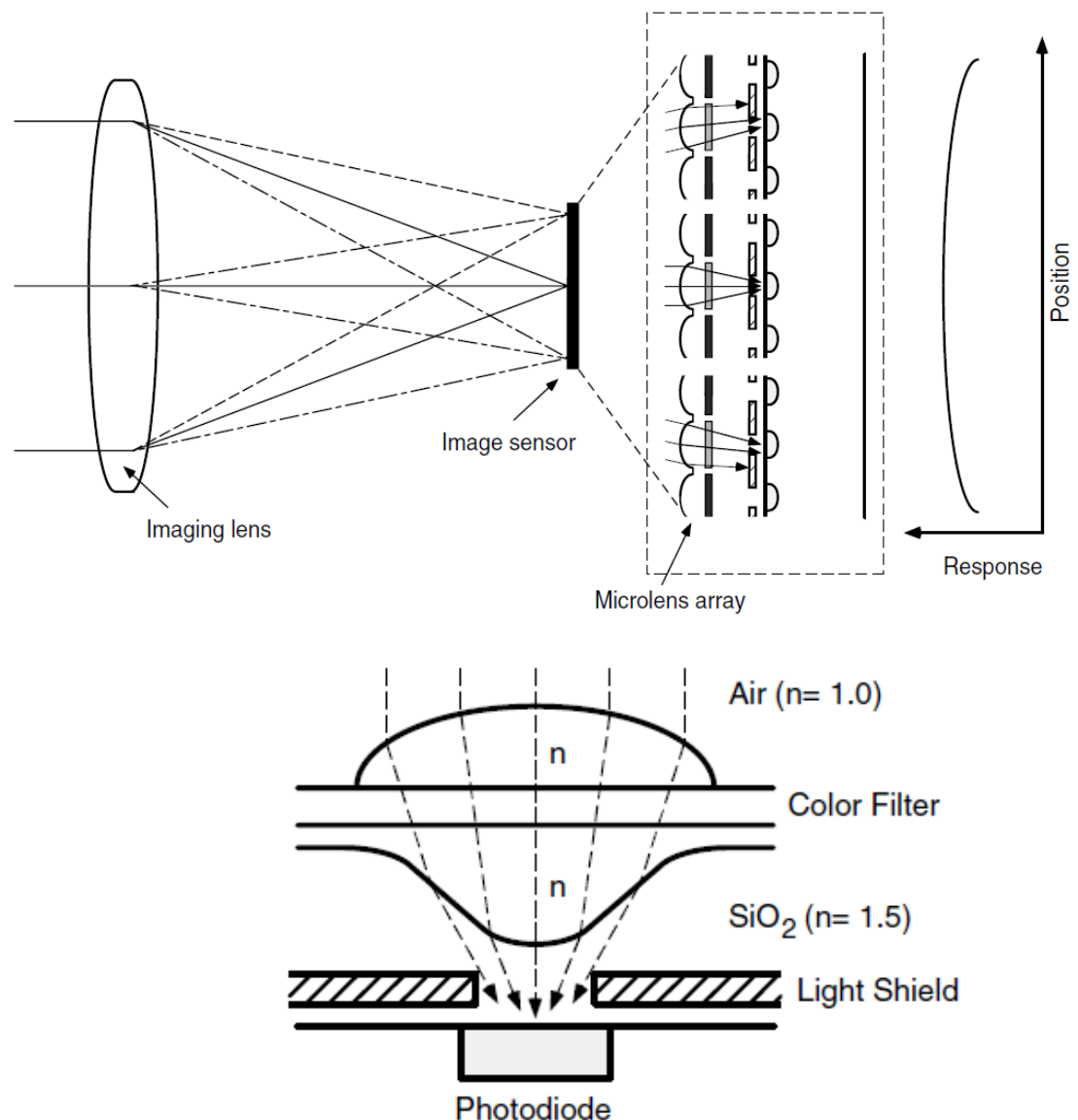
- **Fill factor = $(A_{ps} / A_{pix}) \times 100\%$**
 - the portion of the pixel covered with the light shield includes the area that holds a transfer gate, a channel stop region that isolates pixels, and a V-CCD shift register
 - active-pixel CMOS image sensors: at least three transistors (a reset transistor, a source follower transistor, and a row select transistor) are covered by light shield
- **Color filter array**
 - on-chip color filter array (CFA)
 - RGB CFAs: superior color reproduction and higher color signal-to-noise ratio
 - luminance differences are associated with green whereas color perception is associated with red and blue
 - CMY CFAs: cyan, magenta, and yellow
 - Materials: pigment type and dye type





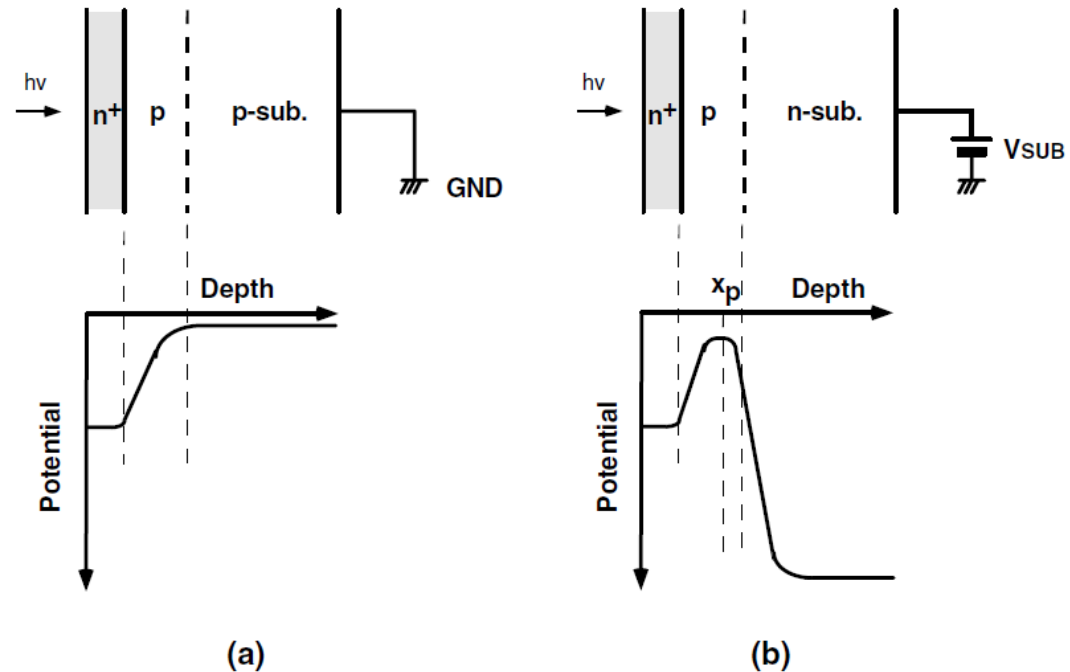
Photodetector in a pixel

- Microlens array
 - On-chip microlens array(OMA)
 - Collimates light to the photodiode
 - color filter layer-> transparent resin
 - photolithographic patterning
 - Increase in sensitivity
 - Shading effect
 - Reduce smear in CCD image sensors and crosstalk between pixels caused by minority carrier diffusion
- Reflection at SiO_2 and Si interface
 - Refractive index variation causes reflection
 - more than 20 to 30% of the incident light is reflected at the silicon surface in the visible light range
 - Anti-reflective films formed above the photodiode



Photodetector in a pixel

- Charge collection efficiency
 - $\eta(\lambda) = \frac{\text{signal charge}}{\text{photo-generated charge}}$
 - Depends on substrate type, impurity profile, minority carrier lifetime in the bulk and photodiode biasing
- Full-well capacity
 - photodiode operates in the charge-integrating mode
 - Limited charge handling capacity
 - Saturation charge
 - $N_{sat} = \frac{1}{q} \int_{V_{reset}}^{V_{max}} C_{PD}(V) dV$



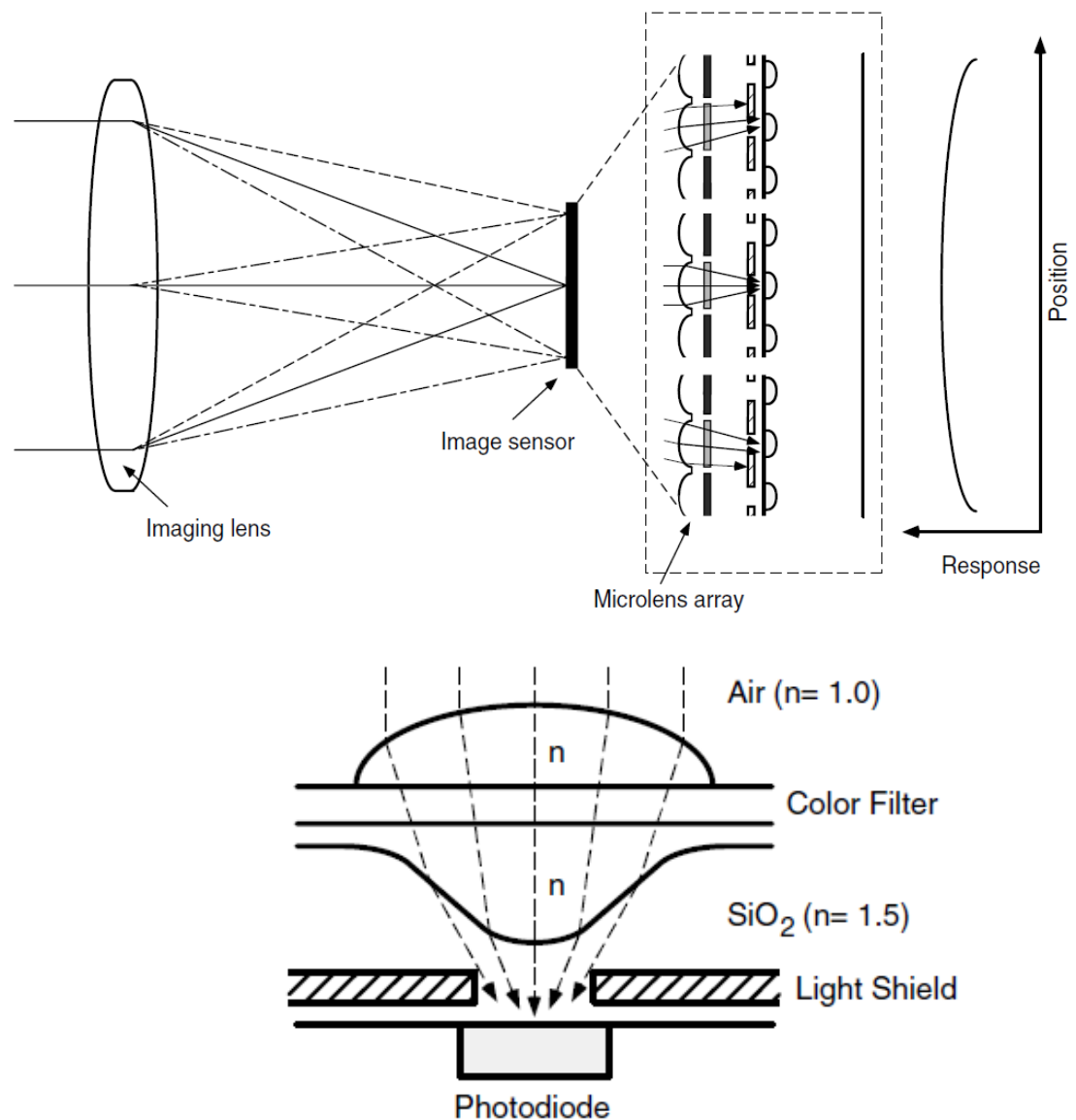
RA 505 Robot Sensing and Vision

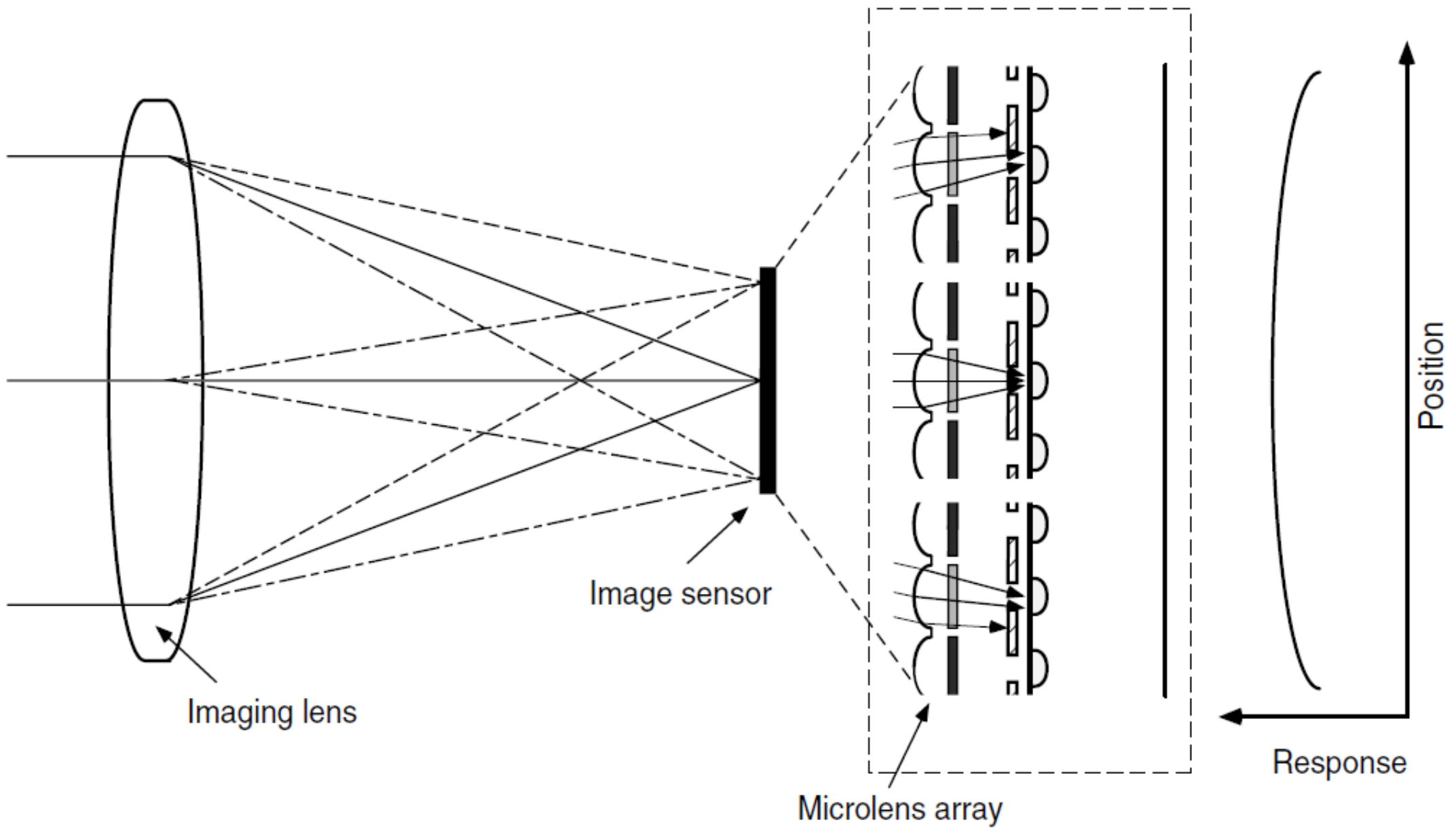
Lecture 27

Dr. Rishikesh Kulkarni
Department of Electronics and Electrical Engineering
IIT Guwahati

Photodetector in a pixel

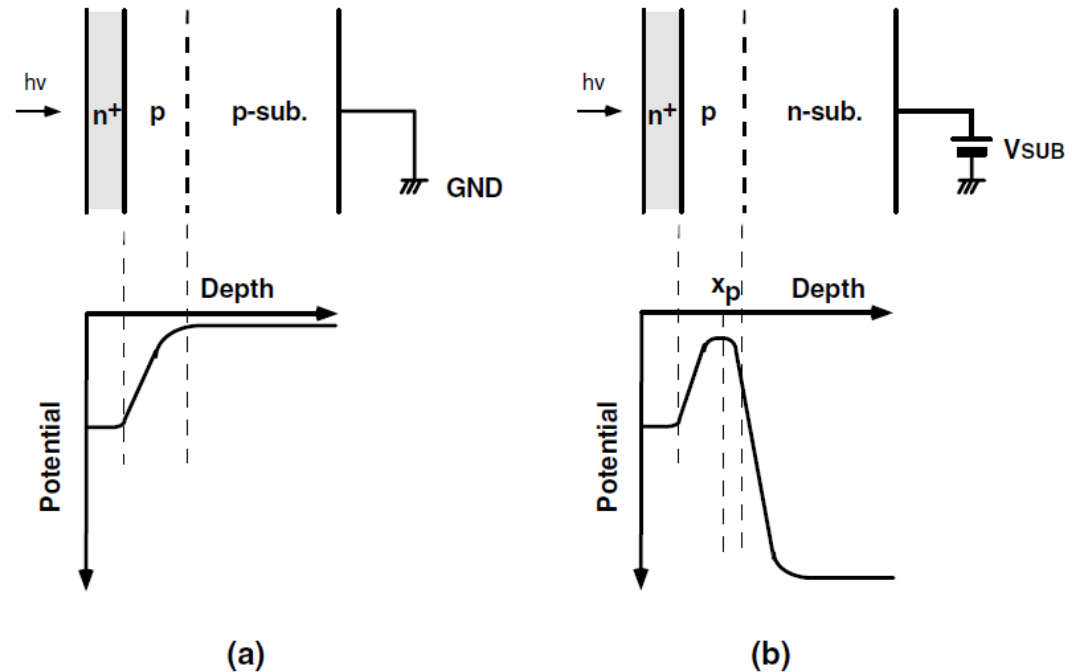
- Microlens array
 - On-chip microlens array(OMA)
 - Collimates light to the photodiode
 - color filter layer-> transparent resin
 - photolithographic patterning
 - Increase in sensitivity
 - Shading effect
 - Reduce smear in CCD image sensors and crosstalk between pixels caused by minority carrier diffusion
- Reflection at SiO_2 and Si interface
 - Refractive index variation causes reflection
 - more than 20 to 30% of the incident light is reflected at the silicon surface in the visible light range
 - Anti-reflective films formed above the photodiode





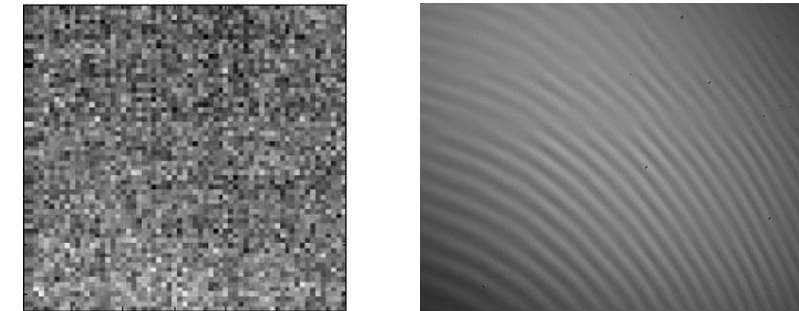
Photodetector in a pixel

- Charge collection efficiency
 - $\eta(\lambda) = \frac{\text{signal charge}}{\text{photo-generated charge}}$
 - Depends on substrate type, impurity profile, minority carrier lifetime in the bulk and photodiode biasing
- Full-well capacity
 - photodiode operates in the charge-integrating mode
 - Limited charge handling capacity
 - Saturation charge
 - $N_{sat} = \frac{1}{q} \int_{V_{reset}}^{V_{max}} C_{PD}(V) dV$



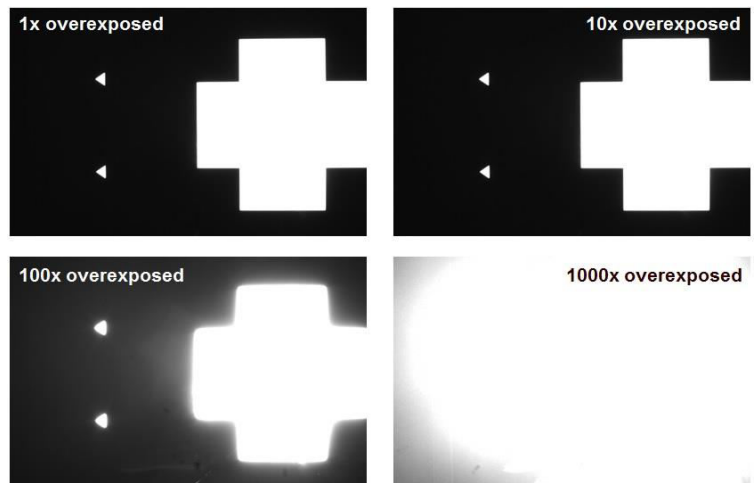
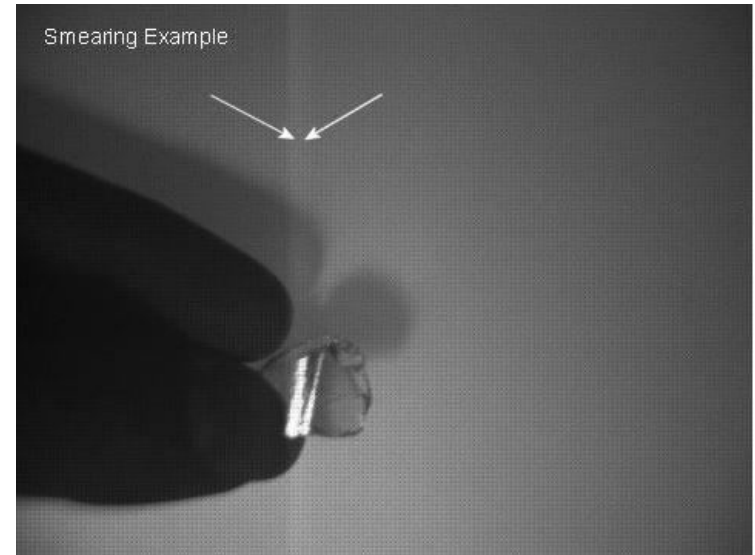
Noise

- Fixed pattern Noise (FPN) vs Random/Temporal noise
- FPN at dark: dark signal non-uniformity (DSNU)
- FPN at illumination: photo-response nonuniformity (PRNU)
- Exposure variation: sensitivity nonuniformity or gain variation
- FPN sources: long exposure times /high temperatures (CCD), dark current nonuniformity and performance variations of an active transistor inside a pixel (CMOS)
- Dark current
 - reduces the imager's useable dynamic range
 - Generation Current in the Depletion Region
 - Surface Generation
 - Diffusion current
 - Temperature Dependence

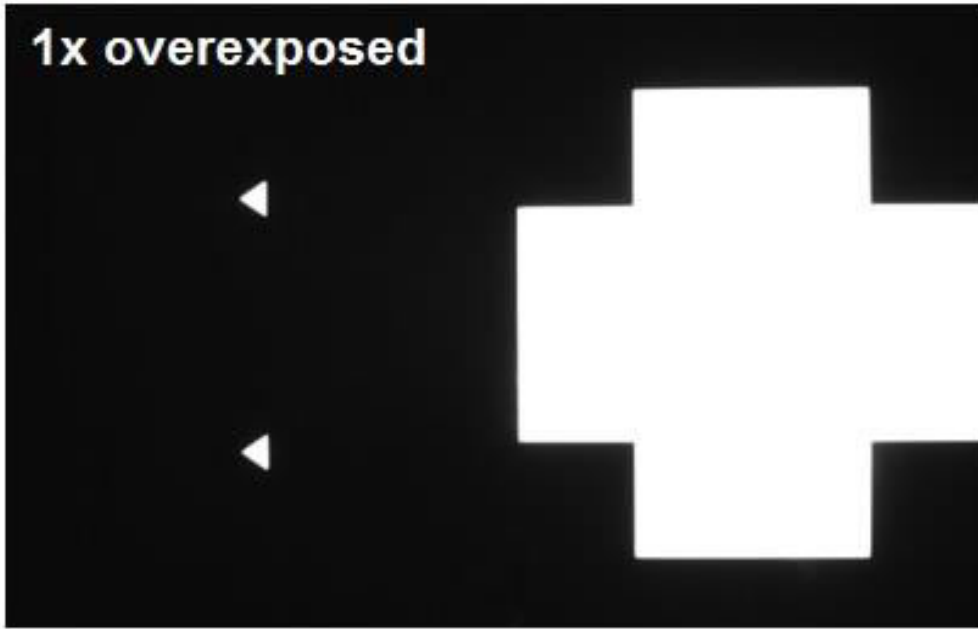


Noise

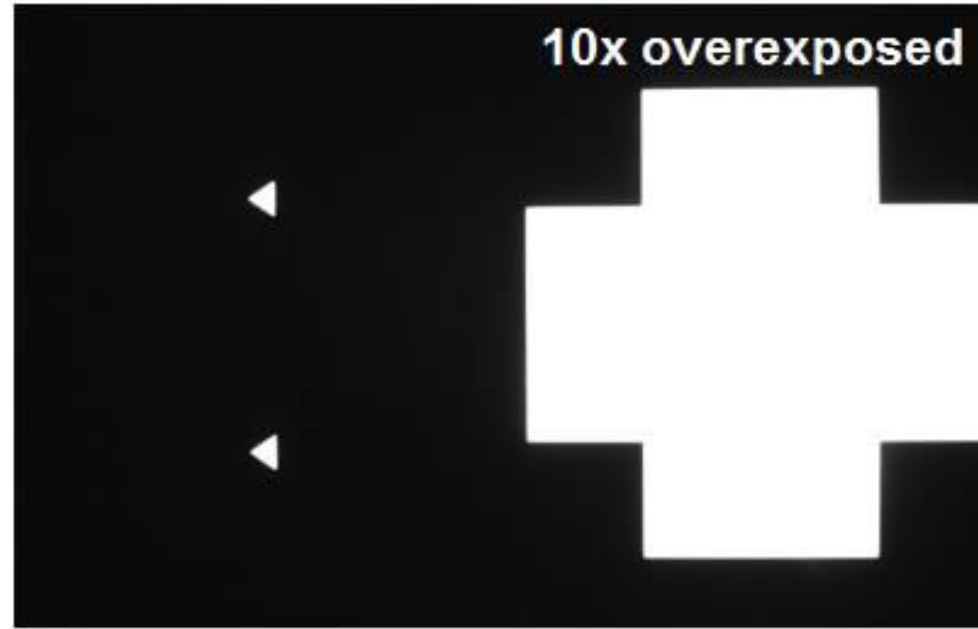
- Shading
 - slowly varying or low spatial frequency output variation
 - Dark-current-oriented, Microlens-oriented, Electrical-oriented shading
- Temporal noise
 - random variation in the signal over time
 - Probability distribution
$$p(x) = \frac{1}{\sqrt{2\pi}\sigma} \exp\left[-\frac{(x-m)^2}{2\sigma^2}\right]$$
- Thermal noise
 - thermal agitation of electrons
- Shot noise
 - arises because of the discrete nature of the charges carried by charge carriers
 - Power spectral densities of thermal noise and shot noise are constant over all frequencies.
 - 1/f noise: correlated double sampling
 - Read noise/noise floor
- Smear: white vertical stripes
- Blooming: photogenerated charge exceeds a pixel's full-well capacity
- Image lag



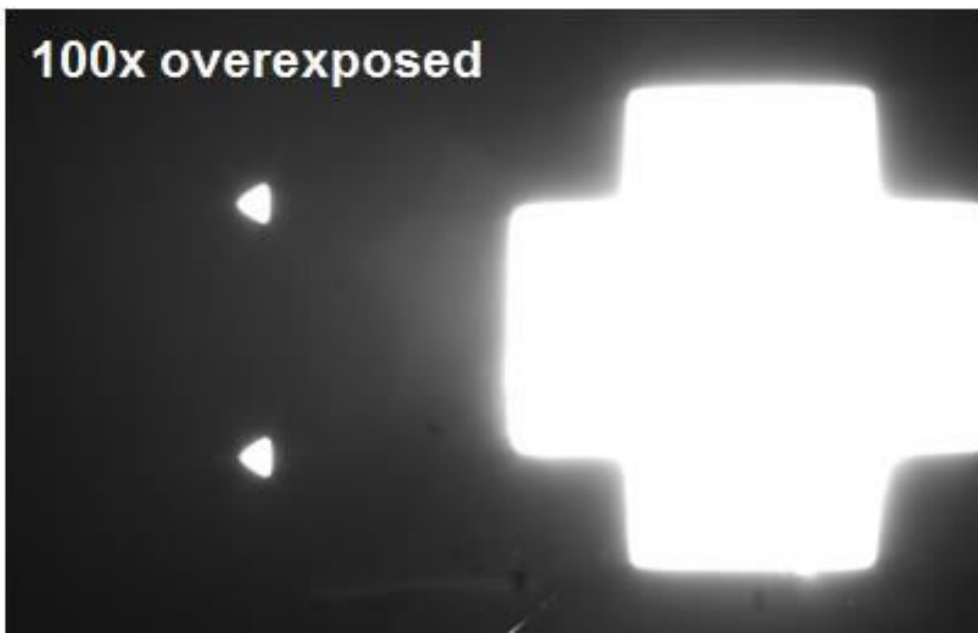
1x overexposed



10x overexposed



100x overexposed



1000x overexposed



Photoconversion characteristics

- Quantum efficiency

$$QE(\lambda) = N_{sig}(\lambda) / N_{ph}(\lambda)$$

$$N_{sig} = \frac{I_{ph} \cdot A_{pix} \cdot t_{INT}}{q}$$

$$QE(\lambda) = T(\lambda) \cdot FF \cdot \eta(\lambda)$$

- Responsivity

$$R = \frac{I_{ph} [A / cm^2]}{P [W / cm^2]} = \frac{qN_{sig}}{h\nu N_{ph}} = QE \cdot \frac{q\lambda}{hc}$$

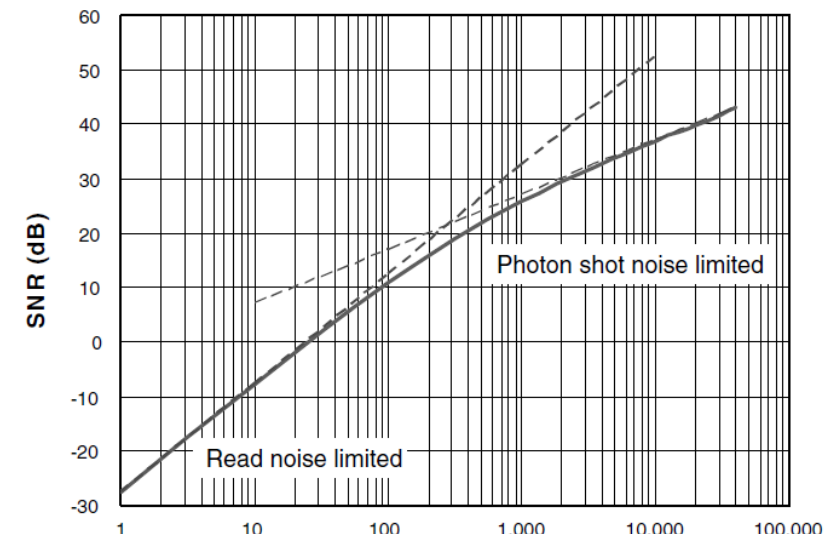
$$N_{ph} = \frac{P \cdot A_{pix} \cdot t_{INT}}{h\nu}$$

- Dynamic range:

$$DR = 20 \log \left(\frac{N_{sat}}{n_{read}} \right) [\text{dB}]$$

- Signal to noise ratio

$$SNR = 20 \log \left(\frac{N_{sig}}{n} \right) [\text{dB}]$$



Photoconversion characteristics

- Estimation of quantum efficiency

$$QE = \frac{N_{sig}}{N_{photon}} = \frac{(S / N)^2}{N_{photon}}$$

$$N_{photon} = \frac{\lambda}{hc} \cdot P \cdot A_{pix} \cdot t_{INT}$$

RA 505 Robot Sensing and Vision

Lecture 27

Dr. Rishikesh Kulkarni
Department of Electronics and Electrical Engineering
IIT Guwahati

Photoconversion characteristics

- Quantum efficiency

$$QE(\lambda) = N_{sig}(\lambda) / N_{ph}(\lambda)$$

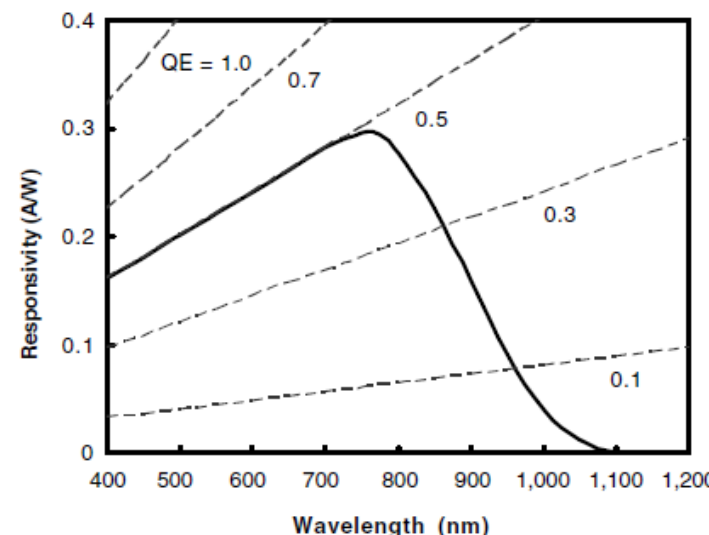
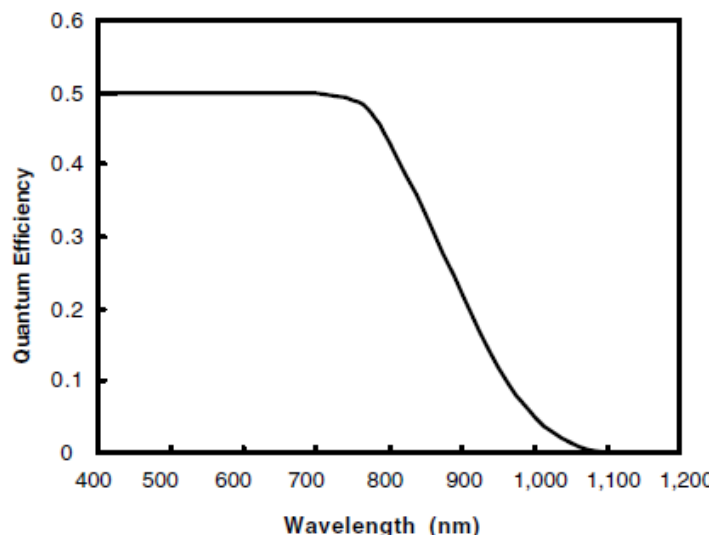
$$QE(\lambda) = T(\lambda) \cdot FF \cdot \eta(\lambda)$$

- Responsivity

$$R = \frac{I_{ph}[A/cm^2]}{P[W/cm^2]} = \frac{qN_{sig}}{h\nu N_{ph}} = QE \cdot \frac{q\lambda}{hc}$$

$$N_{sig} = \frac{I_{ph} \cdot A_{pix} \cdot t_{INT}}{q}$$

$$N_{ph} = \frac{P \cdot A_{pix} \cdot t_{INT}}{h\nu}$$



Photoconversion characteristics

- Dynamic range:

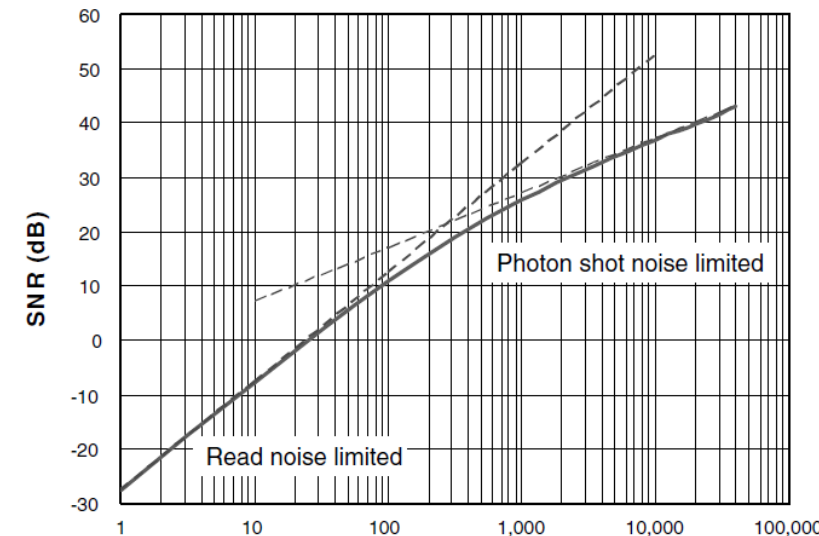
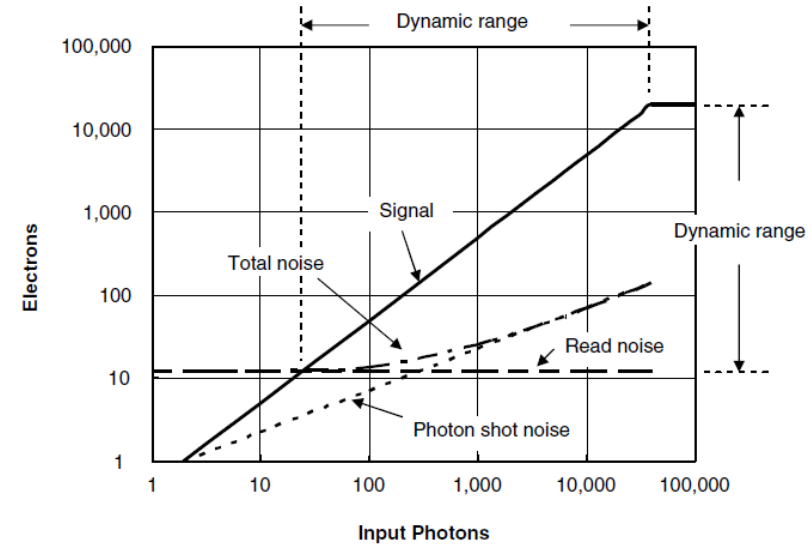
$$DR = 20 \log \left(\frac{N_{sat}}{n_{read}} \right) [\text{dB}]$$

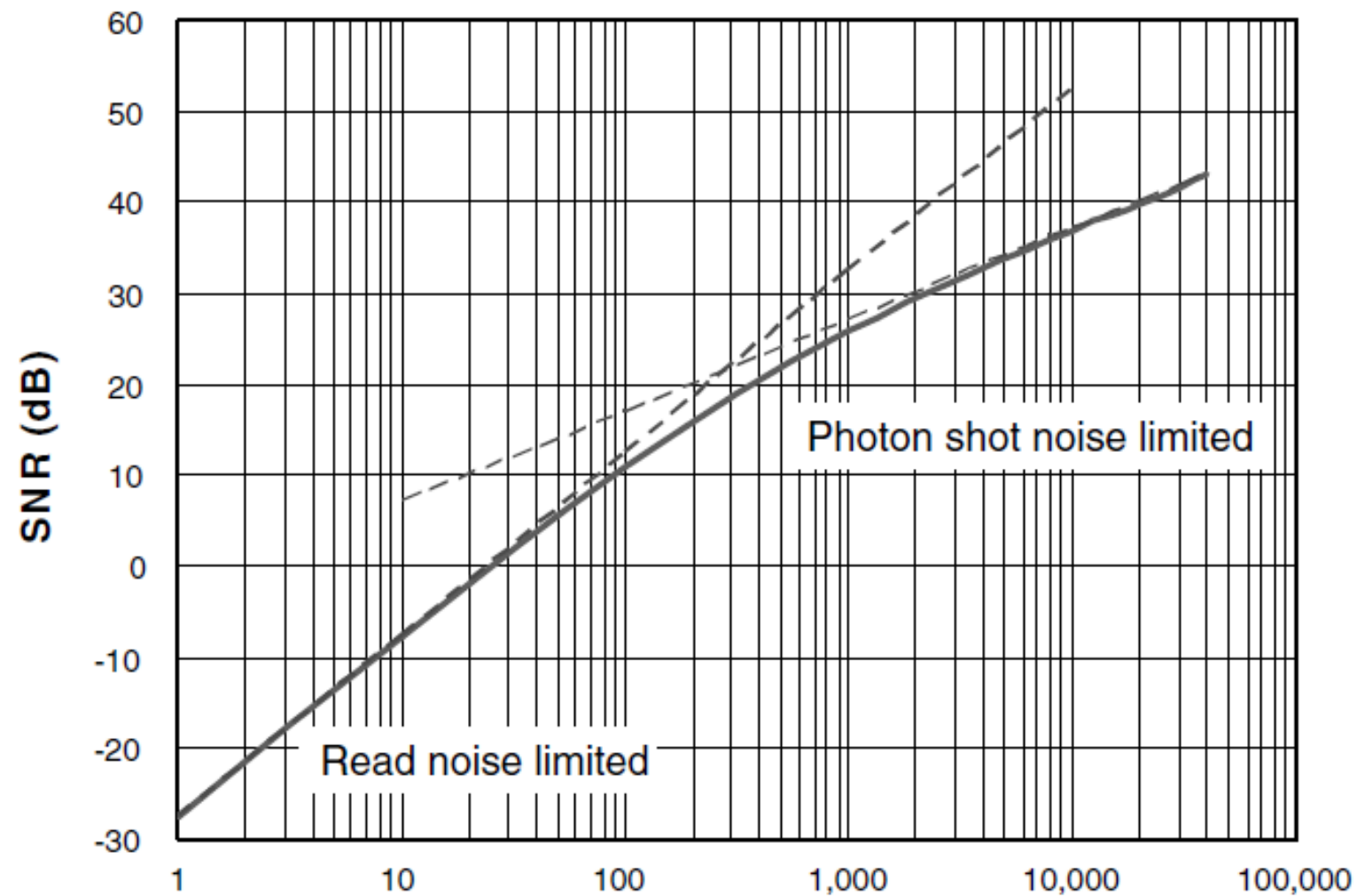
- Signal-to-noise ratio

$$SNR = 20 \log \left(\frac{N_{sig}}{n} \right) [\text{dB}]$$

$$SNR = 20 \log \left(\frac{N_{sig}}{n_{read}} \right)$$

$$SNR = 20 \log \left(\frac{N_{sig}}{n_{photon}} \right) = 20 \log \left(\frac{N_{sig}}{\sqrt{N_{sig}}} \right) = 20 \log \sqrt{N_{sig}}$$





Photoconversion characteristics

- Estimation of quantum efficiency

$$QE = \frac{N_{sig}}{N_{photon}} = \frac{(S / N)^2}{N_{photon}}$$

$$N_{photon} = \frac{\lambda}{hc} \cdot P \cdot A_{pix} \cdot t_{INT}$$

- Estimation of conversion gain

$$V_{sig} = C.G. \cdot N_{sig}$$

$$v_{photon} = C.G. \cdot \sqrt{N_{sig}}$$

$$v_{photon}^2 = (C.G.) \cdot V_{sig}$$

Photoconversion characteristics

- Estimation of full well capacity $N_{sat} = 10^{SNR_{max}/10}$
- Noise Equivalent Exposure : $SNR = 1$
- Linearity
- Crosstalk
- Sensitivity and SNR
 - ratio of the output change to the input light change
 - volts/lux-sec, bits/lux-sec

Modulation transfer function

$$o(x, y) = \iint h(x - x_0, y - y_0) \cdot i(x_0, y_0) \cdot dx_0 \cdot dy_0$$

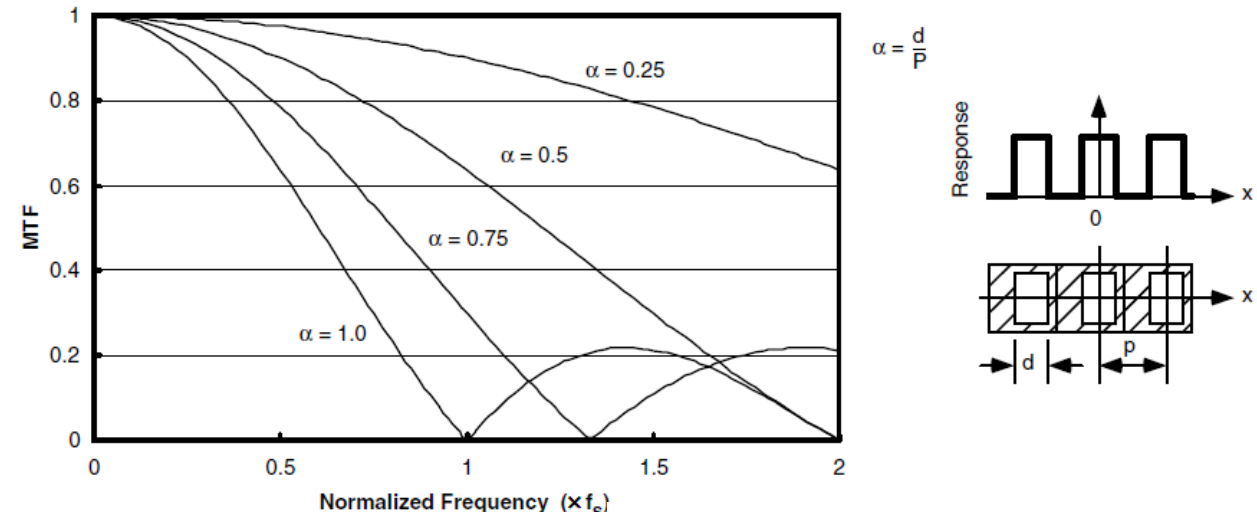
$$O(f_x, f_y) = H(f_x, f_y) \cdot I(f_x, f_y)$$

$$H(f_x, f_y) = MTF(f_x, f_y) \cdot \exp \left\{ -\phi(f_x, f_y) \right\}$$

$$MTF_{System} = MTF_{Lens} \cdot MTF_{Optical_Filter} \cdot MTF_{Imager} \cdot MTF_{Signal_Processing}$$

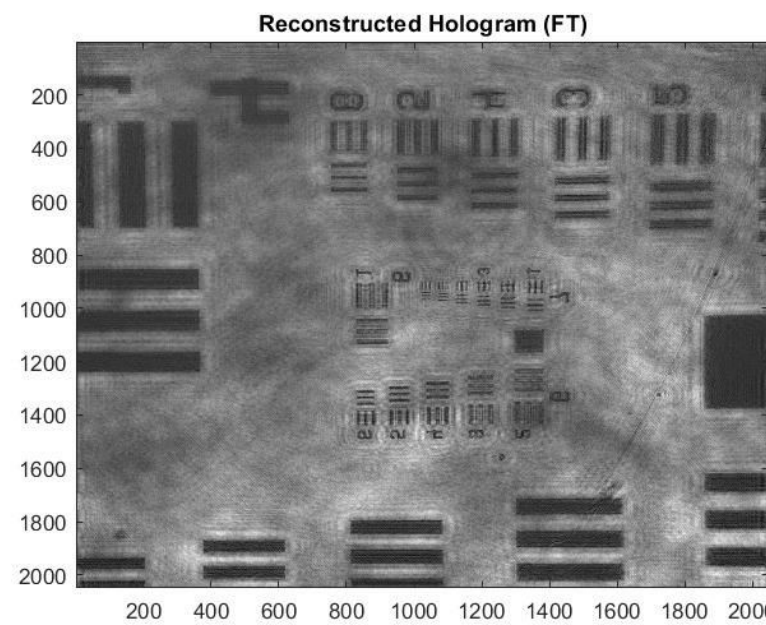
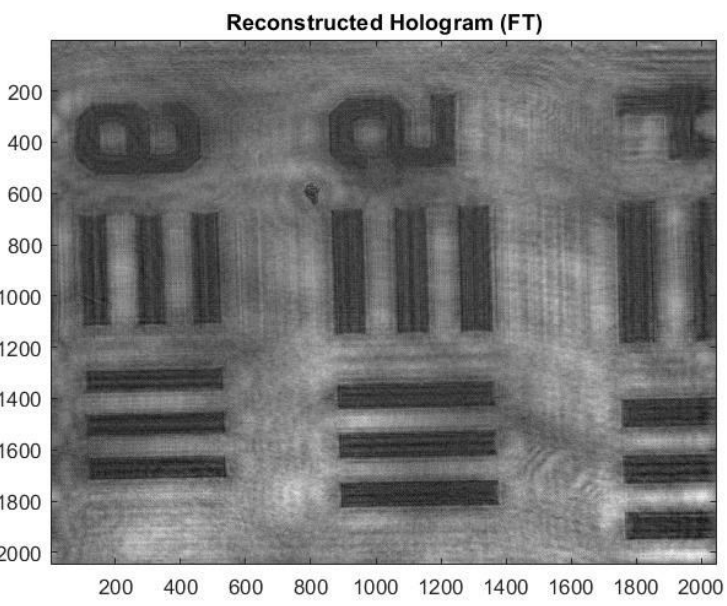
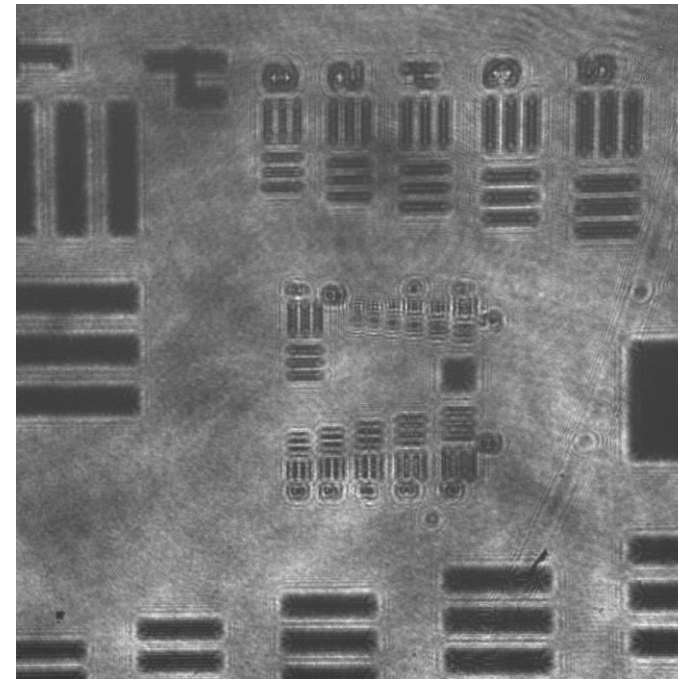
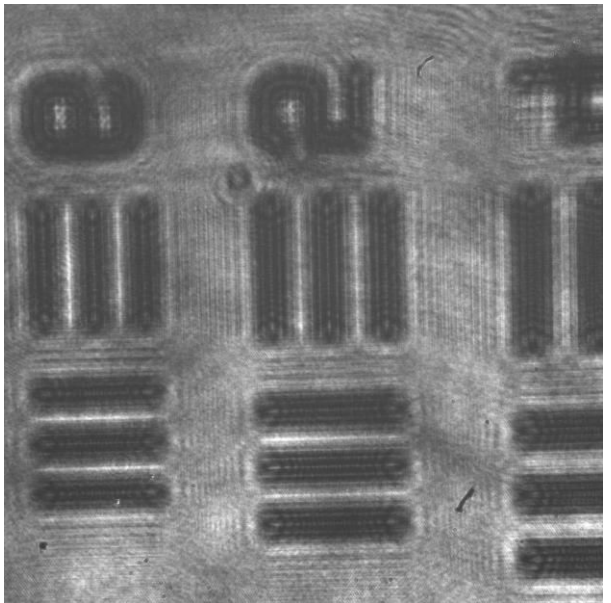
$$MTF(f_x, f_y) = \left| \iint S(x, y) \cdot \exp \left\{ -j2\pi(f_x \cdot x + f_y \cdot y) \right\} \cdot dx \cdot dy \right|$$

$$MTF(f_x) = \left| \int_{-\infty}^{+\infty} Rect(x_0, d) \cdot \exp(-j2\pi f_x x) dx \right| = \frac{\sin\left(2\pi f_x \cdot \frac{d}{2}\right)}{2\pi f_x \cdot \frac{d}{2}}$$

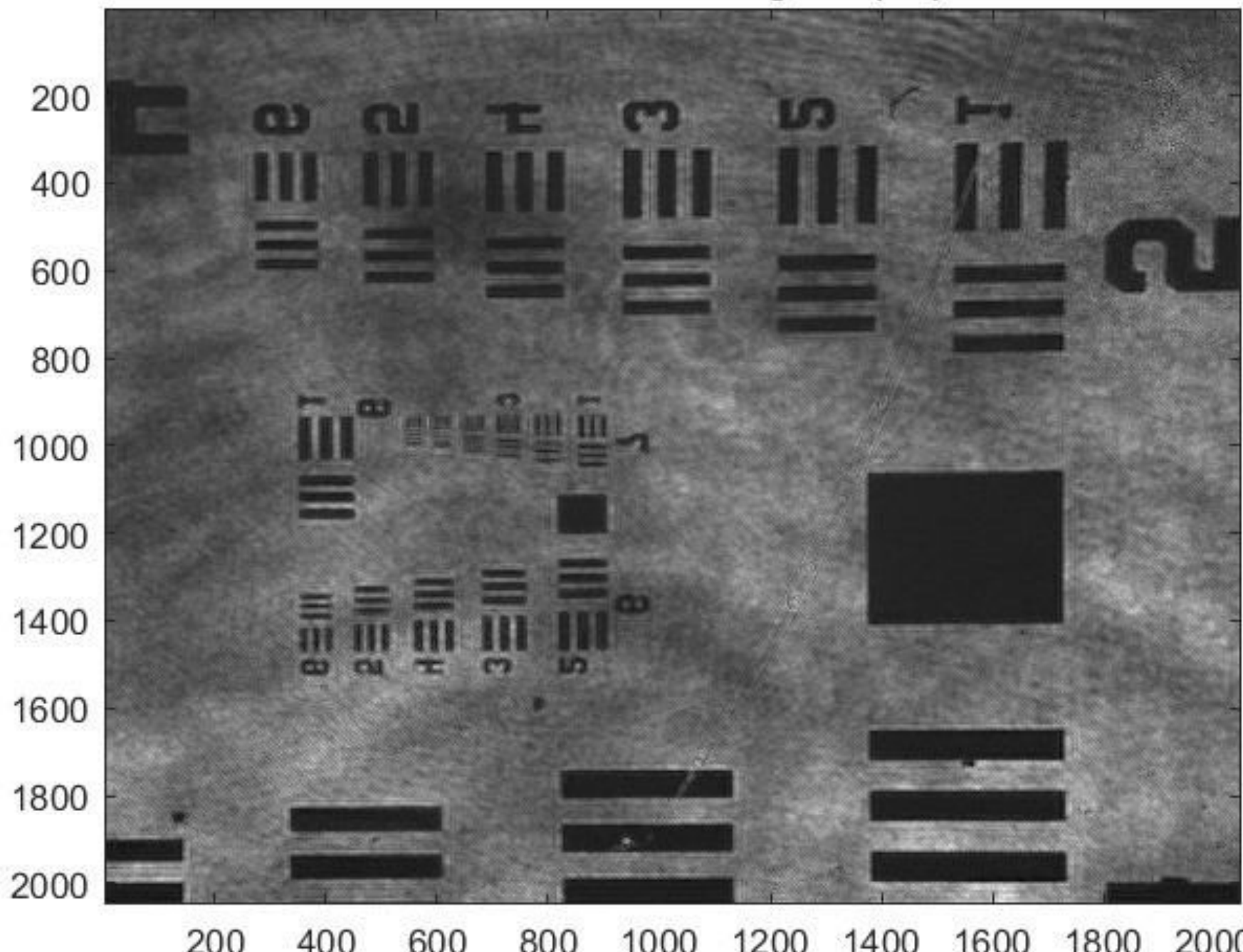


$$f_s = \frac{1}{p}$$

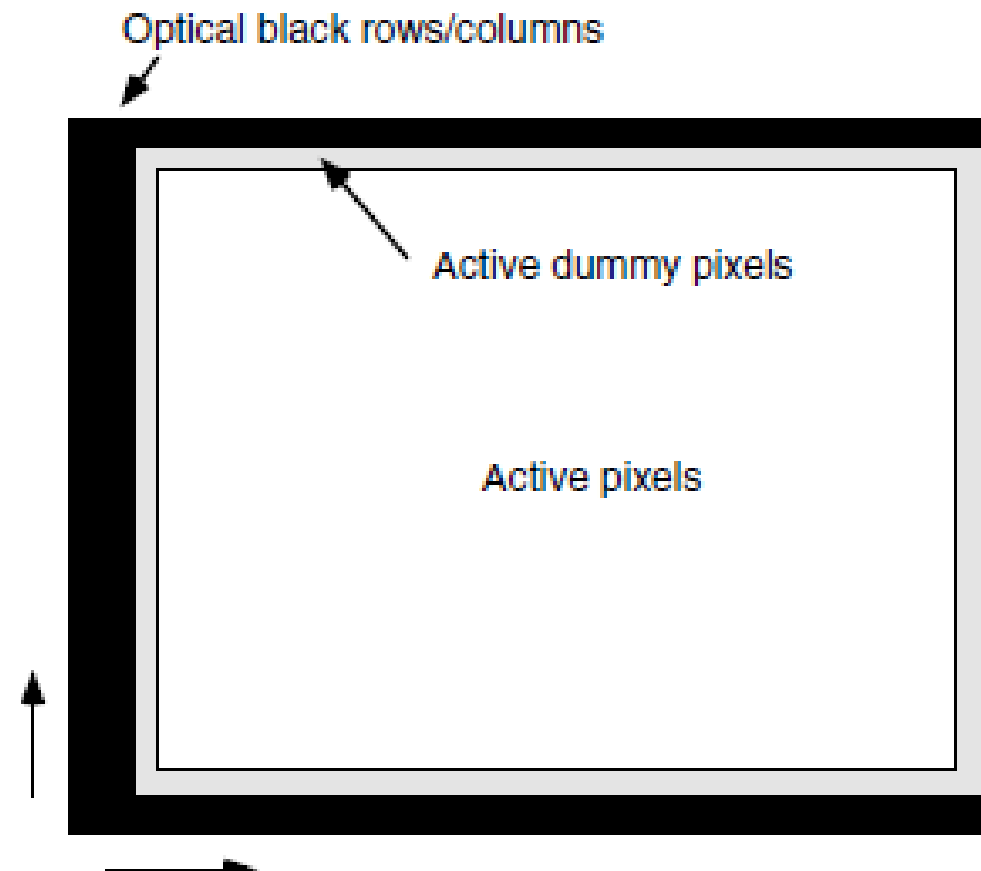
$$f_N = \frac{f_s}{2} = \frac{1}{2p}$$



Reconstructed Hologram (FT)



Optical black pixels and dummy pixels



Optical format and pixel size

Optical Format and Effective Array Size

Format (type)	Diagonal (mm)	H (mm)	V (mm)	
1	16.0	12.80	9.60	16 mm/in.
2/3	11.0	8.80	6.60	
1/1.8	8.89	7.11	5.33	
1/2	8.00	6.40	4.80	
1/2.5	7.20	5.76	4.32	18 mm/in.
1/2.7	6.67	5.33	4.00	
1/3	6.00	4.80	3.60	
1/3.2	5.63	4.50	3.38	
1/4	4.50	3.60	2.70	
1/5	3.60	2.88	2.16	
1/6	3.00	2.40	1.80	
For DSLR Format	Diagnal (mm)	H (mm)	V (mm)	Aspect ratio
35 mm	43.27	36.00	24.00	3:2
APS-DX	28.37	23.7	15.6	
APS-C	27.26	22.7	15.1	
APS-H	33.93	28.7	19.1	
Four-thirds	21.63	17.3	13.0	4:3

Resolution of PC Displays

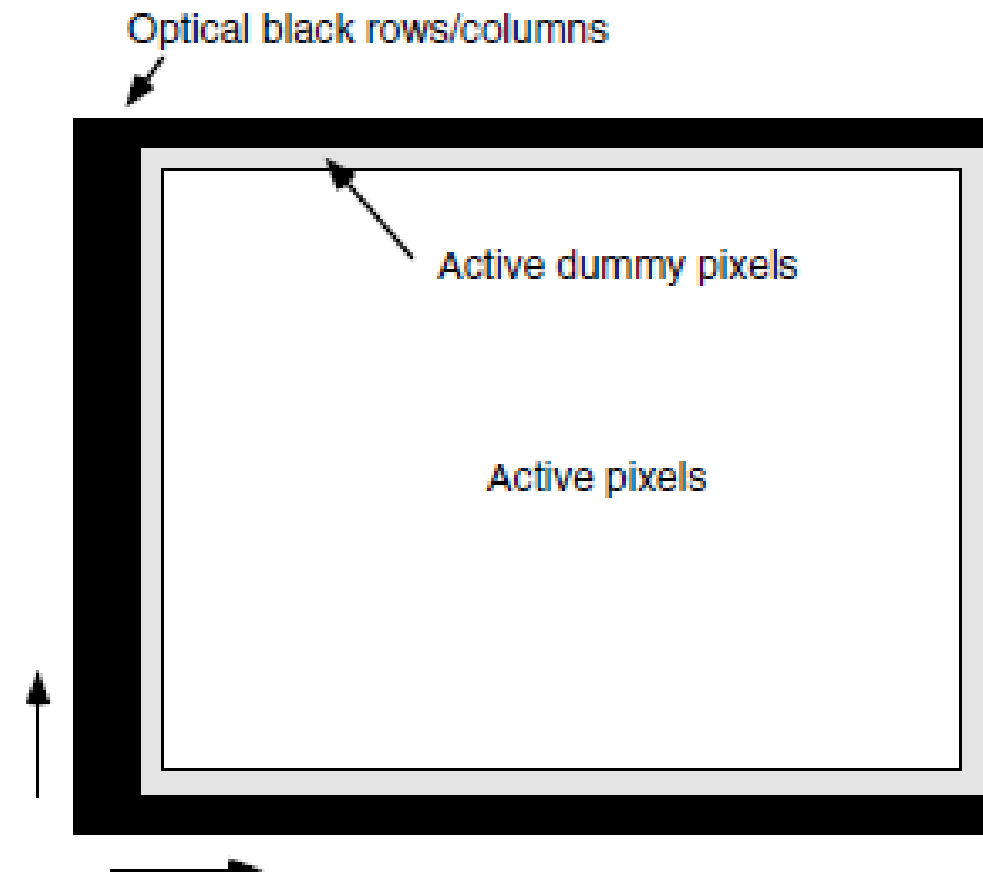
Format	Resolution (pixels)
QCIF	Quarter common intermediate format
CIF	Common intermediate format
QVGA	Quarter video graphics array
VGA	Video graphics array
SVGA	Super video graphics array
XGA	Extended graphics array
SXGA	Super extended graphics array
UXGA	Ultra extended graphics array
QXGA	Quad extended graphics array

RA 505 Robot Sensing and Vision

Lecture 29

Dr. Rishikesh Kulkarni
Department of Electronics and Electrical Engineering
IIT Guwahati

Optical black pixels and dummy pixels



Optical format and pixel size

Optical Format and Effective Array Size

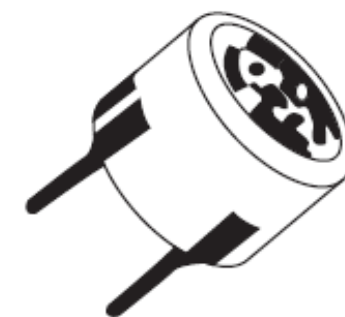
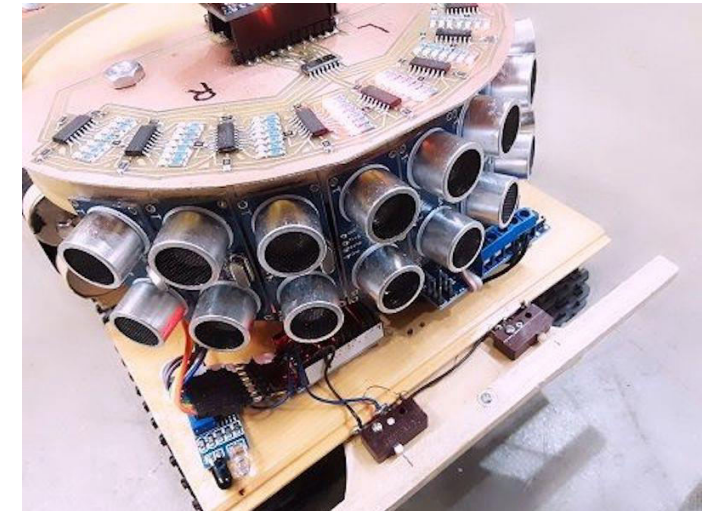
Format (type)	Diagonal (mm)	H (mm)	V (mm)	
1	16.0	12.80	9.60	16 mm/in.
2/3	11.0	8.80	6.60	
1/1.8	8.89	7.11	5.33	
1/2	8.00	6.40	4.80	
1/2.5	7.20	5.76	4.32	18 mm/in.
1/2.7	6.67	5.33	4.00	
1/3	6.00	4.80	3.60	
1/3.2	5.63	4.50	3.38	
1/4	4.50	3.60	2.70	
1/5	3.60	2.88	2.16	
1/6	3.00	2.40	1.80	
For DSLR Format	Diagnal (mm)	H (mm)	V (mm)	Aspect ratio
35 mm	43.27	36.00	24.00	3:2
APS-DX	28.37	23.7	15.6	
APS-C	27.26	22.7	15.1	
APS-H	33.93	28.7	19.1	
Four-thirds	21.63	17.3	13.0	4:3

Resolution of PC Displays

Format	Resolution (pixels)
QCIF	Quarter common intermediate format
CIF	Common intermediate format
QVGA	Quarter video graphics array
VGA	Video graphics array
SVGA	Super video graphics array
XGA	Extended graphics array
SXGA	Super extended graphics array
UXGA	Ultra extended graphics array
QXGA	Quad extended graphics array

Ultrasonic rangefinder

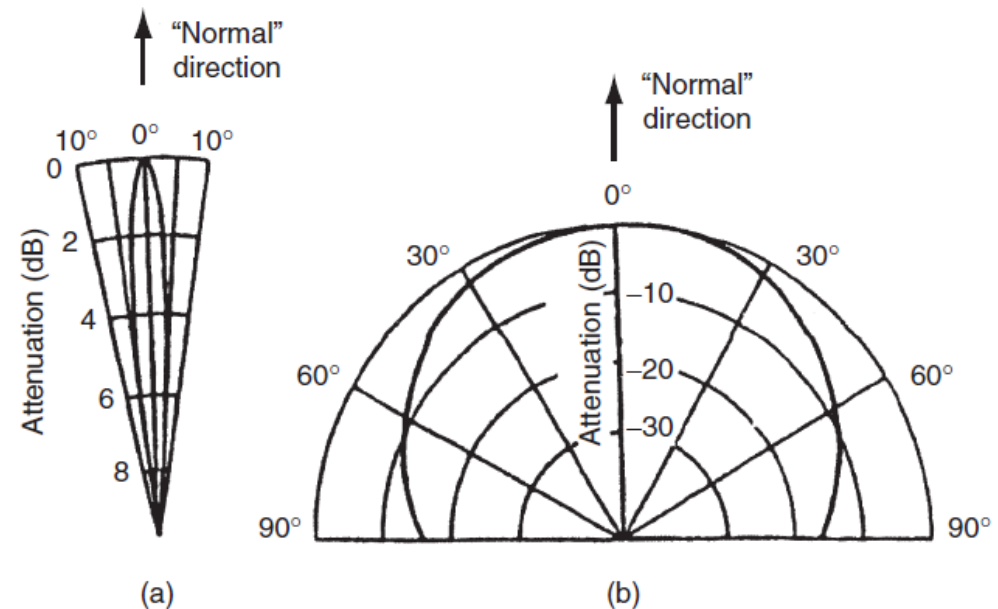
- Ultrasonic devices
 - Measurement of flow rate, liquid level, translational displacements
- Band of frequencies in the range above 20 kHz
- Transmitter and Receiver
- Time-of-flight/ Change in phase/frequency
- Piezoelectric crystal
 - Can operate as transmitter and receiver interchangeably
 - 20 kHz - 15 MHz
 - Quartz, lithium sulphate
 - application of a sinusoidal voltage at a frequency causes sinusoidal variations in the thickness of the material
 - As a result, sound wave are emitted at the chosen frequency



Ultrasonic rangefinder

- Transmission speed
 - varies according to the medium
 - Dependence on temperature, humidity, and air turbulence
 - $V = 331.6 + 0.6 T \text{ m/s}$
- Directionality of ultrasound waves
 - Spherical wave emission of energy
 - Peak energy in particular direction
 - Magnitude of energy emission in any direction proportional to angle made with respect to normal to the surface (direction of travel)
 - attenuation of the transmission magnitude with respect to normal increases
 - 40 kHz : $\pm 50^\circ$, 400 kHz: $\pm 3^\circ$
 - Effect of air currents

Medium	Velocity (m/s)
Air	331.6
Water	1440
Wood (pine)	3320
Iron	5130
Rock (granite)	6000



Ultrasonic rangefinder

- Wavelength and frequency $\lambda = v/f$

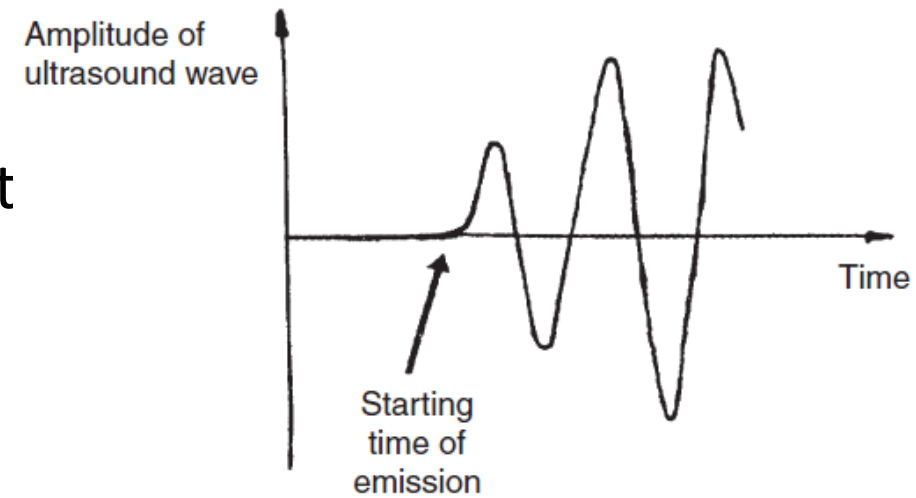
Nominal Frequency (kHz)	23	40	400
Wavelength (in air at 0°C)	14.4	8.3	0.83
Cone angle of transmission (-6 dB limits)	$\pm 80^\circ$	$\pm 50^\circ$	$\pm 3^\circ$

- Directionality also depends on the transmission horn
- Attenuation of Ultrasound Waves: depends on the nominal frequency of the ultrasound and the adsorption characteristics of the medium.
Level of humidity, dust

$$\frac{X_d}{X_0} = \frac{\sqrt{e^{-\alpha d}}}{fd}$$

Ultrasonic rangefinder

- Ultrasonic range sensor
 - time between transmission of a burst of ultrasonic energy from an ultrasonic transmitter and receipt of that energy by an ultrasonic receiver
- Object distance d $d = vt$
- Compensation for variability of v with temperature
- Degree of directionality is of not much important if 'normal lines to Tx and Rx faces are coincident
- Low-frequency elements have to be used for the measurement of large ranges
- Compromise between measurement resolution and range
- Measurement accuracy



Ultrasonic rangefinder

- Effect of noise
 - Outputs are usually of low amplitude
 - prone to contamination by electromagnetic noise
 - Locating amplifier as close as possible to the receiver
- serious form of noise: background ultrasound
- sound-absorbing material: minimizes interference
- ultrasonic energy emission at angles other than the direction
 - transmission-time counter

Ultrasonic rangefinder

- Doppler Shift in Ultrasound Transmission

$$f' = \frac{ft + rt/\lambda}{t} = f + r/\lambda = f + \frac{rf}{v} = \frac{f(r + v)}{v}$$

$$\Delta f = f' - f = \frac{f(v + r)}{v} - f = \frac{fr}{v}$$

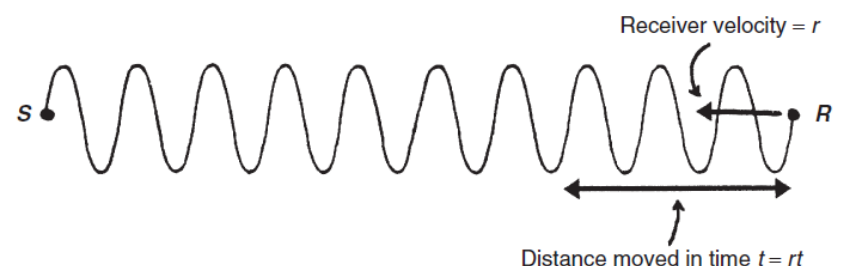
$$f' = \frac{f(v - r)}{v}$$

$$\Delta f = -\frac{fr}{v}$$



Wave frequency = f ; Velocity of wave = v

(a)



Receiver velocity = r
Distance moved in time $t = rt$

(b)

RA 505 Robot Sensing and Vision

Lecture 29

Dr. Rishikesh Kulkarni
Department of Electronics and Electrical Engineering
IIT Guwahati

Ultrasonic rangefinder

- Doppler Shift in Ultrasound Transmission

$$f' = \frac{ft + rt/\lambda}{t} = f + r/\lambda = f + \frac{rf}{v} = \frac{f(r + v)}{v}$$

$$\Delta f = f' - f = \frac{f(v + r)}{v} - f = \frac{fr}{v}$$

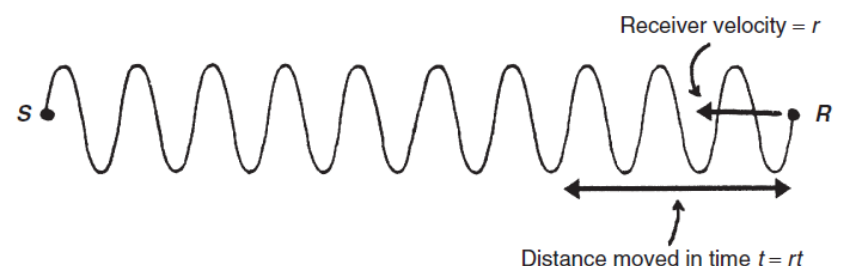
$$f' = \frac{f(v - r)}{v}$$

$$\Delta f = -\frac{fr}{v}$$



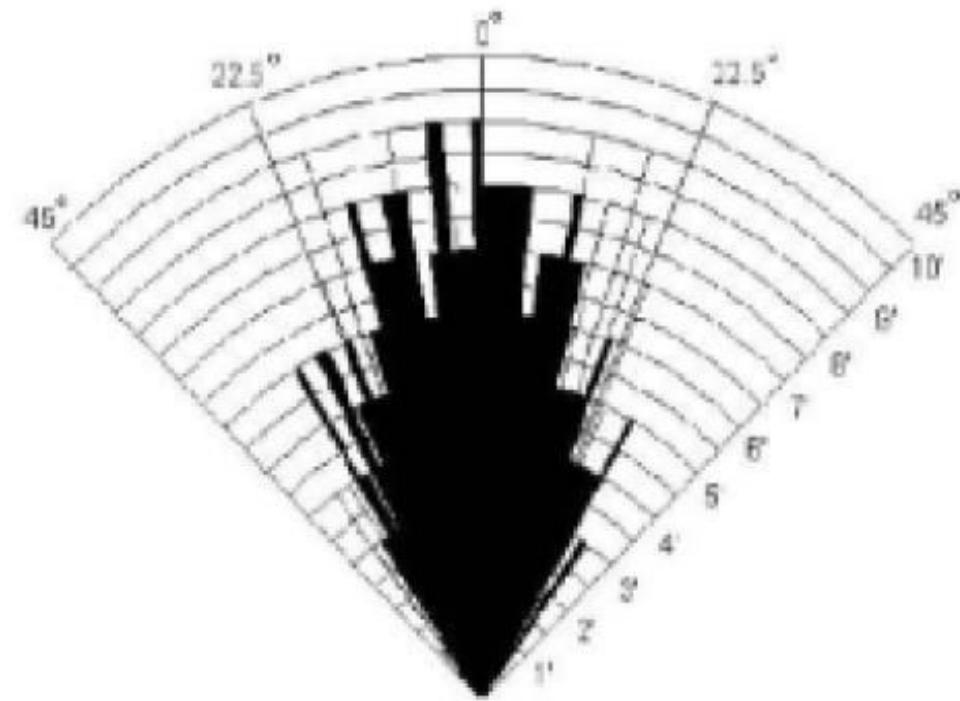
Wave frequency = f ; Velocity of wave = v

(a)

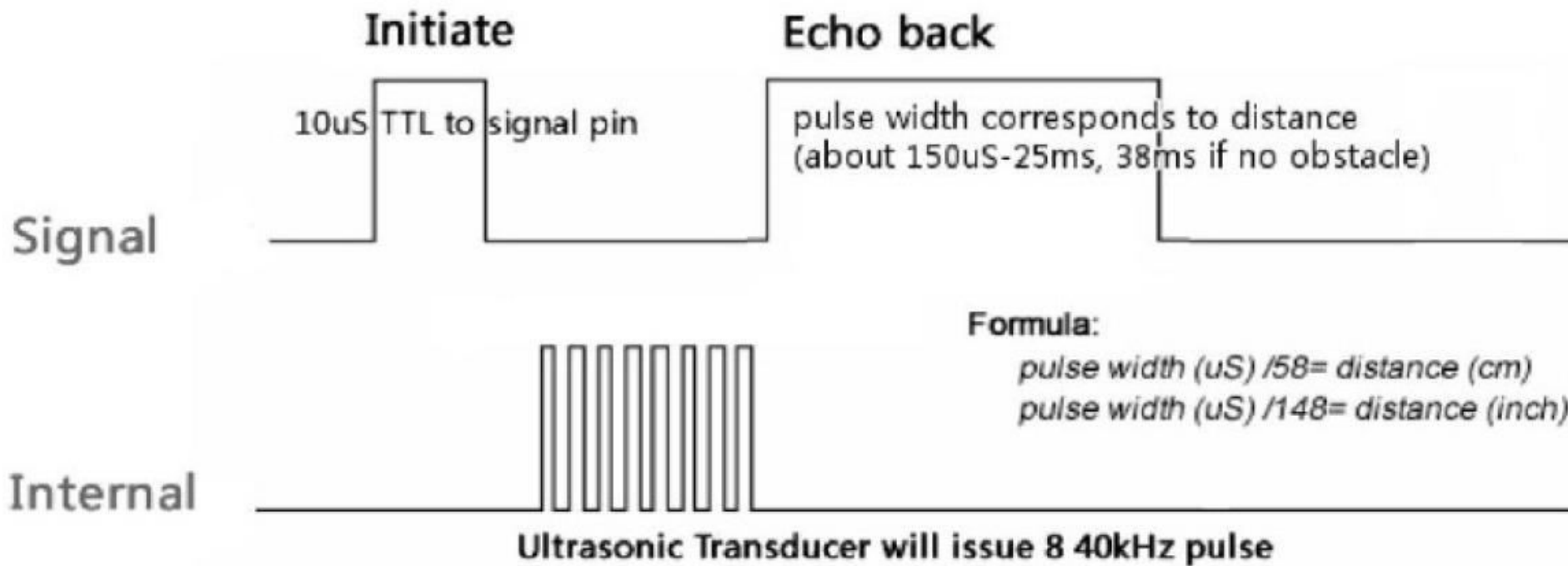


Distance moved in time $t = rt$

(b)



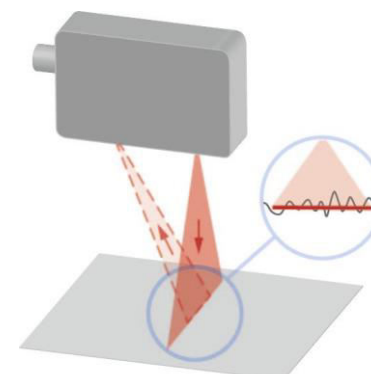
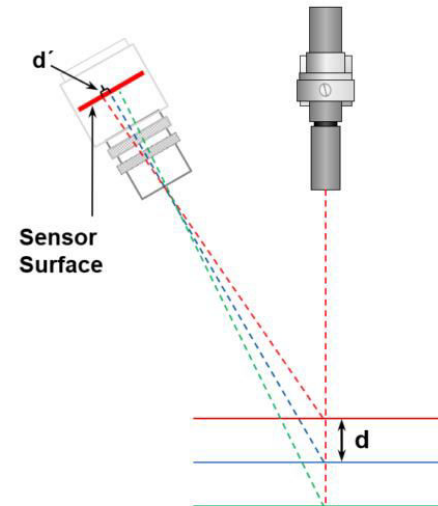
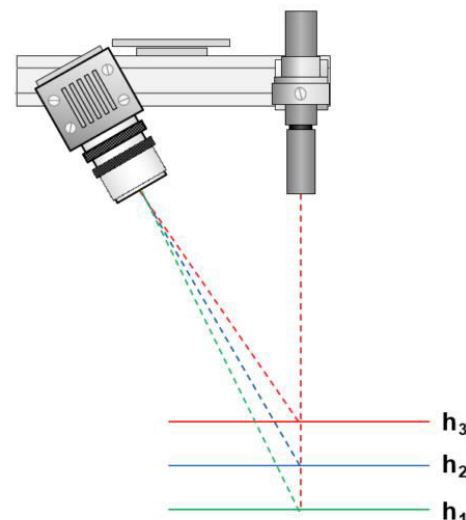
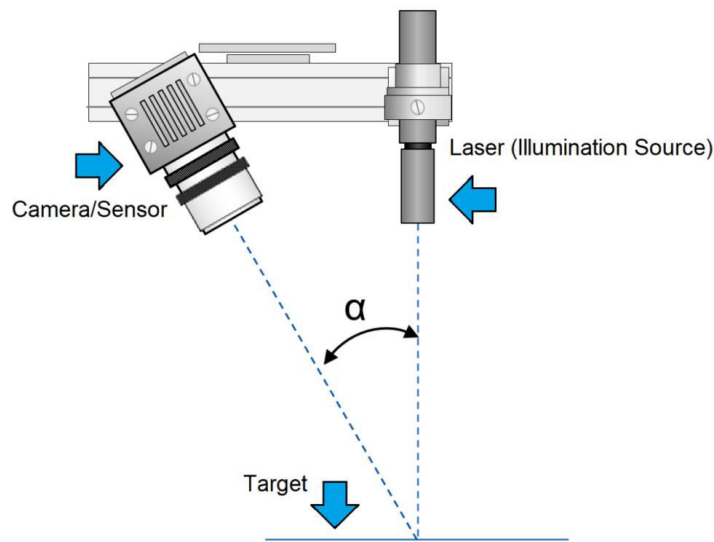
*Practical test of performance,
Best in 30 degree angle*



- Distance between sensors
- Actual distance measured
- Dead zone
- Detectable range

Optical rangefinder

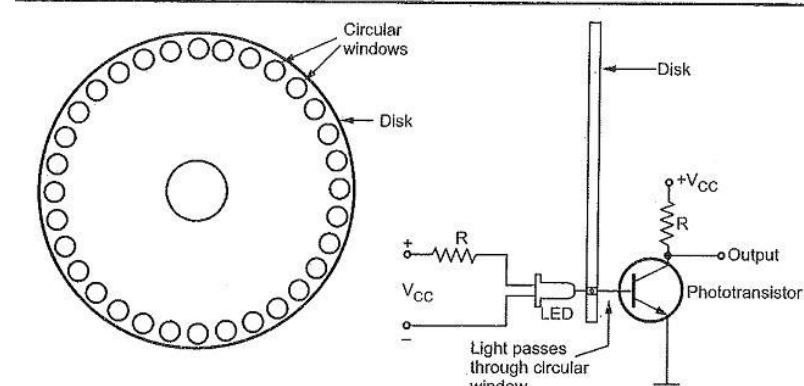
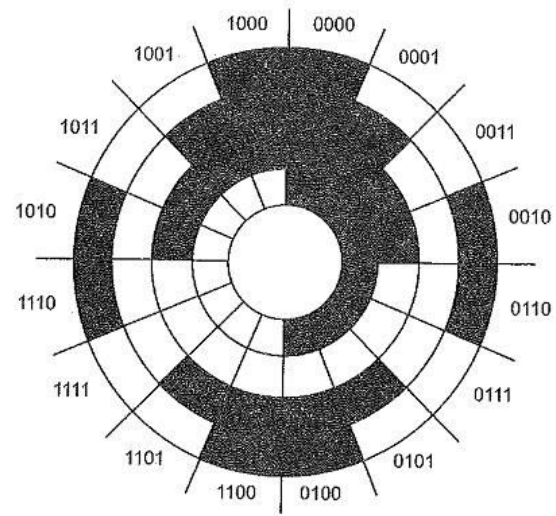
Laser triangulation



- 1D, 2 ½-D and 3-D Sensors
- IR sensors

Position measurement

- Optical encoder
 - Measurement of rotational angle



- Reference grating and direction of rotation

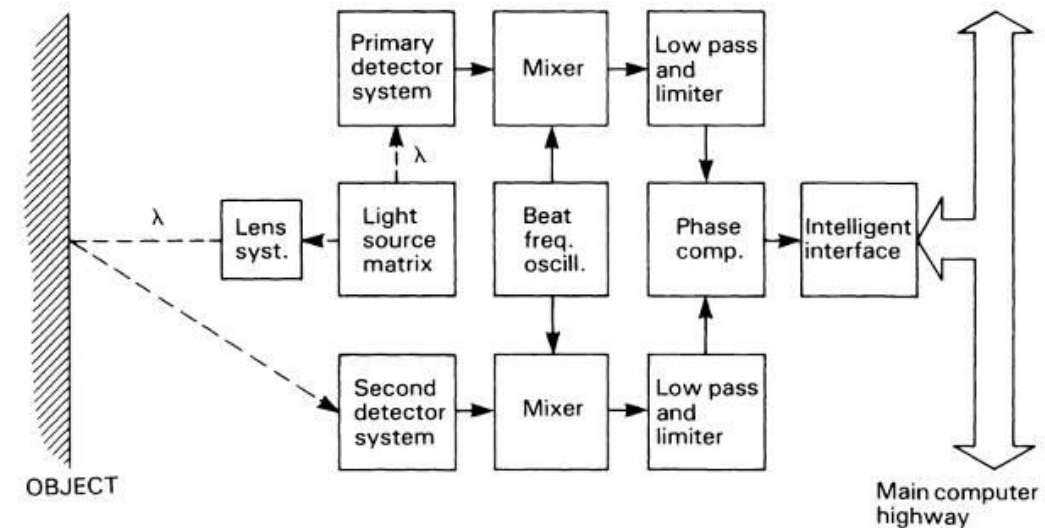
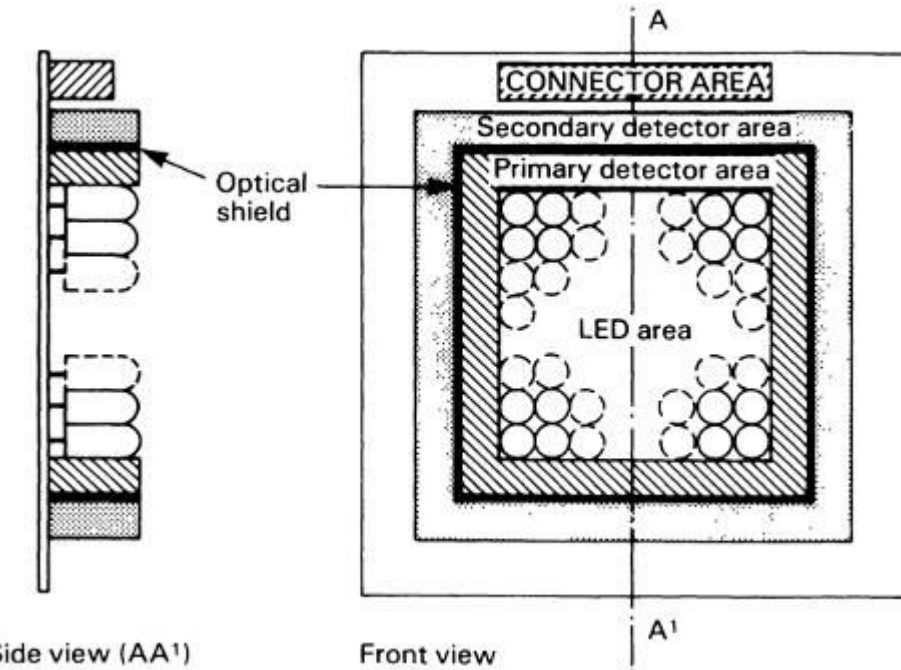
RA 505 Robot Sensing and Vision

Lecture 31

Dr. Rishikesh Kulkarni
Department of Electronics and Electrical Engineering
IIT Guwahati

LED array range-finder

- No moving parts
- Cheap light sources
- Lower optical launch power and lower x-y resolution
- suitable for eye-in-hand robot vision applications
- Electronic multiplexing of LED driver
- Principle
- Obstacle avoidance and pick-and-place operations



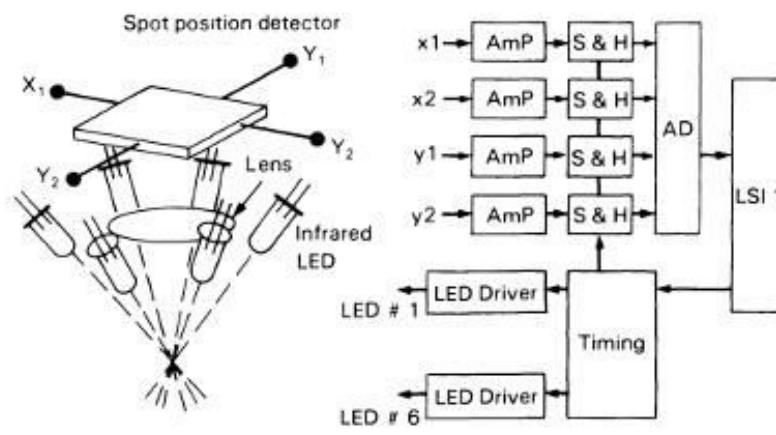
LED array range-finder

- Circular LED-array
- Simplicity of the operating principle
- Fast speed (~ 1000 range measurements per second)
- Precision (0.07 mm)
- Large size
- Smaller range of operation ($\sim 4\text{-}5$ cm)

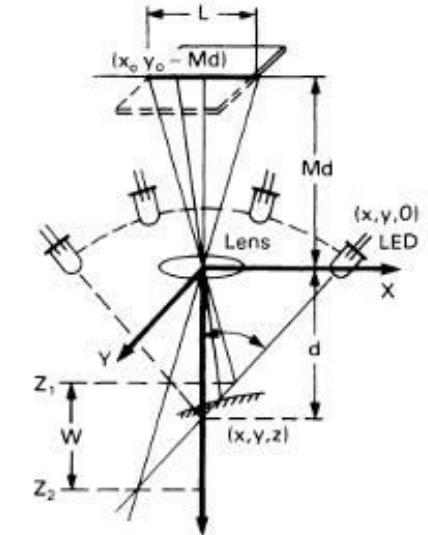
$$X_c = \frac{I_{x_1} - I_{x_2}}{I_{x_1} + I_{x_2}} = \frac{2rx_c}{rL2R_0} \quad (3)$$

$$Y_c = \frac{I_{y_1} - I_{y_2}}{I_{y_1} + I_{y_2}} = \frac{2ry_c}{rL2R_0} \quad (4)$$

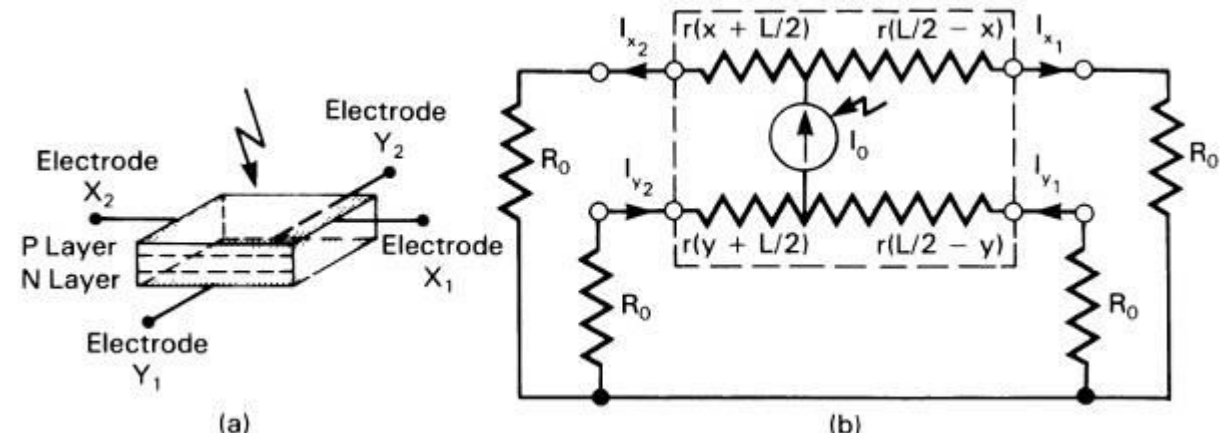
$$Z = \frac{d}{1 - \left(\frac{X_c}{dM \tan \theta} \right)} \quad (5)$$



(a): Configuration and block diagram

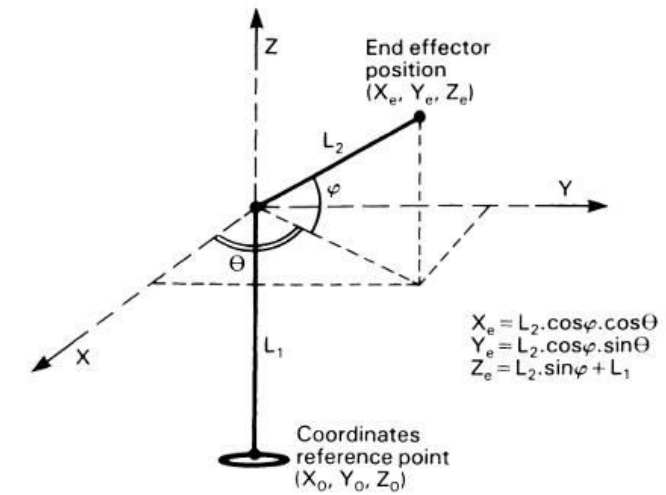
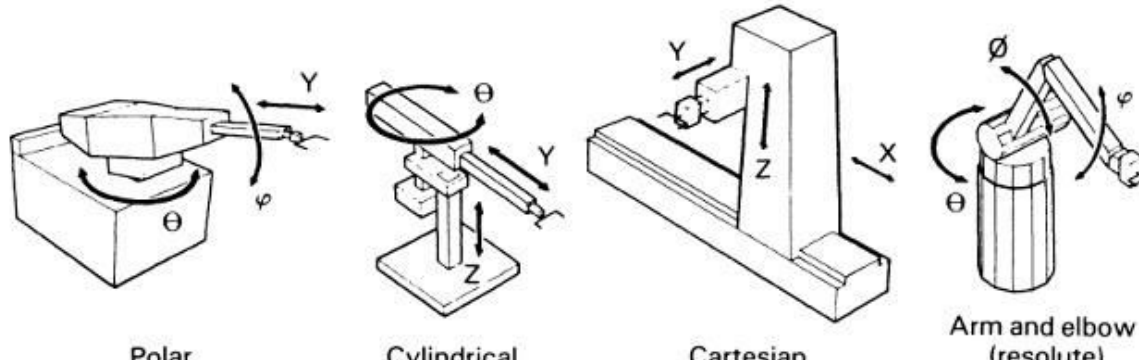


(b): Geometry of distance measurement



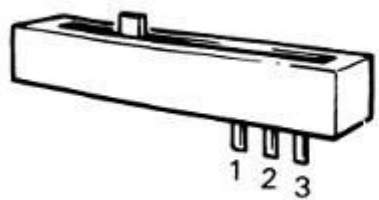
Position sensors

- In robot structure, position of each joint is required to calculate the position of the end effector
 - Enables successful completion of programmed task
 - robot coordinate systems
 - Internal position transducers (proprioceptors)

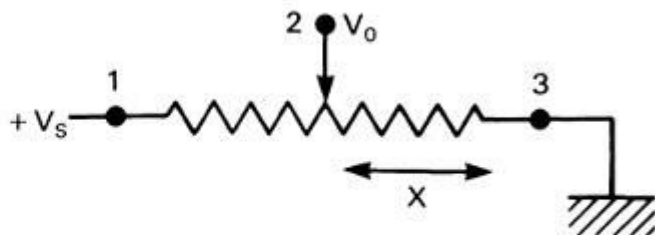


Position sensors

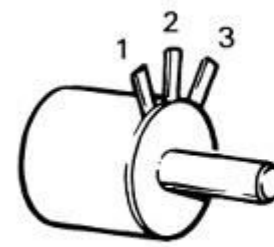
Type	Class	Device description
Absolute	Resistive	Potentiometer
	Optical	Coded optical encoder disks
Incremental	Optical	Slotted optical encoder disks



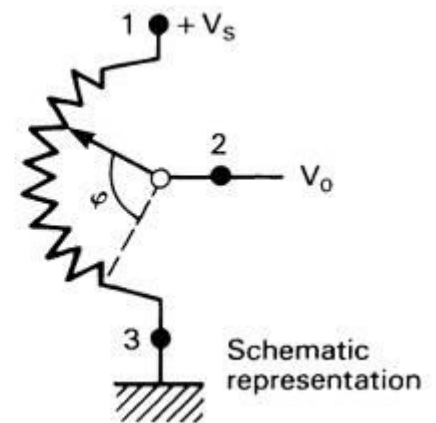
Physical construction



Schematic representation



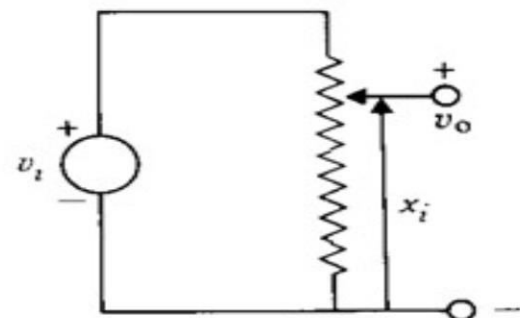
Physical construction



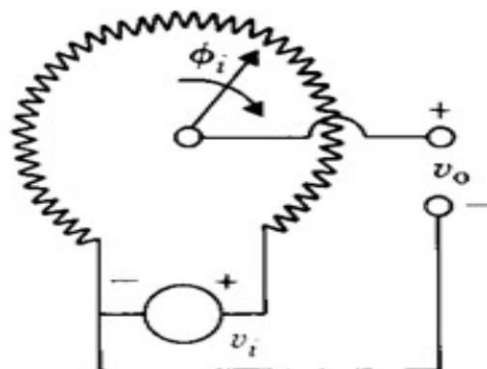
Schematic representation

Position measurement

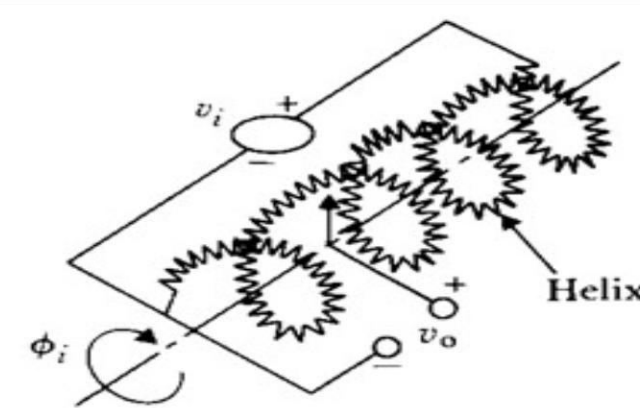
- Resistive potentiometers
 - Resistive element with movable contact
 - contact motion can be translation, rotation or combination of the two
 - The resistive element is excited with either AC or DC voltage
 - resistive elements come with different types such as wire-wound, conductive plastic, deposited film or cermet (ceramic + metal)



(a) Translational



(b) Single-turn



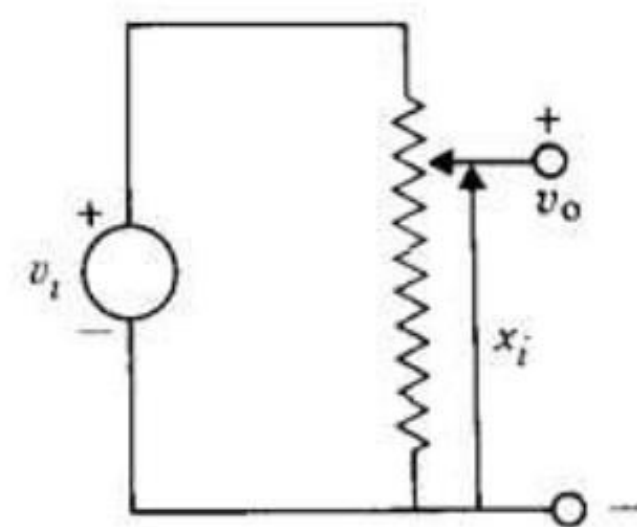
(c) Multi-turn

Position measurement

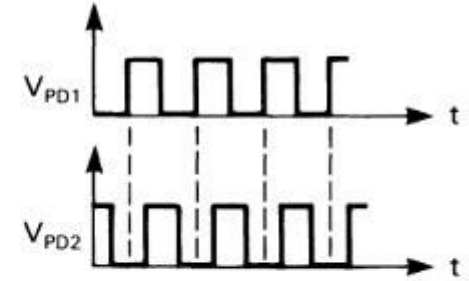
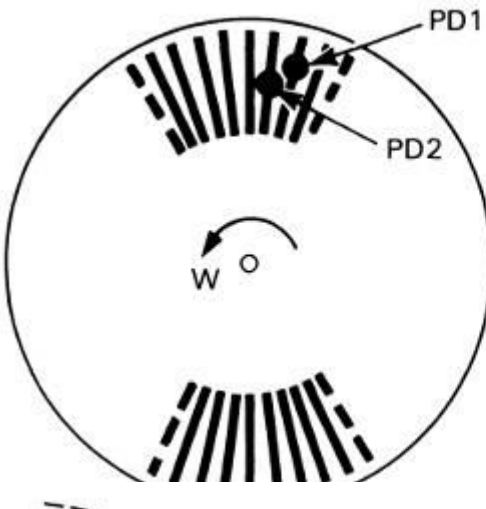
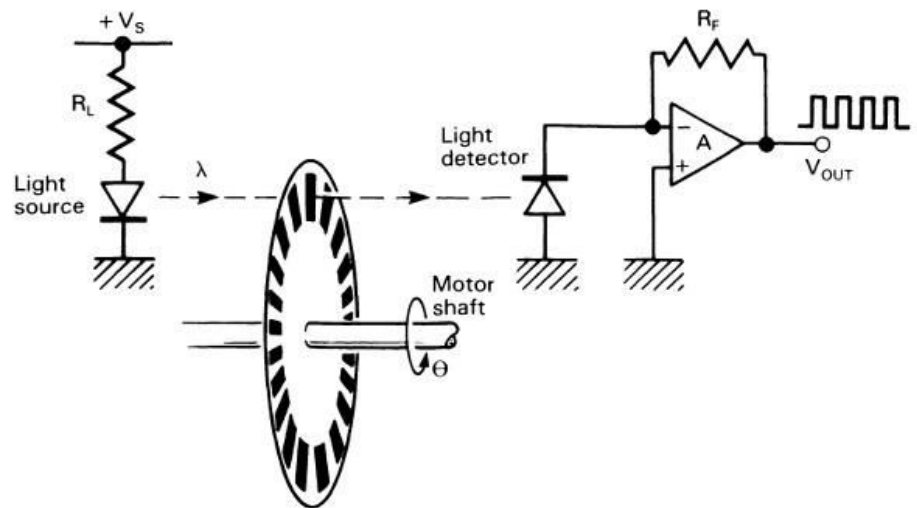
- Resistive potentiometers

$$\frac{v_0}{v_i} = \frac{1}{1 + (1 - x_i/x_t)(R_p/R_m + x_t/x_i)}$$

- Trade-off between linearity and sensitivity
- Resolution Vs Range: continuous strip of resistive element/ wire-wound
- Low cost, small size
- Educational and light industrial robots

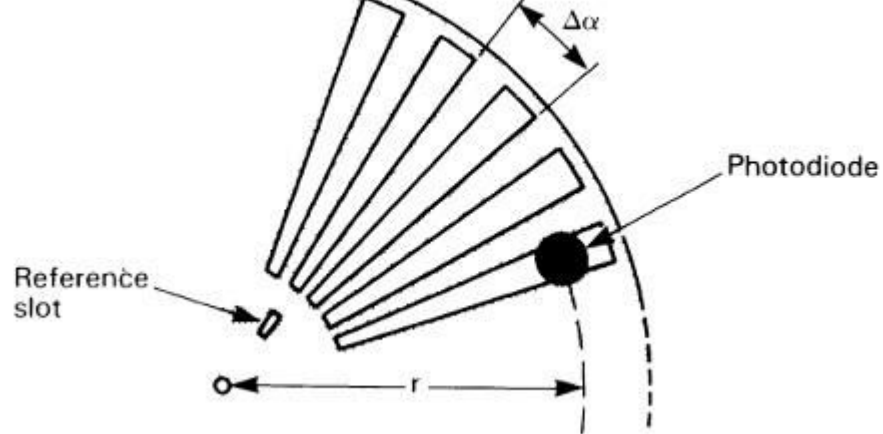


Incremental optical encoder

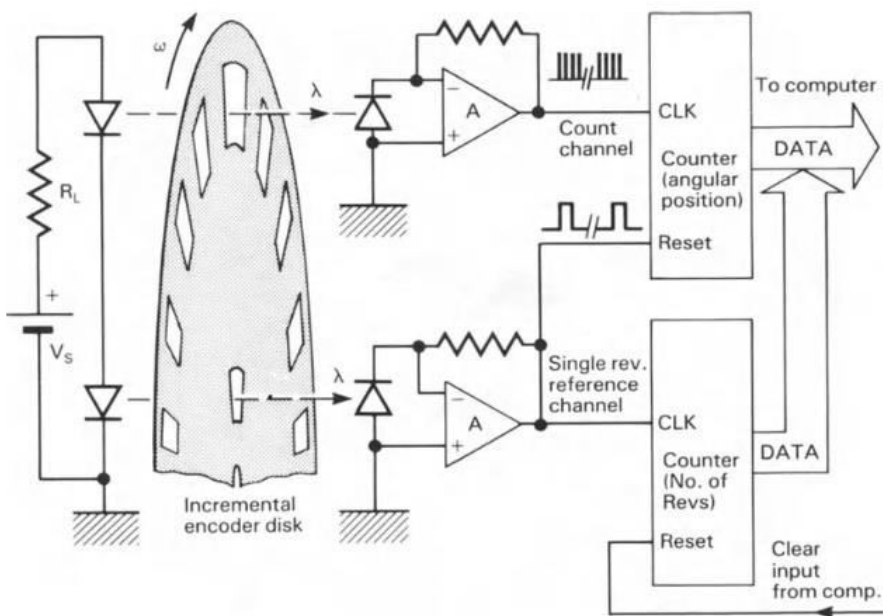
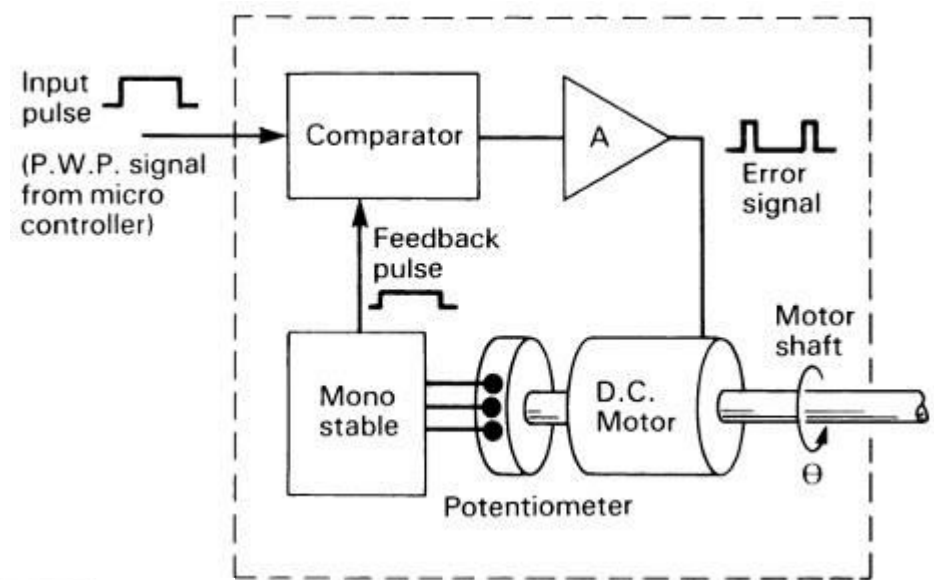
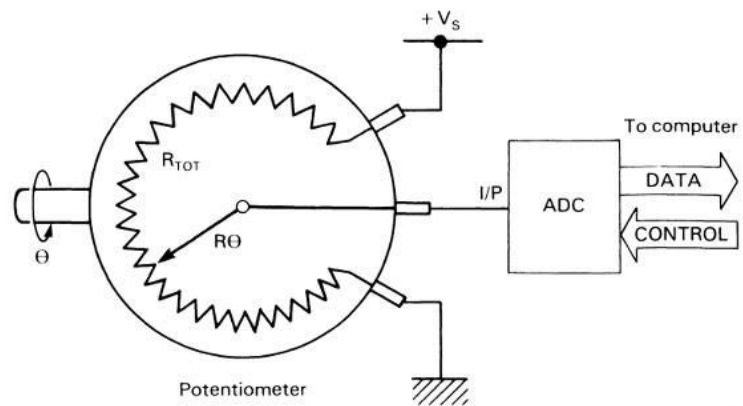


$$\Delta\alpha = \frac{360}{n}$$

$$W_p = r \sin\left(\frac{\Delta\alpha}{2}\right) = r \sin\left(\frac{360}{n}\right)$$



Position sensor interfacing



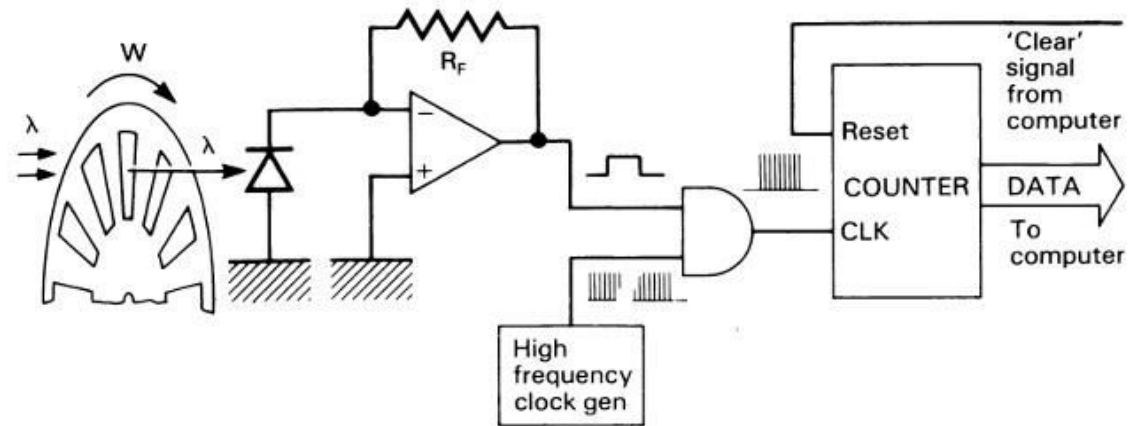
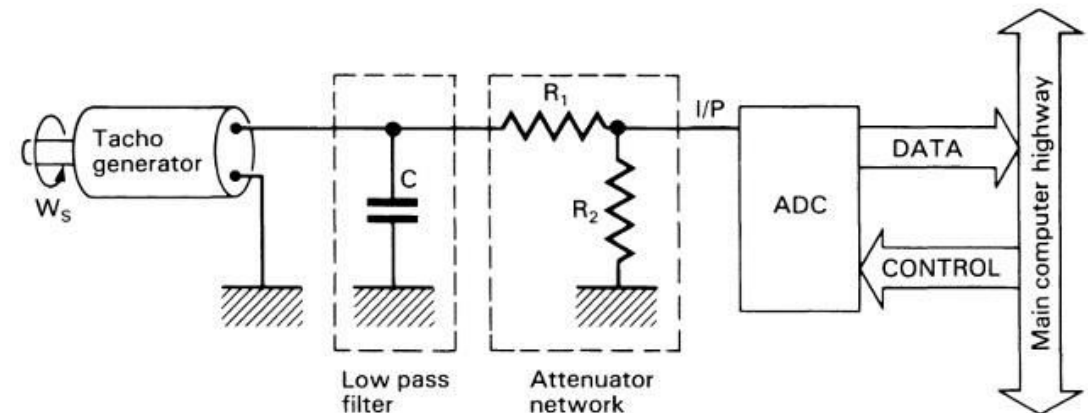
Velocity sensors

Direct

Transducers which measure the shaft velocity directly. These are analogue devices whose variable output is proportional to the shaft rotational velocity. Examples are d.c. and a.c. tachogenerators.

Derived

Transducers which are used mainly for measuring shaft position but which, by external electronic processing, can also provide a shaft velocity measurement. These are digital devices whose output is a pulse train proportional to the shaft rotation, which is then processed electronically using digital counters, to produce a signal proportional to the shaft position and/or angular velocity.



RA 505 Robot Sensing and Vision

Lecture 32

Dr. Rishikesh Kulkarni
Department of Electronics and Electrical Engineering
IIT Guwahati

Velocity sensors

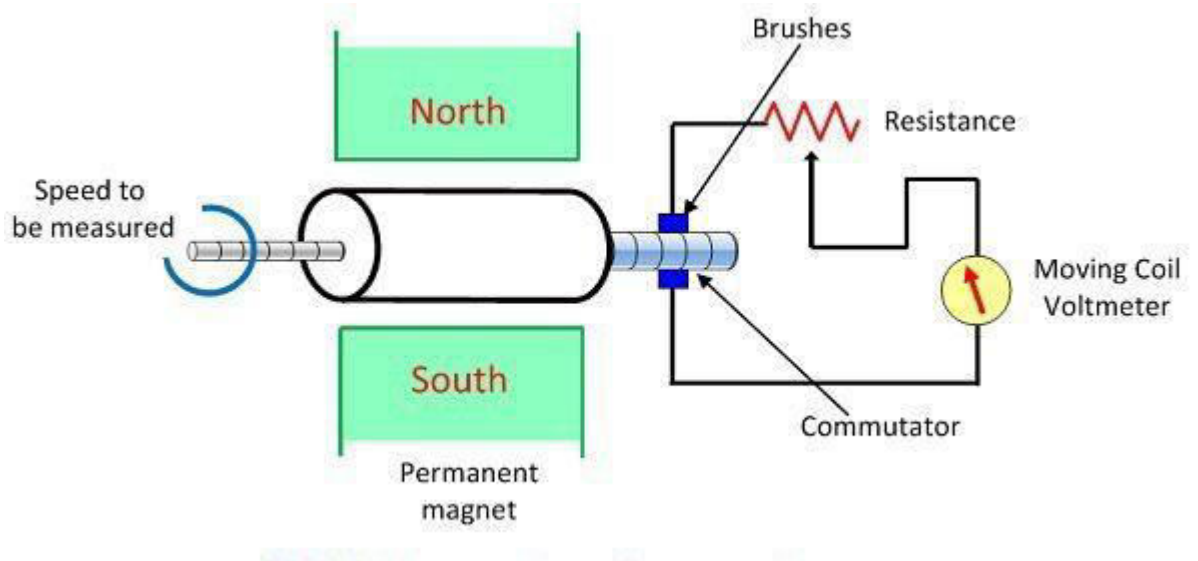
- Optical, capacitive or magnetic
- potentiometer as a velocity transducer
 - require interfacing to a differentiator circuit
 - difficult to stabilize
 - use is not recommended
- Tachogenerator
 - Dual of electric motor
 - DC type (dynamo)
 - AC type (alternator)
 - Need no power supply
 - Analog output, requires ADC

Direct

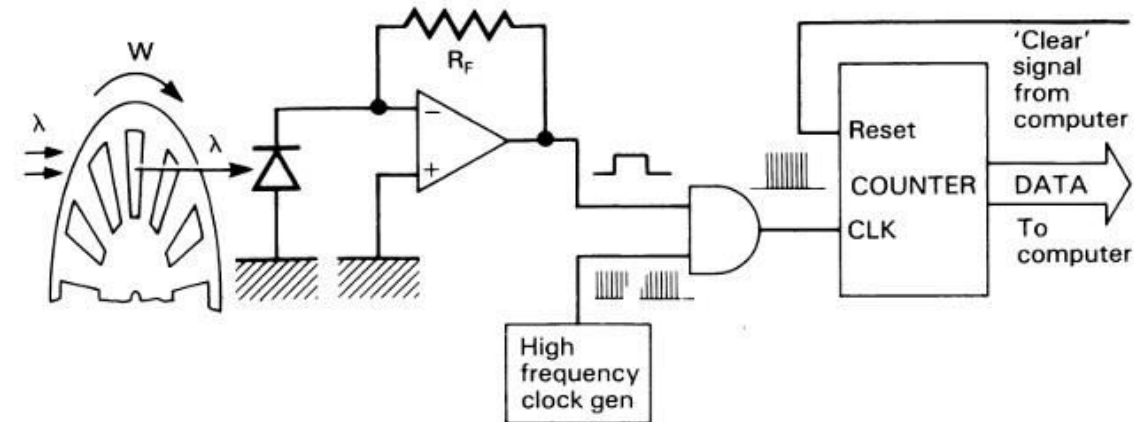
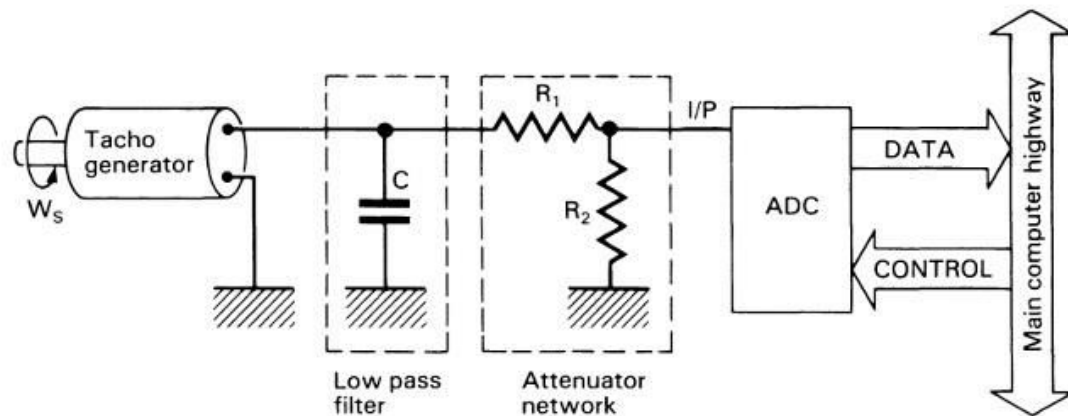
Transducers which measure the shaft velocity directly. These are analogue devices whose variable output is proportional to the shaft rotational velocity. Examples are d.c. and a.c. tachogenerators.

Derived

Transducers which are used mainly for measuring shaft position but which, by external electronic processing, can also provide a shaft velocity measurement. These are digital devices whose output is a pulse train proportional to the shaft rotation, which is then processed electronically using digital counters, to produce a signal proportional to the shaft position and/or angular velocity.

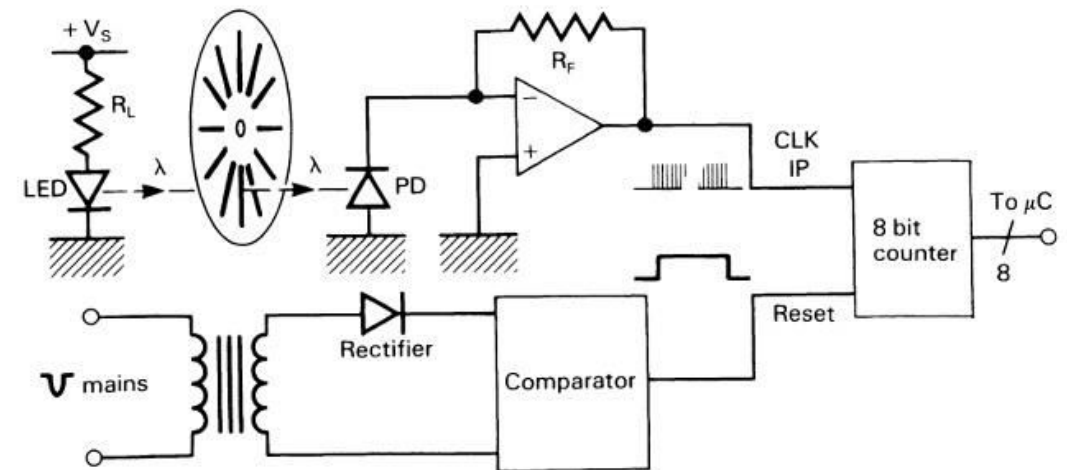


Interfacing of Velocity sensors



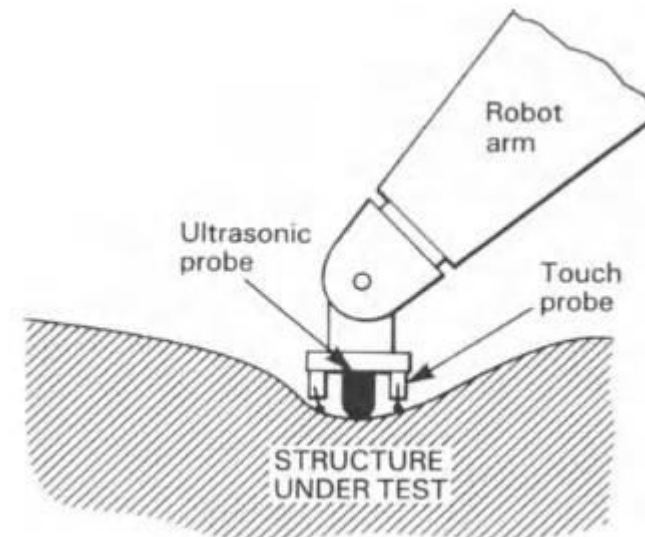
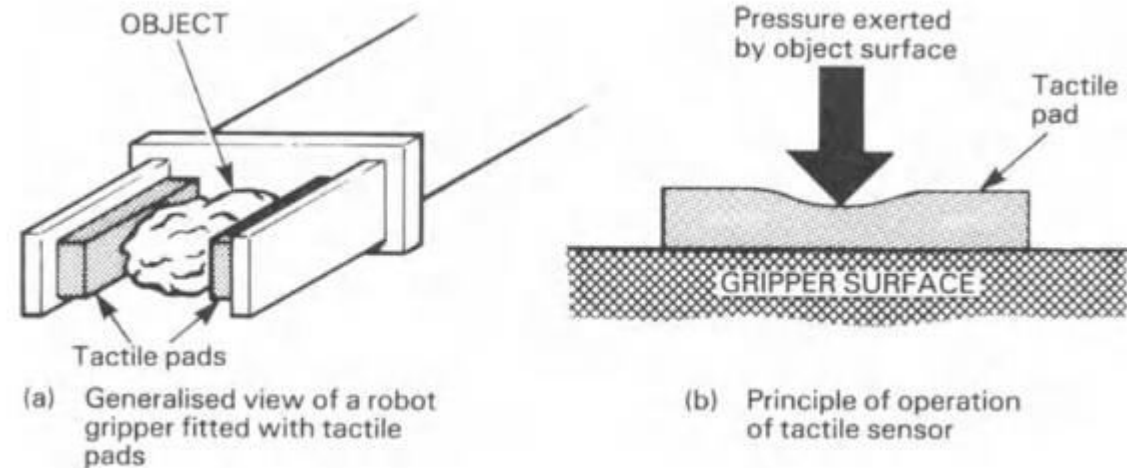
Tachogenerator

- Optical Encoder
- Low voltage pulse train
- frequency is proportional to angular speed
- Counting number of lines detected by photo-diode in unit time
- Time taken by the photo-diode to detect a single line



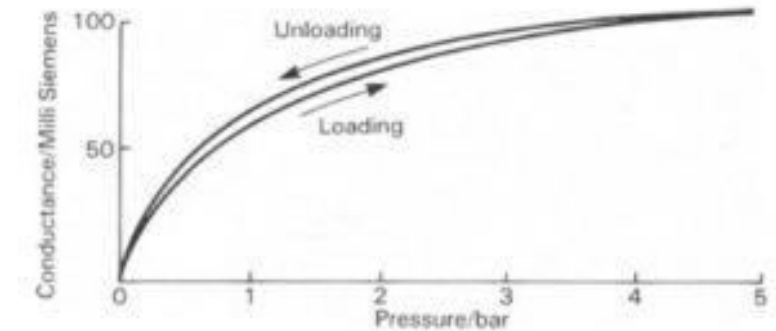
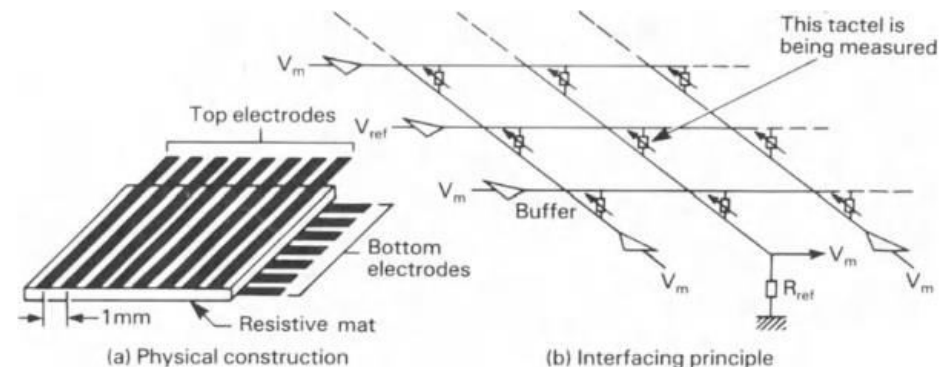
Tactile sensors

- Tactile sensing allows continuous measurement of the pressure distribution across an array of so called 'tactels'
- detection of slippage
- Inspection



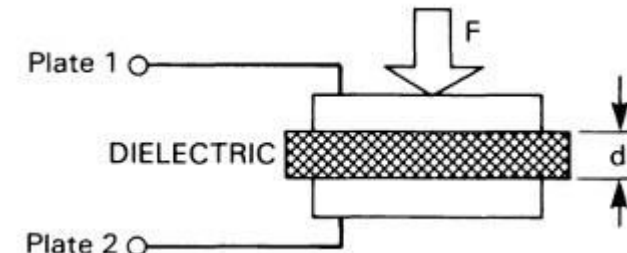
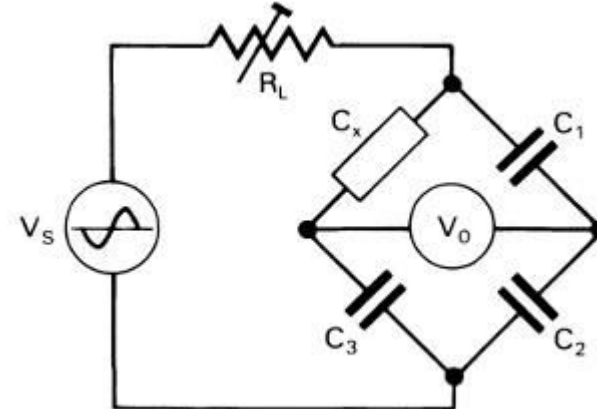
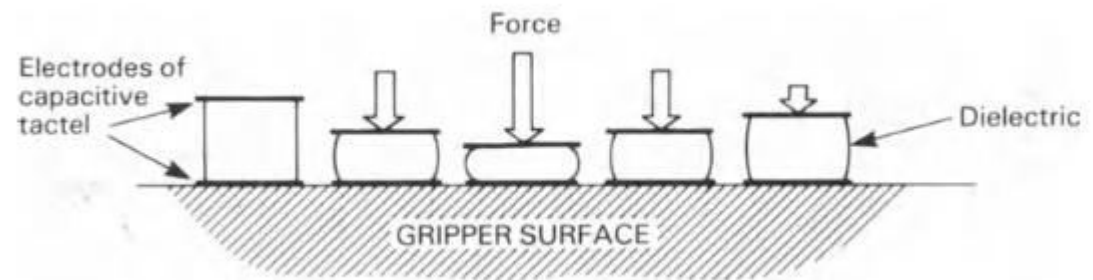
Resistive Tactile sensors

- Most popular
- higher sensitivity and x-y resolution
- carbon fibres, conductive rubbers, media impregnated with conductive dopants (lower hysteresis and larger dynamic range)
- Change in resistance in function of pressure
- Capacitive effect



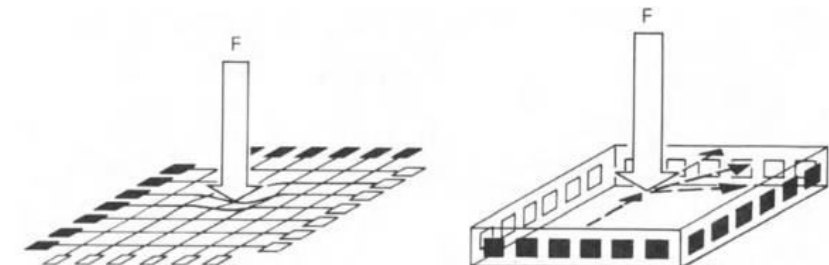
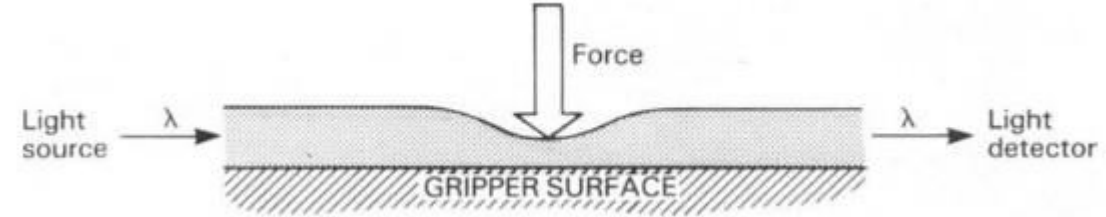
Capacitive Tactile Sensors

- potential for measuring higher pressures
- inherently less malleable
- more mechanically robust
- bigger tactel size
- lower x-y tactel resolution

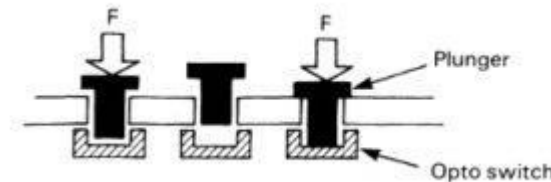


Optical Tactile Sensors

- changing the light absorption characteristics of the transparent medium under the effect of an applied force
- plastics and glass fibres
- used within a robot multisensory feedback system



(a) Optical tactile sensor based on X-Y array of glass fibres.
(b) Optical tactile sensor based on linear arrays of light sources and detectors around the sides of a plastic layer.
(note: ■ represents a light source and □ represents a detector)

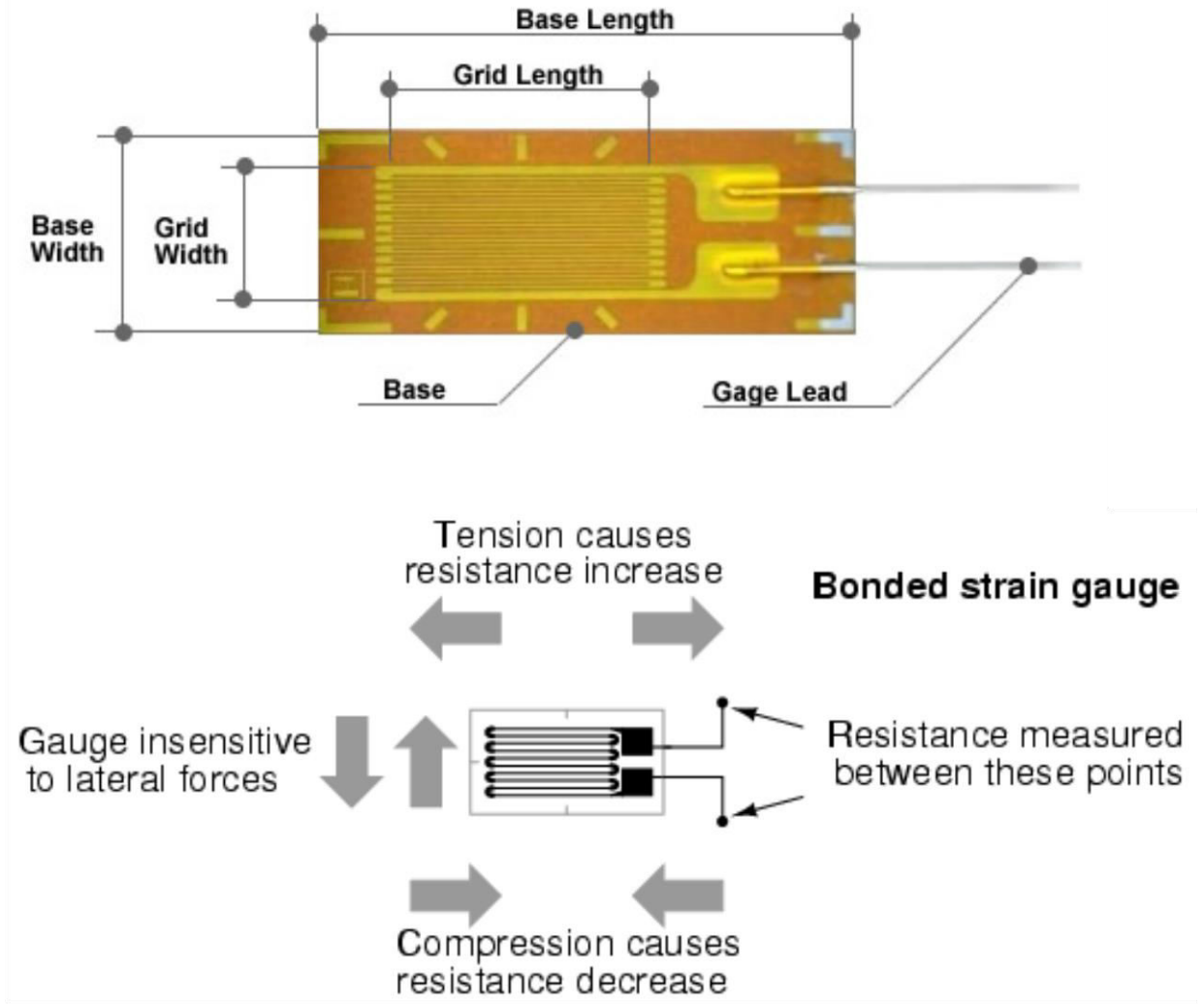


Resistance Strain Gauge

- Highly popular passive type transducers
- stress (force/unit area) and strain (elongation or compression/unit length) is developed on a object due to applied pressure
- strain is used as an index of pressure
- If a metal is compressed or stretched, its resistance changes on account of changes in its dimensions, i.e., length and cross-sectional area
- Types
 - Wire strain gauges
 - Foil strain gauges
 - Semiconductor strain gauges

Resistance Strain Gauge

- Wire strain gauges
 - unbonded resistance wire strain gauges
 - Bonded resistance wire strain gauges.
 - Fine wire: about 25 μm or less
 - Carrier: thin sheet of paper.
 - the carrier mounting of wire structure and carrier adhesion on the object surface plays a crucial role in strain measurement accuracy



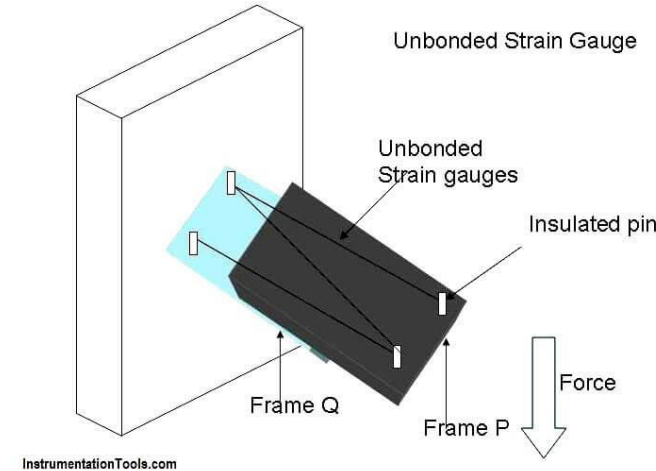
Resistance Strain Gauge

- Resistance of a conductor $R = \frac{\rho L}{A}$
- change in resistance due to the change in dimension and change is fundamental property of the material (*piezoresistance*)
- Strain $\varepsilon = dL/L$
- Poisson ratio: $\nu = -\frac{\delta r/r}{dL/L}$

$$\text{Gauge factor} \triangleq \frac{dR/R}{dL/L} = 1 + 2\nu + \frac{d\rho/\rho}{dL/L}$$

Resistance Strain Gauge

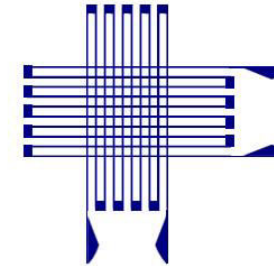
- Unbonded metal-wire gage
- Bonded metal-wire gage
- Bonded metal-foil gage
- Vacuum-deposited thin-metal-film gage
- Sputter-deposited thin-metal-film gage
- Bonded semiconductor gage
- Diffused semiconductor gage



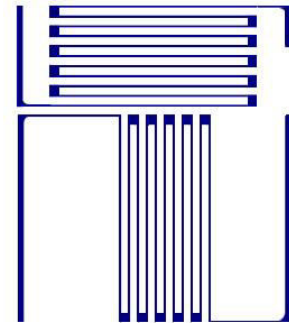
Resistance Strain Gauge

- Bonded metal foil strain gauges

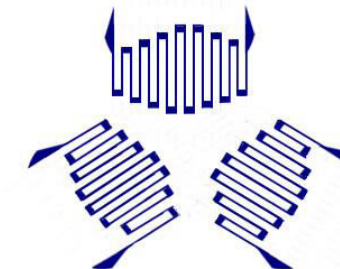
- Copper-Nickel, Nickel-Iron alloys;
- Thin metal grid mounted on flexible or brittle carrier;
- measurement of average strain over an area;
- Types of gauges are: Grid, Rosette, Torque and Helical.
- The area is comparatively more than the wire strain
- The resistive film thickness is typically 0.2mm thick.
- $120\ \Omega$, $350\ \Omega$, $1000\ \Omega$



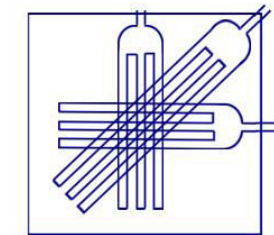
Two-Element, 90 Degree Planar (Shear)
Rosette Strain Gauge



Two-Element 90 Degree Planar
Rosette Strain Gauge

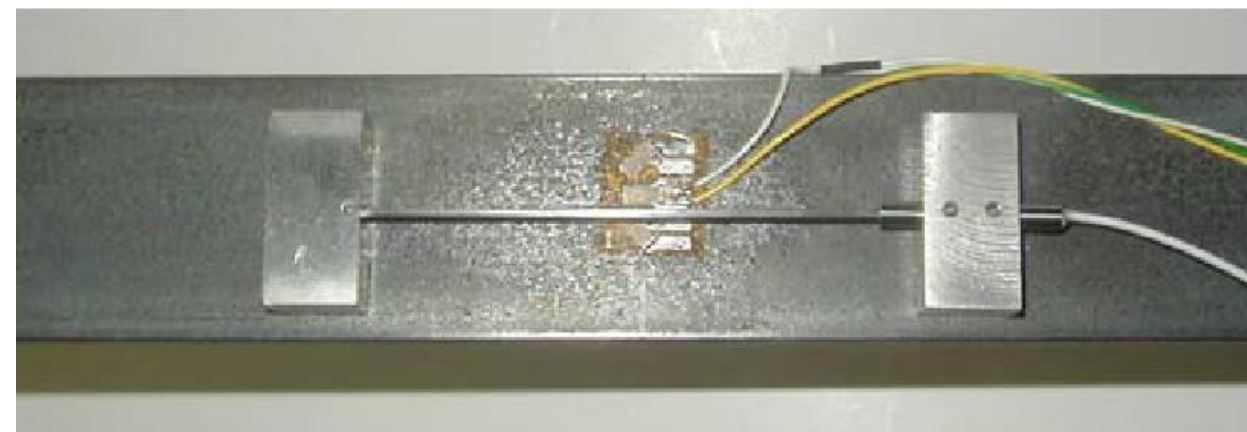


Three Element, 60 Degree Delta
Rosette Strain Gauge



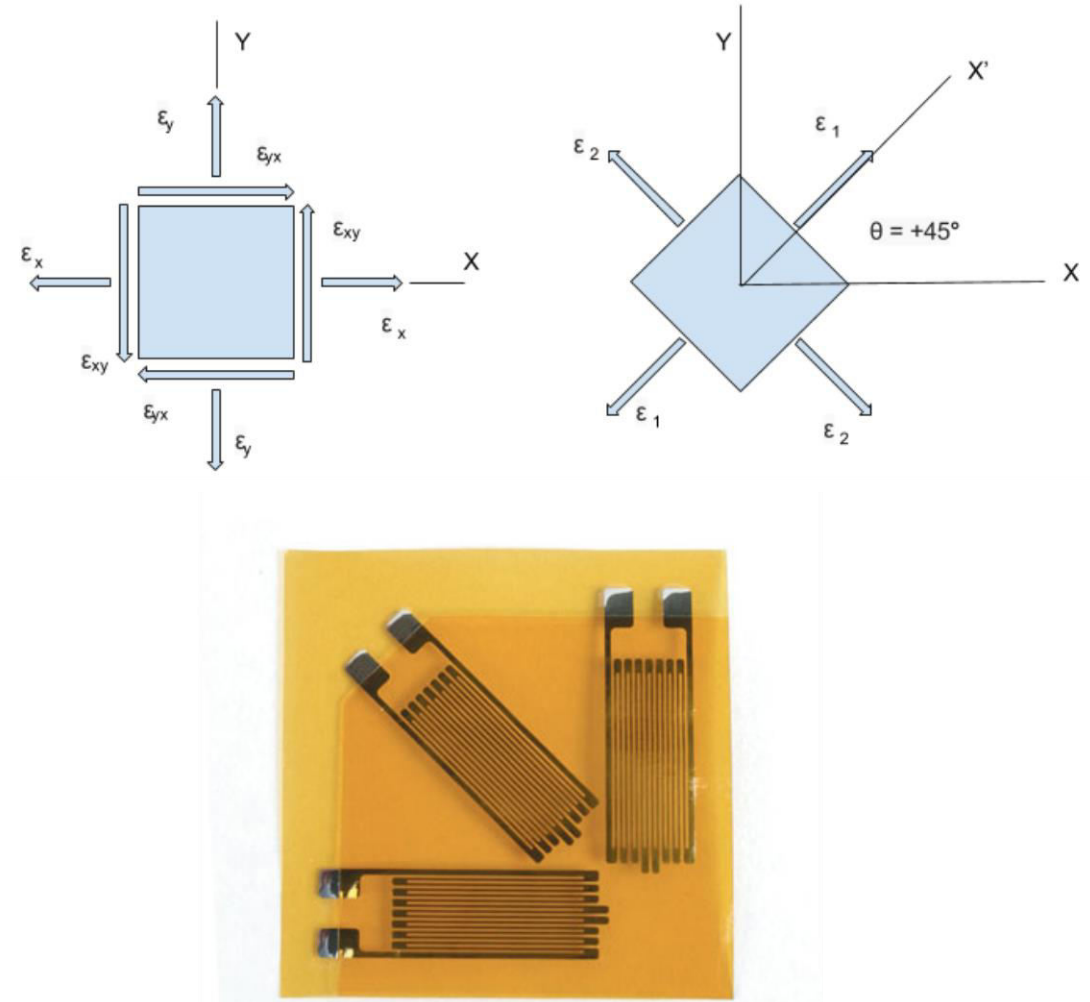
Three Element, 45 Degree Planar
Rectangular Rosette Strain Gauge

www.InstrumentationToday.com

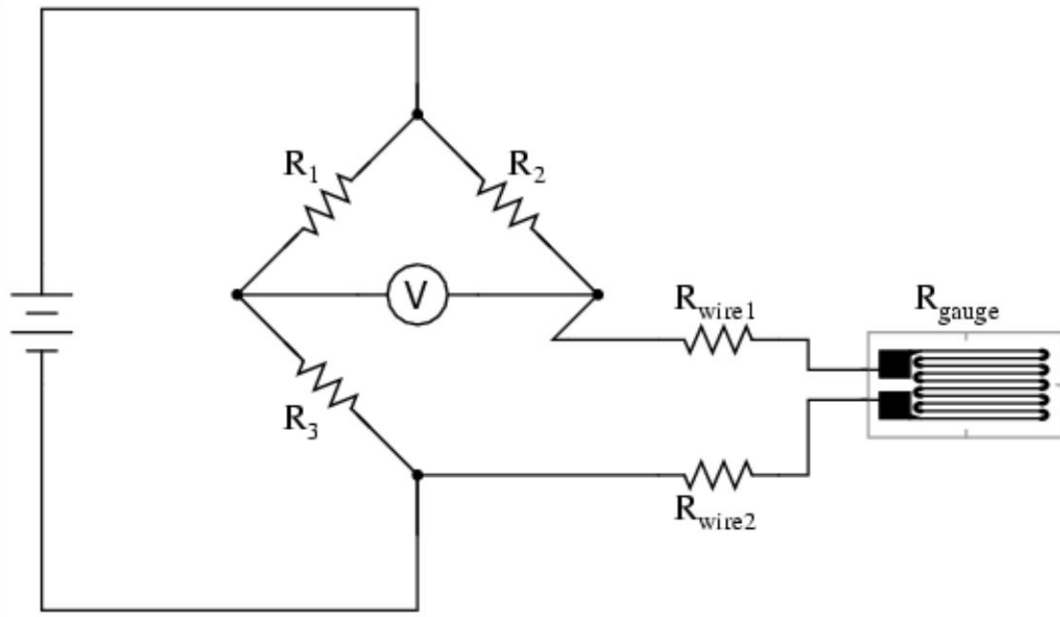


Resistance Strain Gauge

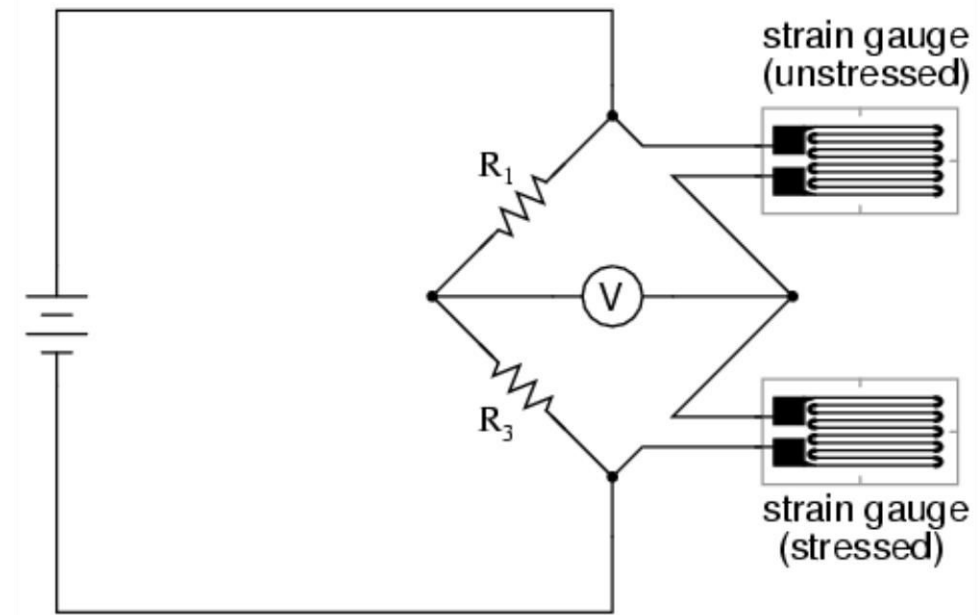
- Rosette are nothing but three strain gauges overlapping at a same point manufactured on the same carrier material.
- Rosettes are used for the measurement of force, velocity, pressure and displacement in applications such as aircraft and missile production, mechanical engineering, railroad, car manufacturing and other industries.



Resistance Strain Gauge

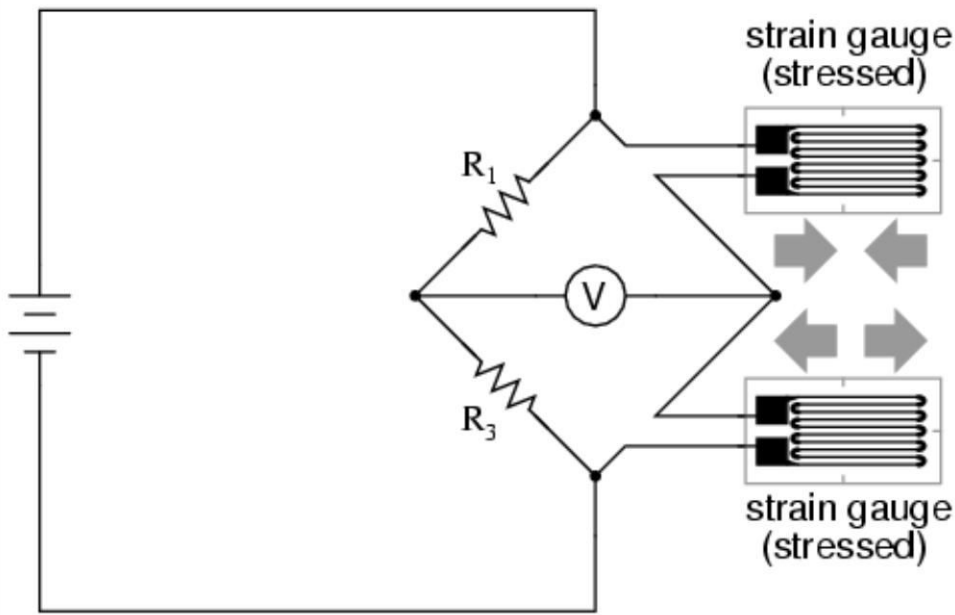


*Quarter-bridge strain gauge circuit
with temperature compensation*

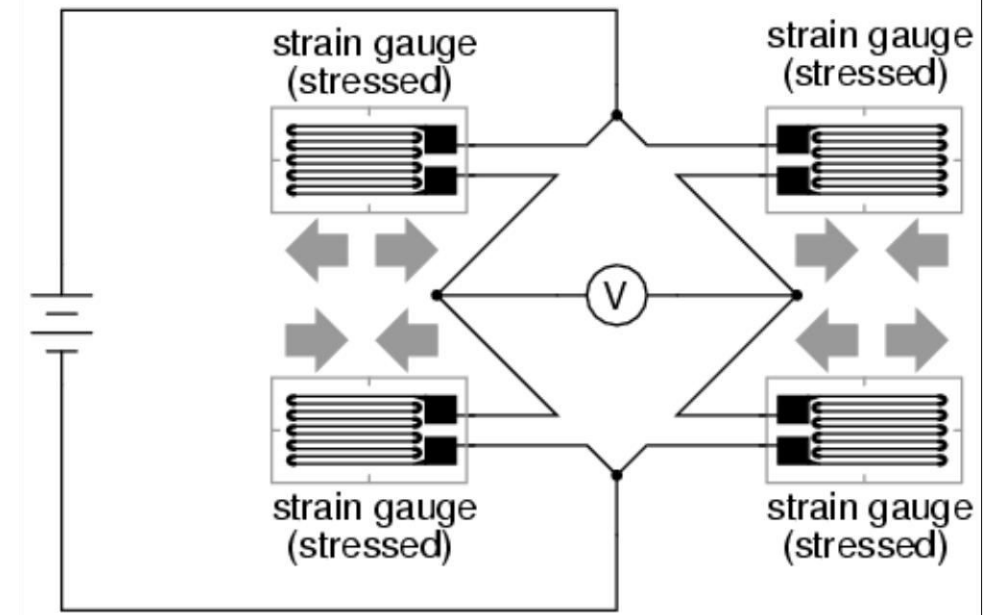


Resistance Strain Gauge

Half-bridge strain gauge circuit



Full-bridge strain gauge circuit



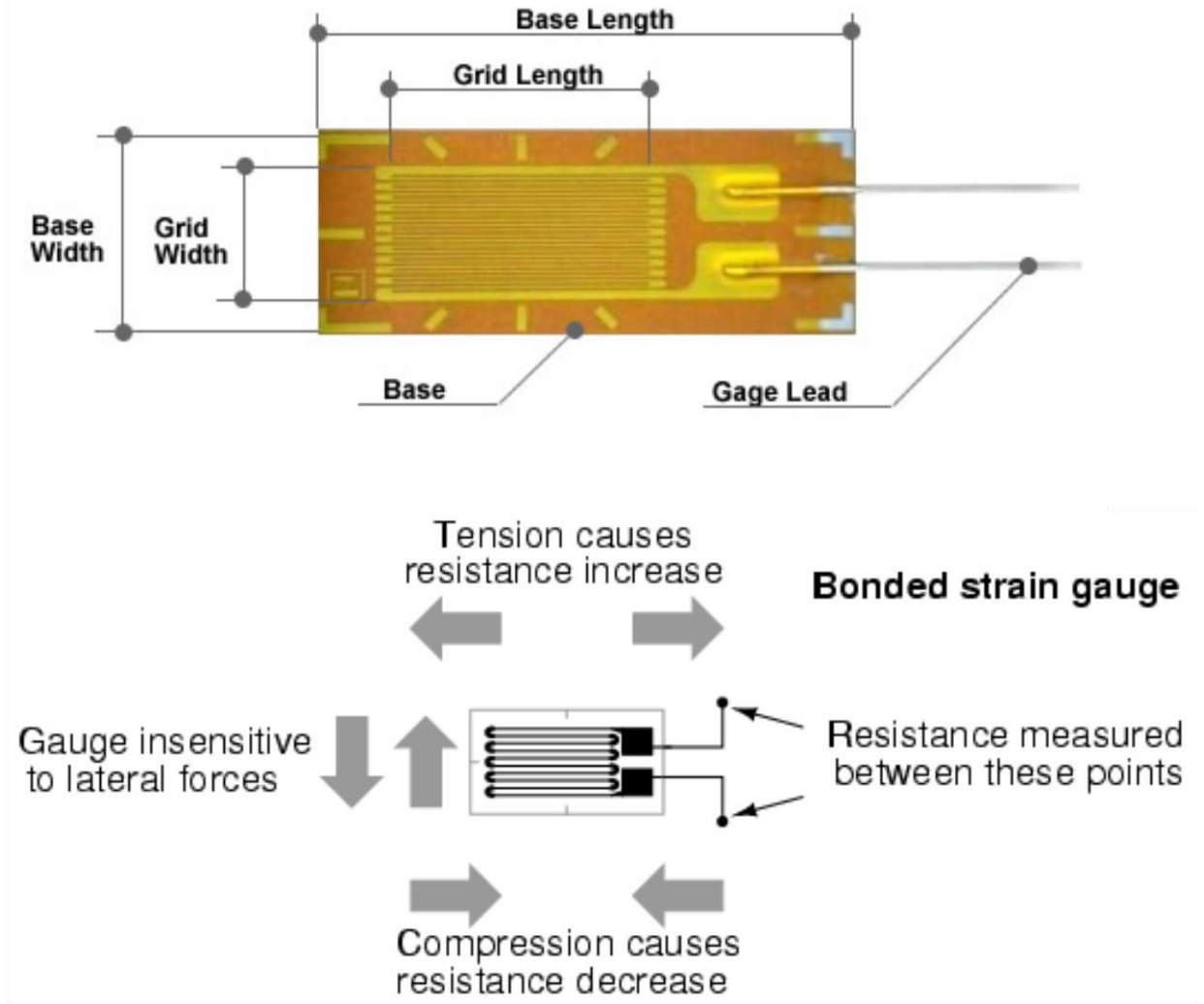
RA 505 Robot Sensing and Vision

Lecture 33

Dr. Rishikesh Kulkarni
Department of Electronics and Electrical Engineering
IIT Guwahati

Resistance Strain Gauge

- Wire strain gauges
 - unbonded resistance wire strain gauges
 - Bonded resistance wire strain gauges.
 - Fine wire: about 25 μm or less
 - Carrier: thin sheet of paper.
 - the carrier mounting of wire structure and carrier adhesion on the object surface plays a crucial role in strain measurement accuracy



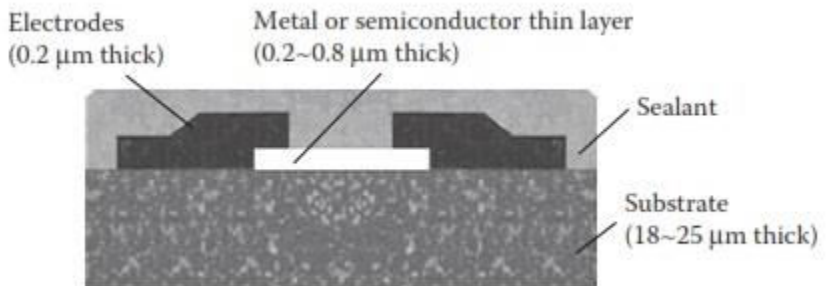
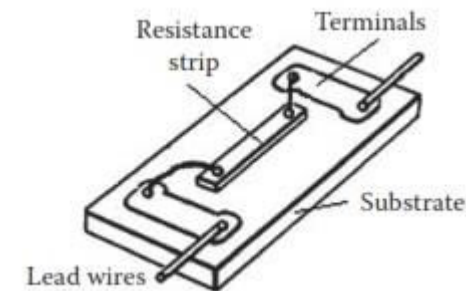
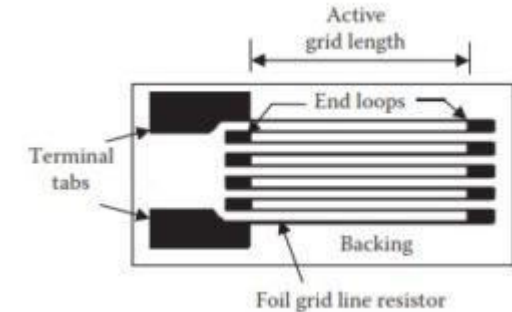
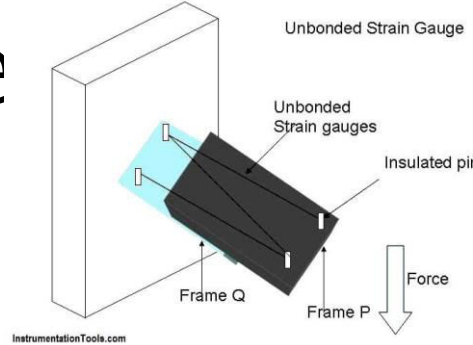
Resistance Strain Gauge

- Resistance of a conductor $R = \frac{\rho L}{A}$
- change in resistance due to the change in dimension and change is fundamental property of the material (*piezoresistance*)
- Strain $\varepsilon = dL/L$
- Poisson ratio: $\nu = -\frac{\delta r/r}{dL/L}$

$$\text{Gauge factor} \triangleq \frac{dR/R}{dL/L} = 1 + 2\nu + \frac{d\rho/\rho}{dL/L}$$

Resistance Strain Gauge

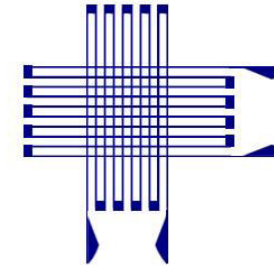
- Unbonded metal-wire gage
- Bonded metal-wire gage
- Bonded metal-foil gage
- Vacuum-deposited thin-metal-film gage
- Sputter-deposited thin-metal-film gage
- Bonded semiconductor gage
- Diffused semiconductor gage



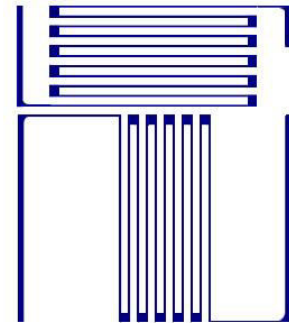
Resistance Strain Gauge

- Bonded metal foil strain gauges
 - Copper-Nickel, Nickel-Iron alloys;
 - Thin metal grid mounted on flexible or brittle carrier;
 - measurement of average strain over an area;
 - Types of gauges are: Grid, Rosette, Torque and Helical.
 - The area is comparatively more than the wire strain
 - The resistive film thickness is typically 0.2mm thick.

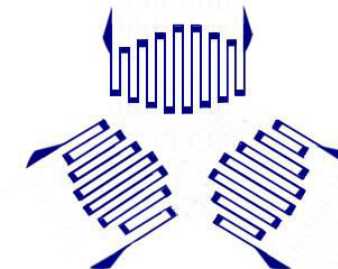
Nominal Resistance of Various Strain Gauges	
Type of Strain Gauge	Nominal Resistance
Wire gauge	60~350 Ω
Foil or semiconductor gauge	120 Ω ~5 k Ω
Thin-film gauge	~10 k Ω



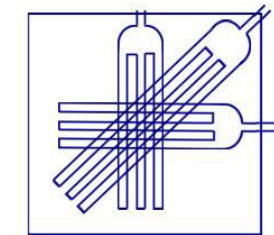
Two-Element, 90 Degree Planar (Shear)
Rosette Strain Gauge



Two-Element 90 Degree Planar
Rosette Strain Gauge

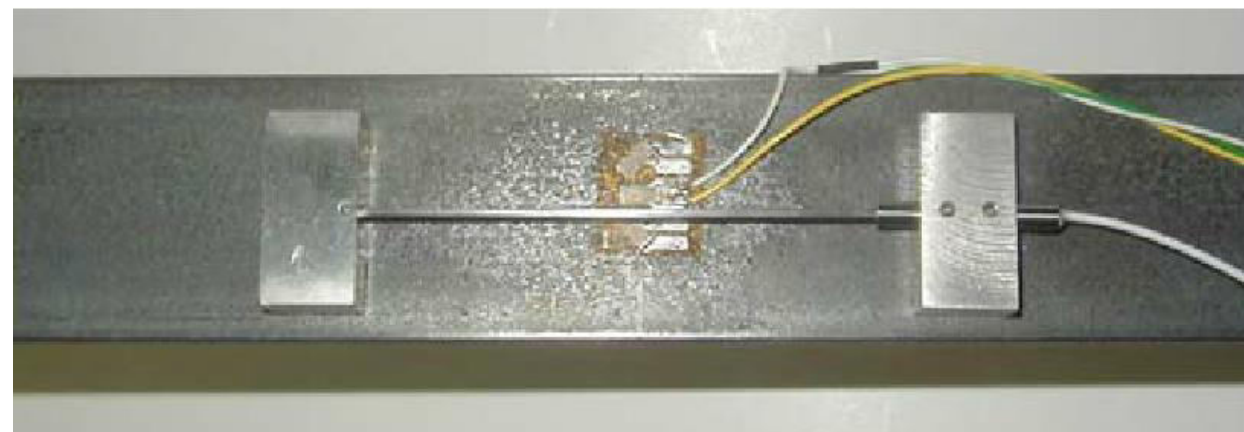


Three Element, 60 Degree Delta
Rosette strain Gauge



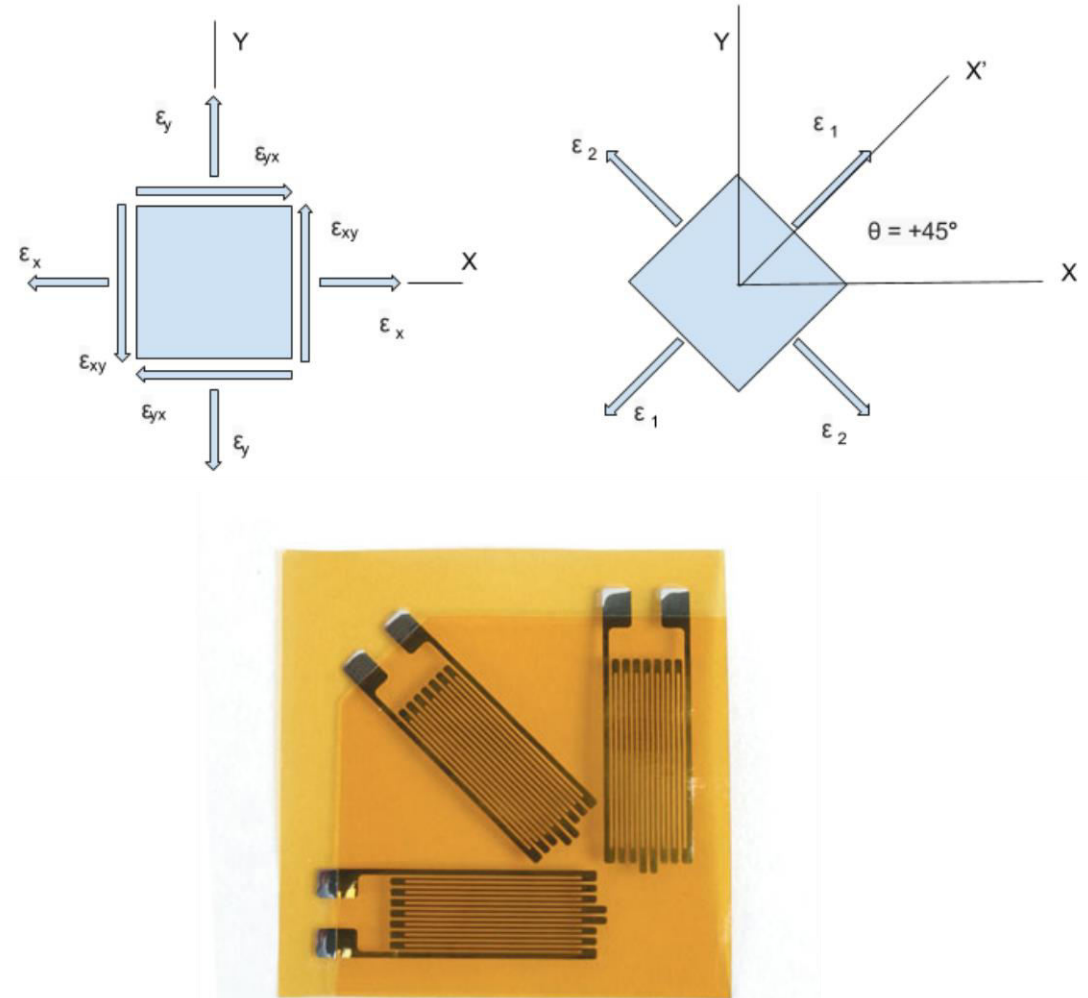
Three Element, 45 Degree Planar
Rectangular Rosette Strain Gauge

www.InstrumentationToday.com



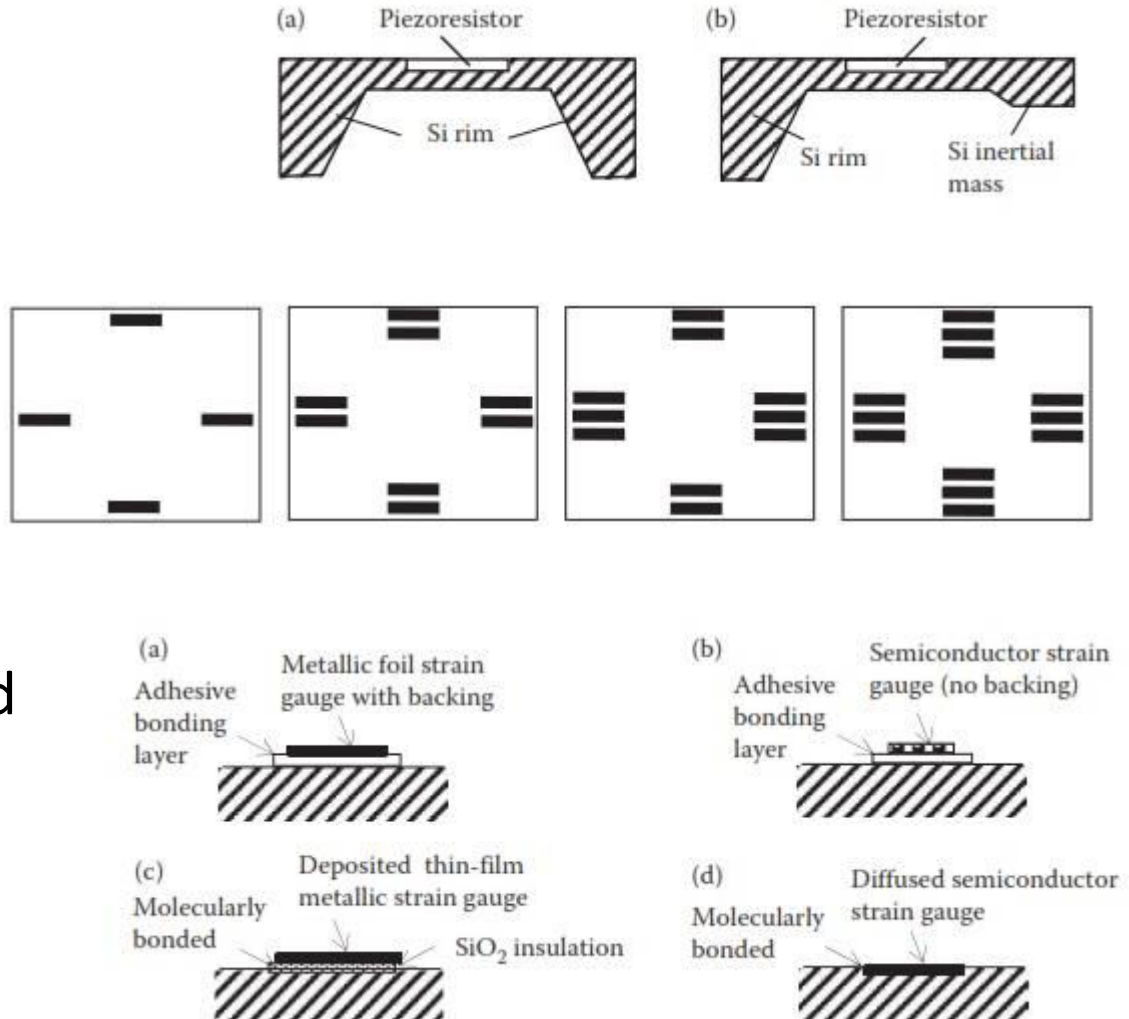
Resistance Strain Gauge

- Rosette are nothing but three strain gauges overlapping at a same point manufactured on the same carrier material.
- Rosettes are used for the measurement of force, velocity, pressure and displacement in applications such as aircraft and missile production, mechanical engineering, railroad, car manufacturing and other industries.

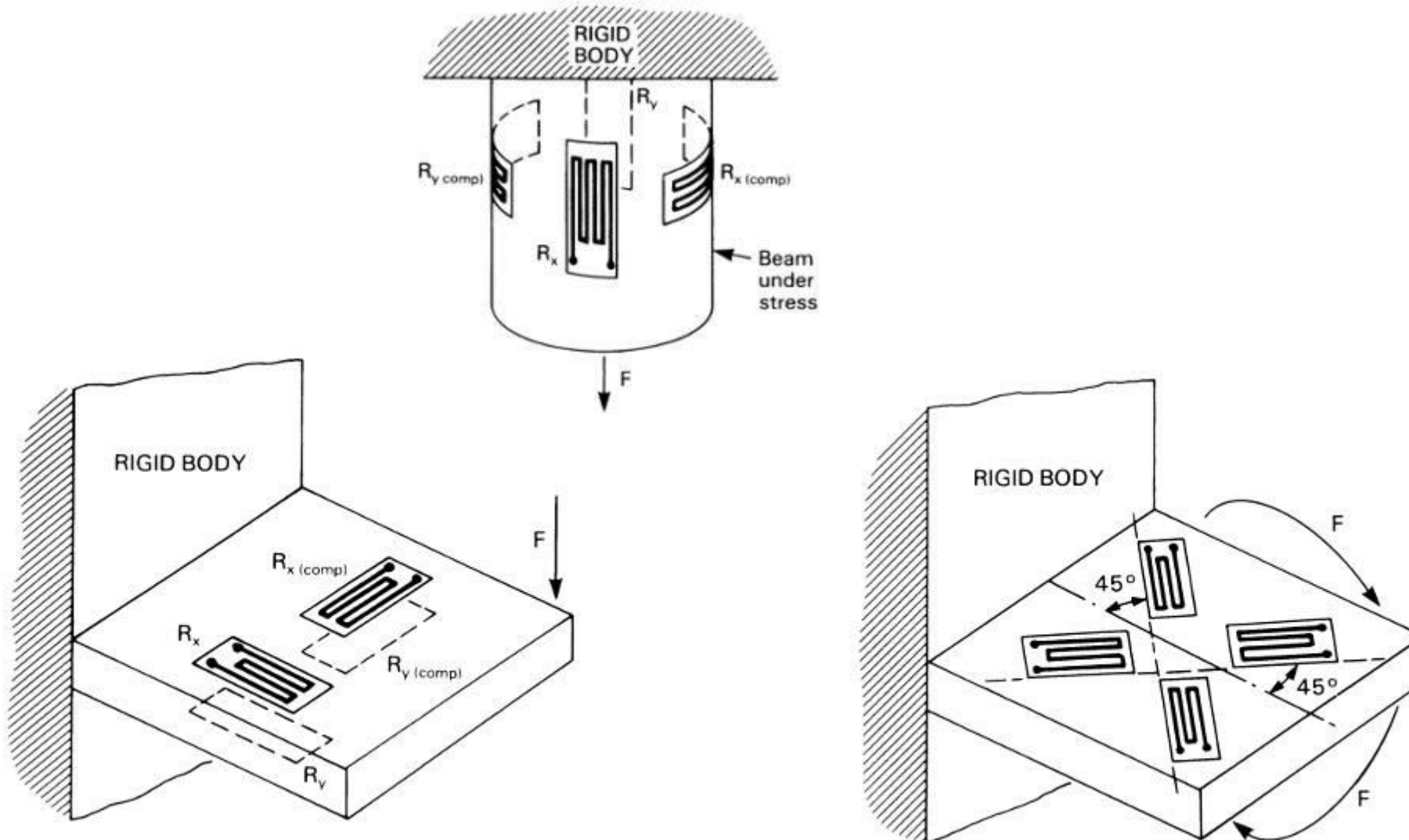


Supporting Structure And Bonding Methods Of Strain Gauges

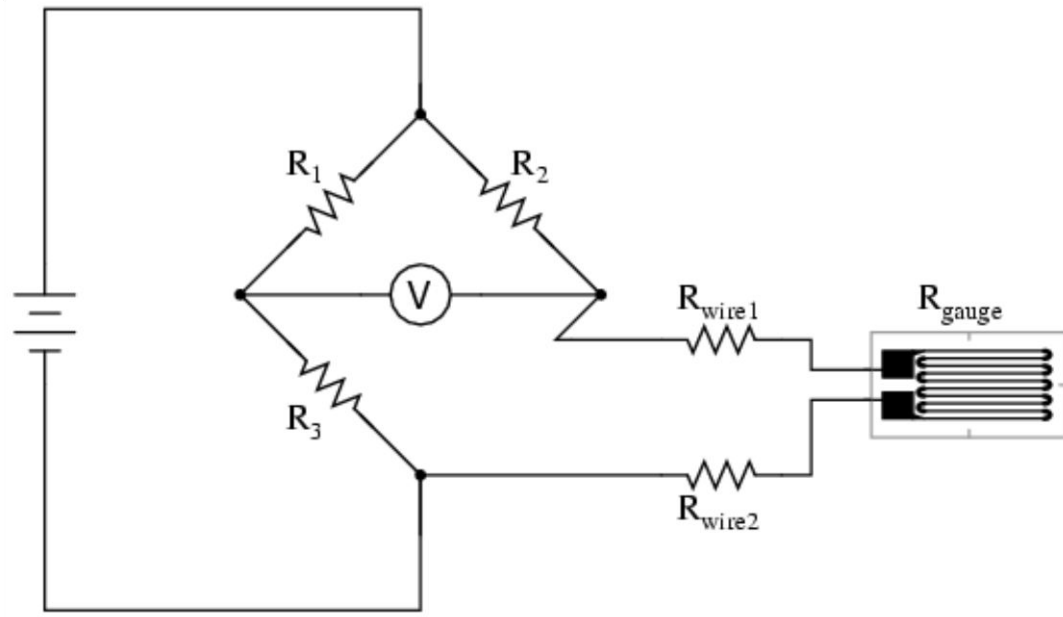
- Membrane-type and cantilever type
- Bonding methods for strain gauge
 - adhesive bonding with backing,
 - adhesive bonding without backing,
 - deposited molecular bonding, and
 - diffused molecular bonding.



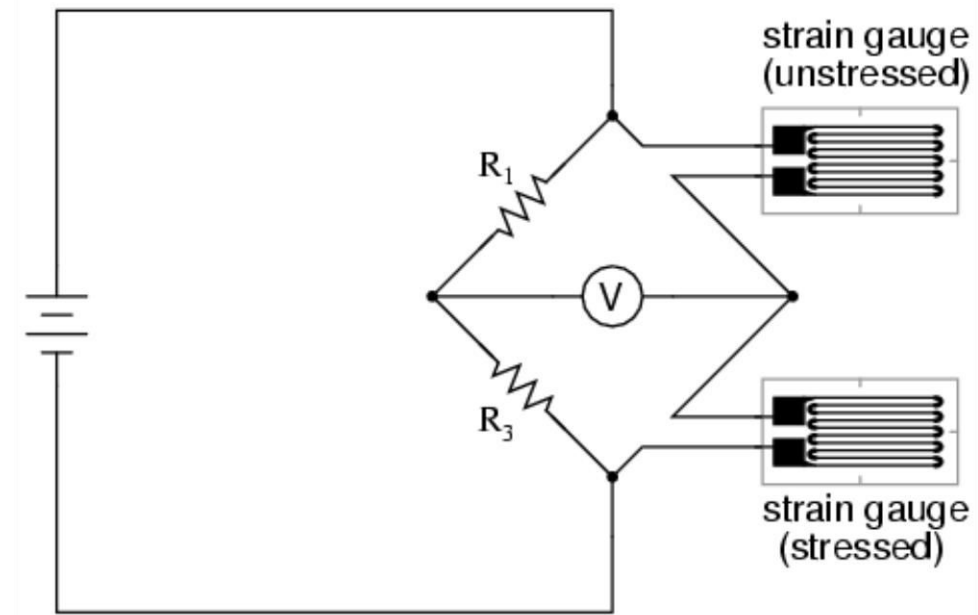
Placement of strain gauges



Resistance Measurement of Strain Gauge

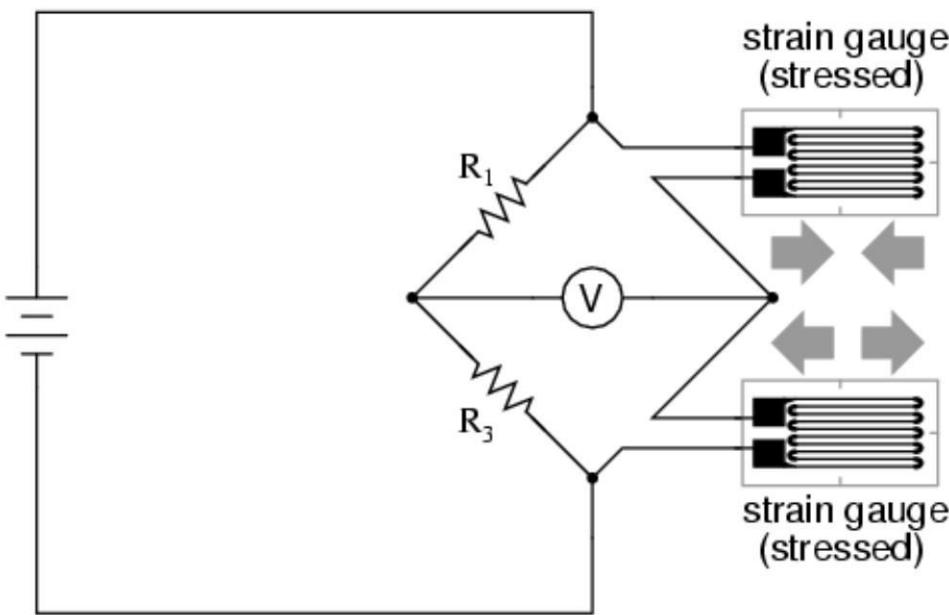


*Quarter-bridge strain gauge circuit
with temperature compensation*

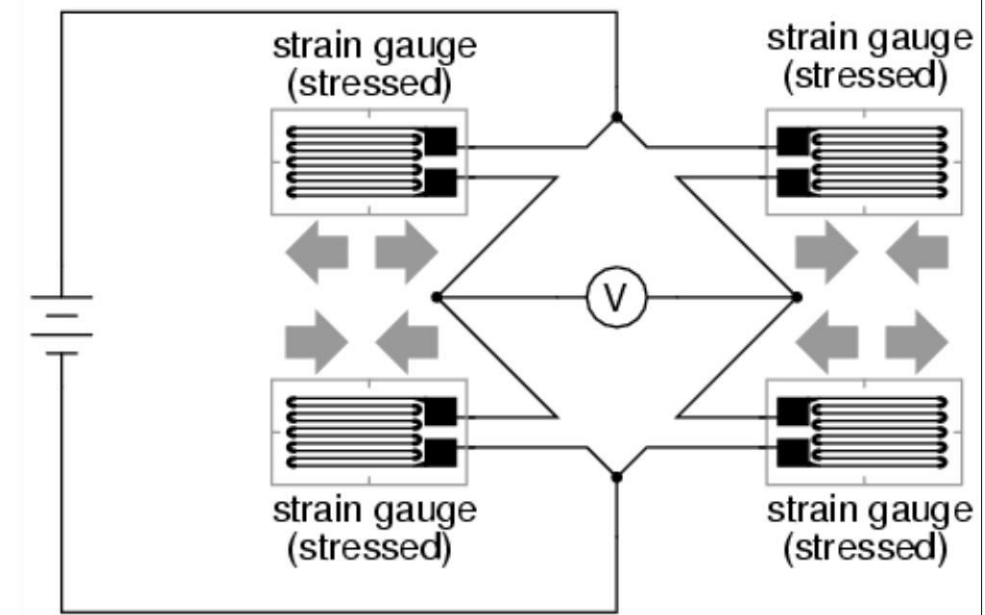


Resistance Strain Gauge

Half-bridge strain gauge circuit

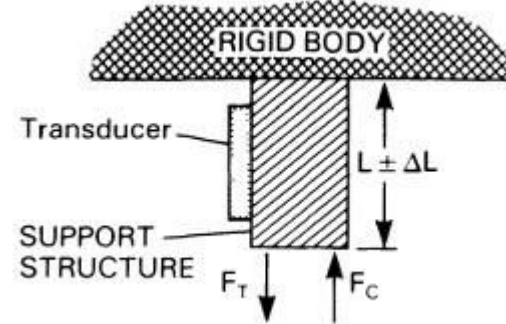


Full-bridge strain gauge circuit

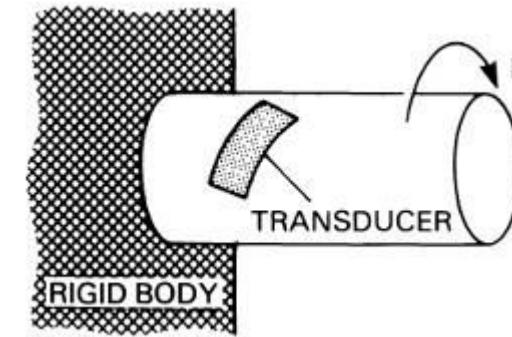
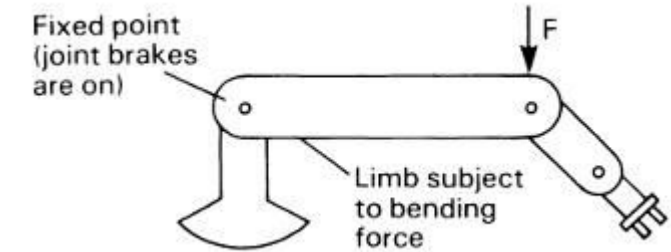
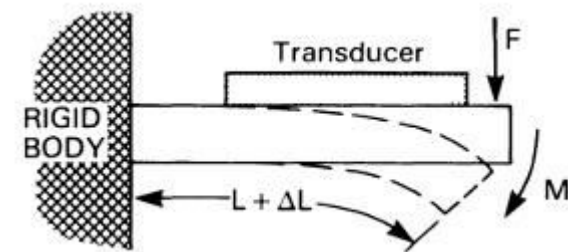


Force sensors

- Kinematic forces
- Static forces
- choice and shape of the support material
 - long-term stability
 - Adhesion
- Traction force: limbs of the robot in the vertical position
- Bending force: a robot limb in a non-vertical position
- Twisting force: drive shaft of a robot actuator



$$F = \frac{EA}{G_f} \left(\frac{\Delta V_t}{V_t} \right) \quad (1)$$



RA 505 Robot Sensing and Vision

Lecture 34

Dr. Rishikesh Kulkarni
Department of Electronics and Electrical Engineering
IIT Guwahati

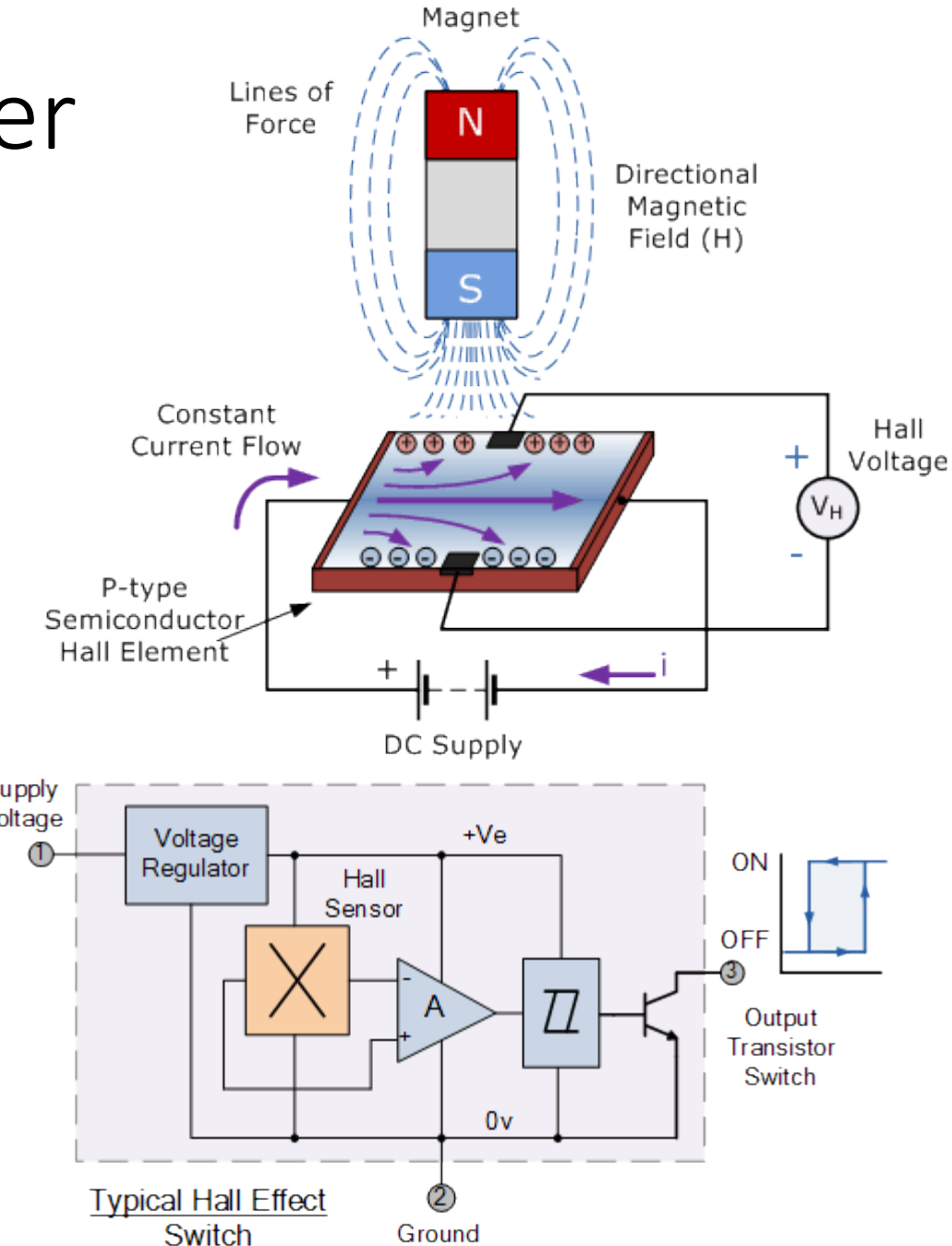
Accelerometer

- Device to measure
 - Acceleration
 - Vibration
 - Shock
 - Velocity
 - Position
- Applications in
 - Automotive
 - Medical
 - Industrial control
 - Robotics
- Types
 - Hall effect
 - Piezoelectric
 - Piezoresistive
 - Capacitive
 - Position

Hall effect based Accelerometer

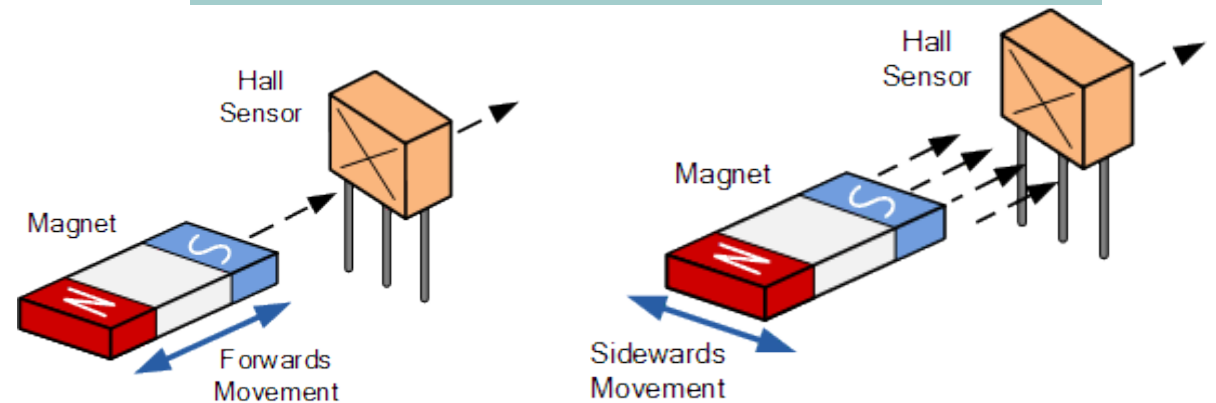
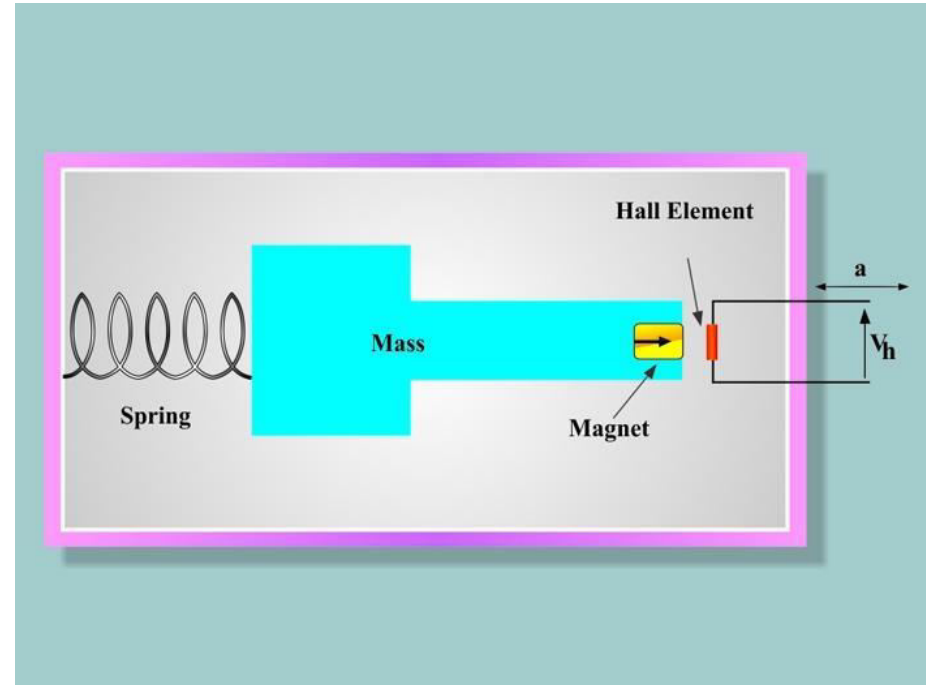
- Output signal from a Hall effect accelerometer is the function of magnetic field density around the device
- Hall Effect Sensors
 - A thin piece of rectangular p-type semiconductor material
 - Gallium arsenide (GaAs), indium antimonide (InSb) or indium arsenide (InAs)
 - A continuous current is passed through it
 - Magnetic force (Lorenz force) experienced by charge carrier displaces them
 - Hall voltage (V_H)
 - Built-in DC amplifiers, logic switching circuits and voltage regulators
 - Bipolar/unipolar

$$V_H = R_H \left(\frac{I}{t} \times B \right)$$



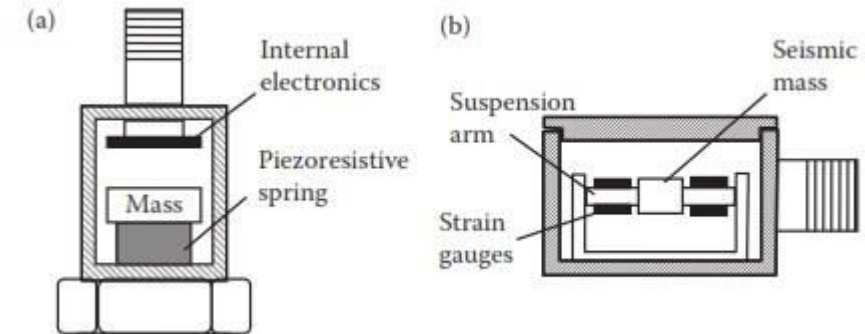
Hall effect based Accelerometer

- Types of magnet movements, such as “Head-on”, “Sideways”, “Push-pull” or “Push-push” etc. sensing movements.
- Useful in environmental conditions consisting of water, vibration, dirt or oil



Piezoresistive Accelerometer

- can measure both dynamic and static accelerations.
- Gauge dimension, gauge factor, power dissipation
- Creep: nonideal elastic behaviors of piezoresistors and adhesive materials
- Temperature coefficient of resistance (TCR)
- Temperature coefficient of sensitivity (TCSR),



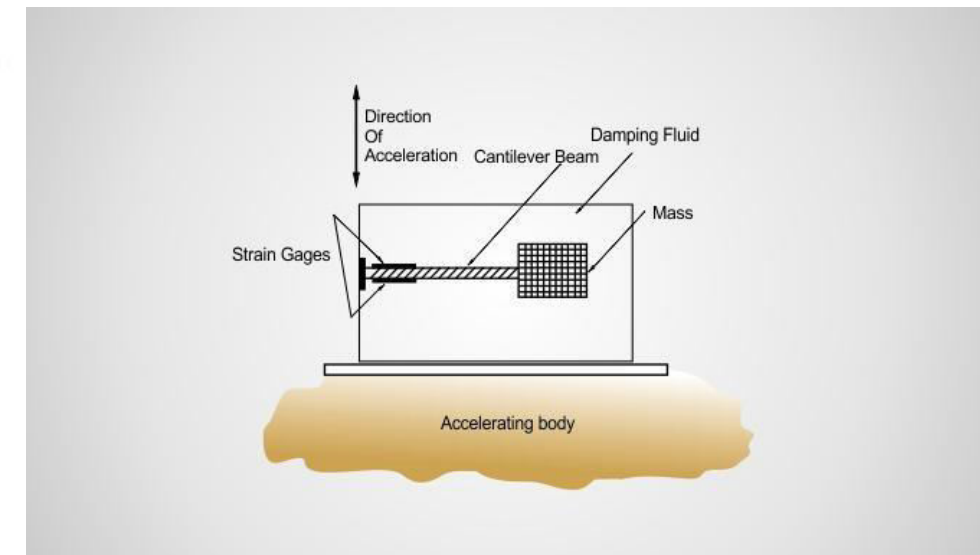
Typical GF Range of Main Types of Strain Gauges

Type of Strain Gauge	Gauge Factor (GF)
Metal foil	1 ~ 5
Thin-film metal	= 2
Bar semiconductor	80 ~ 150
Diffused semiconductor	80 ~ 200

$$\text{Creep (\%)} = \frac{\Delta\epsilon/\epsilon}{\Delta t} \times 100\%$$

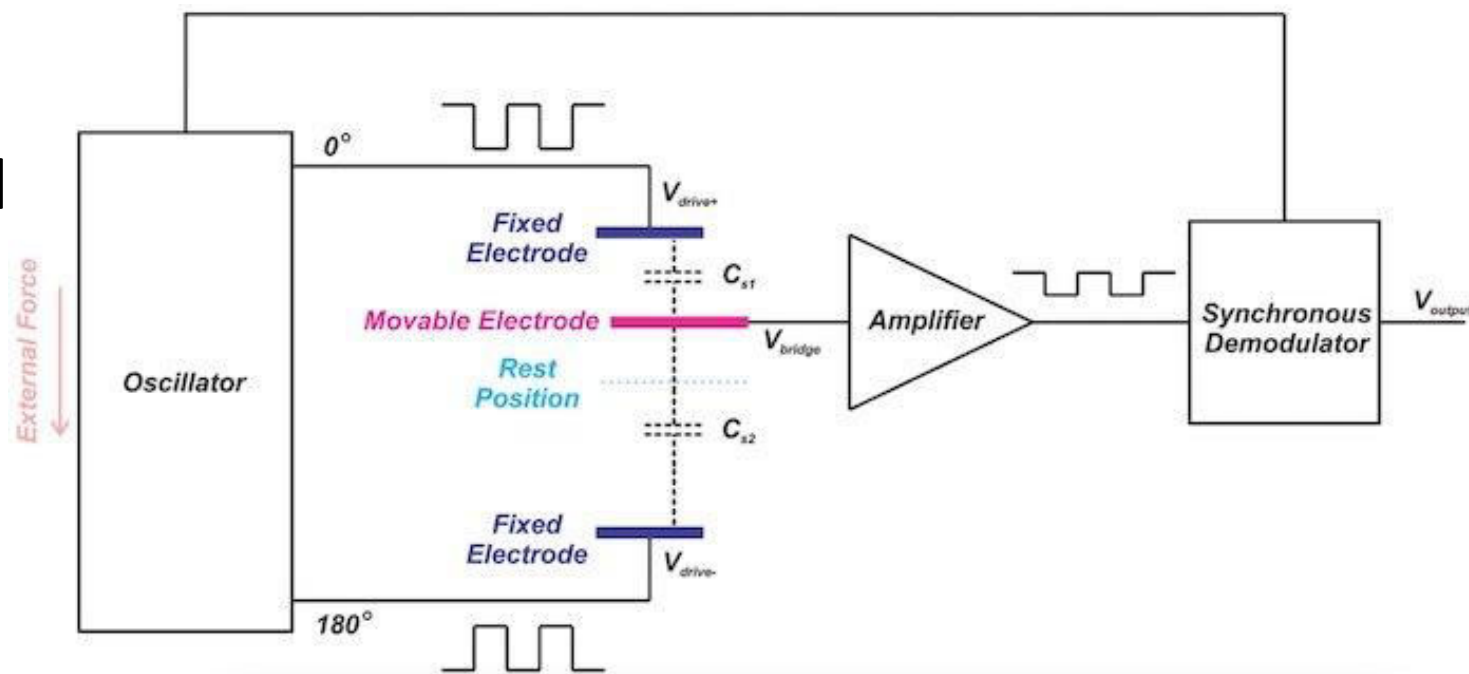
$$\text{TCR} = \left. \frac{\Delta R/R}{\Delta T} \right|_{\text{Free}}$$

$$\text{TCS} = \frac{\Delta \text{GF/GF}}{\Delta T}$$



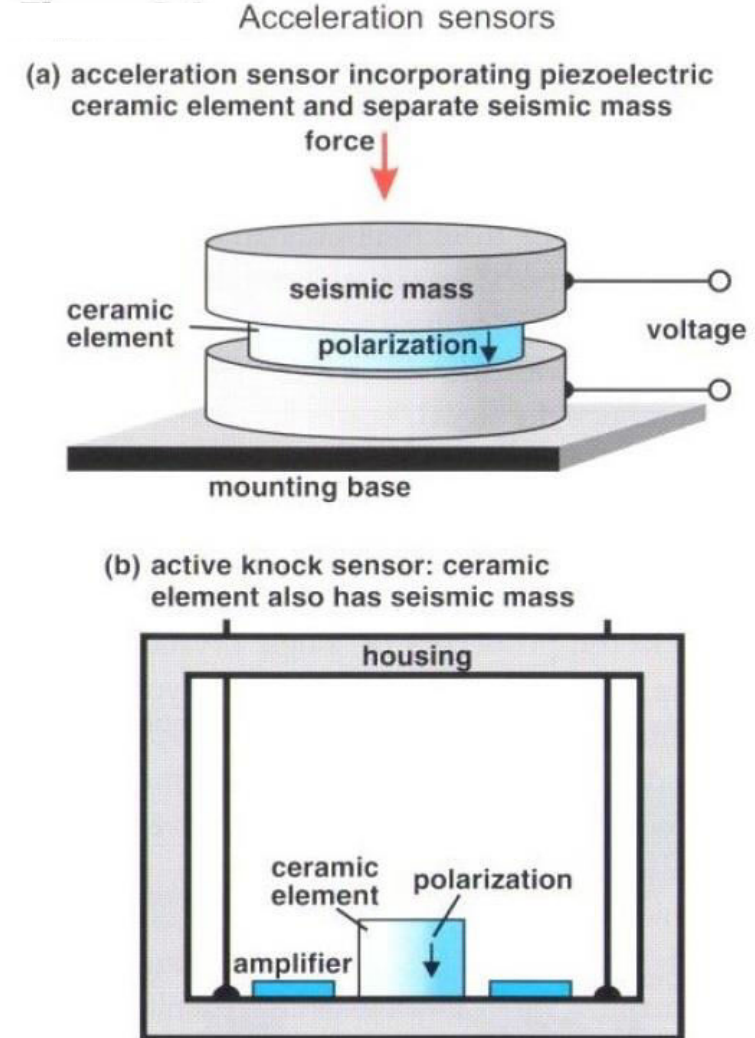
Capacitive Accelerometer

- Spring-mass system
- Change in capacitance due to change in distance between movable and fixed plate

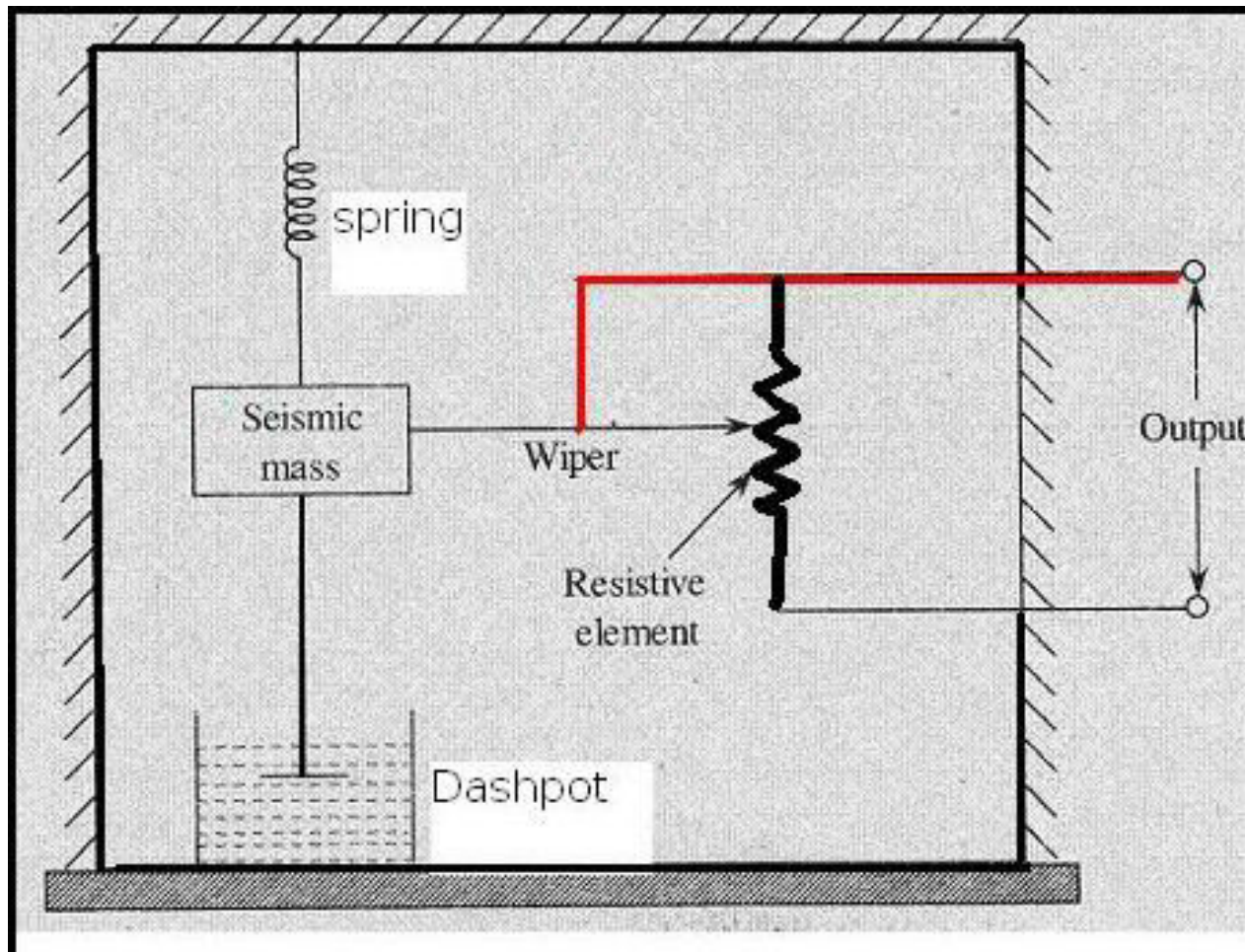


Piezoelectric Accelerometer

- Piezoelectric material slice: Polarized ceramic
- Advantages
 - Frequency response
 - Temperature stability
 - Ruggedness
 - Adaptability
 - Electrical characteristics



Potentiometric Accelerometer



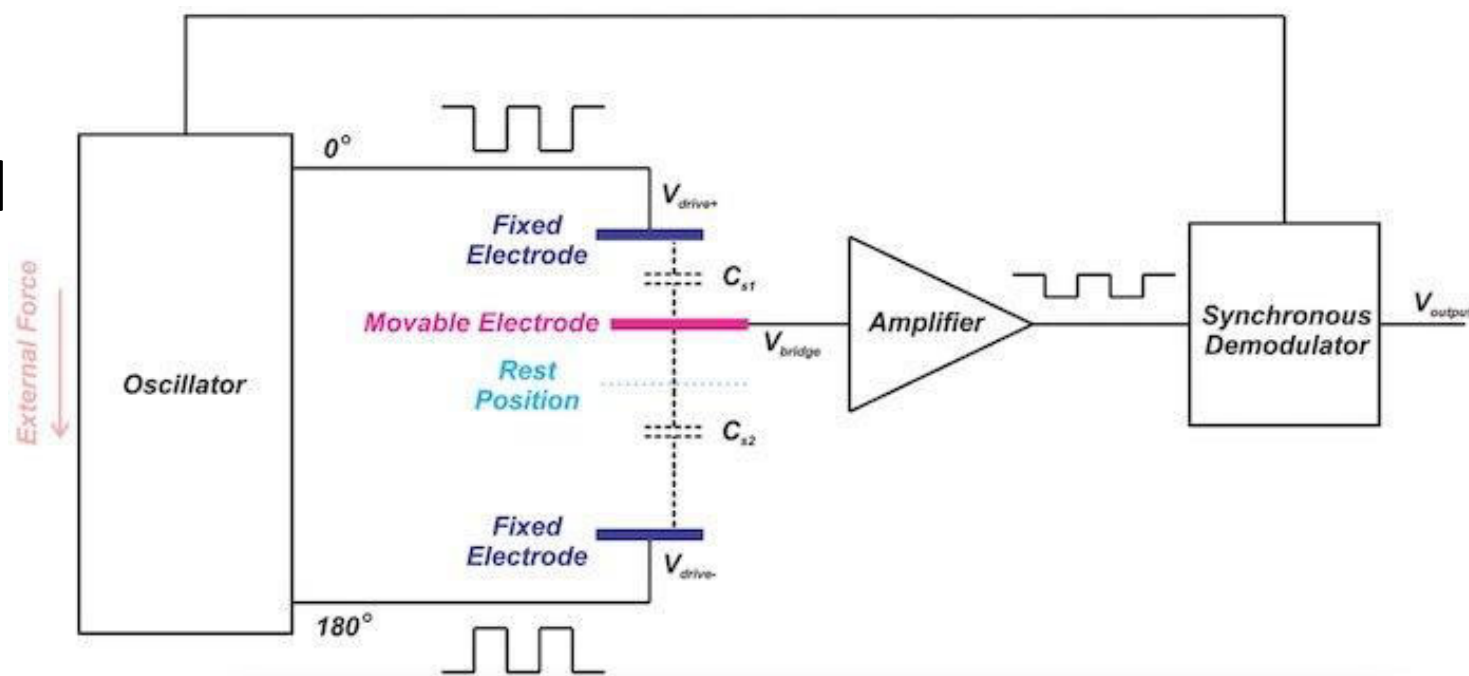
RA 505 Robot Sensing and Vision

Lecture 35

Dr. Rishikesh Kulkarni
Department of Electronics and Electrical Engineering
IIT Guwahati

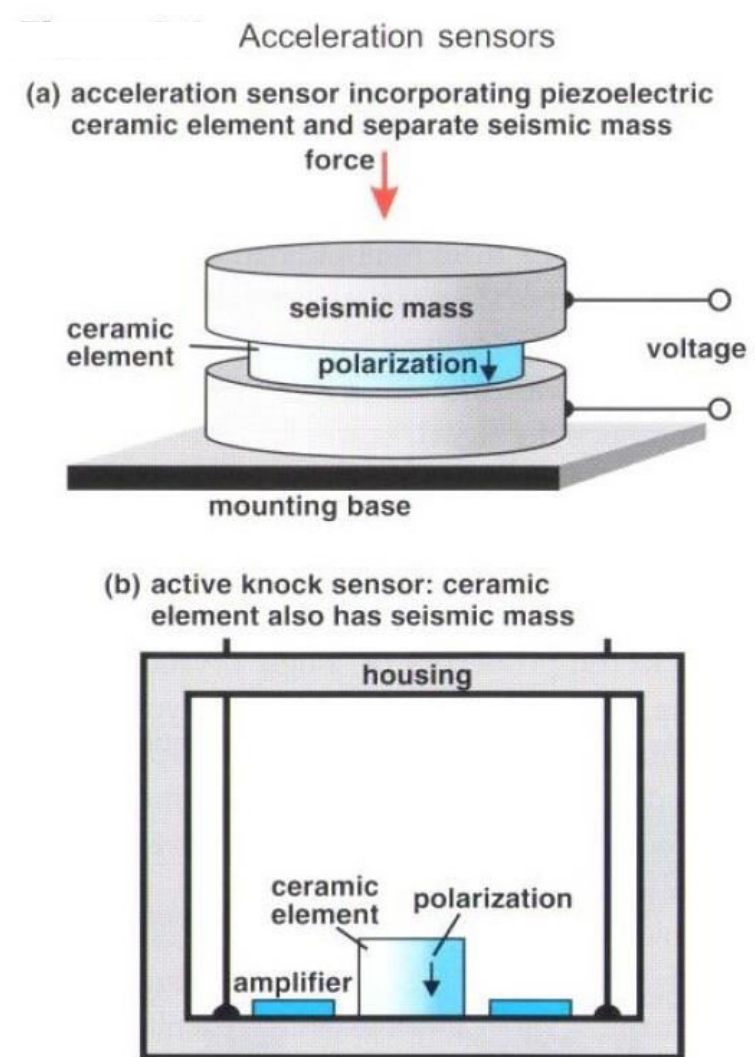
Capacitive Accelerometer

- Spring-mass system
- Change in capacitance due to change in distance between movable and fixed plate

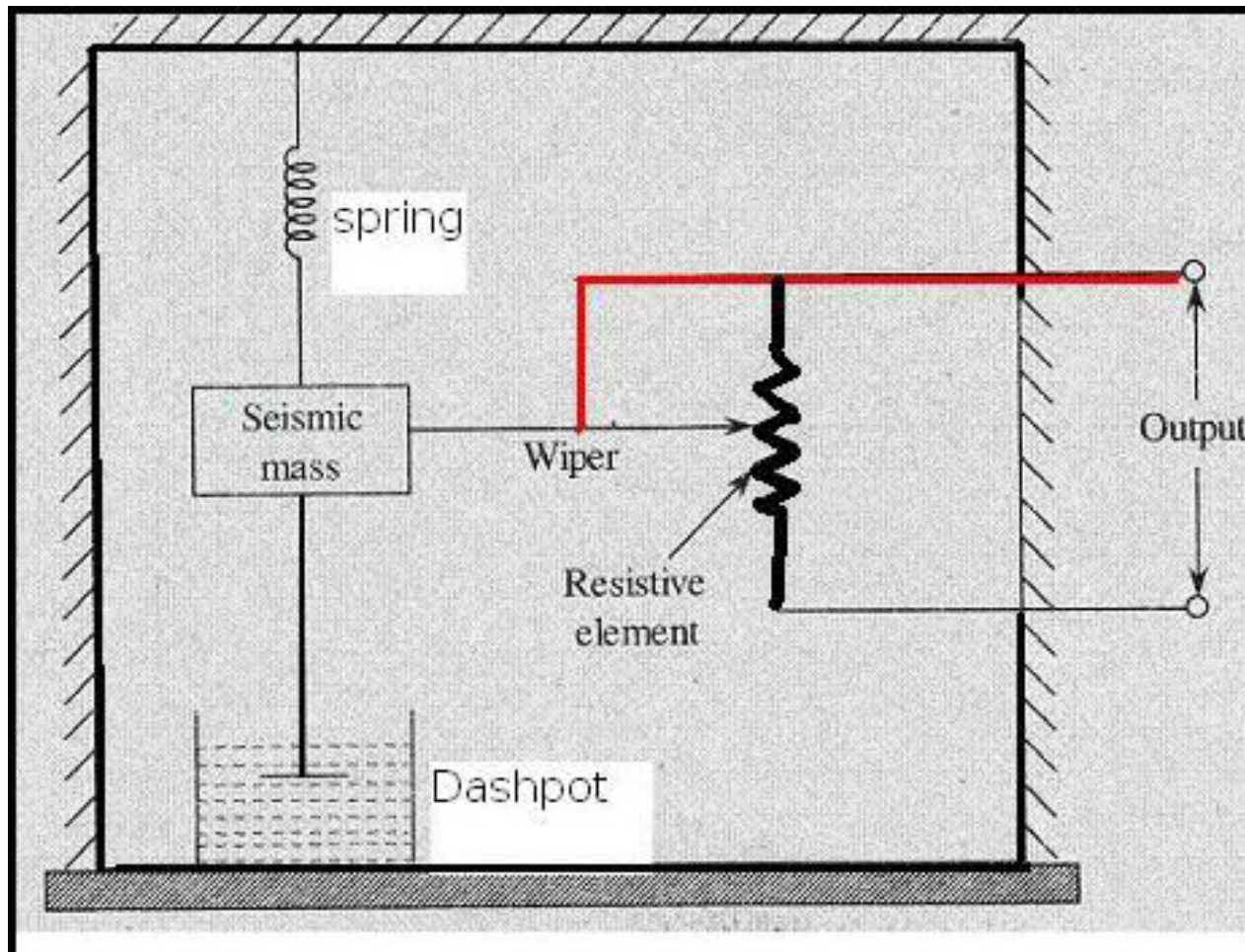


Piezoelectric Accelerometer

- Piezoelectric material slice: Polarized ceramic
- Advantages
 - Frequency response
 - Temperature stability
 - Ruggedness
 - Adaptability
 - Electrical characteristics

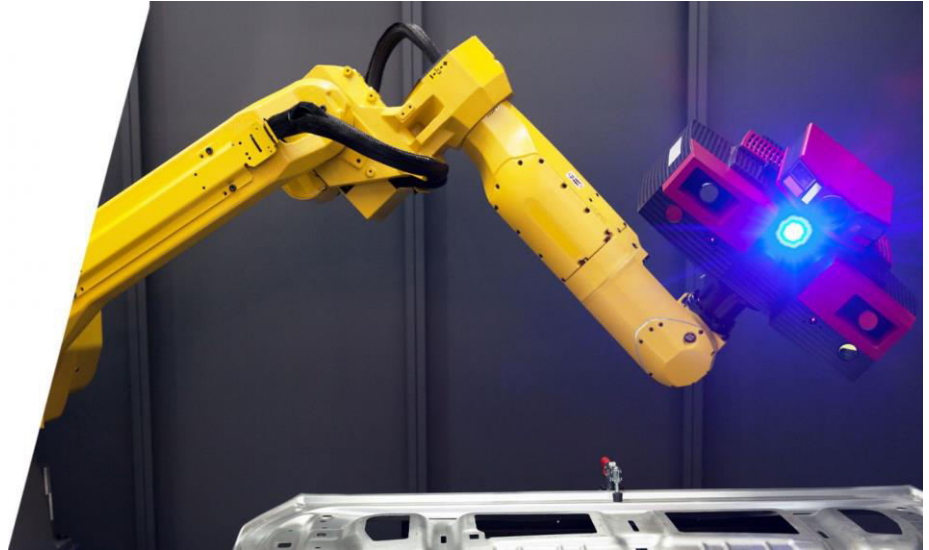


Potentiometric Accelerometer



Structured Light Illumination

- Introduction
- Principle of Method
 - Triangulation
 - Fringe Projection
 - Phase Evaluation
 - Phase Calibration
- Applications of Method
 - Line Scan and Fringe Projection
 - Quality Guided Phase Unwrapping
 - Multifrequency Fringe Projection
 - Carrier Phase Removal
 - 360-degree Fringe Projection
- Concluding Remarks

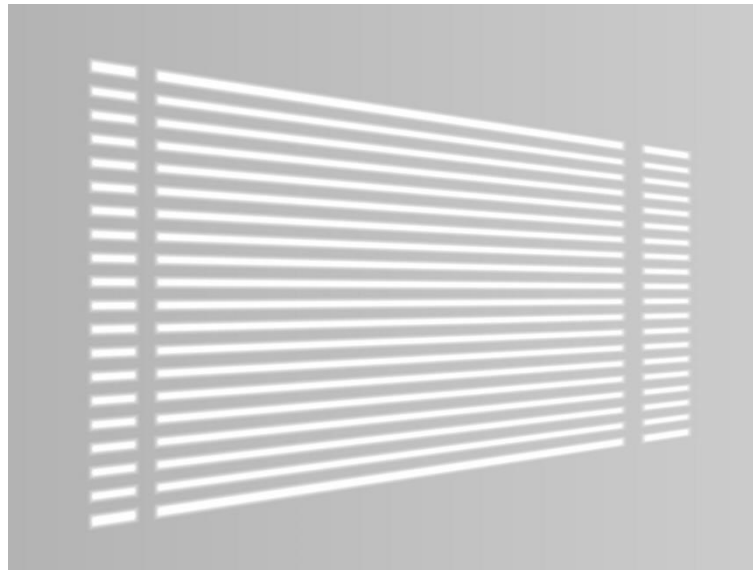


Introduction

- Data-processing methods based on those developed for interferometry
- Interferometry is based on the optical path difference and fringe projection profilometry is based on principle of triangulation.
- Projection of a pattern generated using gratings or a digital projector.

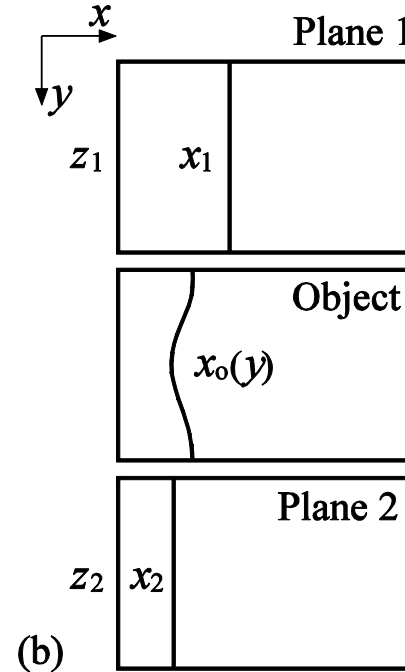
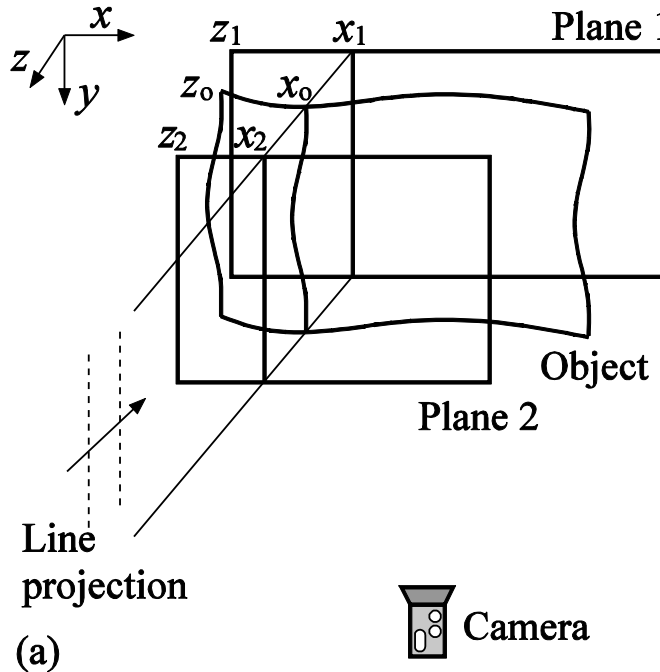
Principle of Method

- Principle of FPP is based on '*Principle of Triangulation*'.



- Quantitative phase evaluation and calibration of the phase values against standard results yields the actual profile of an object.

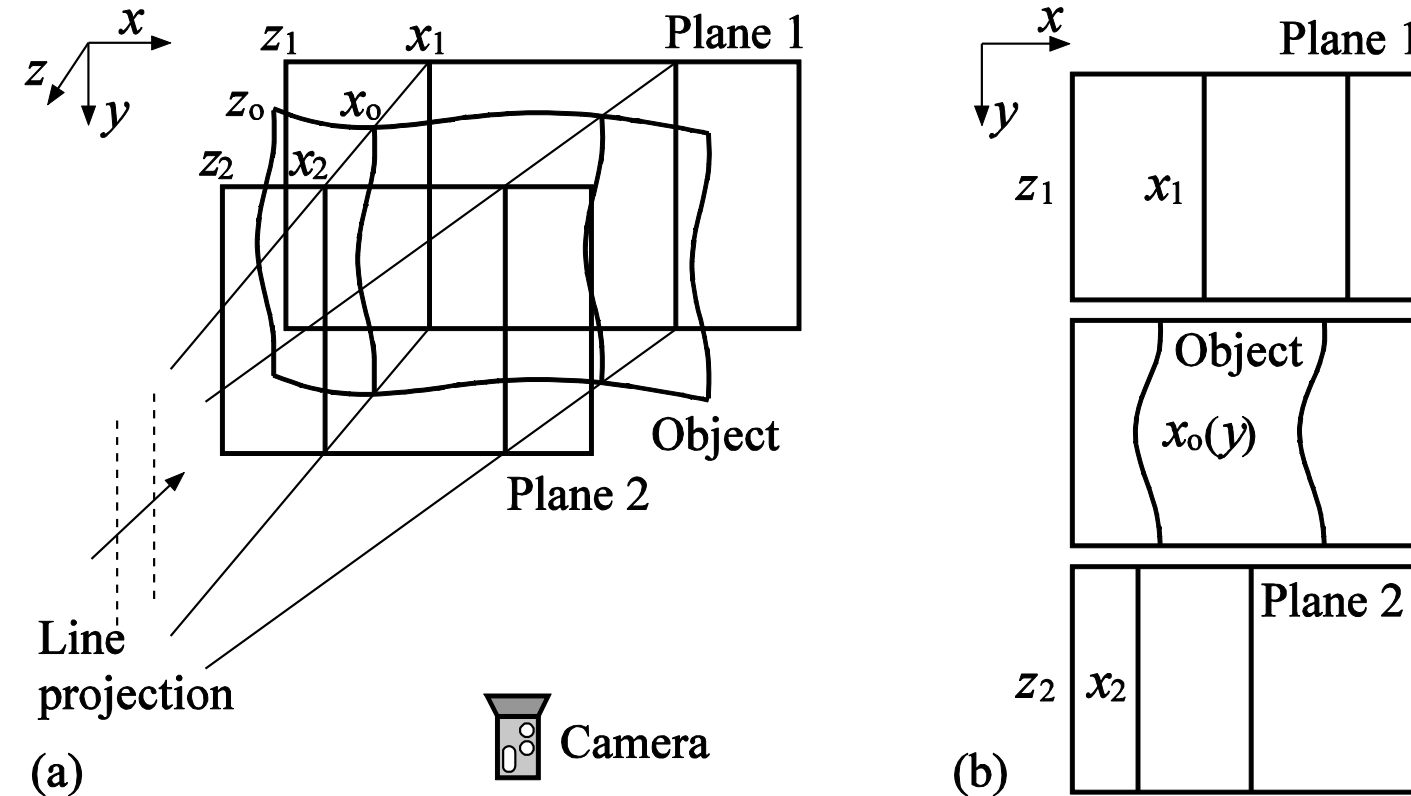
Fringe Projection



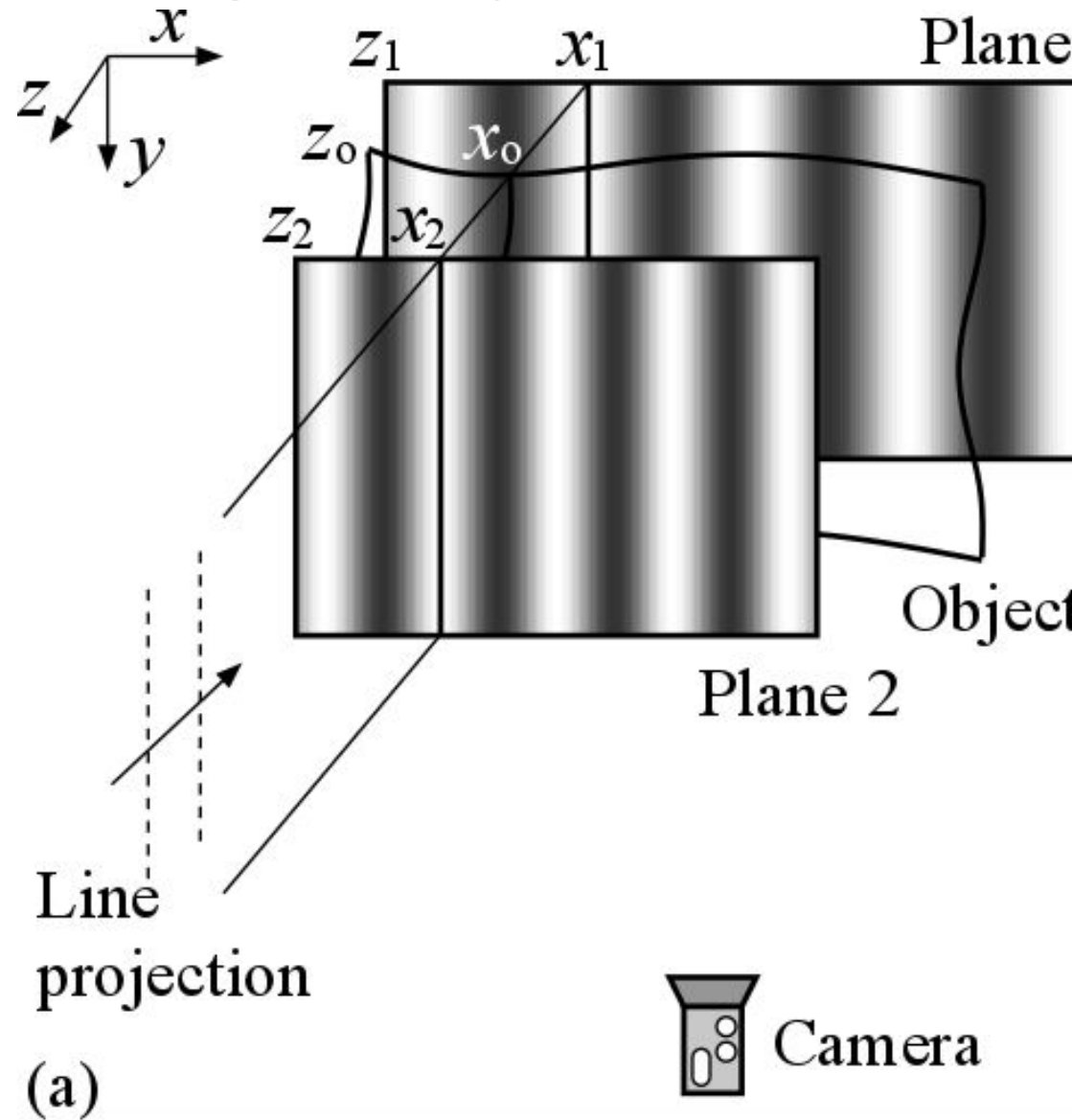
$$\frac{z_o - z_1}{z_2 - z_1} = \frac{x_o - x_1}{x_2 - x_1}$$

- How do we obtain a whole-field depth map of an object?
- Line-scan method

Fringe Projection: Line-scan method



Fringe Projection: Phase-based method



Advantages of using a fringe pattern

1. One single image would provide information on the entire surface and hence scanning is not needed.
2. The problem of a gap between two projected lines no longer exists as every point on the surface is sampled.
3. The order of a phase value at each point can be detected accurately by various methods (discussed next).
4. The accuracy is related to that of phase measurement, which is much higher than the accuracy of the line detection method.

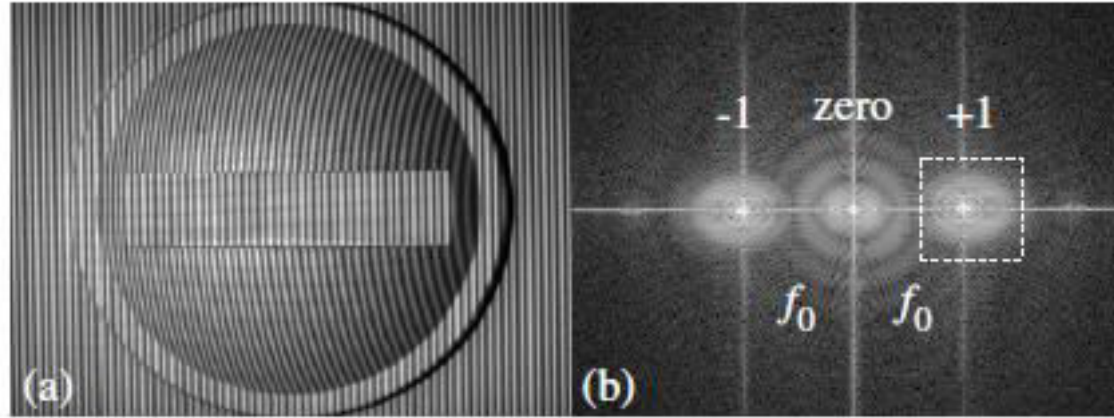
Phase Evaluation

- In the fringe projection method, it is important to obtain the correct phase for each pixel of a fringe pattern.
- This is carried out in two steps: *wrapped phase extraction* and *phase unwrapping*.
- Fourier Transform:
 - The spatial intensity distribution of a fringe pattern is sinusoidal in the direction of progressing phase

$$I(x, y) = a(x, y) + b(x, y) \cos \theta(x, y)$$

$$I = a + \frac{be^{j\theta}}{2} + \frac{be^{-j\theta}}{2}$$

Phase Evaluation: Fourier Transform

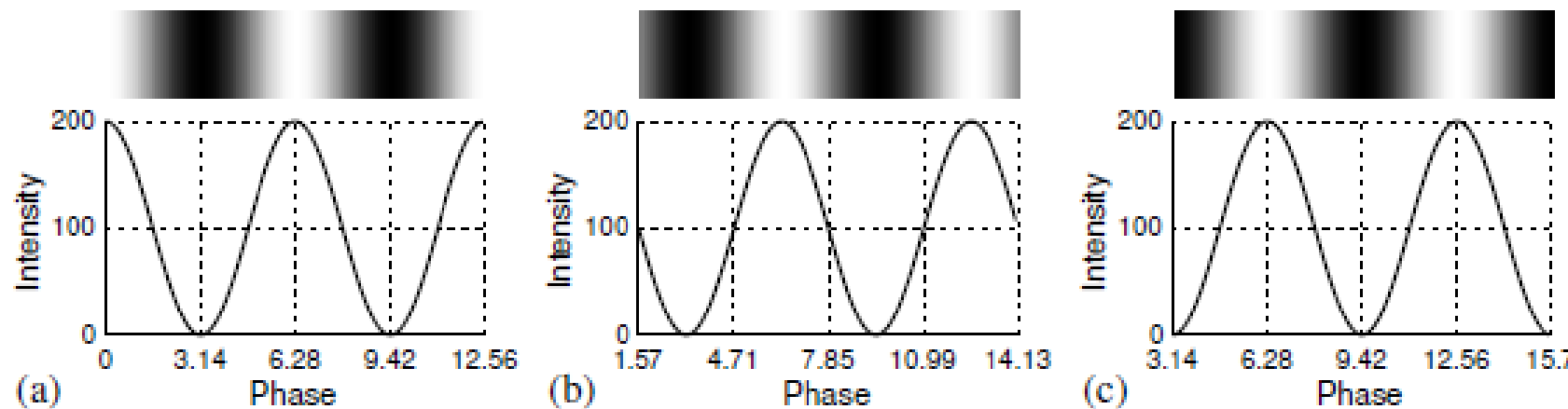


$$c = \frac{be^{j\theta}}{2} = \frac{b}{2}(\cos \theta + j \sin \theta)$$

$$\theta = \arctan \frac{\text{Im}(c)}{\text{Re}(c)}$$

Phase Evaluation: Phase-Shifting

- Phase-shifting method requires the input of at least three phase-shifted fringe patterns as in a sinusoidal intensity distribution there are three unknowns.
- Generating a phase-shifted fringe pattern is straightforward: this is done by changing the initial phase of a fringe pattern and project them sequentially onto the object



Phase Evaluation: Phase-Shifting

- The intensity of a pixel in a fringe pattern, which is phase-shifted n times, is expressed as

$$I_i = a + b \cos(\theta + \delta_i)$$

- If n is 3, the unknowns a , b and θ can be determined. If n is more than 3, the unknowns can be obtained using least-squares error.

$$I_i = a + b \cos \theta \cos \delta_i - b \sin \theta \sin \delta_i$$

- Let $B = b \cos \theta$ and $C = -b \sin \theta$

$$E(a, B, C) = \sum_{i=1}^n (I_i - a - B \cos \delta_i - C \sin \delta_i)^2$$

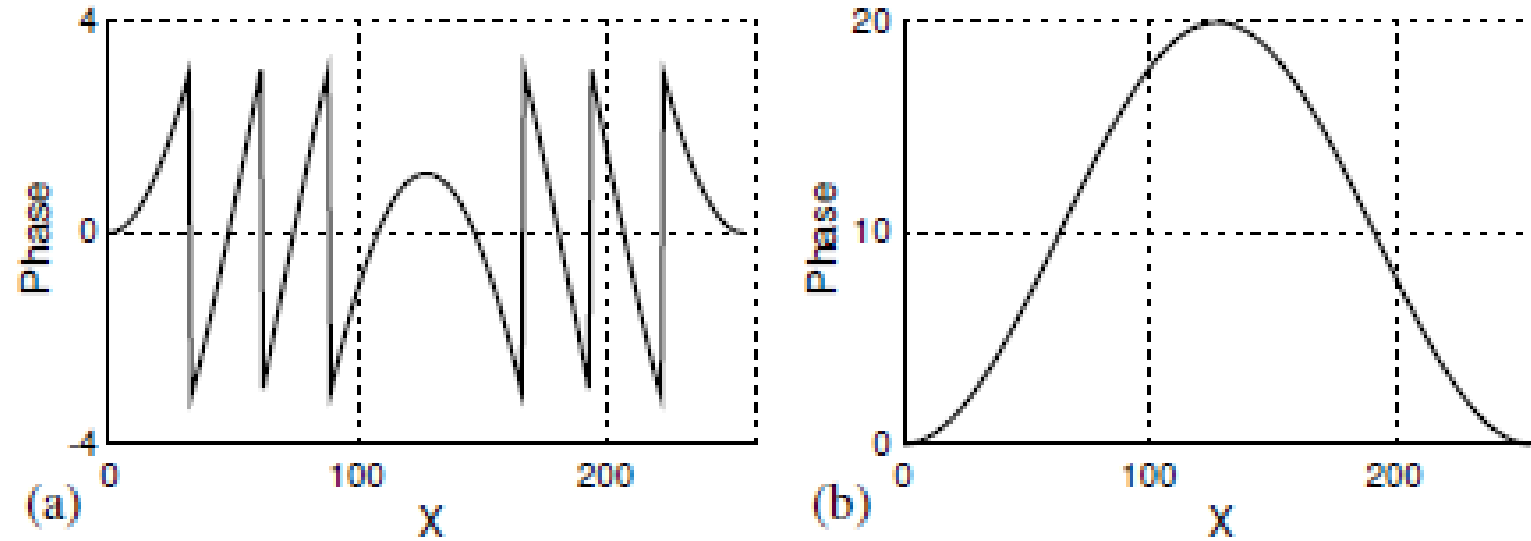
Phase Evaluation: Phase-Shifting

$$\sum_{i=1}^n \begin{bmatrix} 1 & \cos \delta_i & \sin \delta_i \\ \cos \delta_i & \cos^2 \delta_i & \sin \delta_i \cos \delta_i \\ \sin \delta_i & \sin \delta_i \cos \delta_i & \sin^2 \delta_i \end{bmatrix} \begin{bmatrix} a \\ B \\ C \end{bmatrix} = \sum_{i=1}^n \begin{bmatrix} I_i \\ I_i \cos \delta_i \\ I_i \sin \delta_i \end{bmatrix}$$

$$\theta = \arctan \frac{-C}{B}$$

Spatial Phase Unwrapping

- After obtaining a wrapped phase map, the next step is to unwrap the phase values to recover a continuous phase distribution without a 2π jump.



- The problem of phase unwrapping becomes significantly complicated in 2D due to the many possible unwrapping paths (as oppose to only one path in the 1D case)

Quality Guided Phase Unwrapping

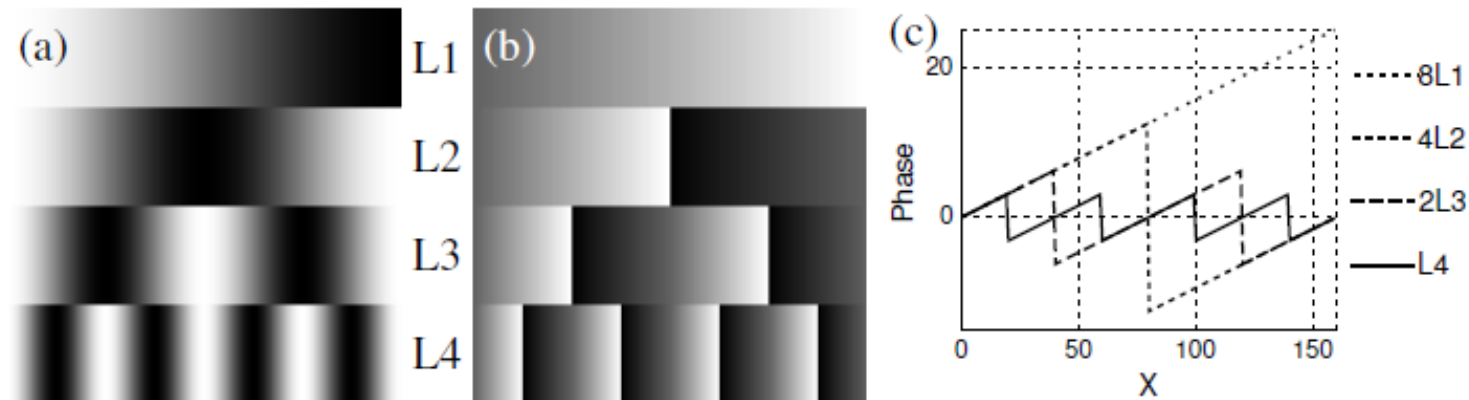
- A particularly effective approach for phase unwrapping is known as quality- guided phase unwrapping.
- It relies on a quality map to determine an unwrapping path.
- At each step, after the current pixel is processed, the next pixel to be processed is determined by a pixel with the highest quality on the propagation boundary.
- This method ensures the unwrapping path moves quickly to a higher quality region before moving to a lower quality region where errors are more likely to be encountered.
- The method is effective for phase fringes where the fringe contrast, which is defined as the ratio between the modulation and background intensity: b/a , is an accurate quality indicator.
- The modulation and background intensity can be obtained from the phase-shifting algorithm.
- Low fringe contrast is usually due to a dark region where a light beam is not able to reach, resulting in a low signal-to-noise ratio, consequently inaccurate results.
- The quality-guided phase unwrapping algorithm would process these low fringe contrast regions at the last stage to minimize error accumulation.

Temporal Phase Unwrapping

- Though spatial phase unwrapping is speedy and requires only one wrapped phase map, there are certain limitations.
- For example, if an object profile is complicated, spatial phase unwrapping often produces suboptimal results.
- In cases where a field of view contains multiple objects whose profiles are disconnected or of different heights, spatial approach may not be able to produce the intended results.
- Unlike spatial phase unwrapping that relies on a pixel's neighbouring pixels to determine its phase value, temporal phase unwrapping deals with each pixel individually
- The method relies on different calculated phase values of a pixel to determine its actual phase value.

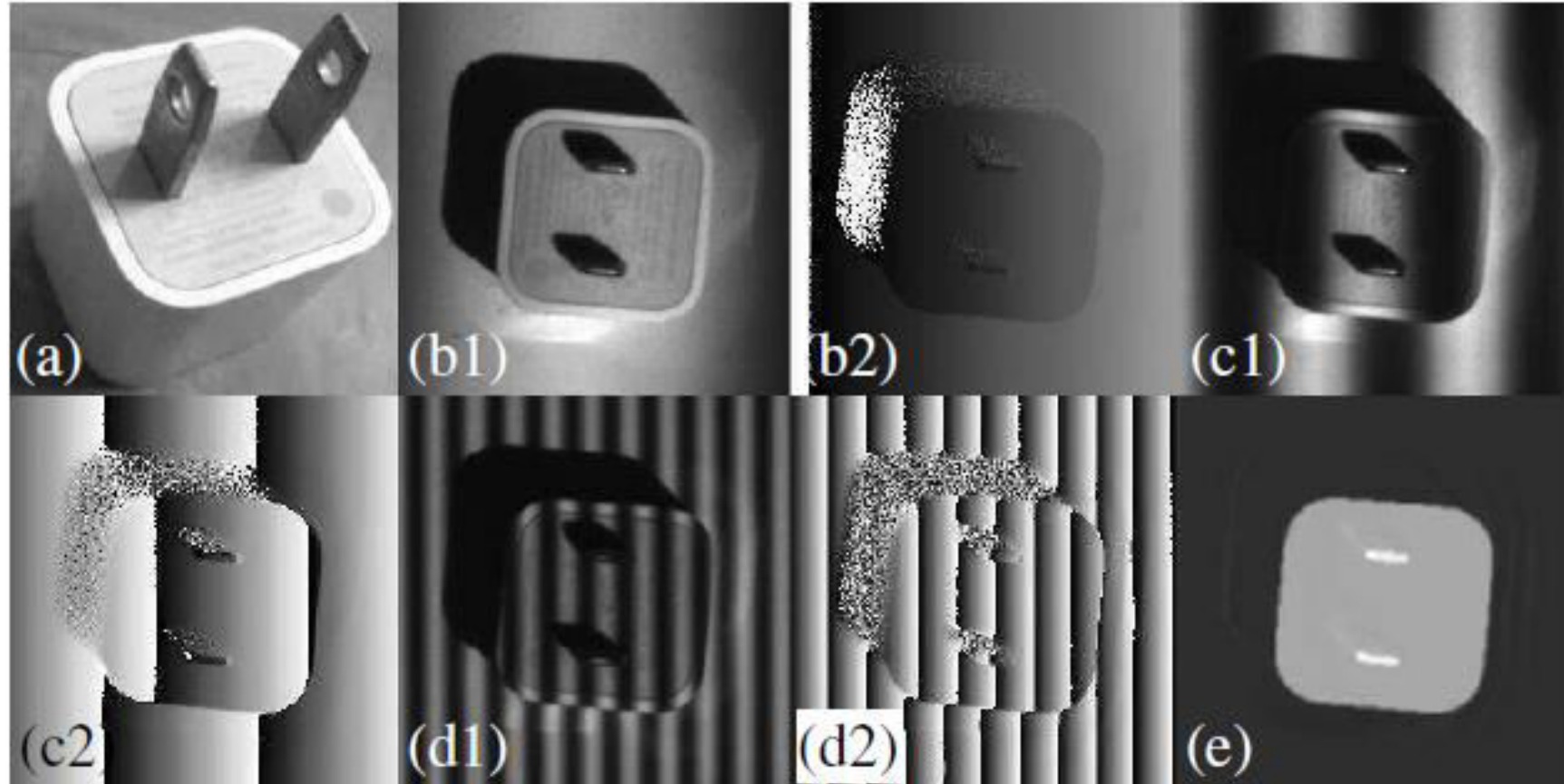
Temporal Phase Unwrapping

- Multi-frequency fringe projection



- Temporal phase unwrapping procedure
- Note that the unwrapped phase map always contains the highest frequency of the fringes.

Temporal Phase Unwrapping



Phase Calibration

- Calibration of a fringe projection system may vary according to its applications.
- If a phase-to-height relationship is required, one may measure an object with a known height and obtain a phase-to-height coefficient by removing the carrier phase component from the unwrapped phase map.
- If a 3D reconstruction of an object is the goal, a full 3D calibration is required.
- Carrier phase removal
 - Carrier fringe deformation which results in phase variations of the fringes would provide the surface profile information of an object.
 - As it is the phase variation and not the original phase of the carrier fringes that is of interest, the latter should be removed from an unwrapped phase map

Phase Calibration: Carrier phase removal

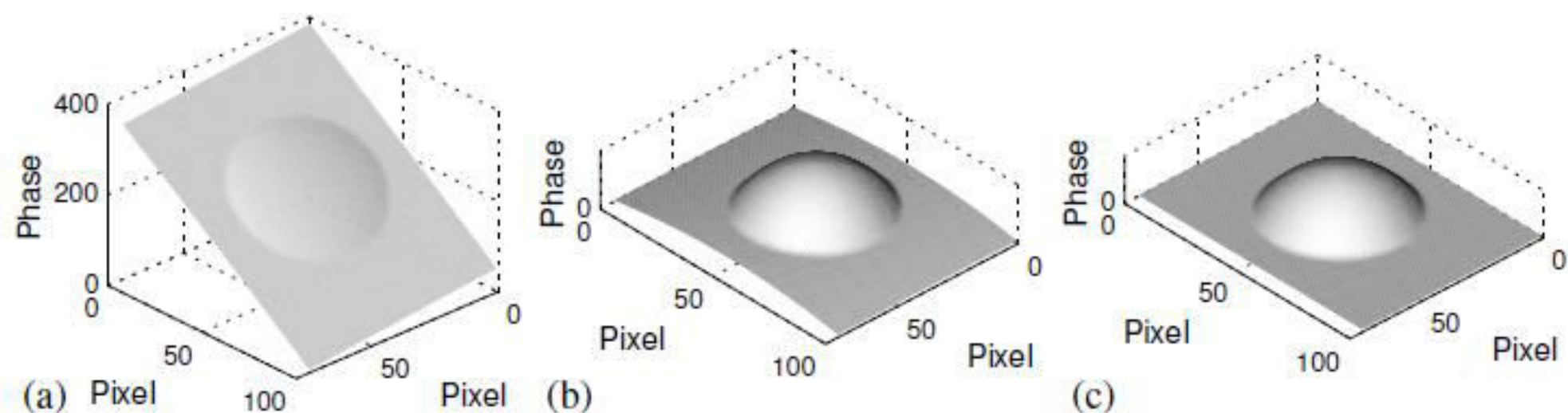
- Determine the component by a 2D polynomial function

$$\begin{aligned} & a_{0,0} + a_{0,1}x + \dots + a_{0,n}x^n \\ & a_{1,0}y + a_{1,1}xy + \dots \\ \theta_p(x, y) = & + \dots \\ & a_{n-1,0}y^{n-1} + a_{n-1,1}xy^{n-1} \\ & a_{n,0}y^n \end{aligned}$$

- Coefficient estimation: Least-squares

$$E(a_{0,0}, \dots, a_{0,n}, \dots, a_{n,0}) = \sum_{(x,y) \in U} [\theta_p(x, y) - \theta_e(x, y)]^2$$

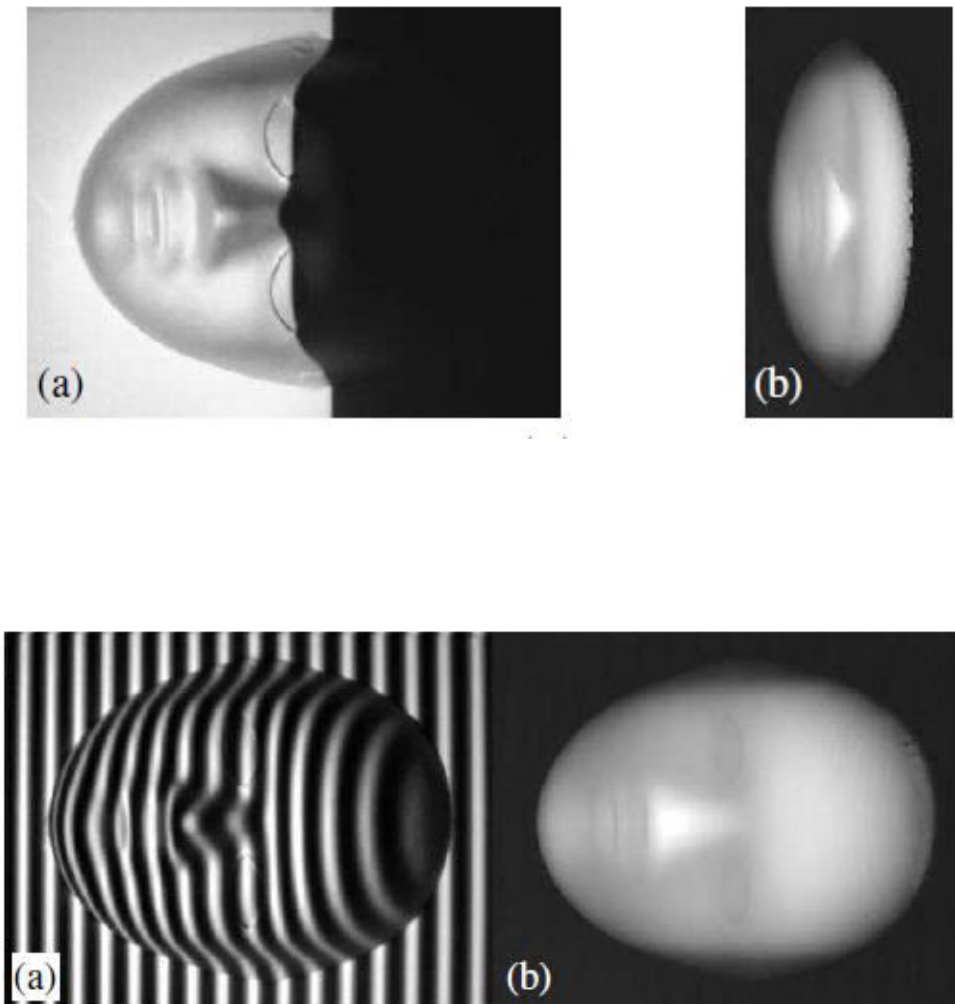
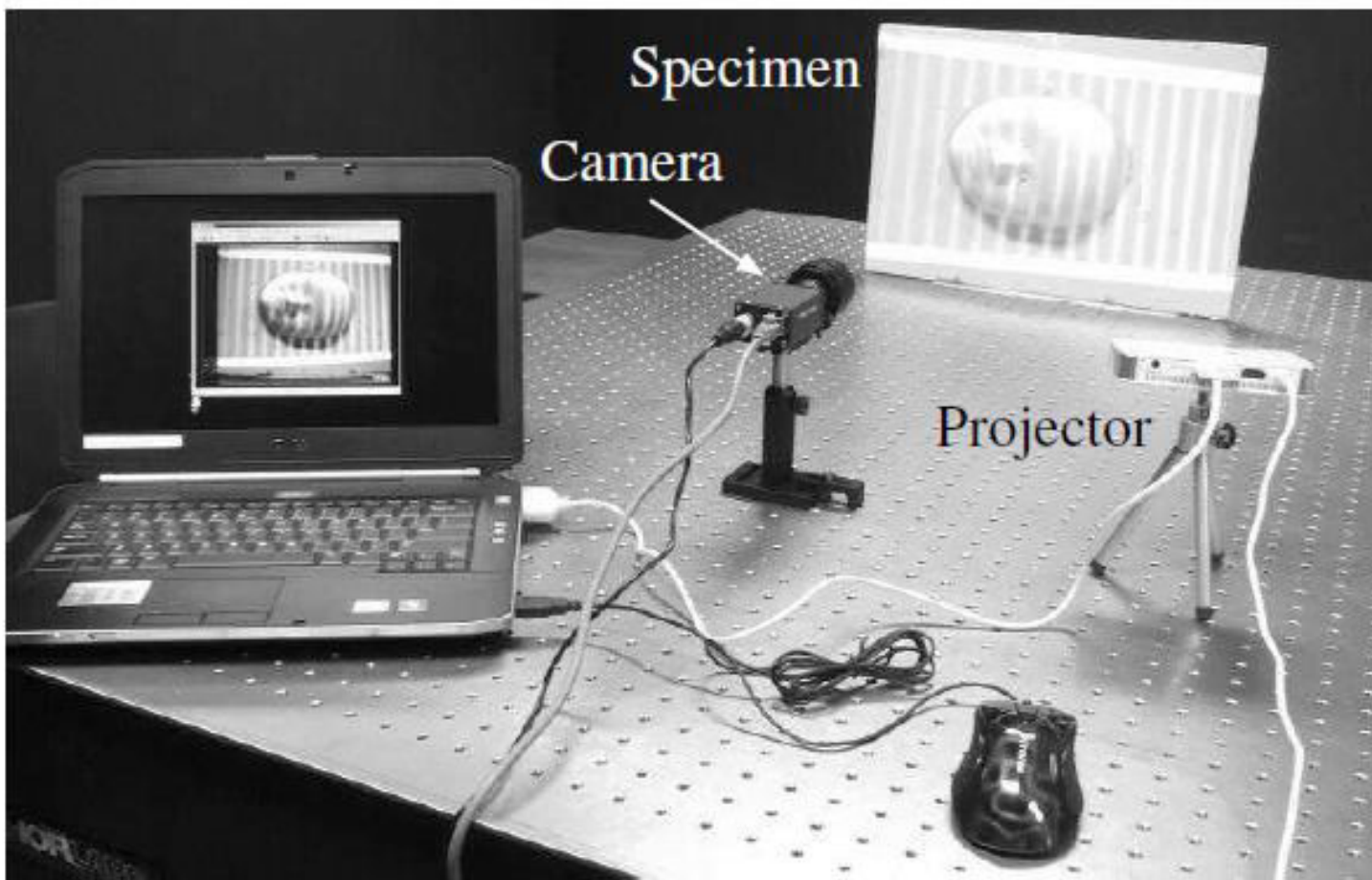
Phase Calibration: Carrier phase removal



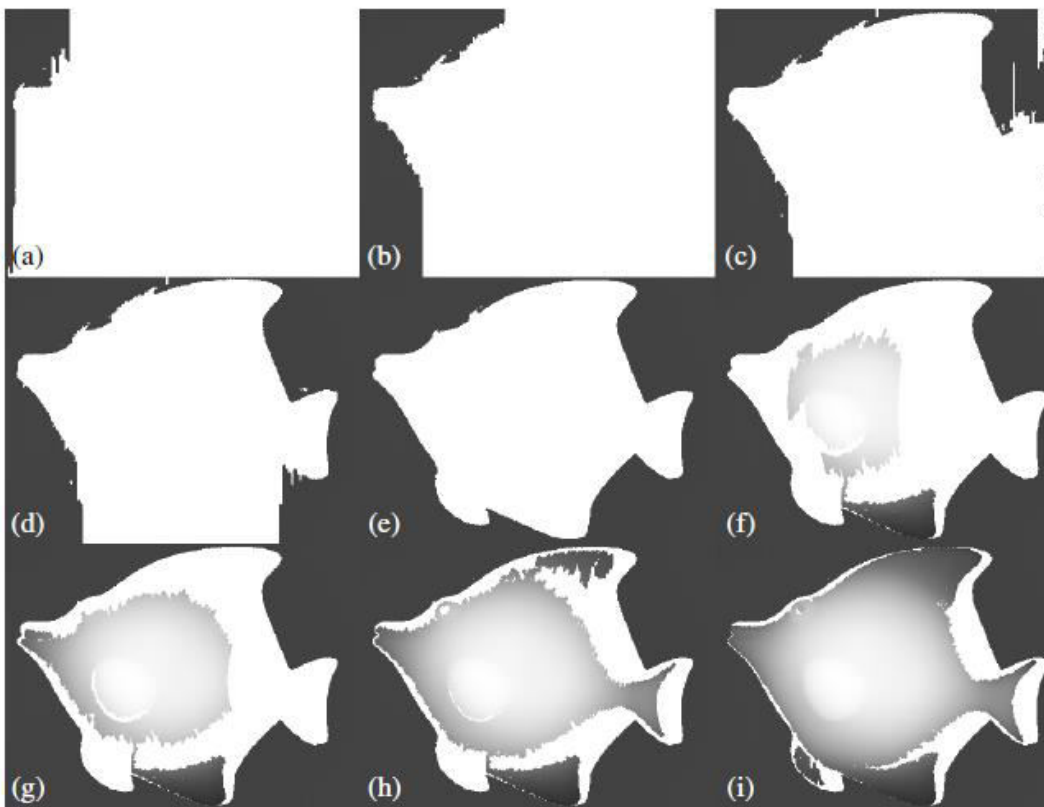
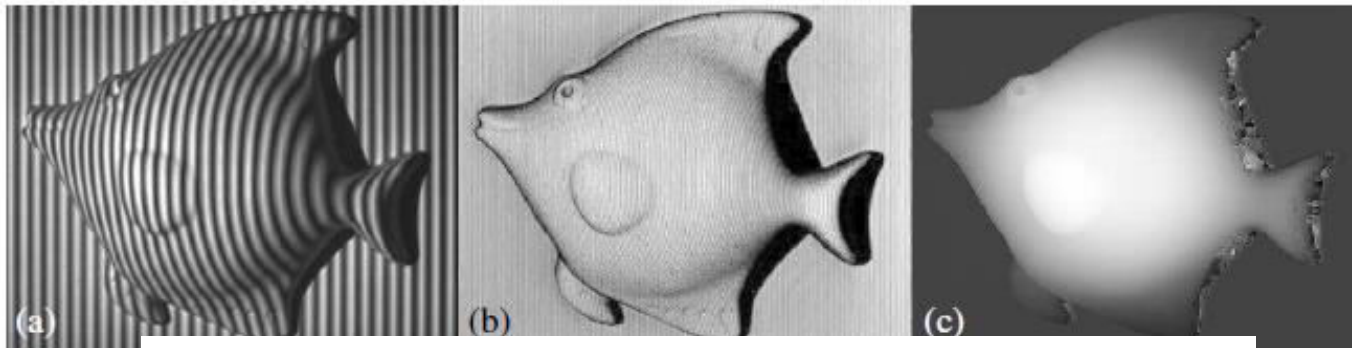
Phase Calibration: Multi-reference-plane

- Measurement pf a reference plane at several axial distances (along the z-axis) with each incremental distance kept reasonably small.
- An unwrapped phase map (without phase removal) at each position is then recorded.
- After the unwrapped phase values of an object are calculated, each pixel phase (θ_0) is compared with the corresponding pixel phase in the reference planes.
- The nearest two reference planes are obtained (phase 1 and 2) and each pixel position (along the z-axis) is interpolated from two reference positions based on the ratio of $(\theta_0 - \theta_1)/(\theta_0 - \theta_2)$.

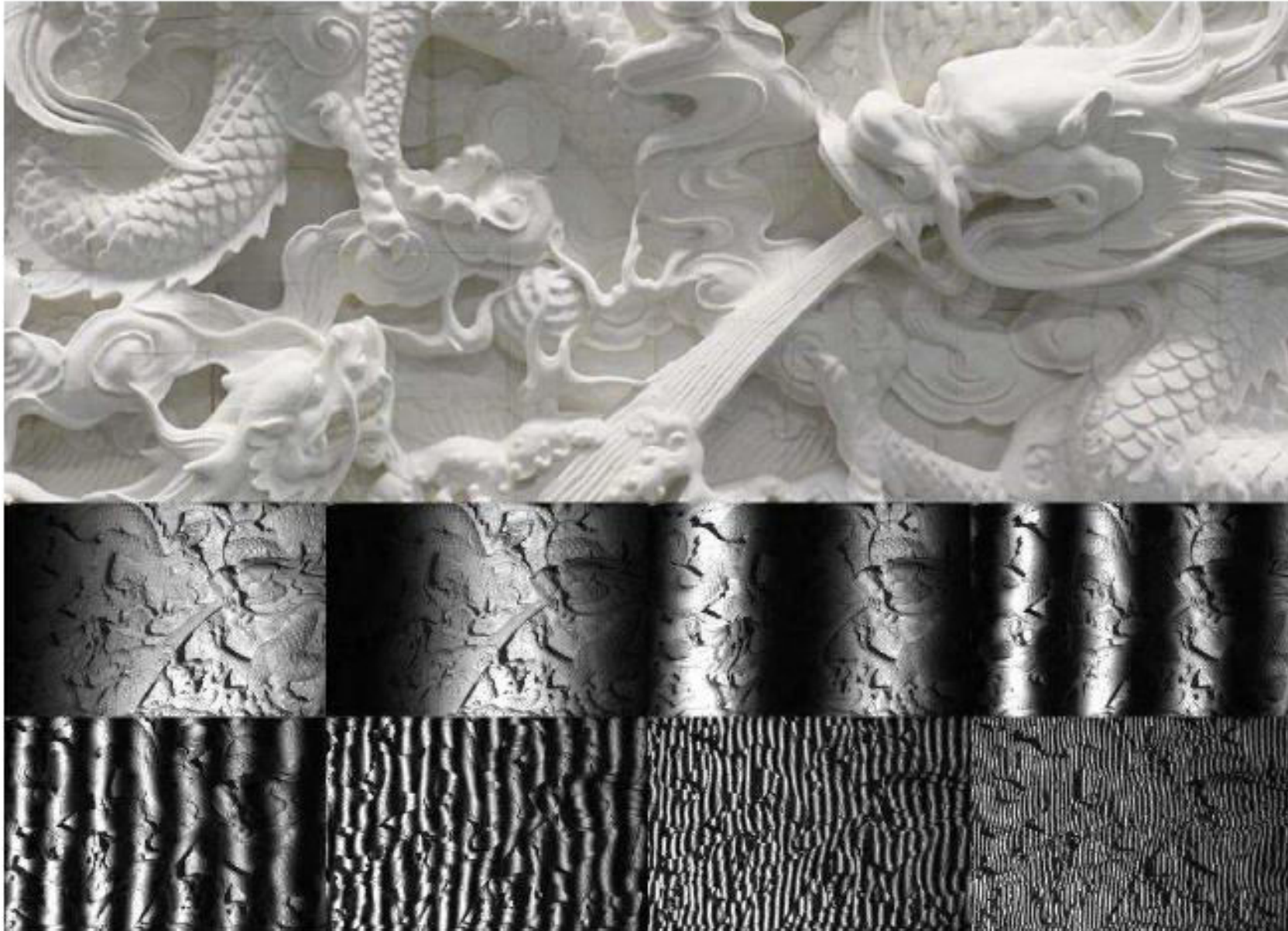
Application of Method



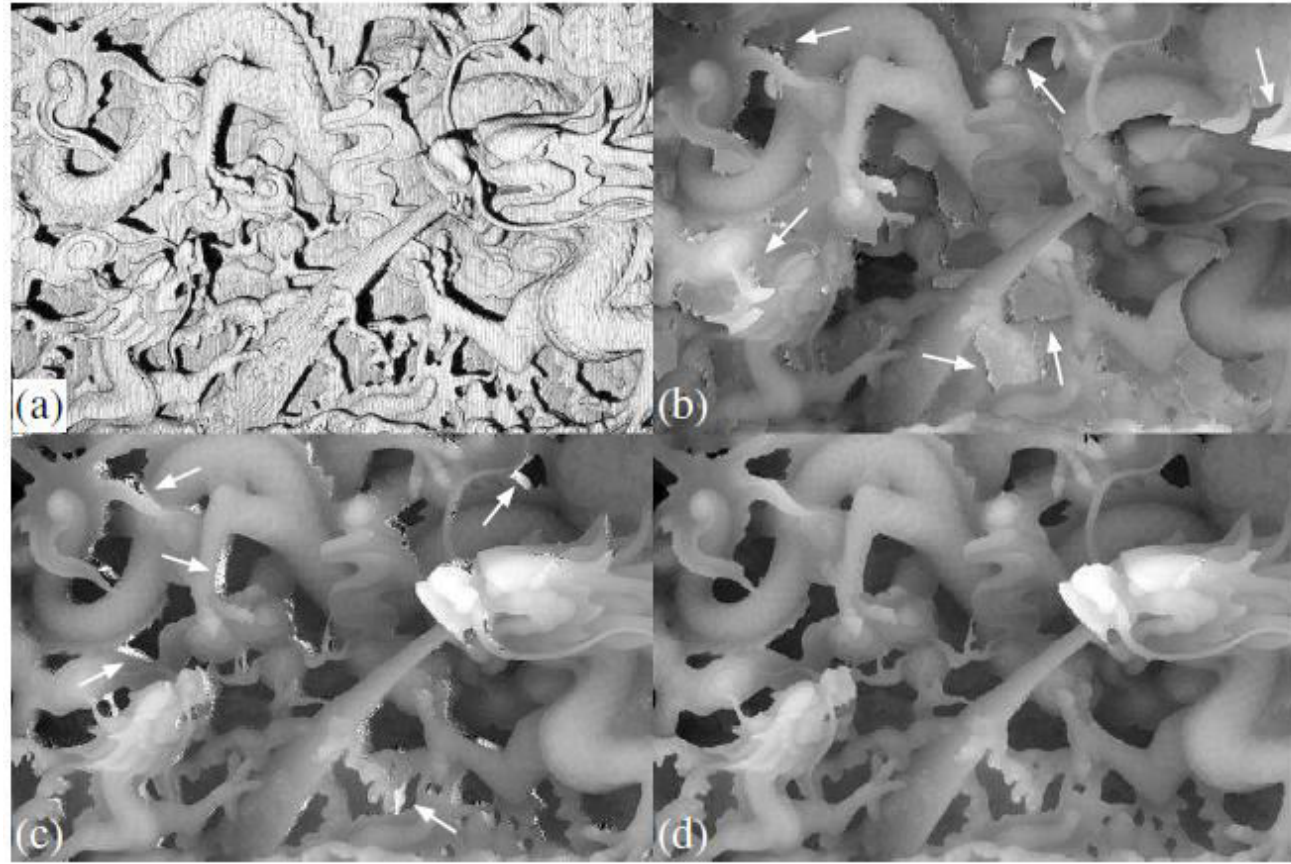
Quality guided phase unwrapping



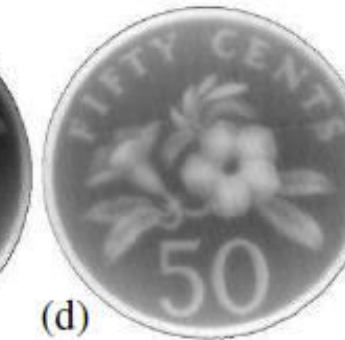
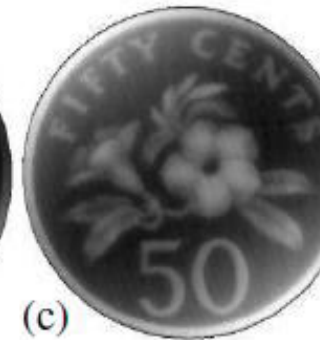
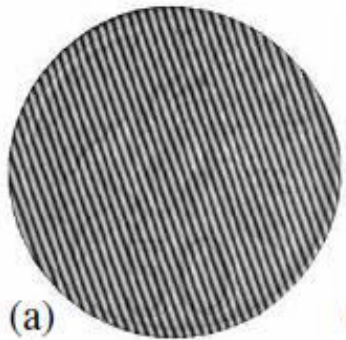
Multi-Frequency Fringe Projection



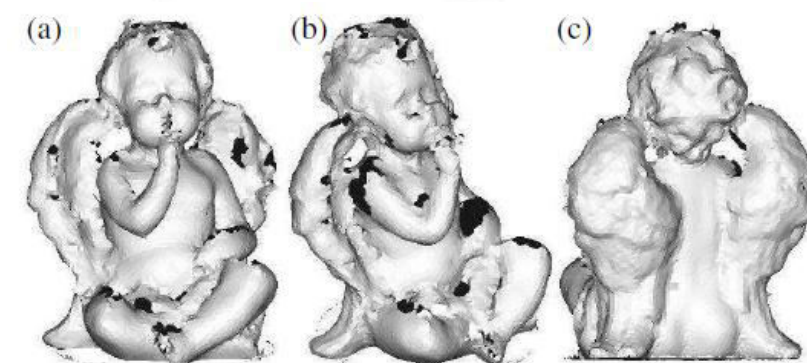
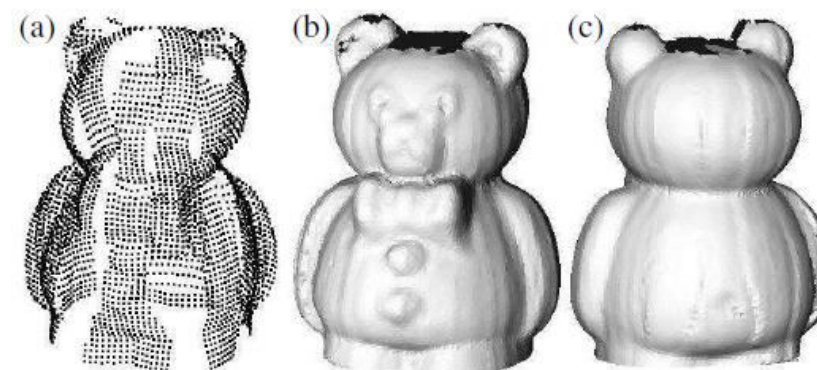
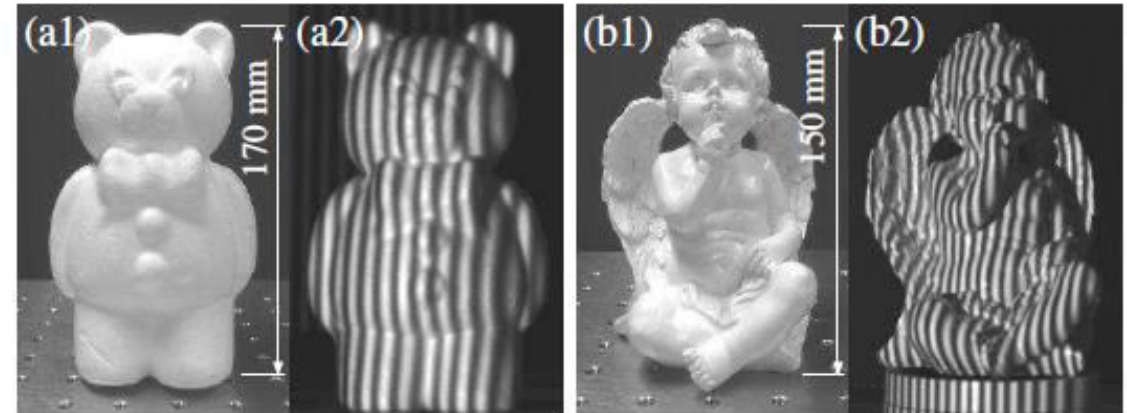
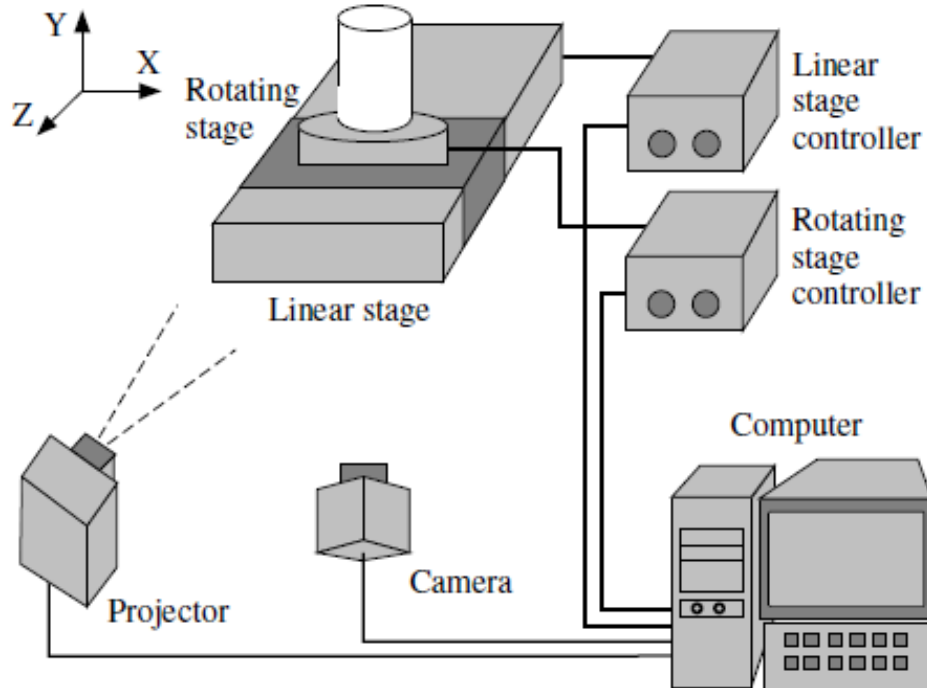
Multi-Frequency Fringe Projection



Carrier Phase Removal



360-degree Fringe Projection



Summary

- Principle of Fringe Projection Profilometry
- Steps involved in calculating height from phase
- Phase unwrapping techniques
- Practical issues
- Examples

References

- L Chen C Quan and CJ Tay, Digital Fringe Projection Profilometry, in Digital Optical Measurement Techniques and Applications, Artech House, 2015.

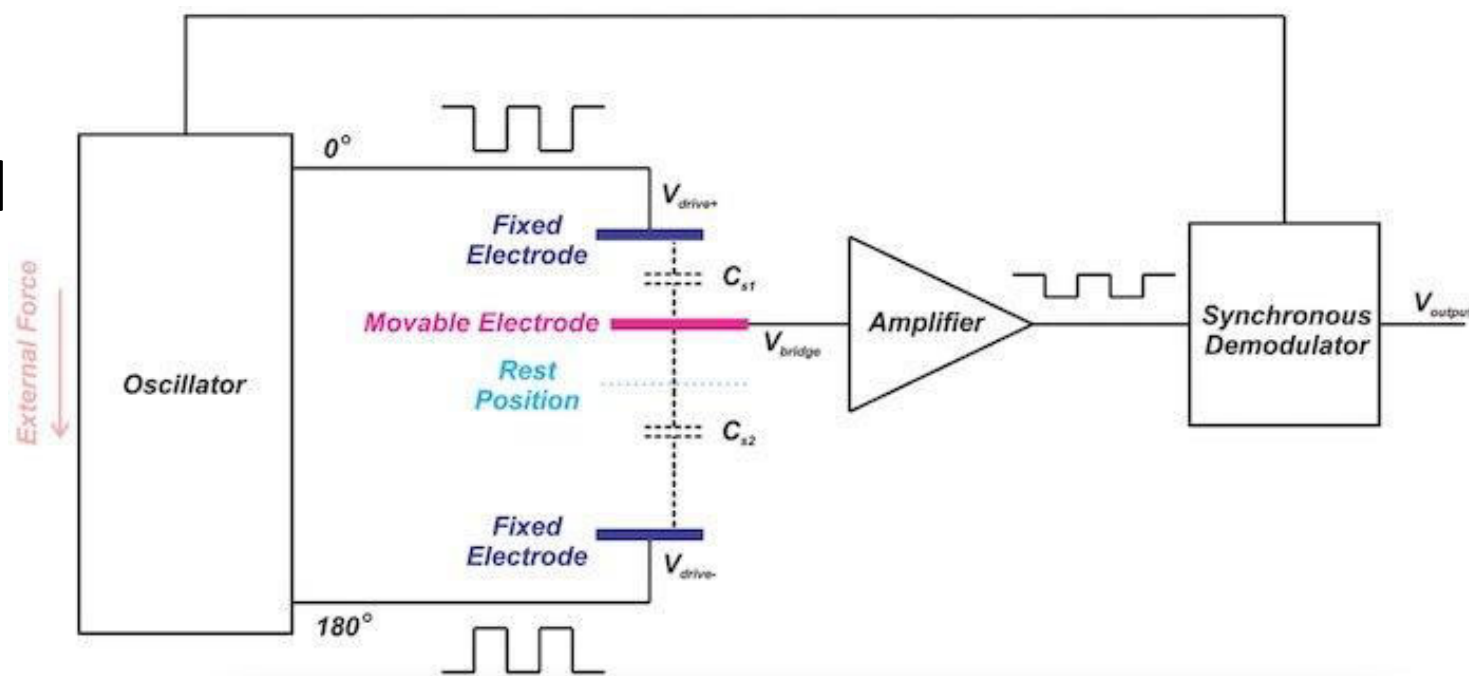
RA 505 Robot Sensing and Vision

Lecture 36

Dr. Rishikesh Kulkarni
Department of Electronics and Electrical Engineering
IIT Guwahati

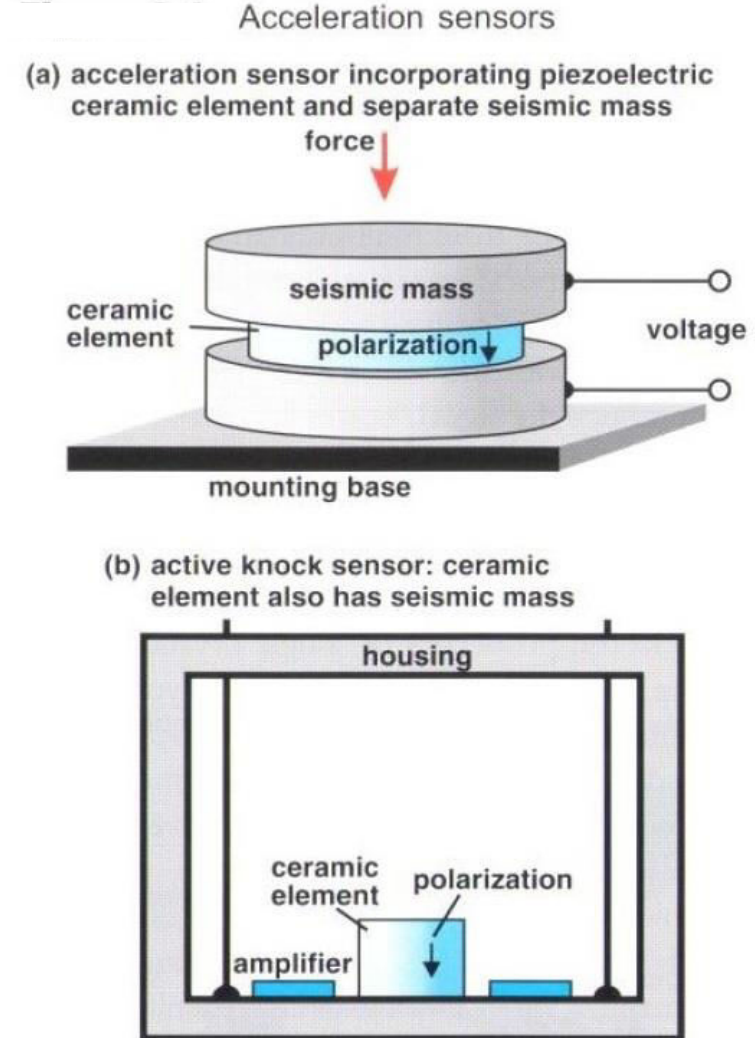
Capacitive Accelerometer

- Spring-mass system
- Change in capacitance due to change in distance between movable and fixed plate

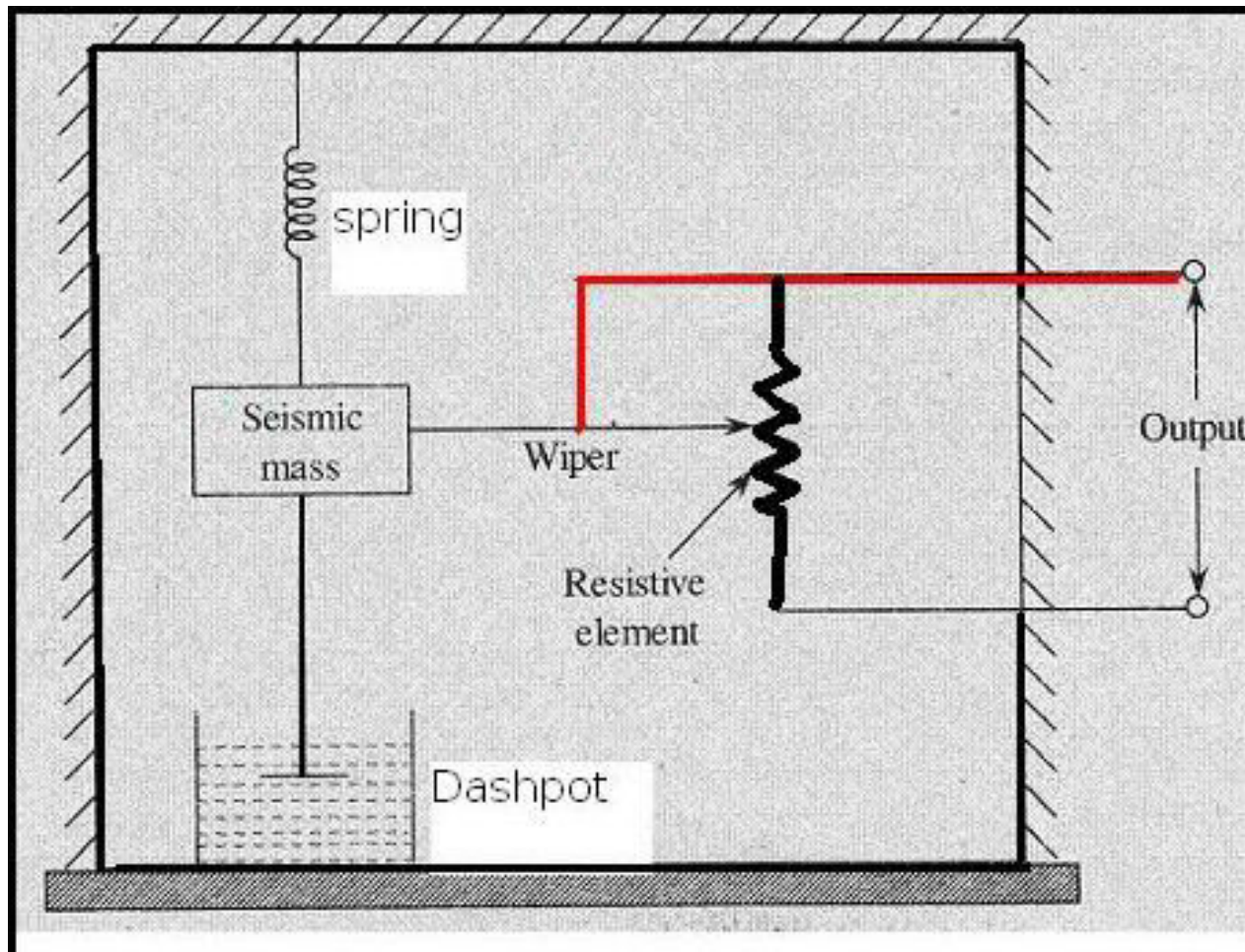


Piezoelectric Accelerometer

- Piezoelectric material slice: Polarized ceramic
- Advantages
 - Frequency response
 - Temperature stability
 - Ruggedness
 - Adaptability
 - Electrical characteristics

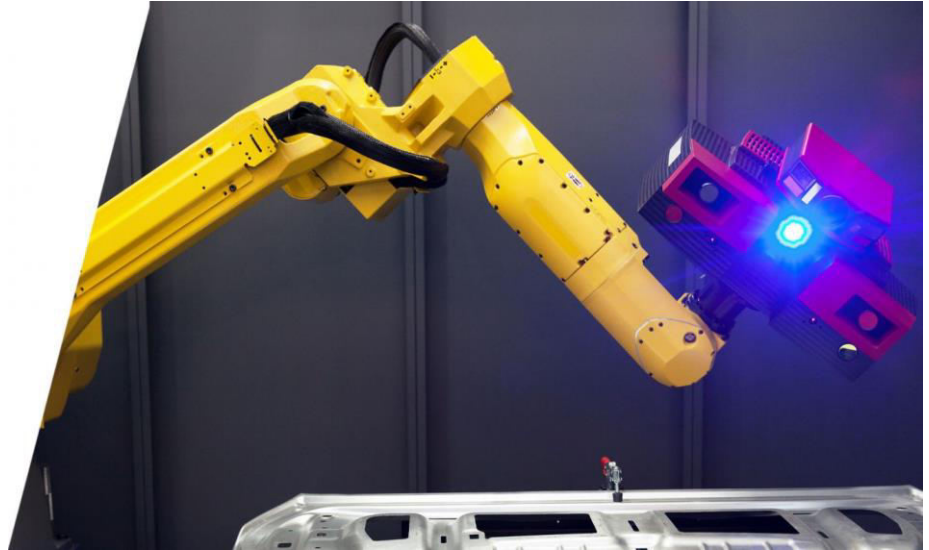


Potentiometric Accelerometer



Structured Light Illumination

- Introduction
- Principle of Method
 - Triangulation
 - Fringe Projection
 - Phase Evaluation
 - Phase Calibration
- Applications of Method
 - Line Scan and Fringe Projection
 - Quality Guided Phase Unwrapping
 - Multifrequency Fringe Projection
 - Carrier Phase Removal
 - 360-degree Fringe Projection
- Concluding Remarks

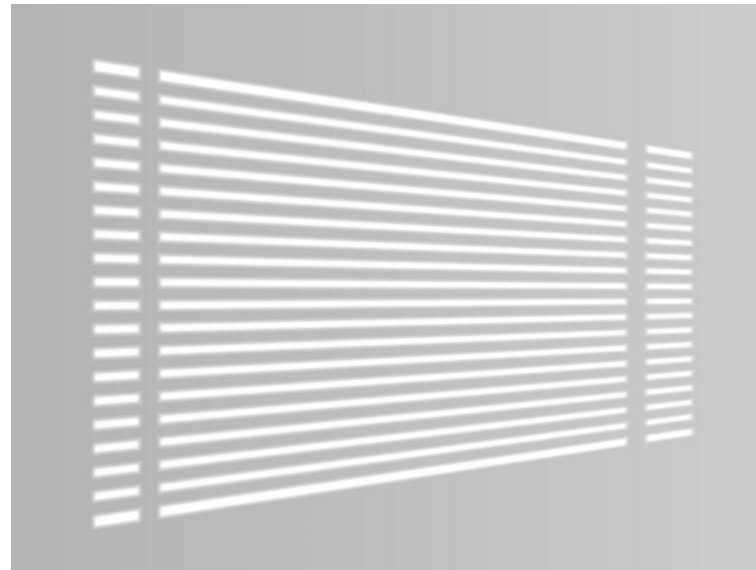


Introduction

- Data-processing methods based on those developed for interferometry
- Interferometry is based on the optical path difference and fringe projection profilometry is based on principle of triangulation.
- Projection of a pattern generated using gratings or a digital projector.

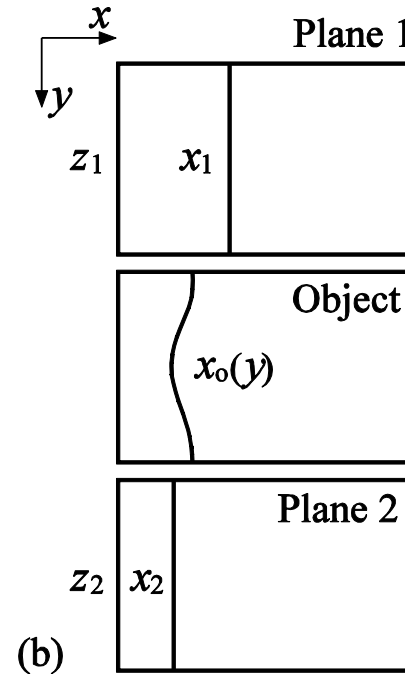
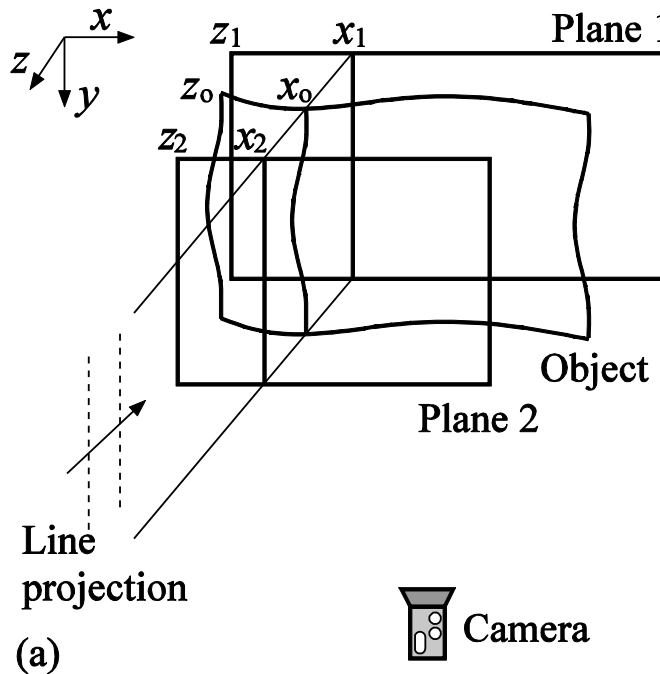
Principle of Method

- Principle of FPP is based on '*Principle of Triangulation*'.



- Quantitative phase evaluation and calibration of the phase values against standard results yields the actual profile of an object.

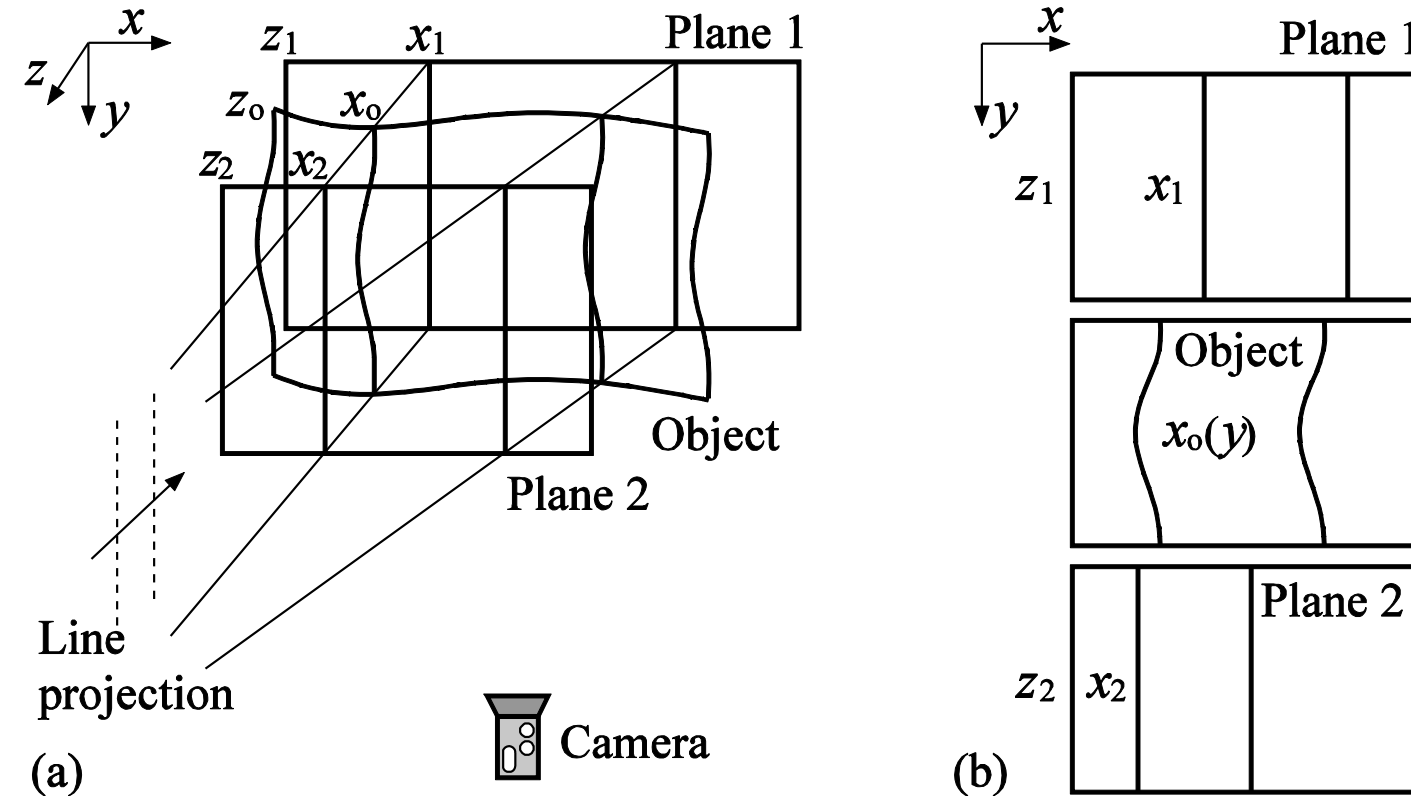
Fringe Projection



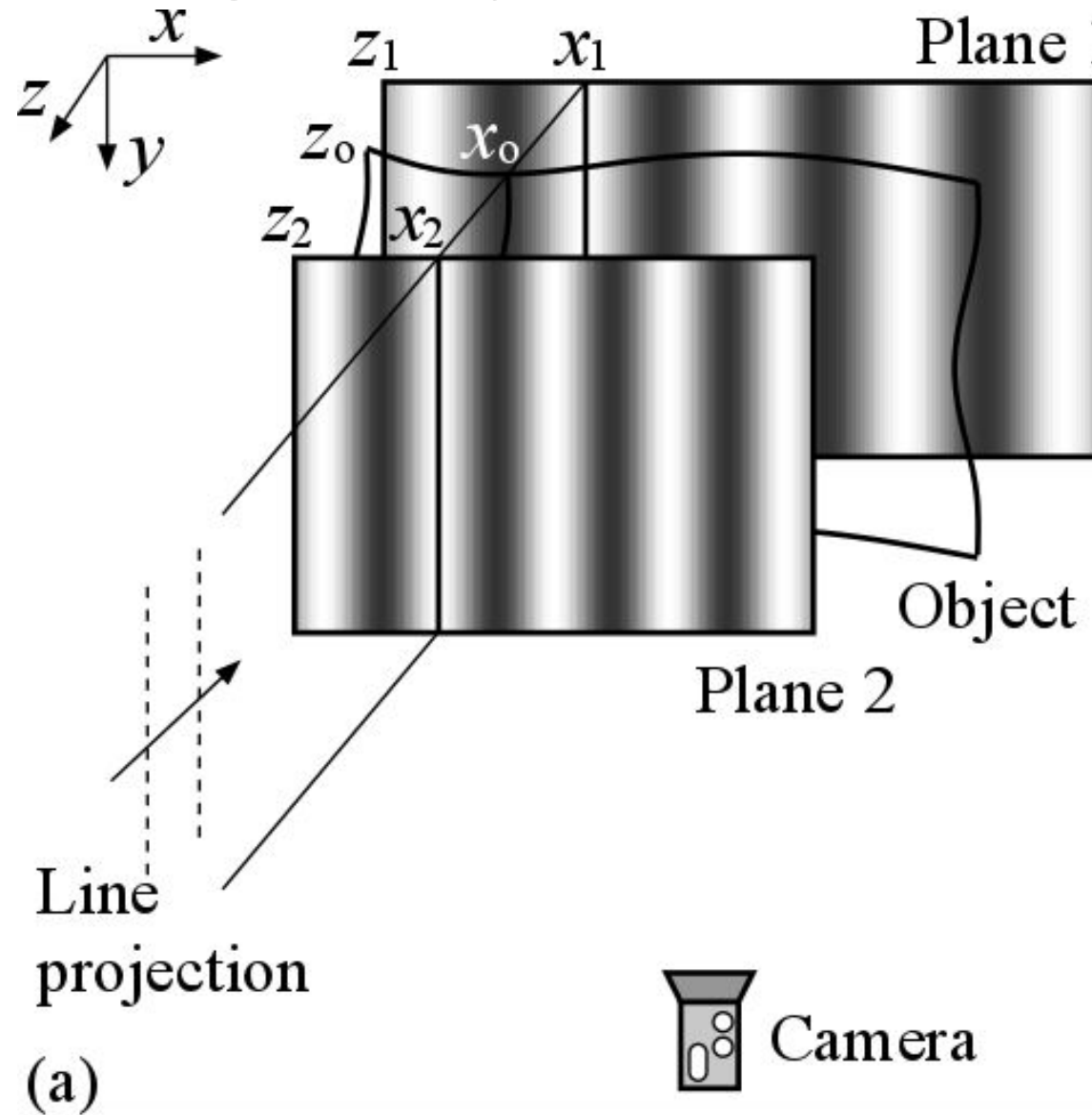
$$\frac{z_o - z_1}{z_2 - z_1} = \frac{x_o - x_1}{x_2 - x_1}$$

- How do we obtain a whole-field depth map of an object?
- Line-scan method

Fringe Projection: Line-scan method



Fringe Projection: Phase-based method



Advantages of using a fringe pattern

1. One single image would provide information on the entire surface and hence scanning is not needed.
2. The problem of a gap between two projected lines no longer exists as every point on the surface is sampled.
3. The order of a phase value at each point can be detected accurately by various methods (discussed next).
4. The accuracy is related to that of phase measurement, which is much higher than the accuracy of the line detection method.

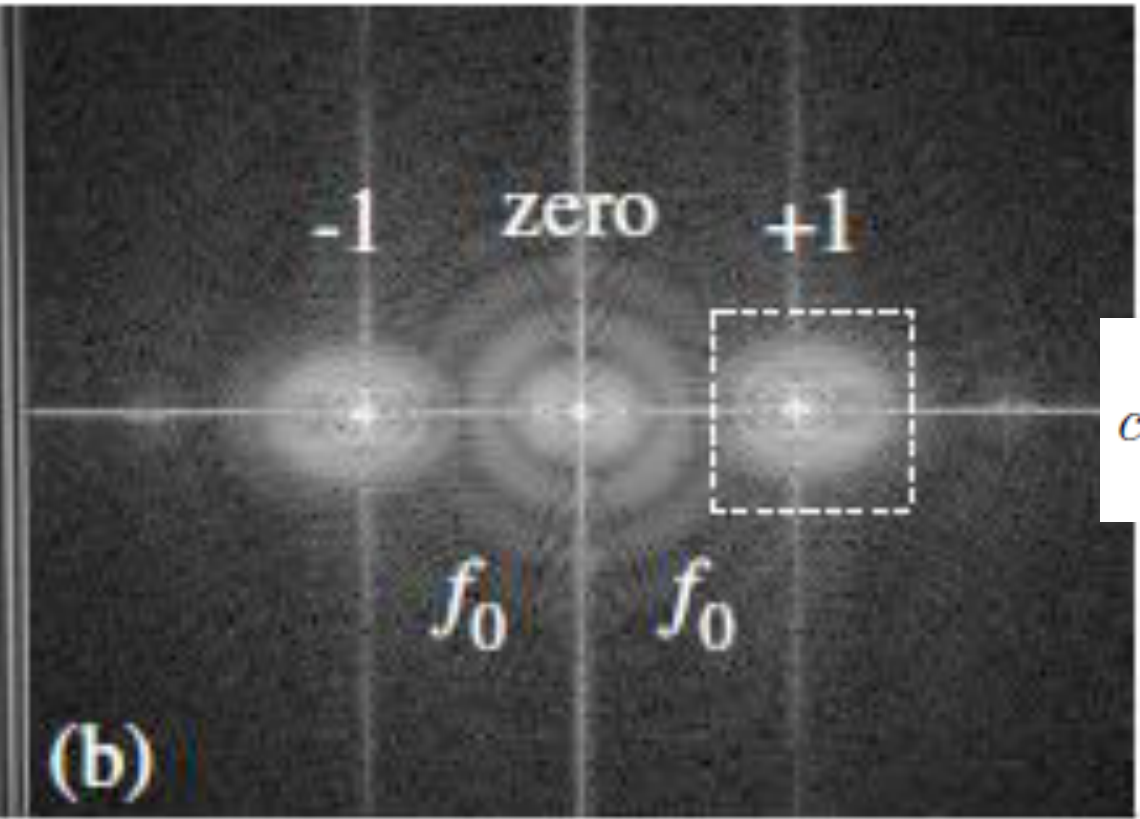
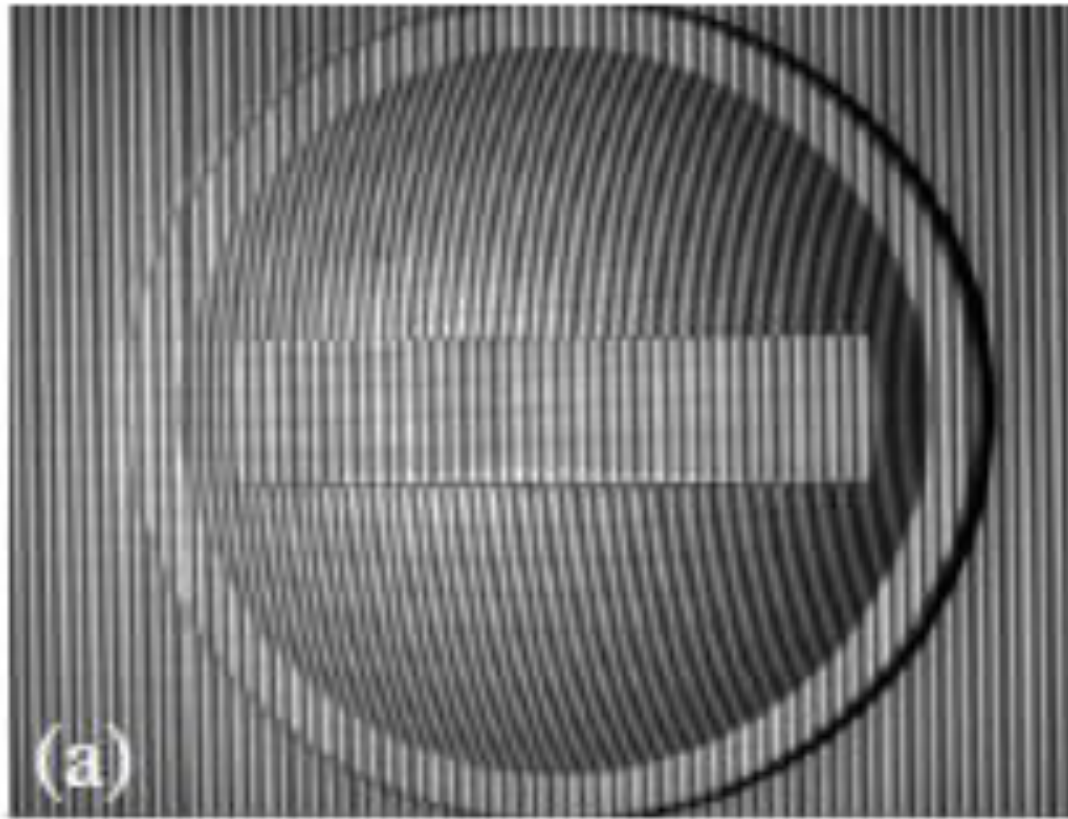
Phase Evaluation

- In the fringe projection method, it is important to obtain the correct phase for each pixel of a fringe pattern.
- This is carried out in two steps: *wrapped phase extraction* and *phase unwrapping*.
- Fourier Transform:
 - The spatial intensity distribution of a fringe pattern is sinusoidal in the direction of progressing phase

$$I(x, y) = a(x, y) + b(x, y) \cos \theta(x, y)$$

$$I = a + \frac{be^{j\theta}}{2} + \frac{be^{-j\theta}}{2}$$

Phase Evaluation: Fourier Transform

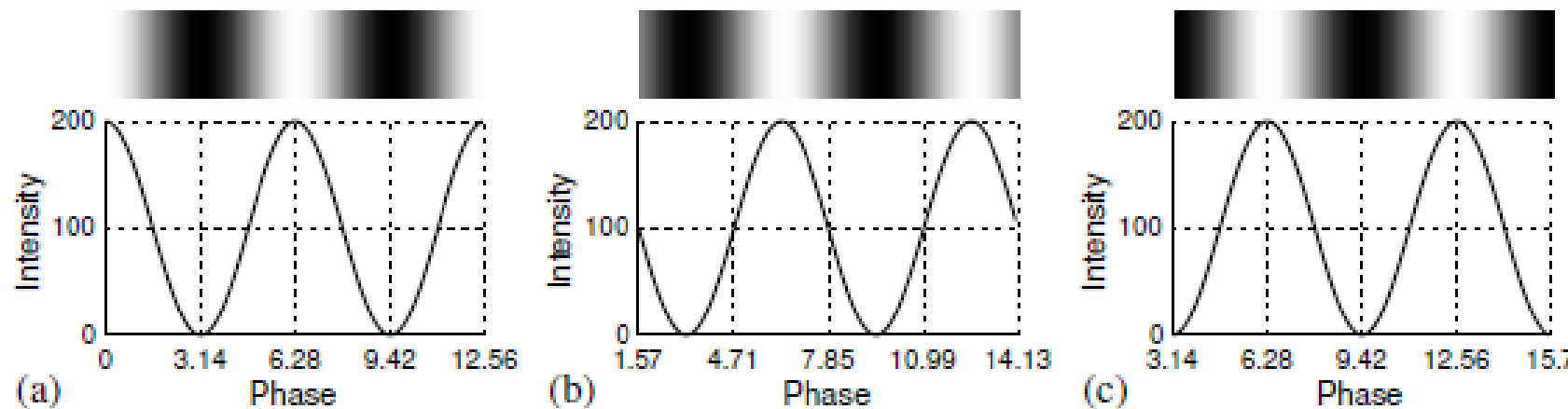


$$c = \frac{be^{j\theta}}{2} =$$

$$\theta = \arctan$$

Phase Evaluation: Phase-Shifting

- Phase-shifting method requires the input of at least three phase-shifted fringe patterns as in a sinusoidal intensity distribution there are three unknowns.
- Generating a phase-shifted fringe pattern is straightforward: this is done by changing the initial phase of a fringe pattern and project them sequentially onto the object



Phase Evaluation: Phase-Shifting

- The intensity of a pixel in a fringe pattern, which is phase-shifted n times, is expressed as

$$I_i = a + b \cos(\theta + \delta_i)$$

- If n is 3, the unknowns a , b and θ can be determined. If n is more than 3, the unknowns can be obtained using least-squares error.

$$I_i = a + b \cos \theta \cos \delta_i - b \sin \theta \sin \delta_i$$

- Let $B = b \cos \theta$ and $C = -b \sin \theta$

$$E(a, B, C) = \sum_{i=1}^n (I_i - a - B \cos \delta_i - C \sin \delta_i)^2$$

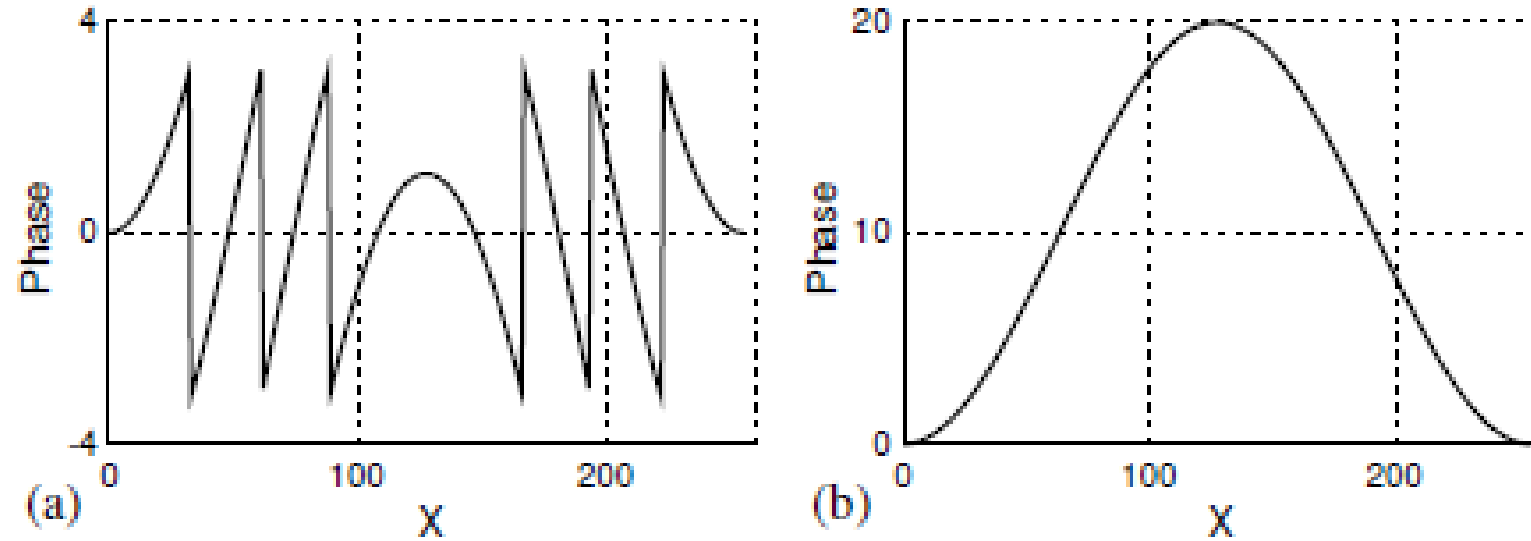
Phase Evaluation: Phase-Shifting

$$\sum_{i=1}^n \begin{bmatrix} 1 & \cos \delta_i & \sin \delta_i \\ \cos \delta_i & \cos^2 \delta_i & \sin \delta_i \cos \delta_i \\ \sin \delta_i & \sin \delta_i \cos \delta_i & \sin^2 \delta_i \end{bmatrix} \begin{bmatrix} a \\ B \\ C \end{bmatrix} = \sum_{i=1}^n \begin{bmatrix} I_i \\ I_i \cos \delta_i \\ I_i \sin \delta_i \end{bmatrix}$$

$$\theta = \arctan \frac{-C}{B}$$

Spatial Phase Unwrapping

- After obtaining a wrapped phase map, the next step is to unwrap the phase values to recover a continuous phase distribution without a 2π jump.



- The problem of phase unwrapping becomes significantly complicated in 2D due to the many possible unwrapping paths (as opposed to only one path in the 1D case)

Quality Guided Phase Unwrapping

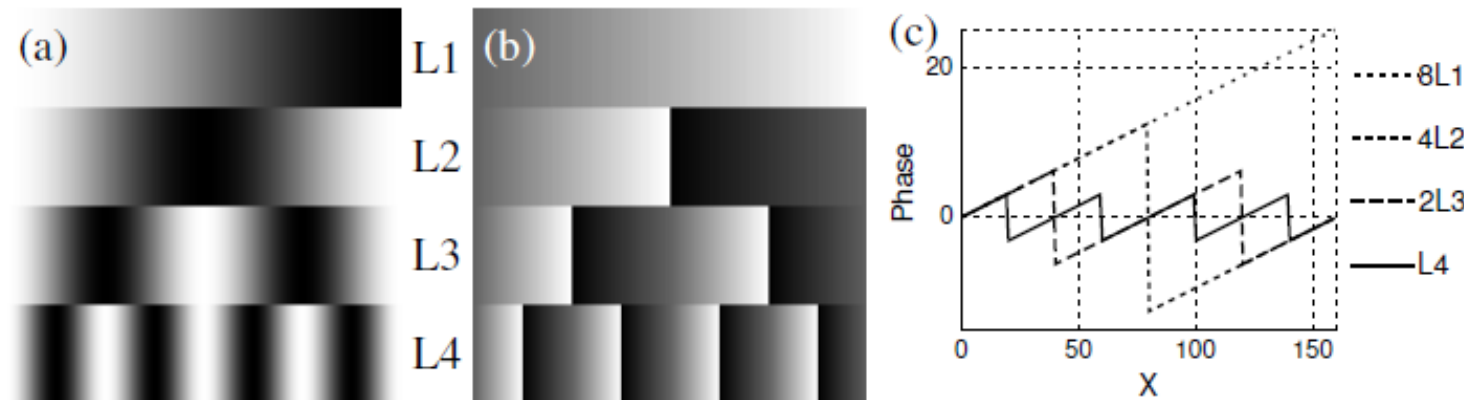
- A particularly effective approach for phase unwrapping is known as quality- guided phase unwrapping.
- It relies on a quality map to determine an unwrapping path.
- At each step, after the current pixel is processed, the next pixel to be processed is determined by a pixel with the highest quality on the propagation boundary.
- This method ensures the unwrapping path moves quickly to a higher quality region before moving to a lower quality region where errors are more likely to be encountered.
- The method is effective for phase fringes where the fringe contrast, which is defined as the ratio between the modulation and background intensity: b/a , is an accurate quality indicator.
- The modulation and background intensity can be obtained from the phase-shifting algorithm.
- Low fringe contrast is usually due to a dark region where a light beam is not able to reach, resulting in a low signal-to-noise ratio, consequently inaccurate results.
- The quality-guided phase unwrapping algorithm would process these low fringe contrast regions at the last stage to minimize error accumulation.

Temporal Phase Unwrapping

- Though spatial phase unwrapping is speedy and requires only one wrapped phase map, there are certain limitations.
- For example, if an object profile is complicated, spatial phase unwrapping often produces suboptimal results.
- In cases where a field of view contains multiple objects whose profiles are disconnected or of different heights, spatial approach may not be able to produce the intended results.
- Unlike spatial phase unwrapping that relies on a pixel's neighbouring pixels to determine its phase value, temporal phase unwrapping deals with each pixel individually
- The method relies on different calculated phase values of a pixel to determine its actual phase value.

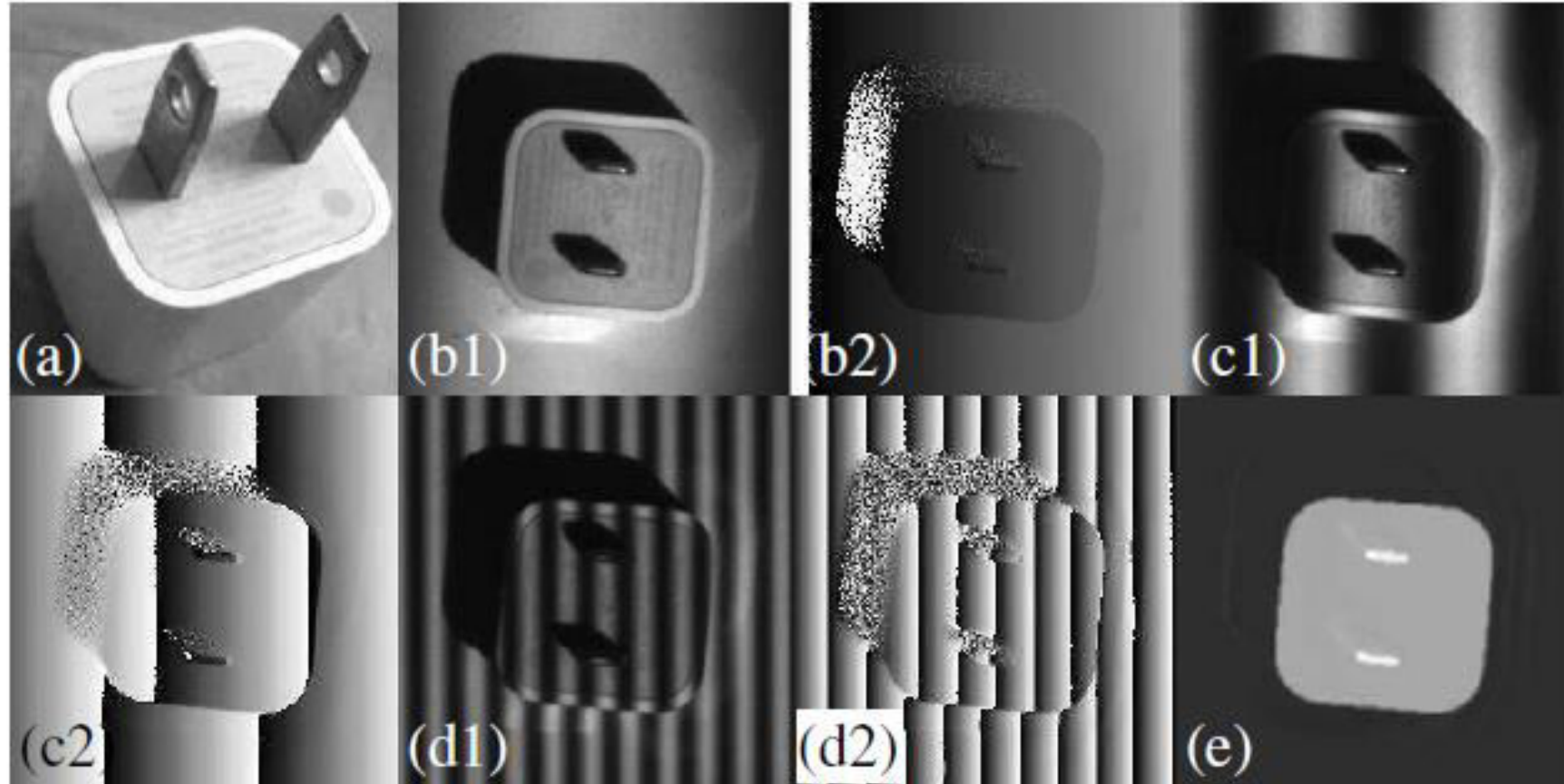
Temporal Phase Unwrapping

- Multi-frequency fringe projection



- Temporal phase unwrapping procedure
- Note that the unwrapped phase map always contains the highest frequency of the fringes.

Temporal Phase Unwrapping



Phase Calibration

- Calibration of a fringe projection system may vary according to its applications.
- If a phase-to-height relationship is required, one may measure an object with a known height and obtain a phase-to-height coefficient by removing the carrier phase component from the unwrapped phase map.
- If a 3D reconstruction of an object is the goal, a full 3D calibration is required.
- Carrier phase removal
 - Carrier fringe deformation which results in phase variations of the fringes would provide the surface profile information of an object.
 - As it is the phase variation and not the original phase of the carrier fringes that is of interest, the latter should be removed from an unwrapped phase map

Phase Calibration: Carrier phase removal

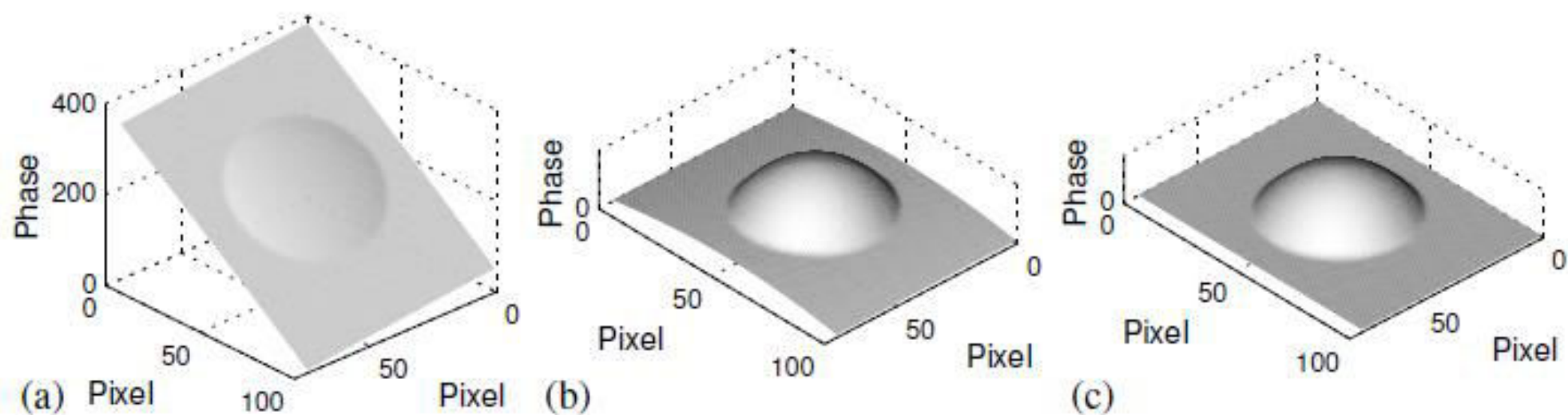
- Determine the component by a 2D polynomial function

$$\begin{aligned} & a_{0,0} + a_{0,1}x + \dots + a_{0,n}x^n \\ & a_{1,0}y + a_{1,1}xy + \dots \\ \theta_p(x, y) = & + \dots \\ & a_{n-1,0}y^{n-1} + a_{n-1,1}xy^{n-1} \\ & a_{n,0}y^n \end{aligned}$$

- Coefficient estimation: Least-squares

$$E(a_{0,0}, \dots, a_{0,n}, \dots, a_{n,0}) = \sum_{(x,y) \in U} [\theta_p(x, y) - \theta_e(x, y)]^2$$

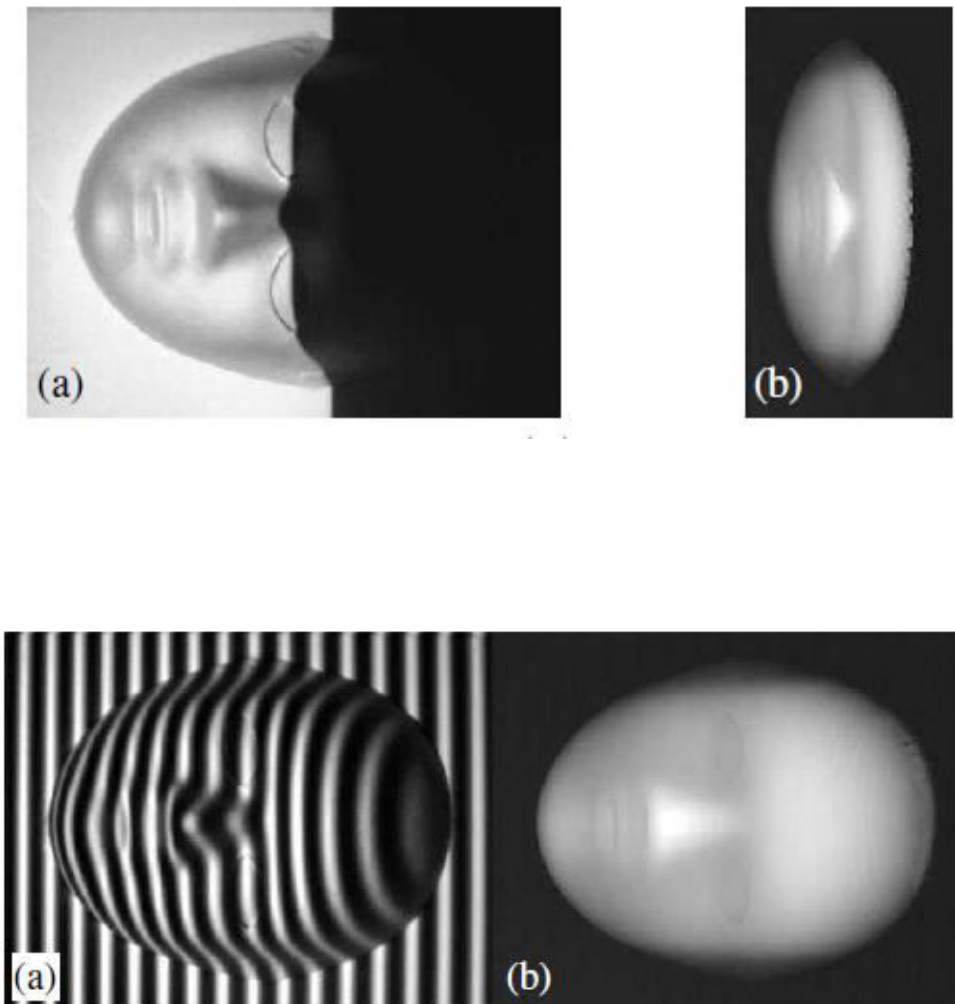
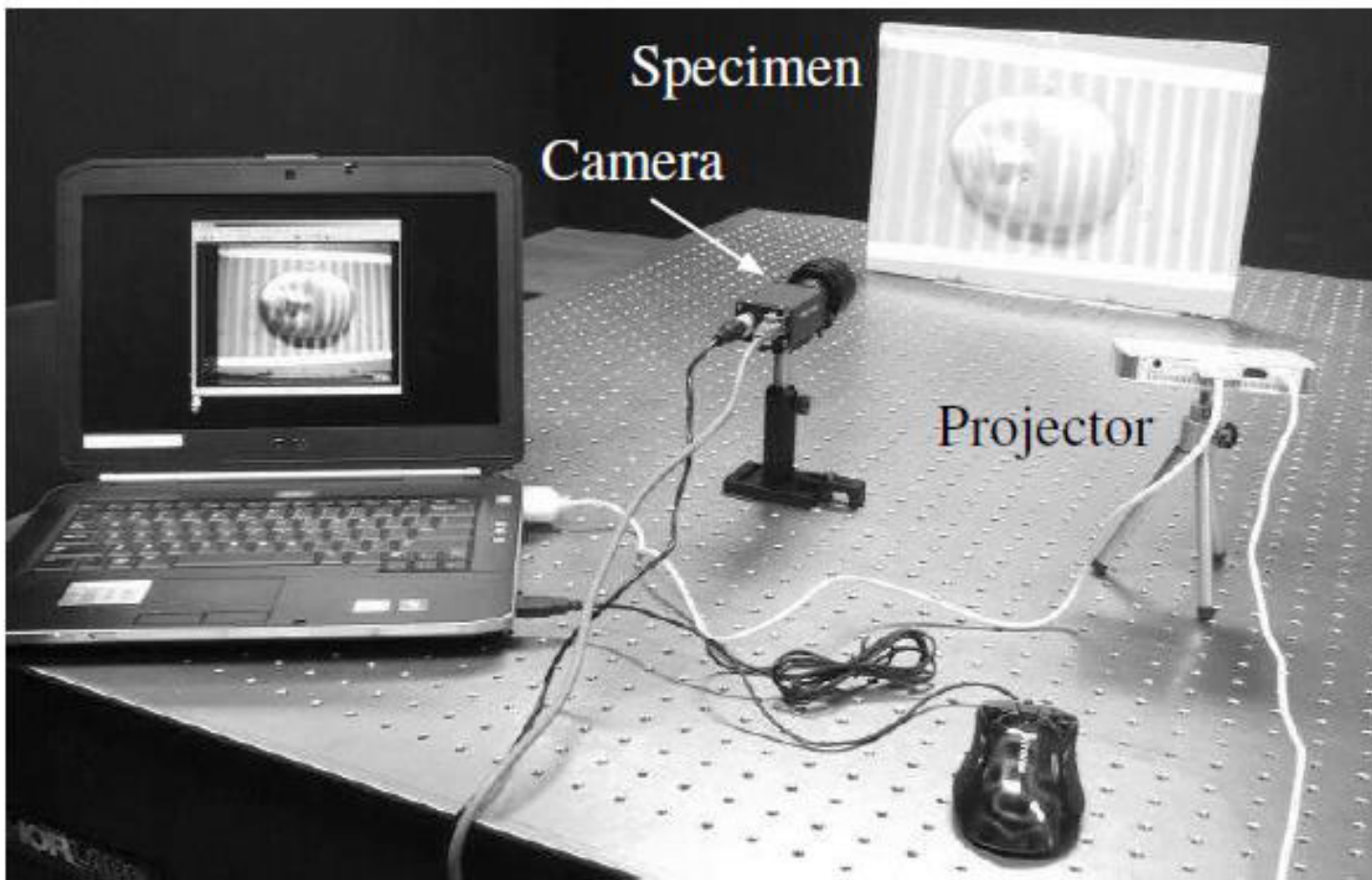
Phase Calibration: Carrier phase removal



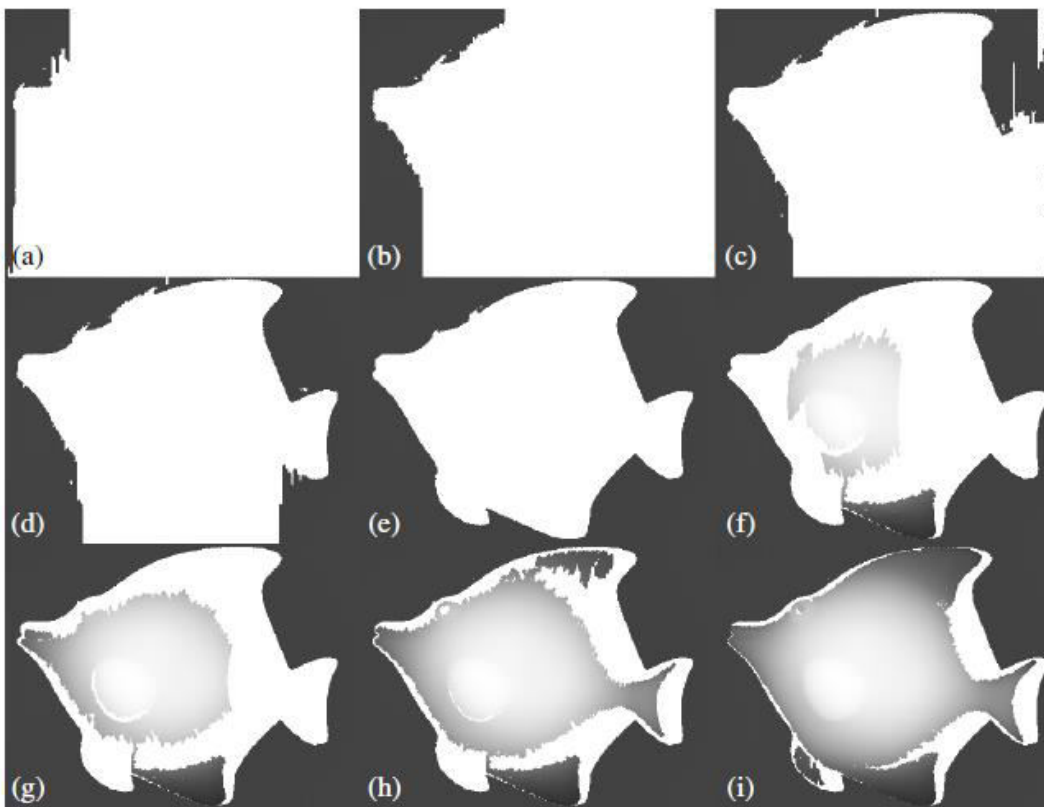
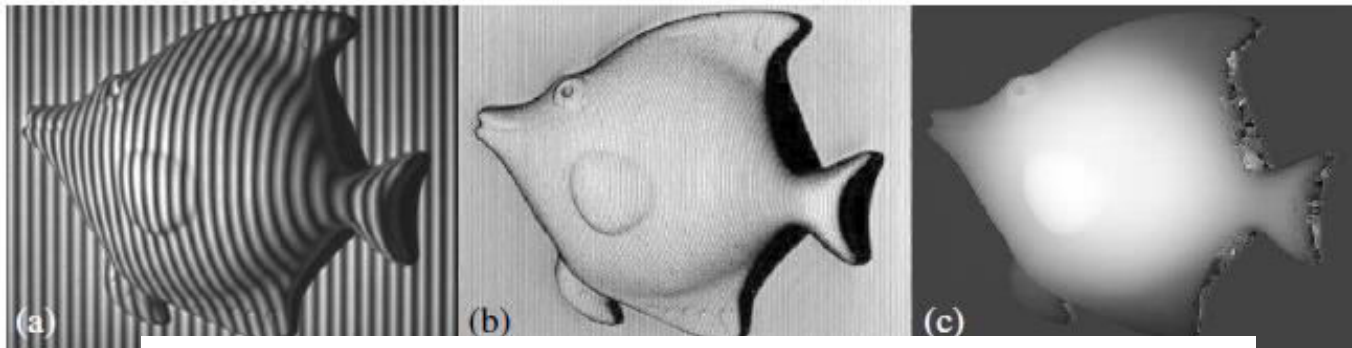
Phase Calibration: Multi-reference-plane

- Measurement pf a reference plane at several axial distances (along the z-axis) with each incremental distance kept reasonably small.
- An unwrapped phase map (without phase removal) at each position is then recorded.
- After the unwrapped phase values of an object are calculated, each pixel phase (θ_0) is compared with the corresponding pixel phase in the reference planes.
- The nearest two reference planes are obtained (phase 1 and 2) and each pixel position (along the z-axis) is interpolated from two reference positions based on the ratio of $(\theta_0 - \theta_1)/(\theta_0 - \theta_2)$.

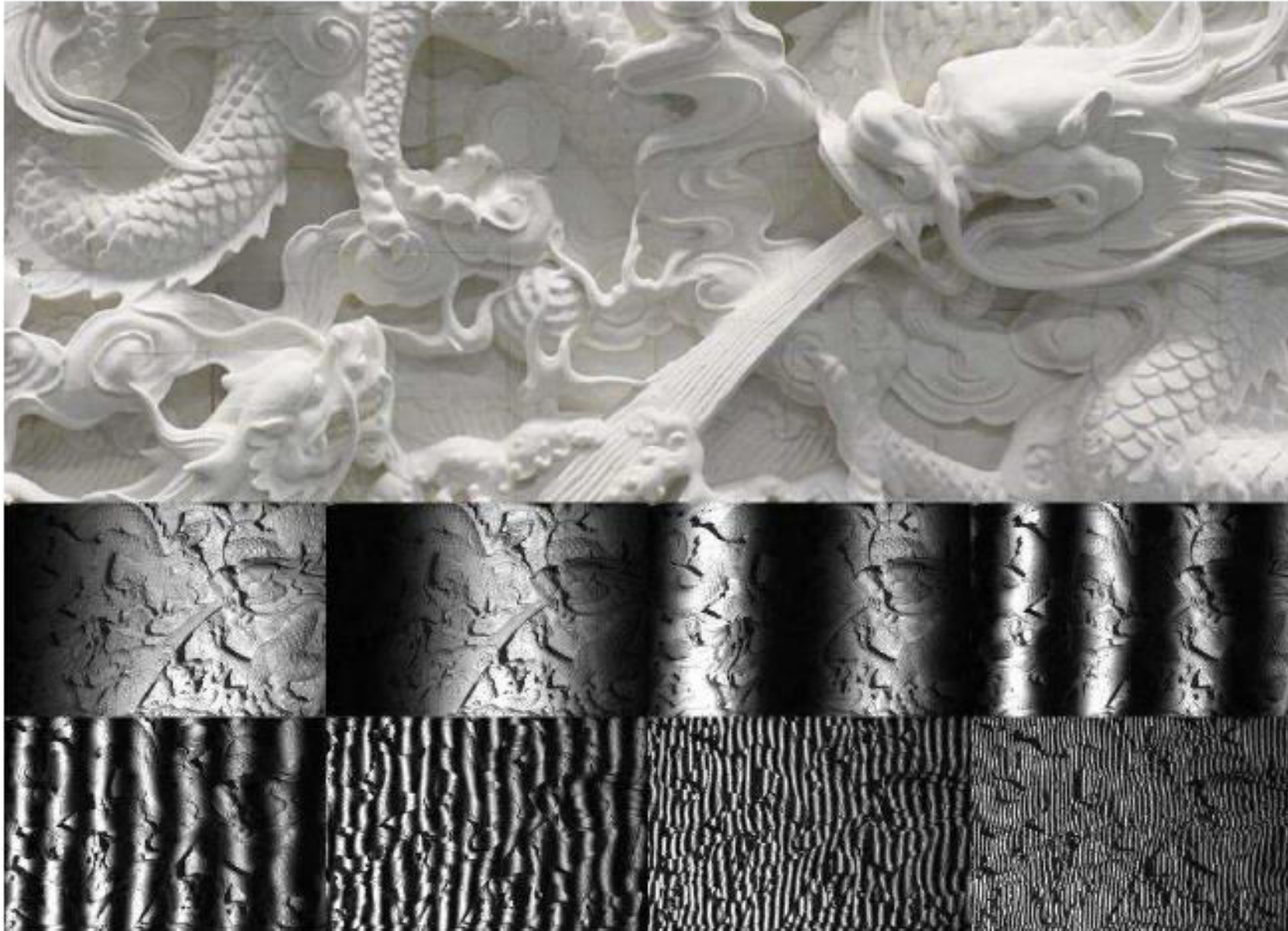
Application of Method



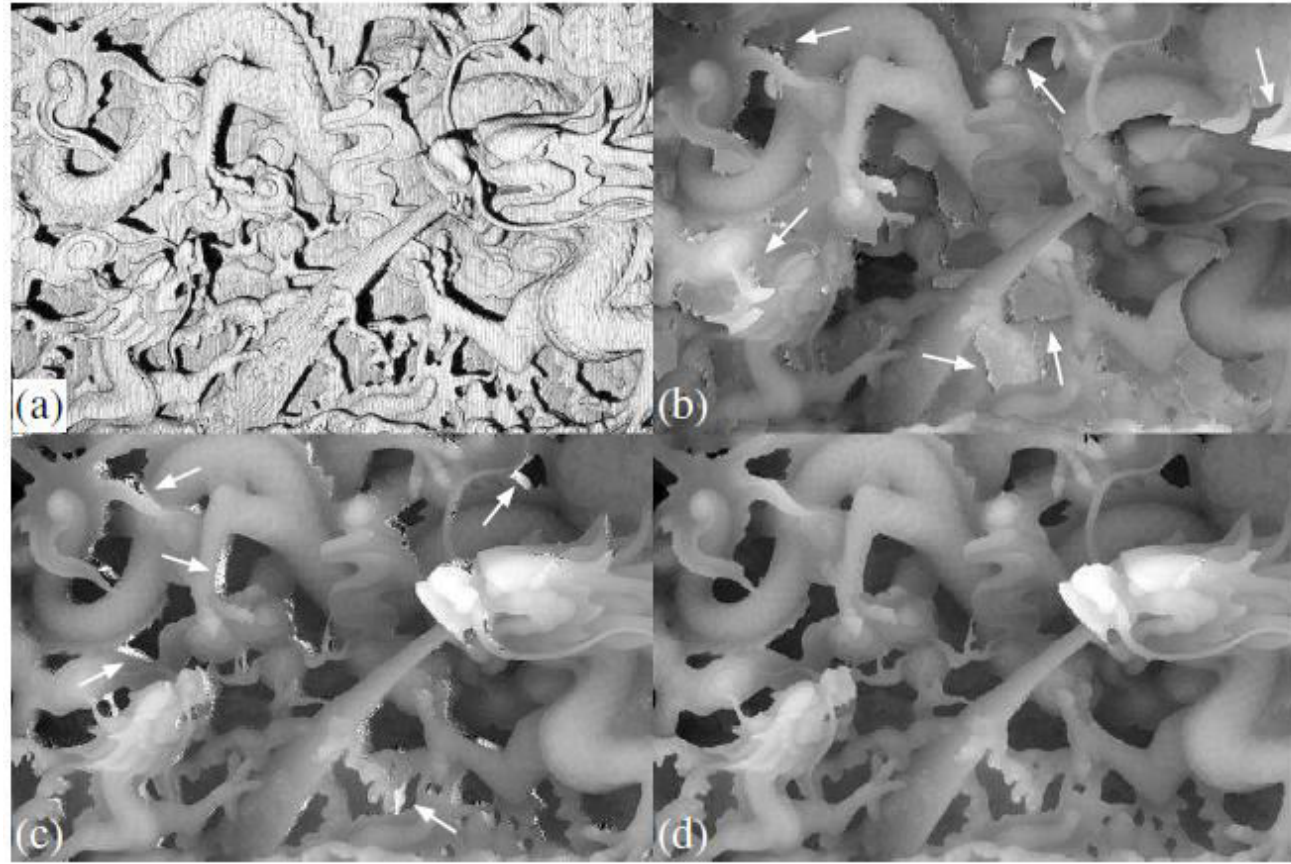
Quality guided phase unwrapping



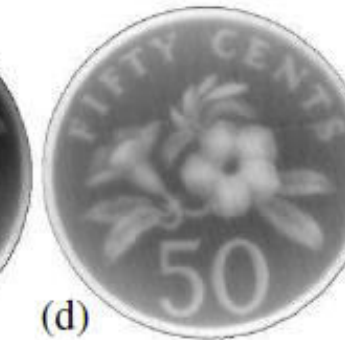
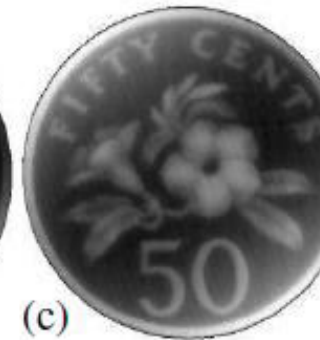
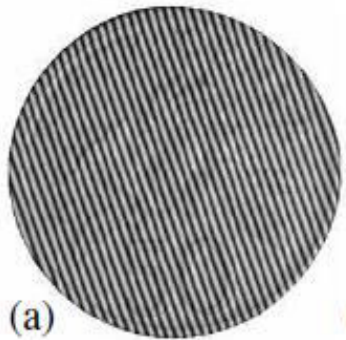
Multi-Frequency Fringe Projection



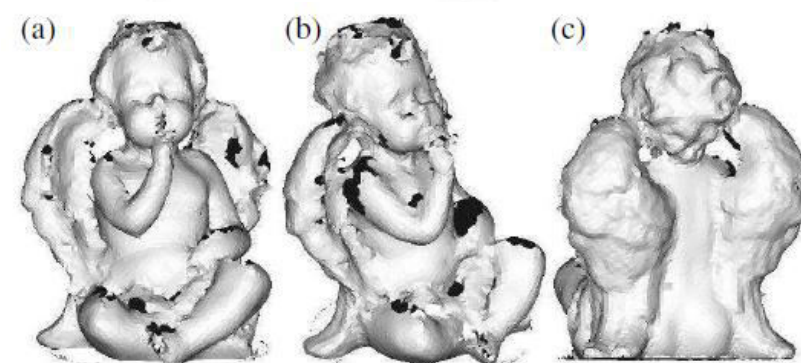
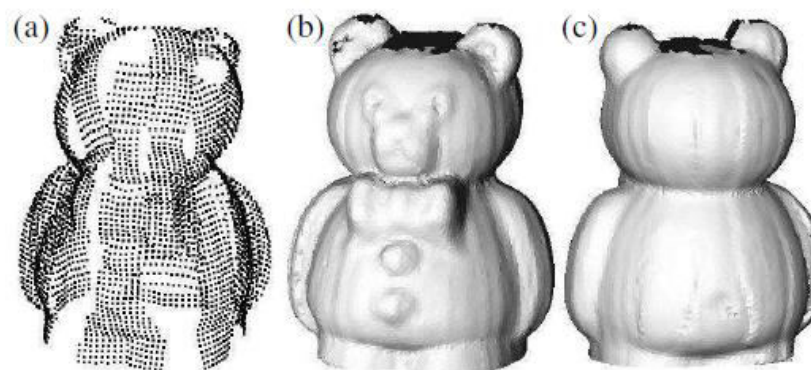
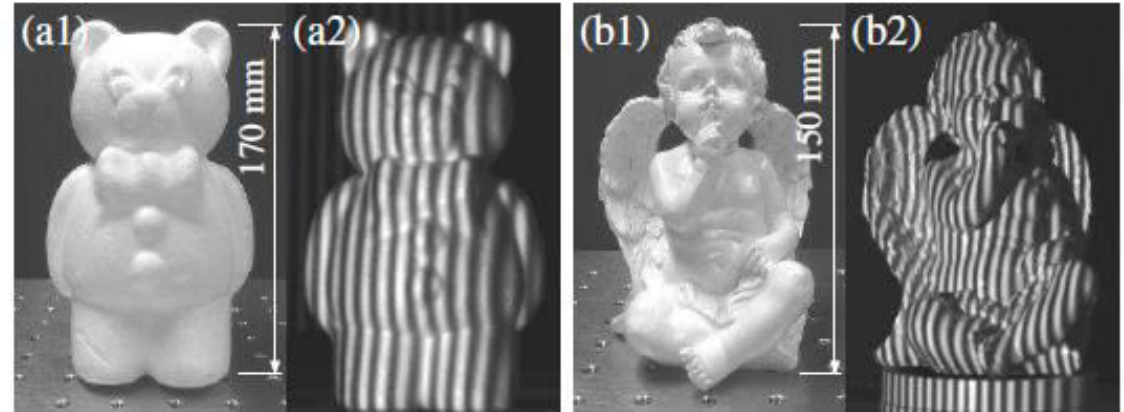
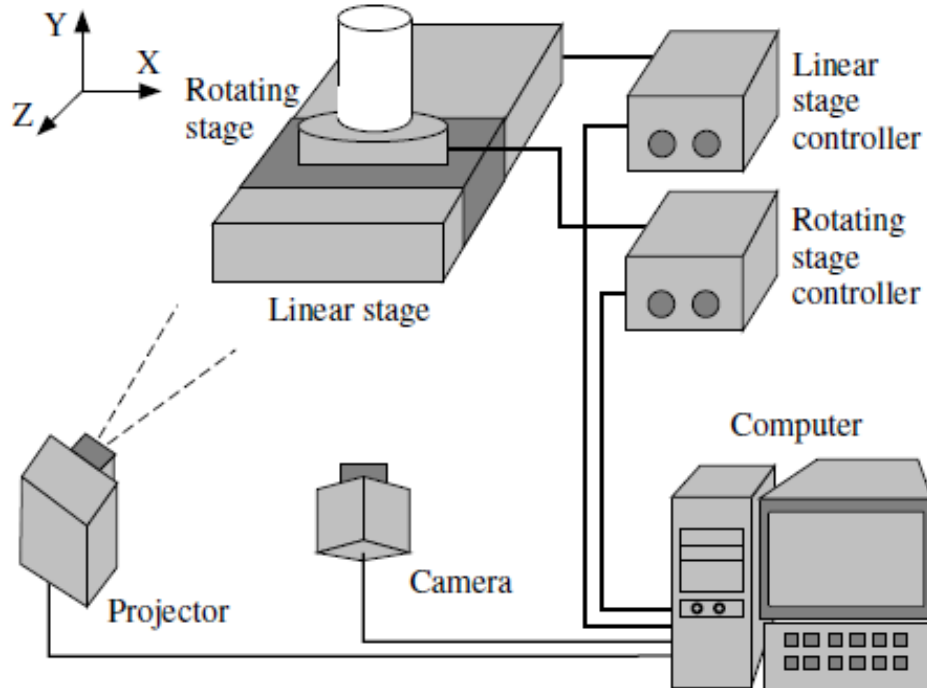
Multi-Frequency Fringe Projection



Carrier Phase Removal



360-degree Fringe Projection



Summary

- Principle of Fringe Projection Profilometry
- Steps involved in calculating height from phase
- Phase unwrapping techniques
- Practical issues
- Examples

References

- L Chen C Quan and CJ Tay, Digital Fringe Projection Profilometry, in Digital Optical Measurement Techniques and Applications, Artech House, 2015.

RA 505 Robot Sensing and Vision

Lecture 37

Dr. Rishikesh Kulkarni
Department of Electronics and Electrical Engineering
IIT Guwahati

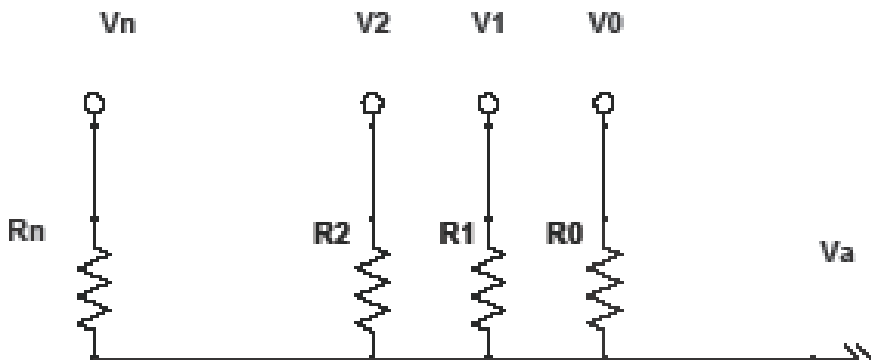
Sensor signal conditioning

- Amplification
- Analog to digital and digital to analog conversion
- Filtering
- Display
- Transmission
- Data Interpretation

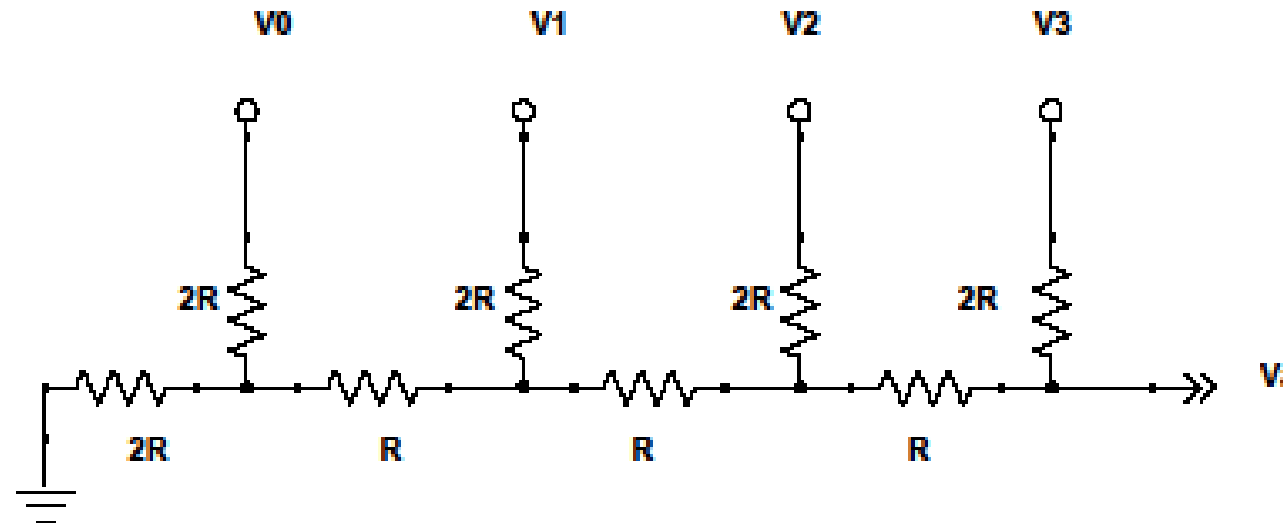
Analog-to-Digital and Digital-to-Analog Converter

- Very important in sensor data processing
- A/D: translating analog signals to equivalent binary signals
- D/A: translating digital information into equivalent analog information
- A/D converters are used to convert analog signal generated by transducers into digital form to feed them into microprocessor system. A/D is referred to as an encoding device.
- D/A converters can be used to drive actuators according to the control output generated by microprocessors. Thus, D/A can also be considered as a decoding device. A D/A converter is usually an integral part of any A/D conversion.

Digital-to-Analog Converter

- Variable resistor network
- As per Millman's theorem
- 
$$V_a = \frac{V_{n-1}/R_{n-1} + \dots + V_2/R_2 + V_1/R_1 + V_0/R_0}{1/R_{n-1} + \dots + 1/R_2 + 1/R_1 + 1/R_0}$$
$$R_1 = R_0/2, R_2 = R_0/4, \text{ and } R_{n-1} = R_0/2^{n-1}$$
$$V_a = \frac{V_{n-1}2^{n-1} + \dots + V_22^2 + V_12^1 + V_02^0}{2^n - 1}$$
1. Each resistance in the network has a different value. Since the dividers are usually constructed using precision resistor, their cost factor increases.
 2. The resistance used in the MSB is required to handle a much higher current than the LSB resistor.

Digital-to-Analog Converter: R-2R laddar

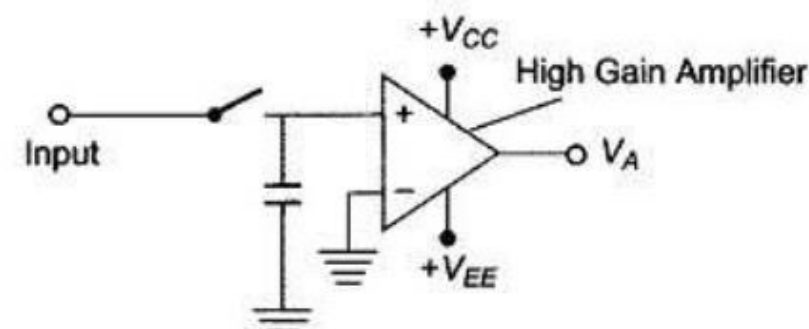
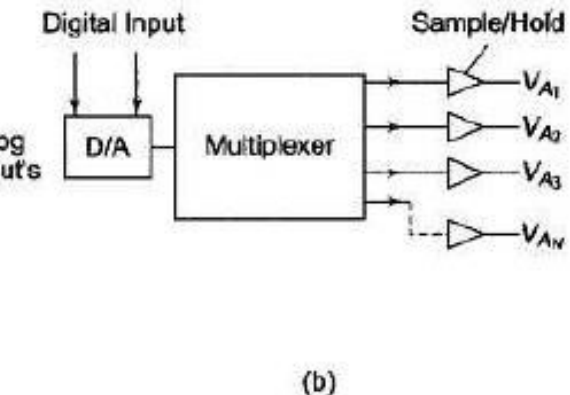
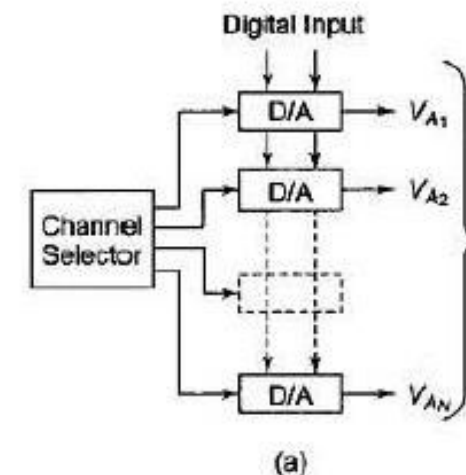
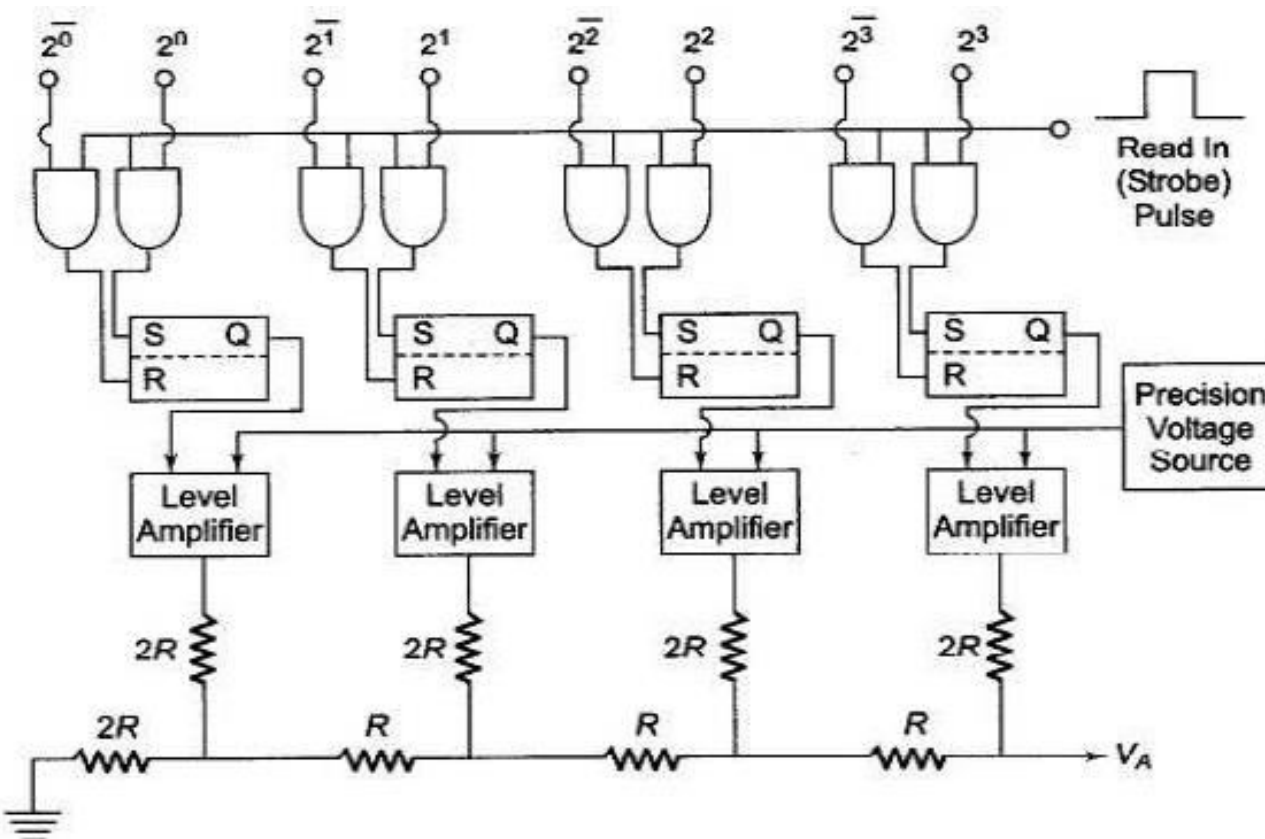


- R-2R laddar

$$V_a = \frac{V_3 2^3 + V_2 2^2 + V_1 2^1 + V_0 2^0}{2^4}$$

$$V_a = \frac{\sum_{k=0}^{n-1} V_k 2^k}{2^n}$$

Digital-to-Analog Converter



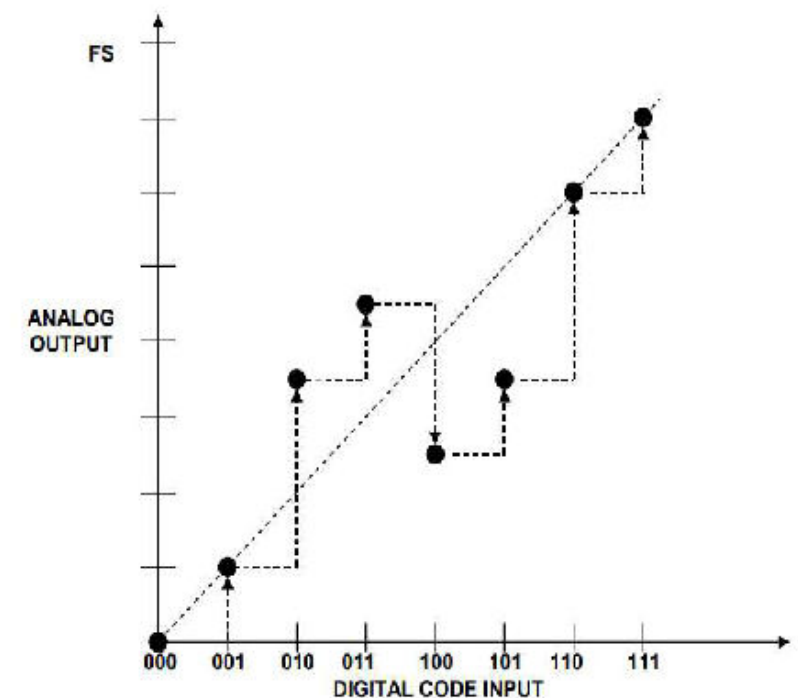
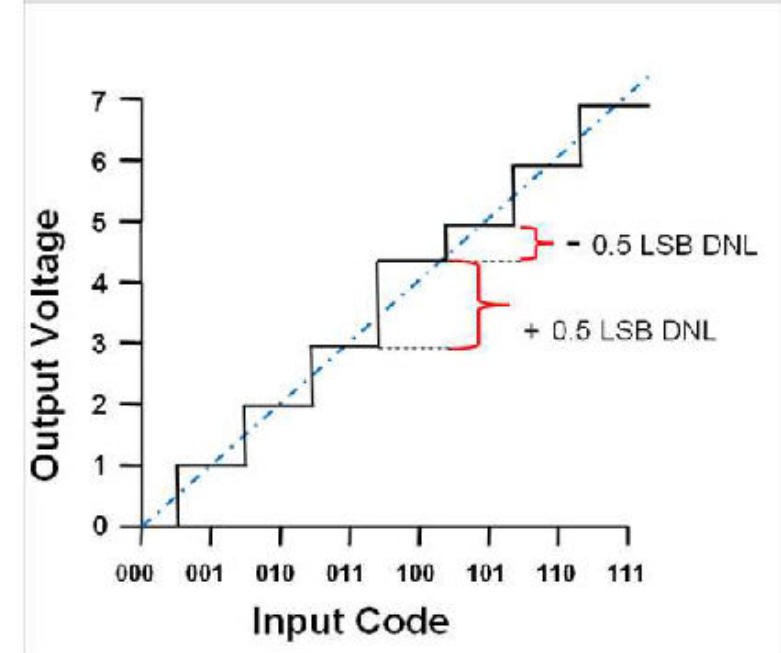
Digital-to-Analog Converter

- Errors in DAC
 - Non-linearity
 - Non-monotonicity
- non-linearity error is quantified as differential non-linearity error (DNL)

$$DNL_{error} = |V_a(i+1) - V_a(i)| - V_{LSB}$$

- Dynamic range

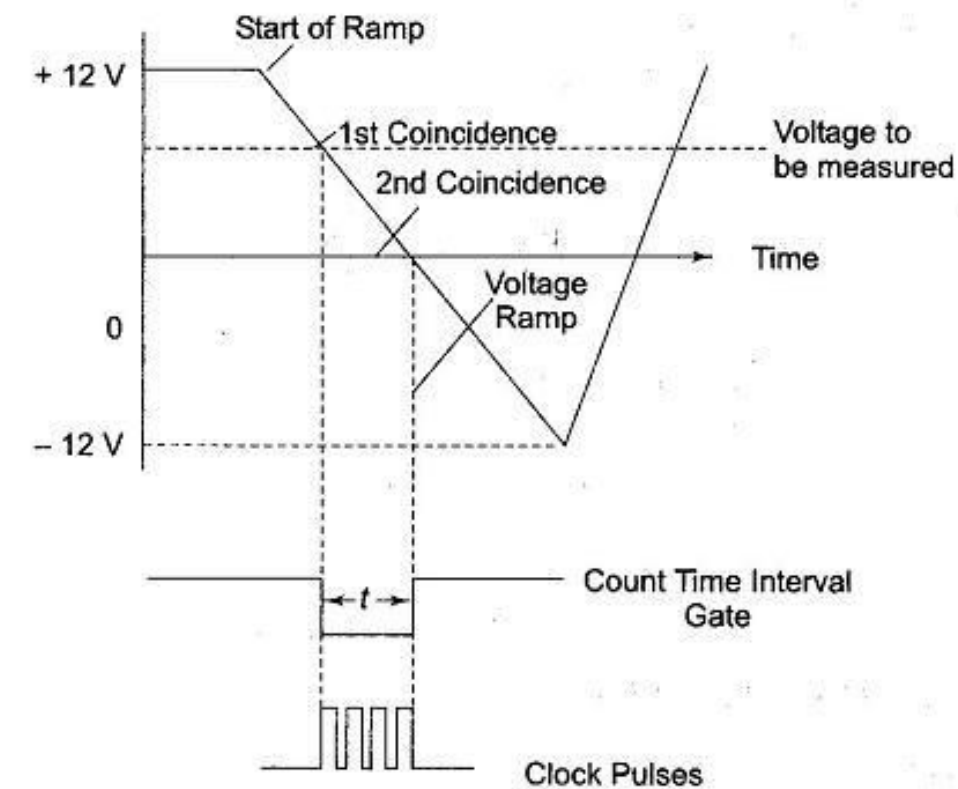
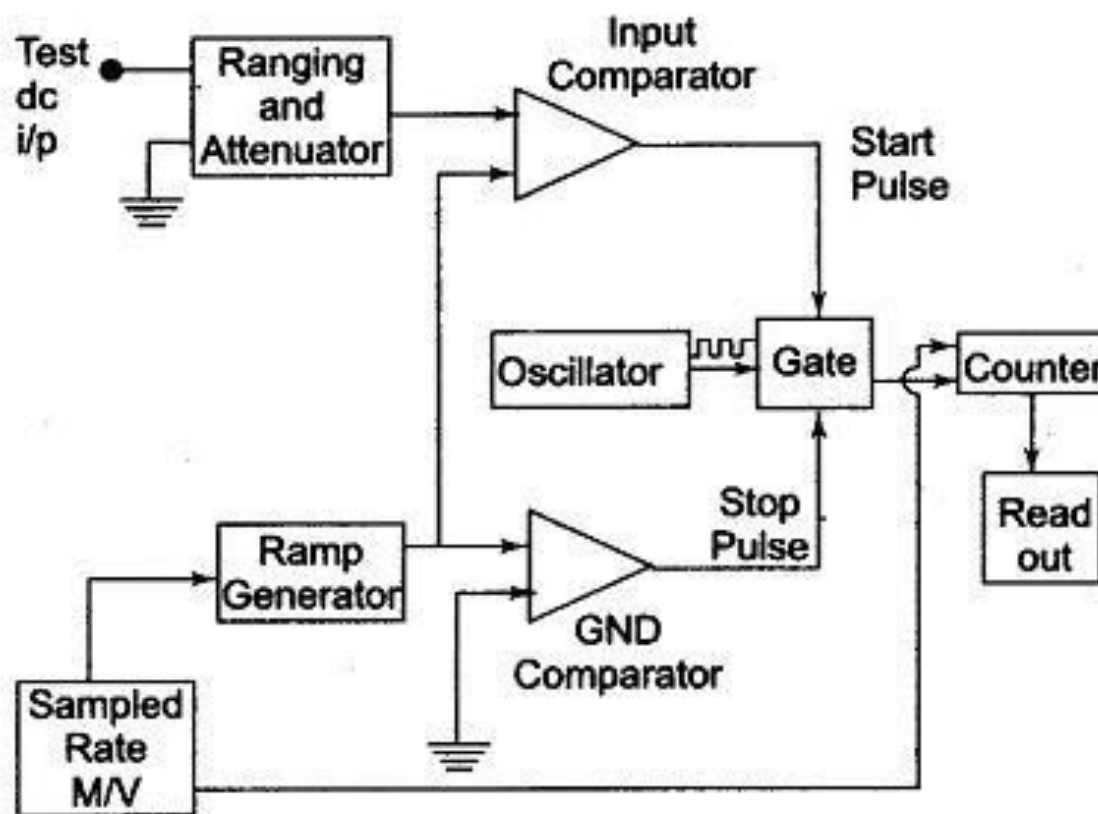
$$20 \log 2^n = 6.02n \text{ dB}$$



Analog-to-Digital Convertor

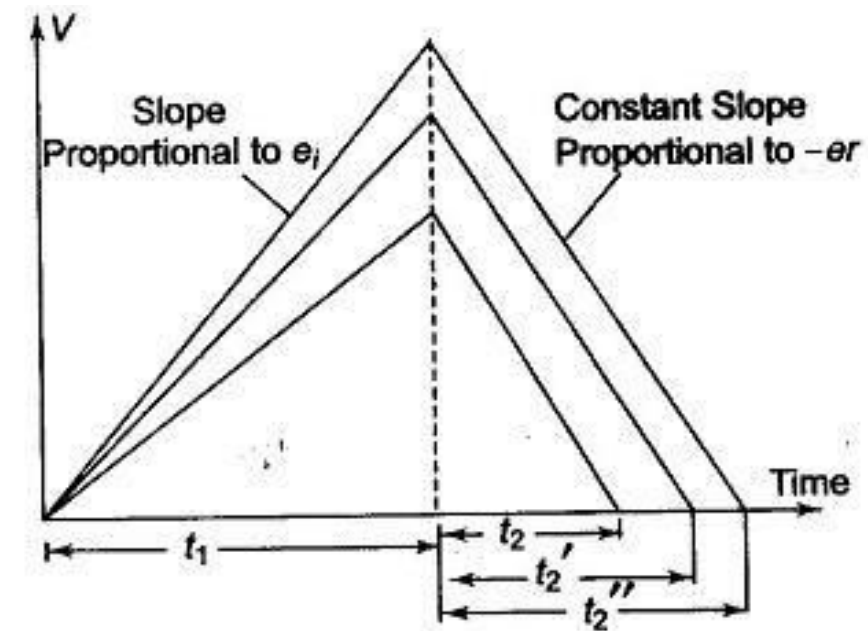
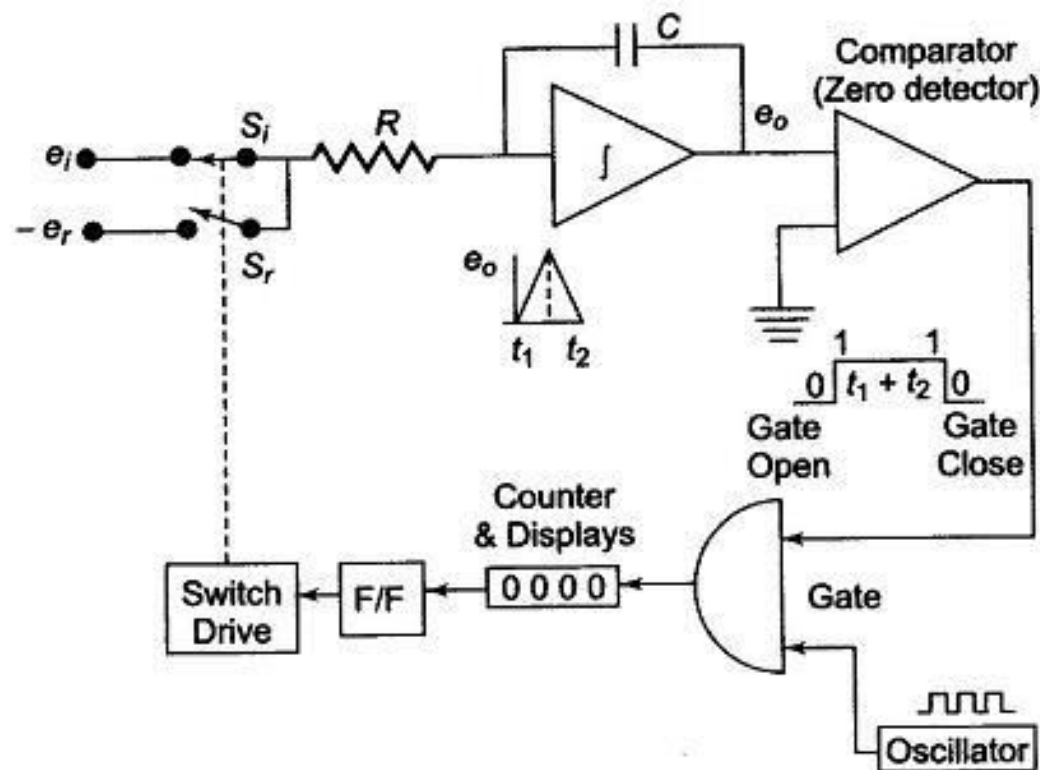
- Analog-to-digital converter as the name suggests, converts the analog signal into equivalent digital signal.
- It is usually referred as A/D, A-D or ADC. For a n-bit A/D, there are 2^n distinct digital levels one of which represents the analog signal.
- We will discuss different A/D techniques in the following.

Analog-to-Digital Converter: Ramp technique



$\pm 0.005\%$ accuracy

Analog-to-Digital Converter: Dual-slope



Excellent noise rejection; +/- 0.05% accuracy in 100 ms.

ADC: Successive Approximation

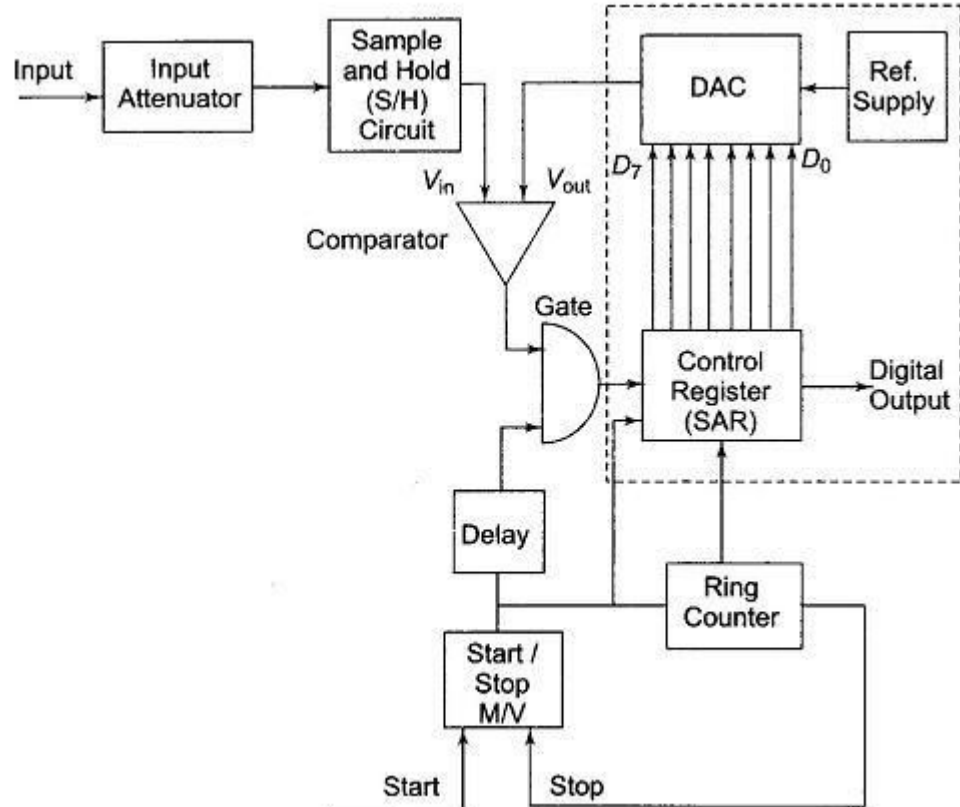


Table 5.1

$V_{in} = 1\text{ V}$	<i>Operation</i>	D_7	D_6	D_5	D_4	D_3	D_2	D_1	D_0	<i>Compare</i>	<i>Output</i>	<i>Voltage</i>
00110011	D_7 Set	1	0	0	0	0	0	0	0	$V_{in} < V_{out}$	D_7 Reset	2.5
"	D_6 Set	0	1	0	0	0	0	0	0	$V_{in} < V_{out}$	D_6 Reset	1.25
"	D_5 Set	0	0	1	0	0	0	0	0	$V_{in} > V_{out}$	D_5 Set	0.625
"	D_4 Set	0	0	1	1	0	0	0	0	$V_{in} > V_{out}$	D_4 Set	0.9375
"	D_3 Set	0	0	1	1	1	0	0	0	$V_{in} < V_{out}$	D_3 Reset	0.9375
"	D_2 Set	0	0	1	1	0	1	0	0	$V_{in} < V_{out}$	D_2 Reset	0.9375
"	D_1 Set	0	0	1	1	0	0	1	0	$V_{in} > V_{out}$	D_1 Set	0.97725
"	D_0 Set	0	0	1	1	0	0	1	1	$V_{in} > V_{out}$	D_0 Set	0.99785

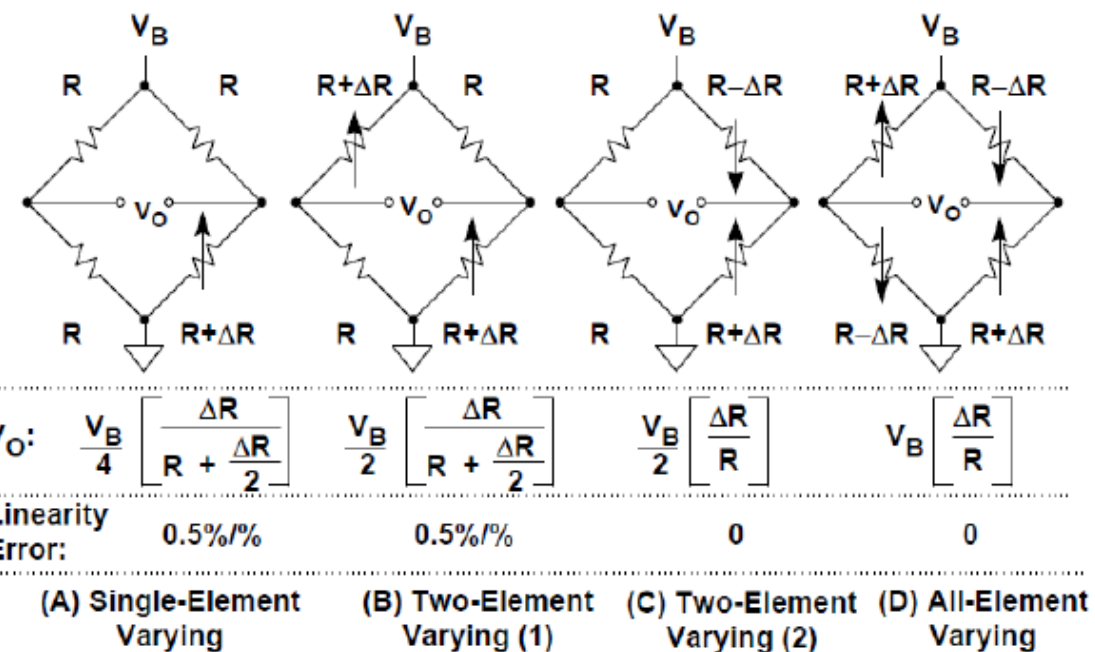
A/D Signal-to-noise ratio

- The quantization process in the A/D converter produces noise in the converted signal.
- The quantification of it is done in terms of signal-to-noise ratio (SNR) of A/D converter.
- $\text{SNR} = 6.02N + 1.76 \text{ dB}$ (N-bit ADC)
- <https://www.analog.com/media/en/training-seminars/tutorials/MT-001.pdf>

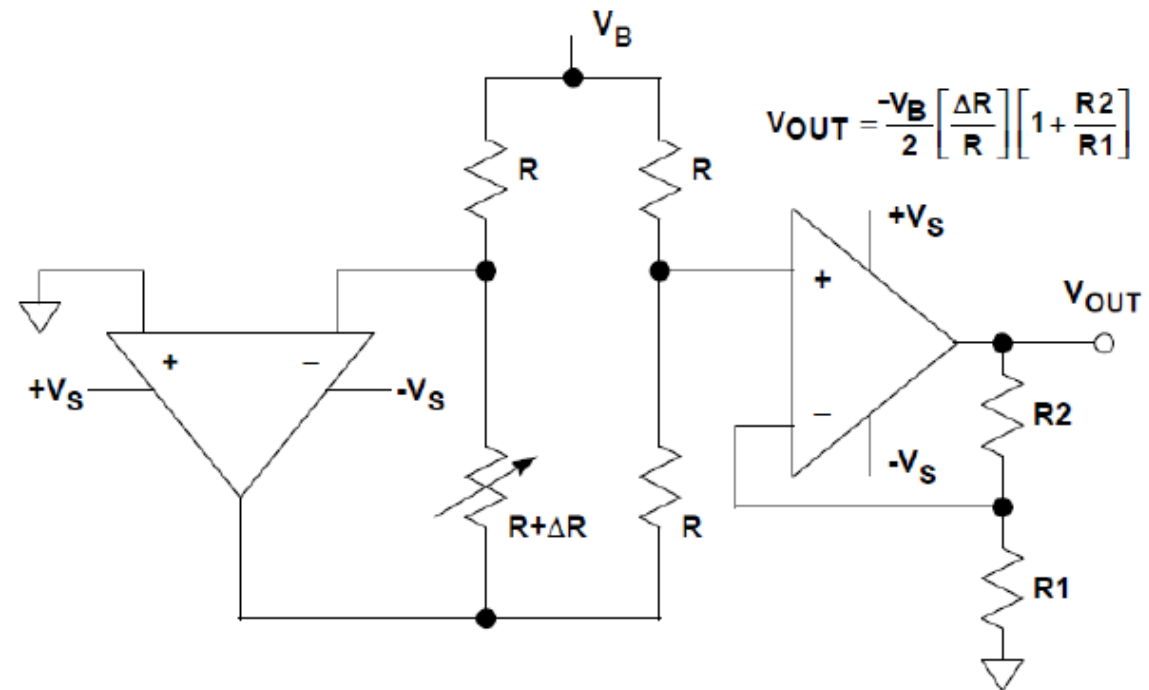
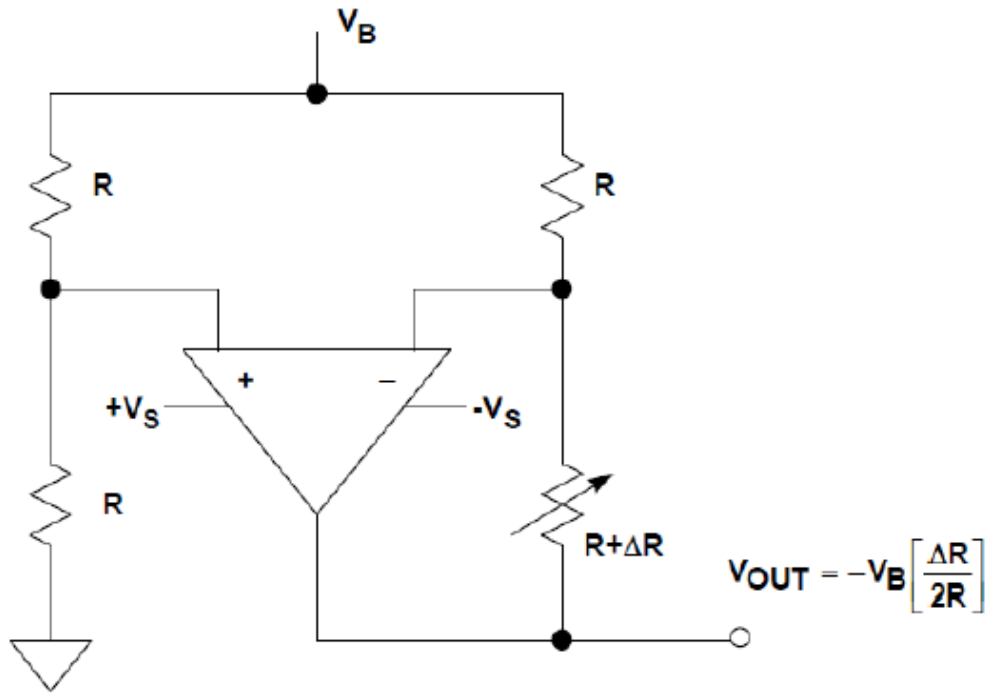
Bridge Circuits

- Ubiquity of resistive sensors
 - Displacement
 - Pressure
 - Temperature
 - Humidity
 - Force
 - Flow
- Bridge configurations
- Non-linearity
- Bridge sensitivity

Strain Gages	$120 \Omega, 350 \Omega, 3500 \Omega$
Load cells	cells 350 Ω - 3500 Ω
Pressure sensors	350 Ω - 3500 Ω
Humidity sensors	100 K Ω - 10 M Ω
RTDs	100 Ω , 1000 Ω
Thermistors	100 Ω - 10 M Ω



Bridge Circuits

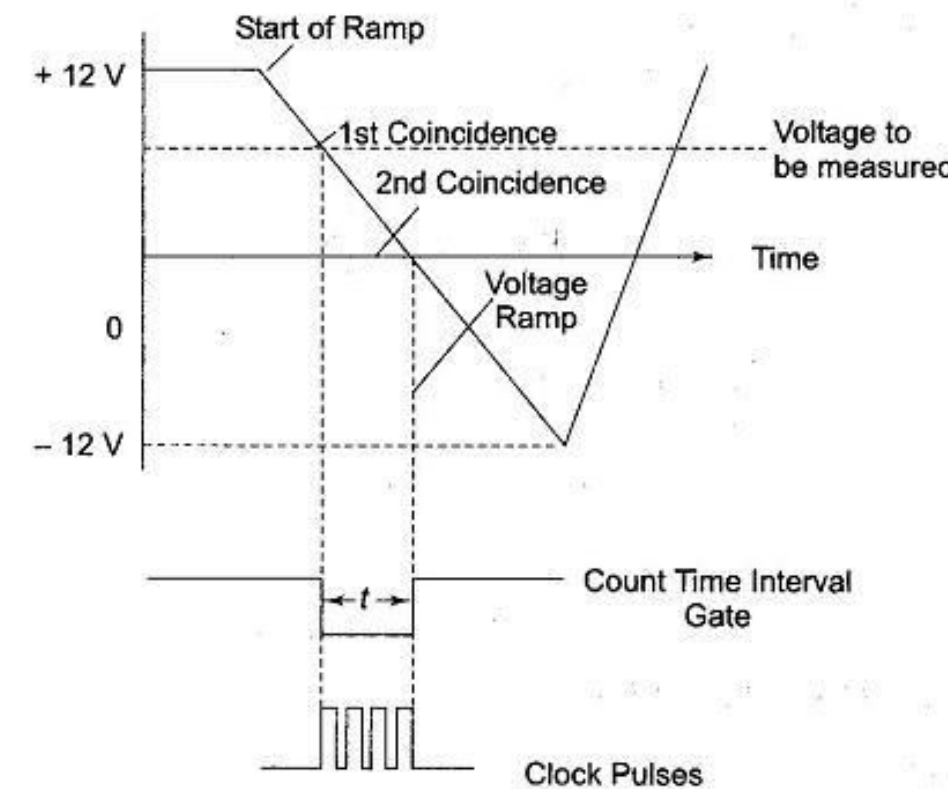
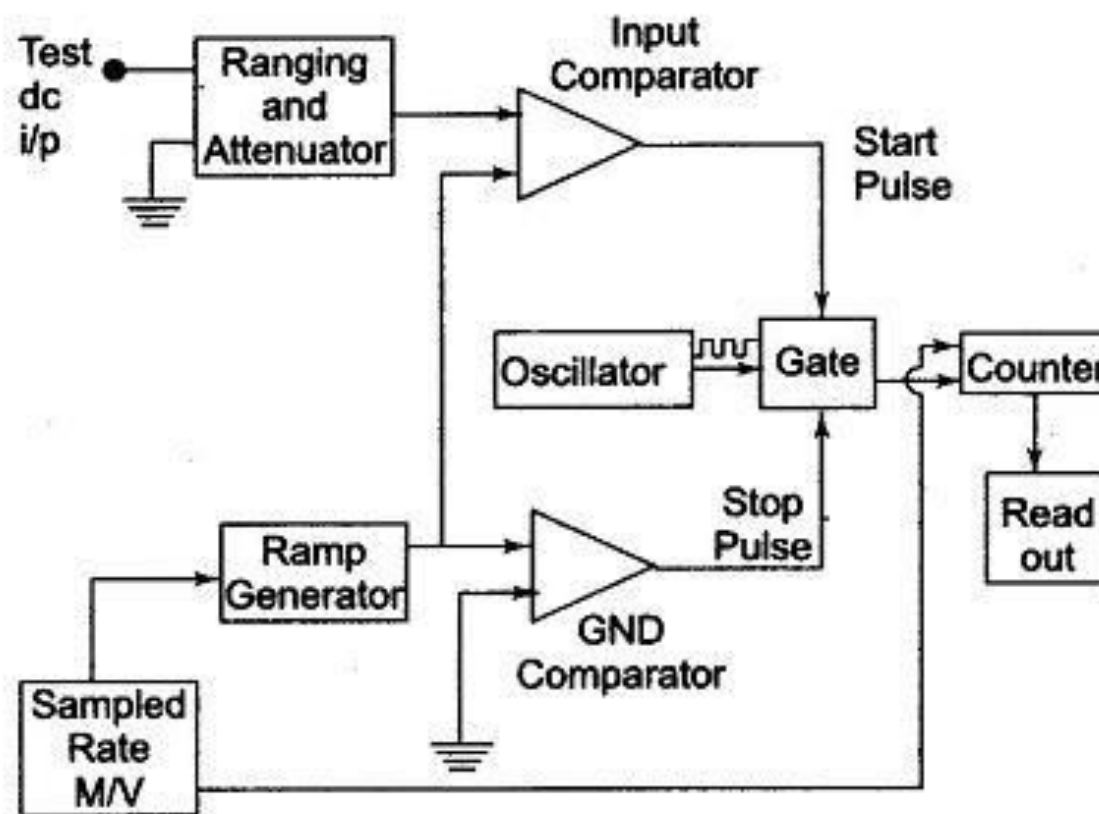


RA 505 Robot Sensing and Vision

Lecture 38

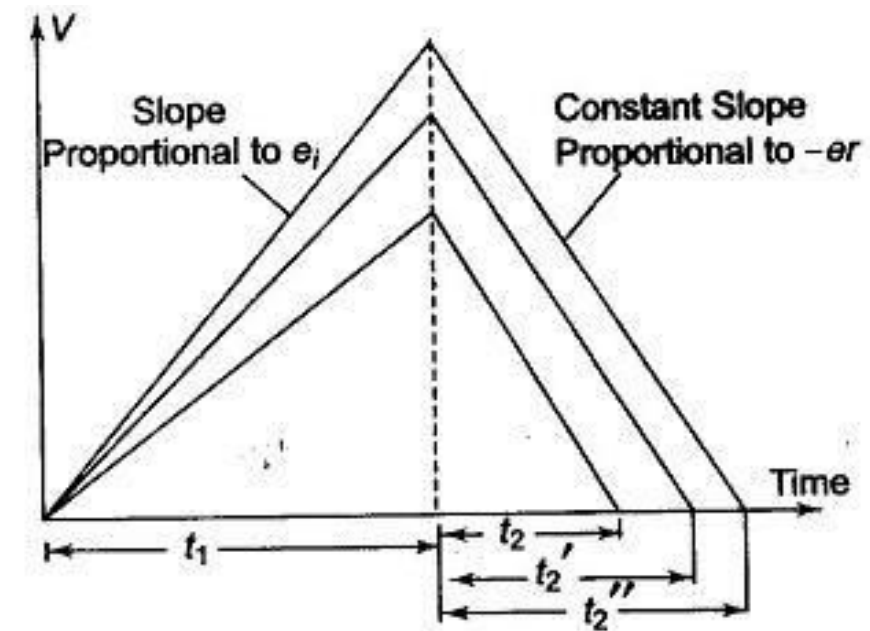
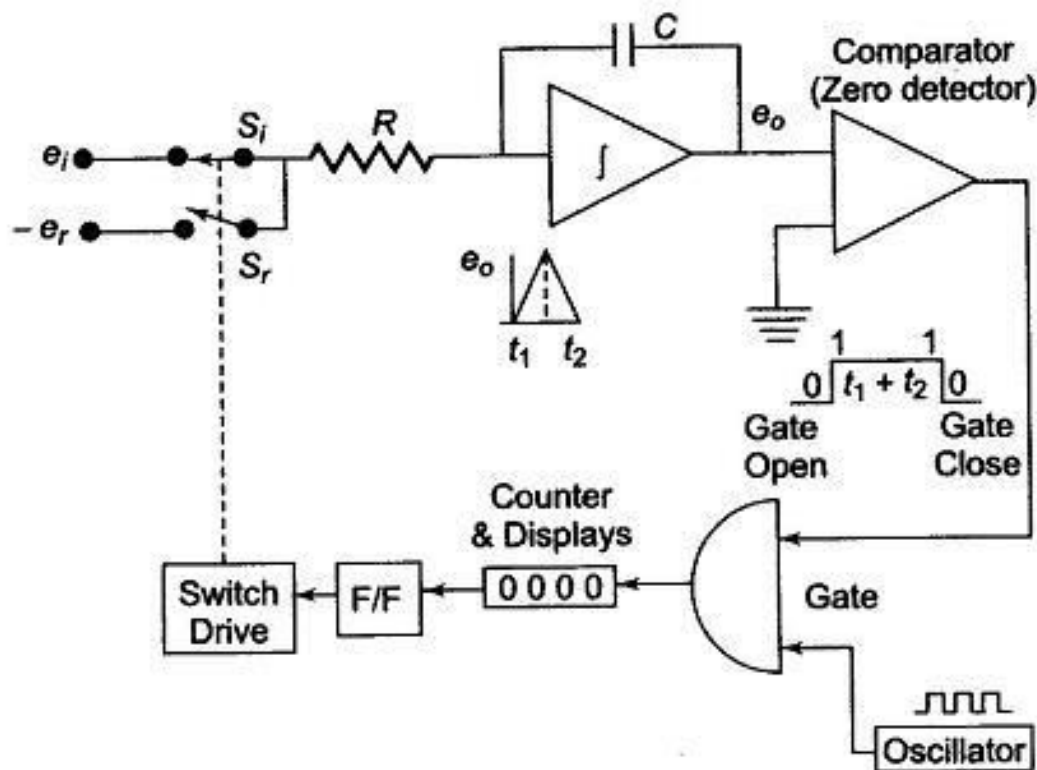
Dr. Rishikesh Kulkarni
Department of Electronics and Electrical Engineering
IIT Guwahati

Analog-to-Digital Converter: Ramp technique



$\pm 0.005\%$ accuracy

Analog-to-Digital Converter: Dual-slope



Excellent noise rejection; $\pm 0.05\%$ accuracy in 100 ms.

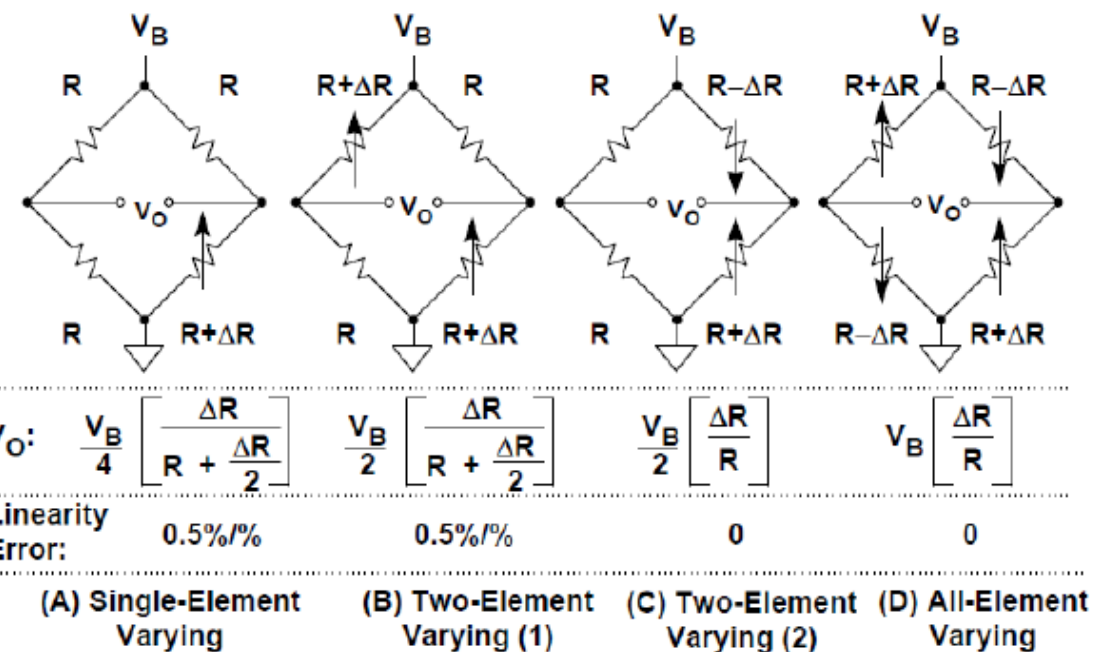
A/D Signal-to-noise ratio

- The quantization process in the A/D converter produces noise in the converted signal.
- The quantification of it is done in terms of signal-to-noise ratio (SNR) of A/D converter.
- $\text{SNR} = 6.02N + 1.76 \text{ dB}$ (N-bit ADC)
- <https://www.analog.com/media/en/training-seminars/tutorials/MT-001.pdf>

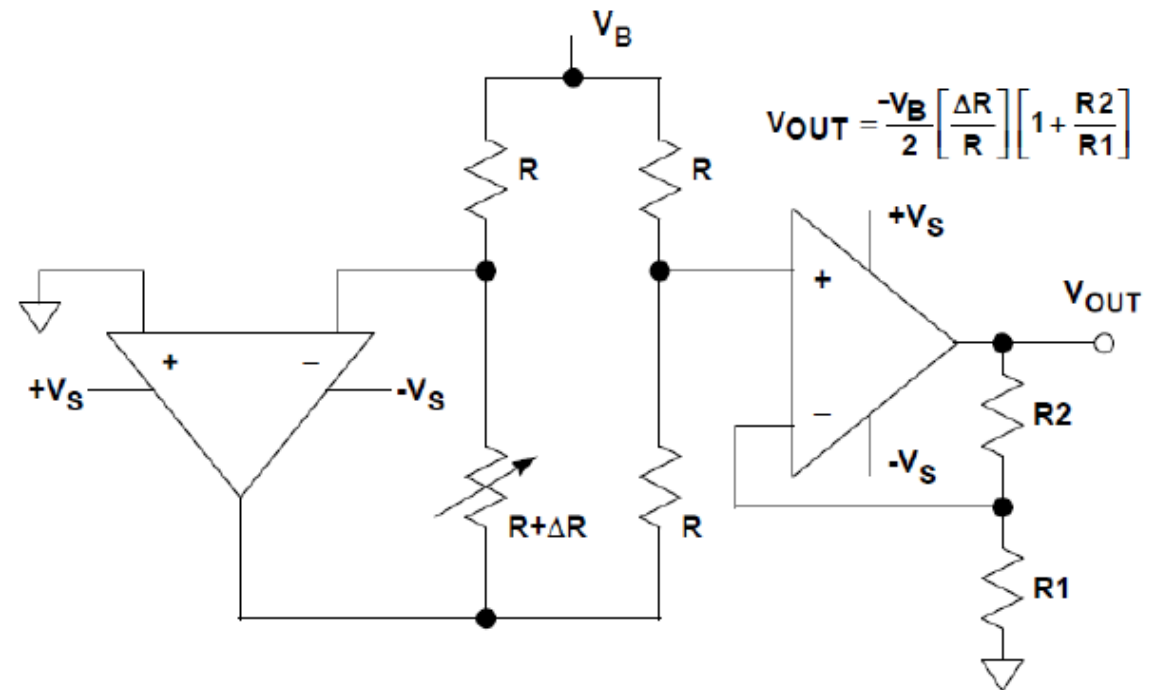
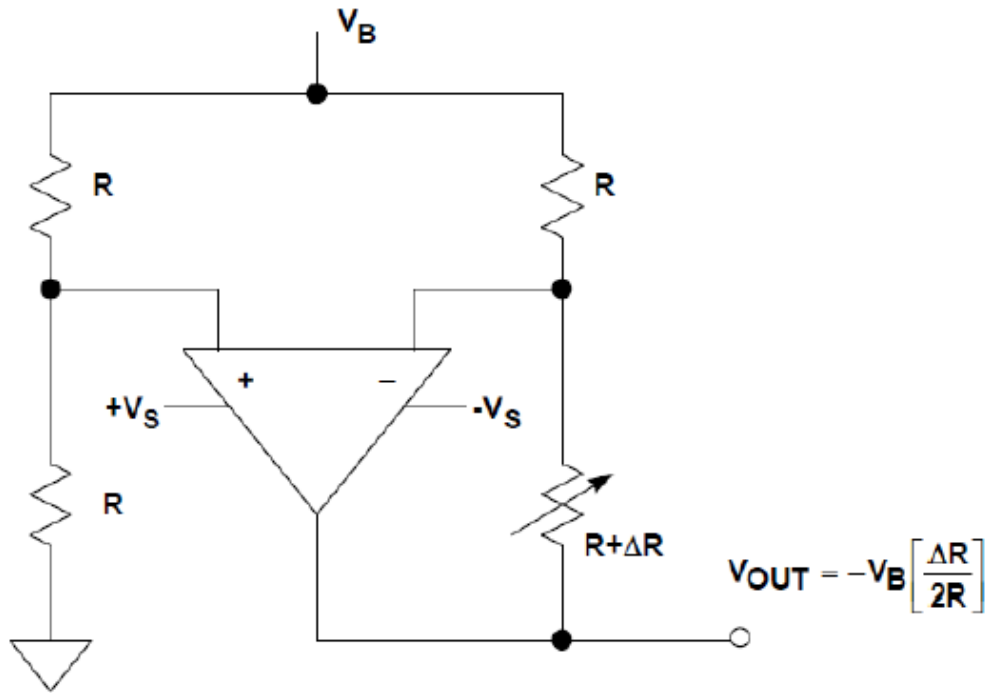
Bridge Circuits

- Ubiquity of resistive sensors
 - Displacement
 - Pressure
 - Temperature
 - Humidity
 - Force
 - Flow
- Bridge configurations
- Non-linearity
- Bridge sensitivity

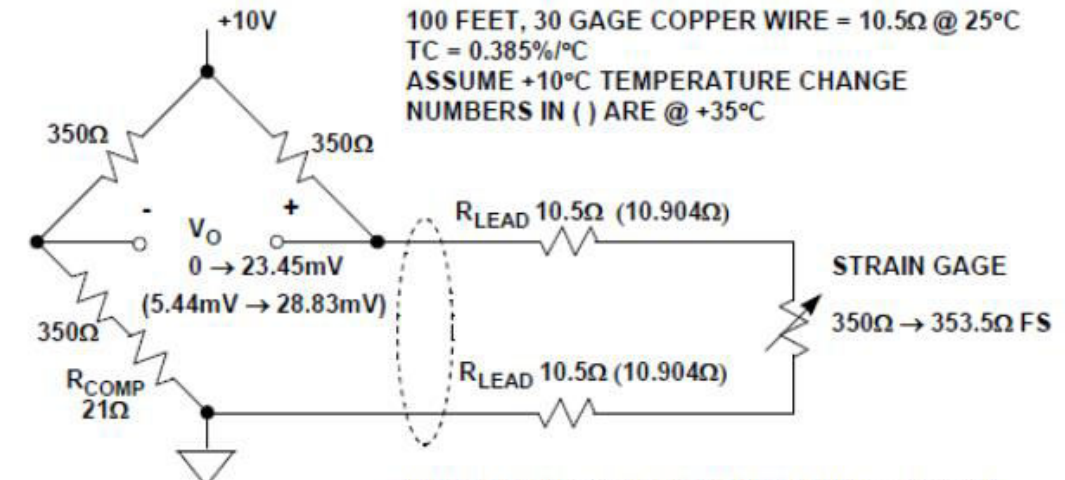
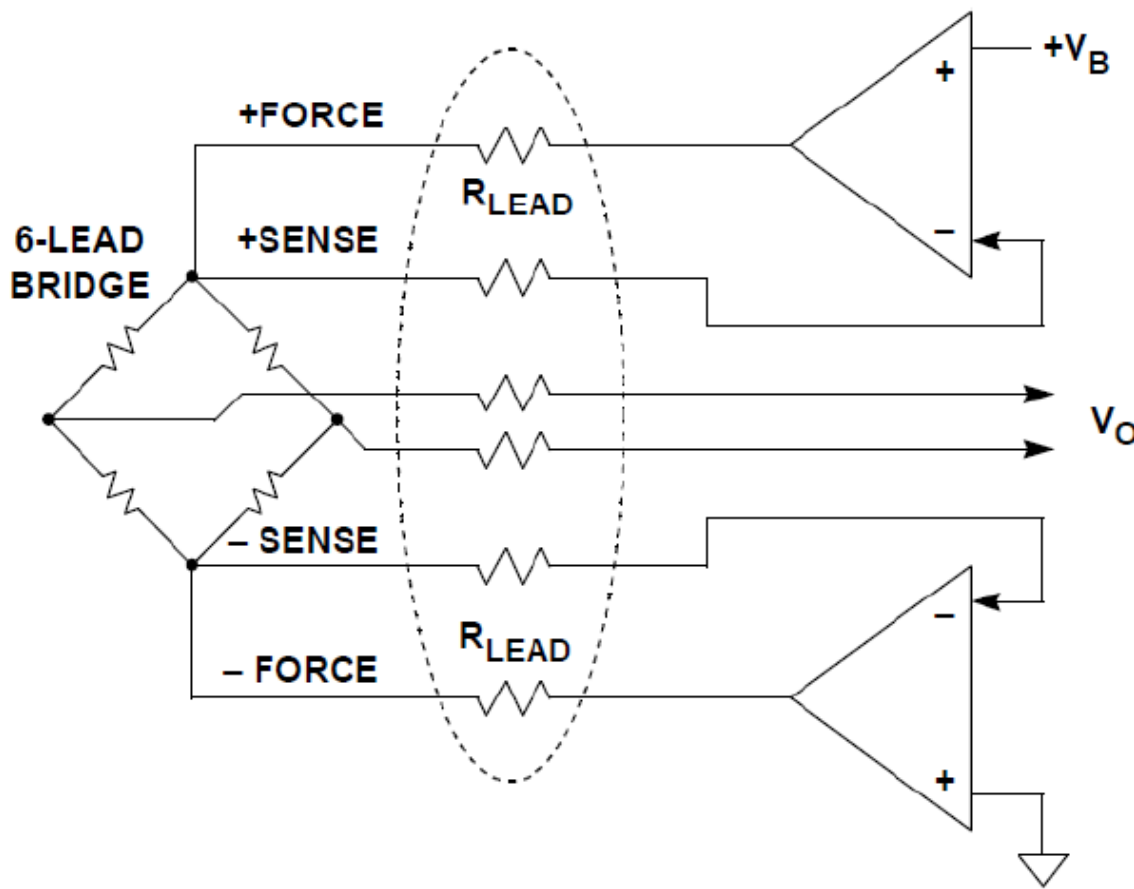
Strain Gages	$120 \Omega, 350 \Omega, 3500 \Omega$
Load cells	cells 350 Ω - 3500 Ω
Pressure sensors	350 Ω - 3500 Ω
Humidity sensors	100 K Ω - 10 M Ω
RTDs	100 Ω , 1000 Ω
Thermistors	100 Ω - 10 M Ω



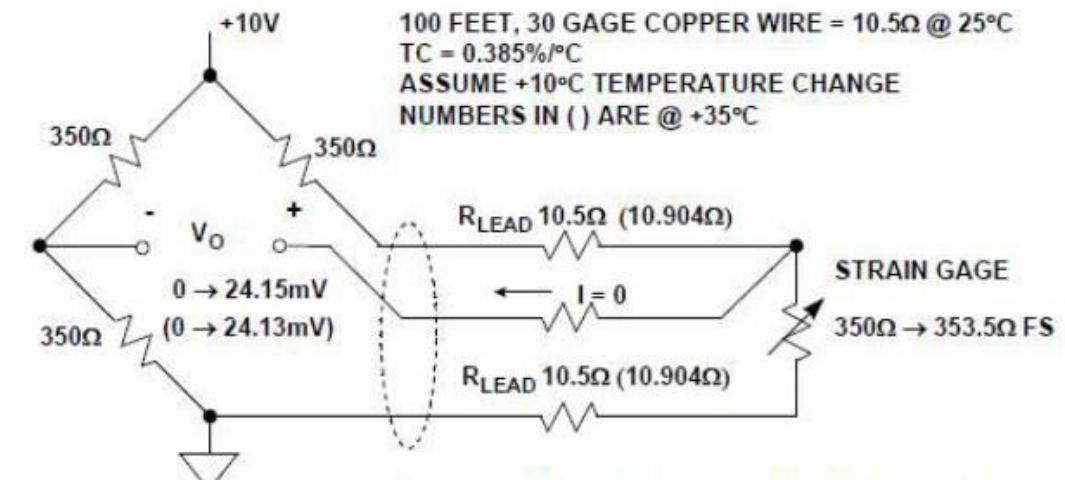
Bridge Circuits



Bridge Compensation



OFFSET ERROR OVER TEMPERATURE = +23%FS
GAIN ERROR OVER TEMPERATURE = -0.26%FS



OFFSET ERROR OVER TEMPERATURE = 0%FS
GAIN ERROR OVER TEMPERATURE = -0.08%FS

Operational Amplifier

- Signal conditioning
 - Amplification
 - Filtering
 - Linearization
- Op-amp parameters
 - Open-Loop Voltage Gain, Slew rate, input offset voltage, input bias current, input offset current, output offset voltage Common Mode Rejection Ratio (CMMR), power supply rejection ratio (PSRR), differential input impedance, output impedance, average temperature coefficient of input offset current, average temperature coefficient of input offset voltage, output short circuit current, etc.

Amplifiers

- Non-inverting amplifier
 - Non-ideal open loop gain

$$V_o = \frac{A(R_1 + R_F)V_{in}}{R_1 + R_F + AR_1}$$
$$= V_{in} \frac{A_{CL}}{1 + A_{CL}/A}$$

$$A_f = \frac{f_u}{f_{sig}}$$

$$\%gain\ error = A_{CL}/(A_{CL} + A_f) \times 100$$

- Inverting amplifier

$$V_o = \frac{1}{R_1 \left[\frac{1}{A} \left(\frac{R_1 + R_F}{R_1 R_F} \right) - \frac{1}{R_F} \right]} V_{in}$$

- Integrator
 - Input signal time period
 - Time-constant

$$\frac{V_{in}}{R_1} = -C_F \frac{dV_o}{dt}$$
$$V_o = -\frac{1}{C_F R_1} \int_0^t V_{in} dt$$

- Differentiator

$$C_1 \frac{dV_{in}}{dt} = -\frac{V_o}{R_F}$$
$$V_o = -C_1 R_F \frac{dV_{in}}{dt}$$

Amplifier

- Summing amplifier

$$V_o = - \left(\frac{R_f}{R_a} V_a + \frac{R_f}{R_b} V_b + \frac{R_f}{R_c} V_c \right)$$

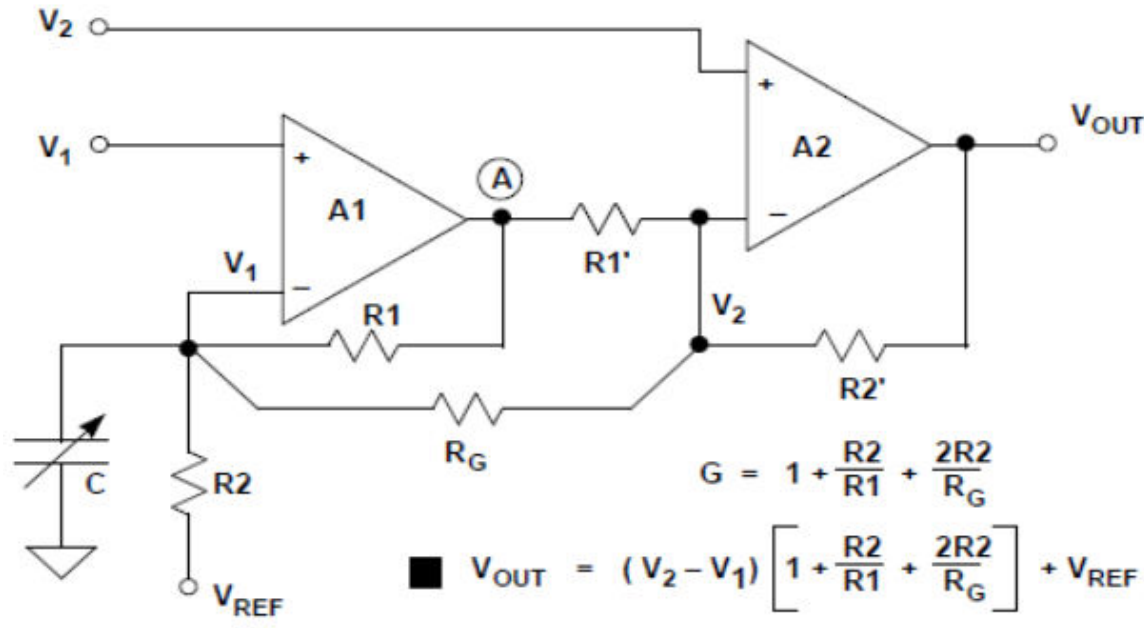
- Subtracting amplifier

$$V_o = V_b - V_a$$

- Instrumentation amplifier

- Selectable gain with high gain accuracy and gain linearity
- Differential input capability with high common mode rejection
- High stability of gain with low temperature coefficient (resistors and other components are manufactured with high precision)
- Low DC offset and drift errors
- Low output impedance

Two-OpAmp Instrumentation amplifier



$$G = 1 + \frac{R_2}{R_1} + \frac{2R_2}{R_G}$$

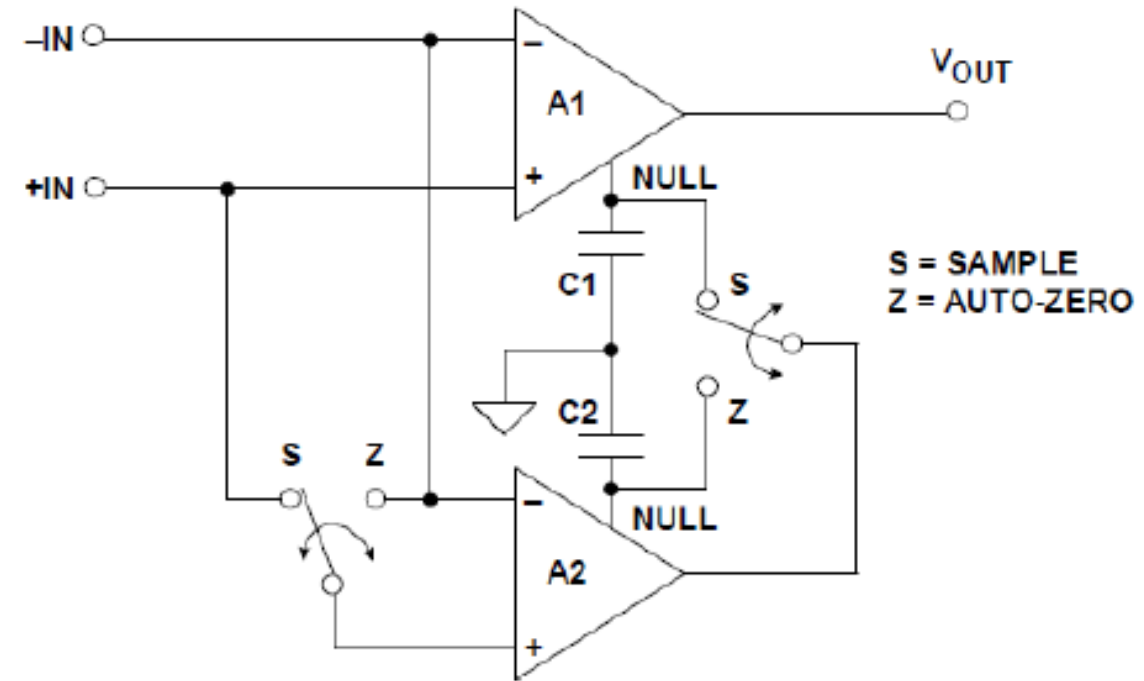
■ $V_{\text{OUT}} = (V_2 - V_1) \left[1 + \frac{R_2}{R_1} + \frac{2R_2}{R_G} \right] + V_{\text{REF}}$

■ $\frac{R_2}{R_1} = \frac{R_{2'}}{R_{1'}}$

■ $\text{CMR} \leq 20 \log \left[\frac{\text{GAIN} \times 100}{\% \text{ MISMATCH}} \right]$

Amplifier

- Chopper amplifier



RA 505 Robot Sensing and Vision

Lecture 39

Dr. Rishikesh Kulkarni
Department of Electronics and Electrical Engineering
IIT Guwahati

Operational Amplifier

- Signal conditioning
 - Amplification
 - Filtering
 - Linearization
- Op-amp parameters
 - Open-Loop Voltage Gain, Slew rate, input offset voltage, input bias current, input offset current, output offset voltage Common Mode Rejection Ratio (CMMR), power supply rejection ratio (PSRR), differential input impedance, output impedance, average temperature coefficient of input offset current, average temperature coefficient of input offset voltage, output short circuit current, etc.

Amplifiers

- Non-inverting amplifier
 - Non-ideal open loop gain

$$V_o = \frac{A(R_1 + R_F)V_{in}}{R_1 + R_F + AR_1}$$
$$= V_{in} \frac{A_{CL}}{1 + A_{CL}/A}$$

$$A_f = \frac{f_u}{f_{sig}}$$

$$\%gain\ error = A_{CL}/(A_{CL} + A_f) \times 100$$

- Inverting amplifier

$$V_o = \frac{1}{R_1 \left[\frac{1}{A} \left(\frac{R_1 + R_F}{R_1 R_F} \right) - \frac{1}{R_F} \right]} V_{in}$$

- Integrator

- Input signal time period
- Time-constant

$$\frac{V_{in}}{R_1} = -C_F \frac{dV_o}{dt}$$
$$V_o = -\frac{1}{C_F R_1} \int_0^t V_{in} dt$$

- Differentiator

$$C_1 \frac{dV_{in}}{dt} = -\frac{V_o}{R_F}$$

$$V_o = -C_1 R_F \frac{dV_{in}}{dt}$$

Amplifier

- Summing amplifier

$$V_o = - \left(\frac{R_f}{R_a} V_a + \frac{R_f}{R_b} V_b + \frac{R_f}{R_c} V_c \right)$$

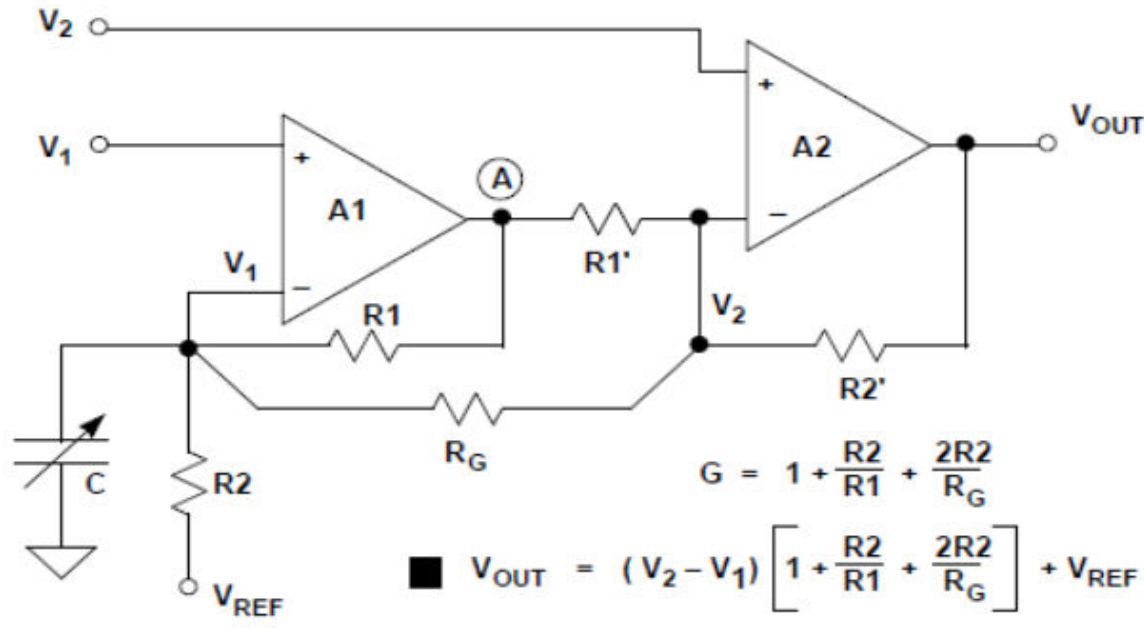
- Subtracting amplifier

$$V_o = V_b - V_a$$

- Instrumentation amplifier

- Selectable gain with high gain accuracy and gain linearity
- Differential input capability with high common mode rejection
- High stability of gain with low temperature coefficient (resistors and other components are manufactured with high precision)
- Low DC offset and drift errors
- Low output impedance

Two-OpAmp Instrumentation amplifier



$$G = 1 + \frac{R_2}{R_1} + \frac{2R_2}{R_G}$$

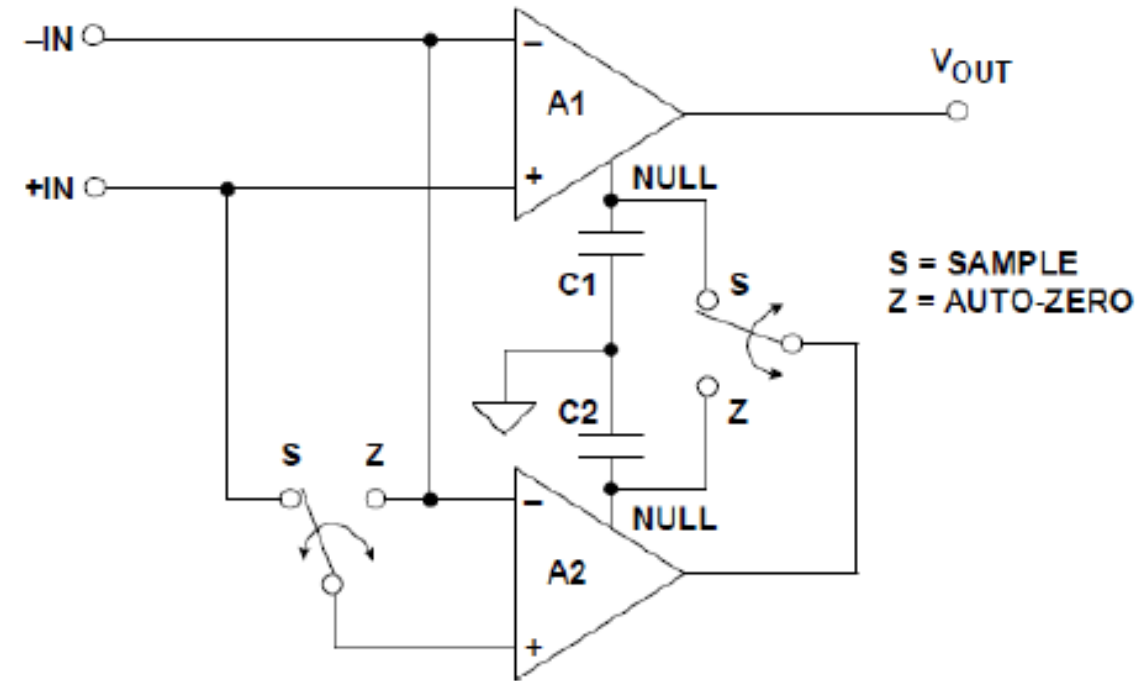
■ $V_{OUT} = (V_2 - V_1) \left[1 + \frac{R_2}{R_1} + \frac{2R_2}{R_G} \right] + V_{REF}$

■ $\frac{R_2}{R_1} = \frac{R_2'}{R_1'}$

■ $CMR \leq 20 \log \left[\frac{\text{GAIN} \times 100}{\% \text{ MISMATCH}} \right]$

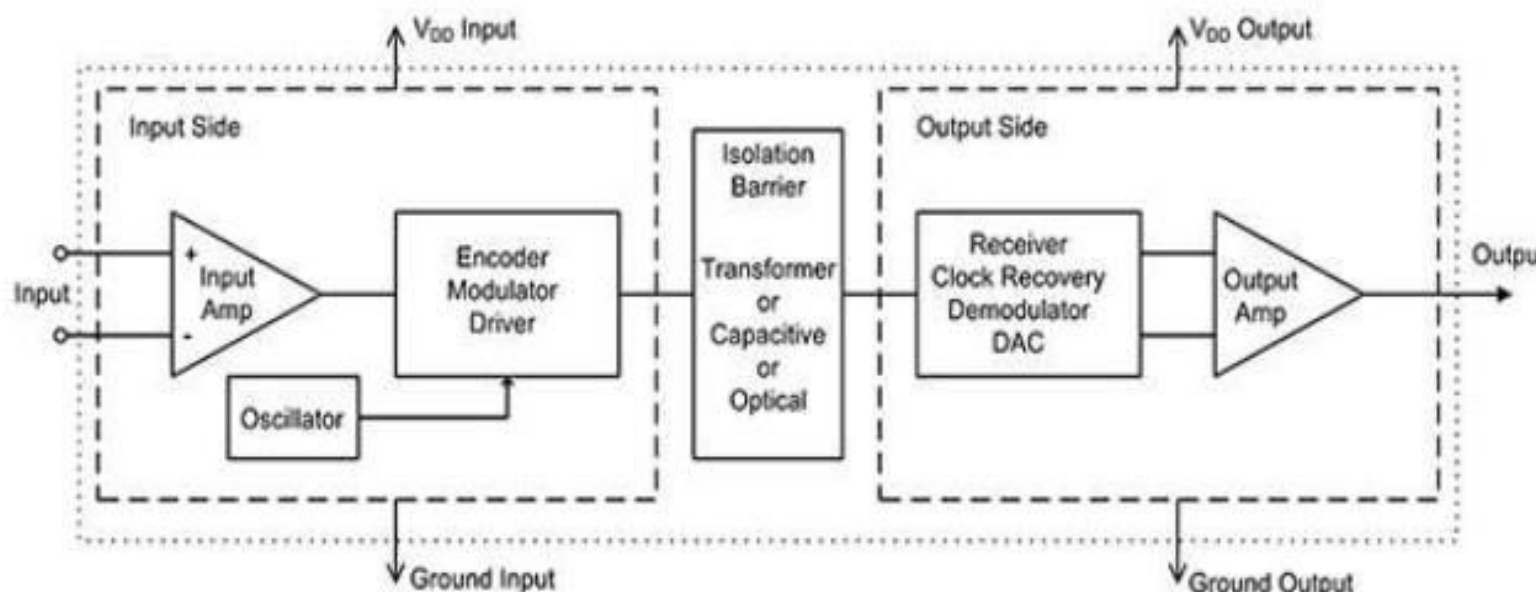
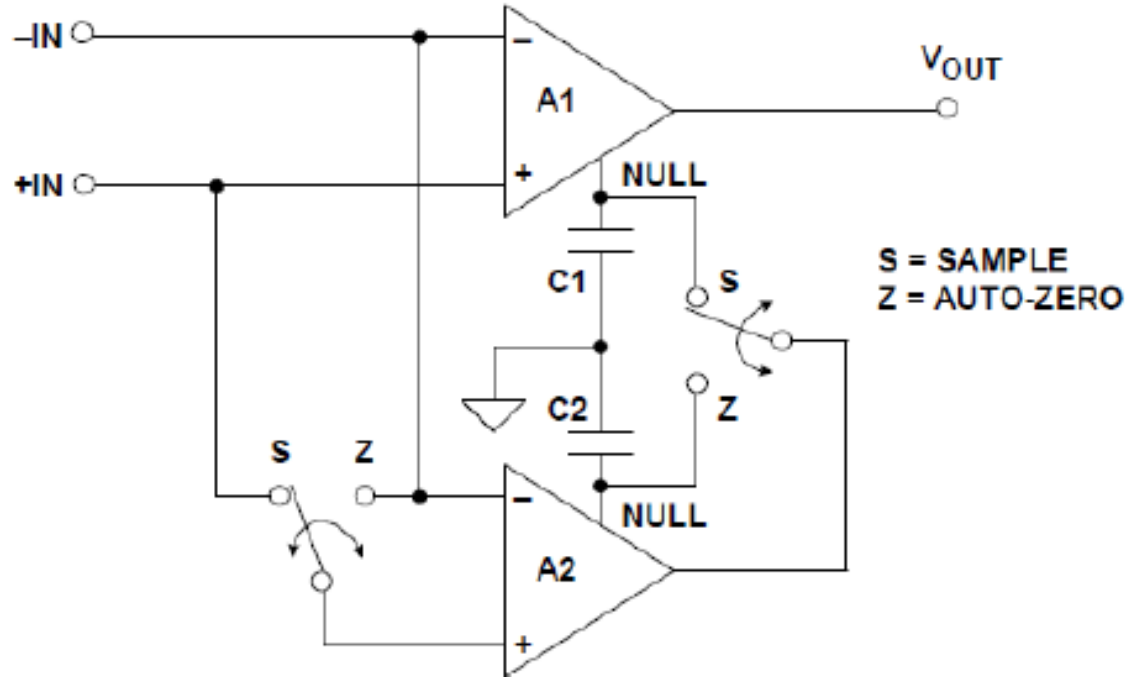
Amplifier

- Chopper amplifier



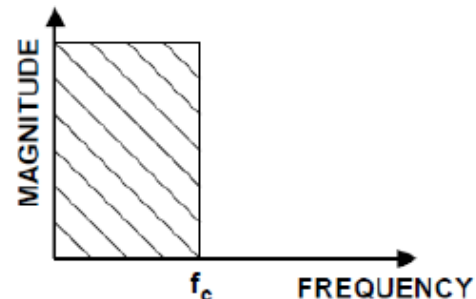
Amplifier

- Chopper amplifier
- Isolation amplifier

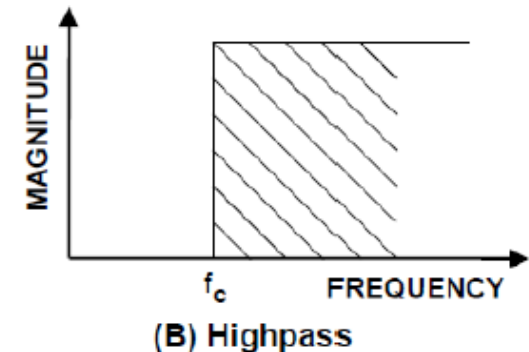


Filters

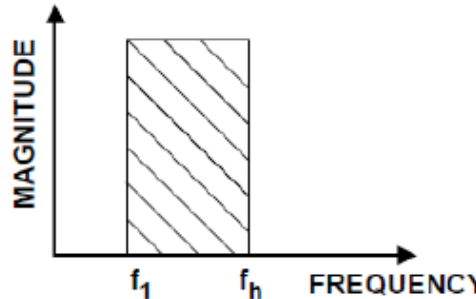
- Noise filtering
- Selecting certain frequency signal
- Anti-aliasing filter
- ADC/DAC
- Filter characteristics
 - Passband
 - Stopband/attenuation band
 - Cut-off frequency



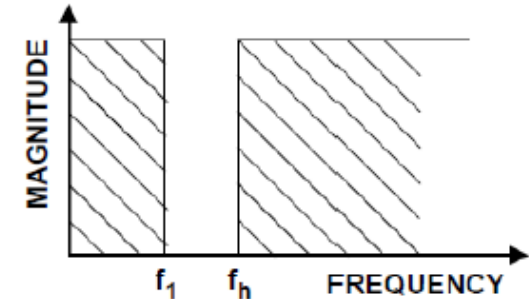
(A) Lowpass



(B) Highpass



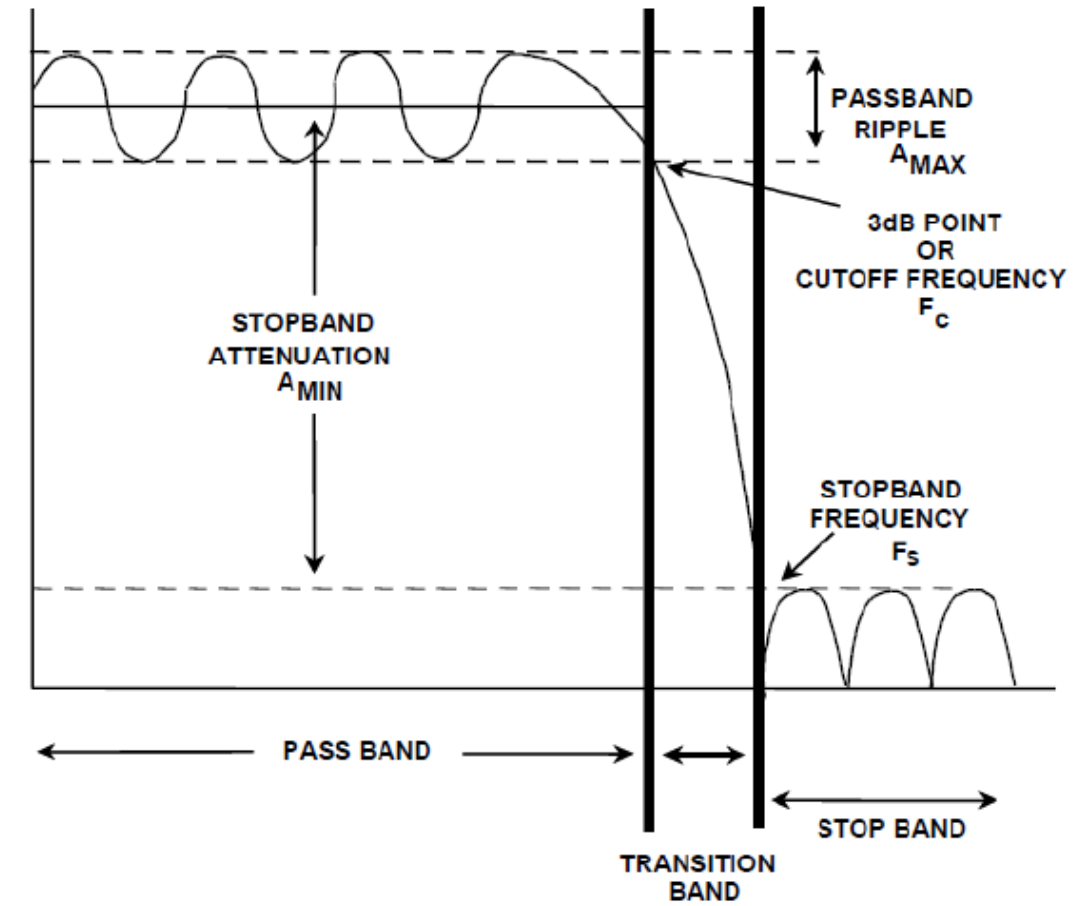
(C) Bandpass



(D) Notch (Bandreject)

Filters

- Cut-off frequency (f_c): Frequency at which the filter amplitude response drops to -3 dB
- Stop band frequency (f_s): Frequency at which the minimum attenuation in the stop-band is reached.
- Pass-band ripple (A_{MAX}): Variation in the pass-band response.
- Pass-band attenuation (A_{MIN}): The minimum signal attenuation within the stop band.
- Filter order (M): The steepness of the filter. M is also the number of poles in the filter transfer function.



Transfer function

- Passive filters
 - R, L, C
- Active filters
 - Op-amp, R, L, C
- ZL, Zc

$$H(s) = \frac{\sum_{n=0}^N a_n s^n}{\sum_{m=0}^M b_m s^m}$$

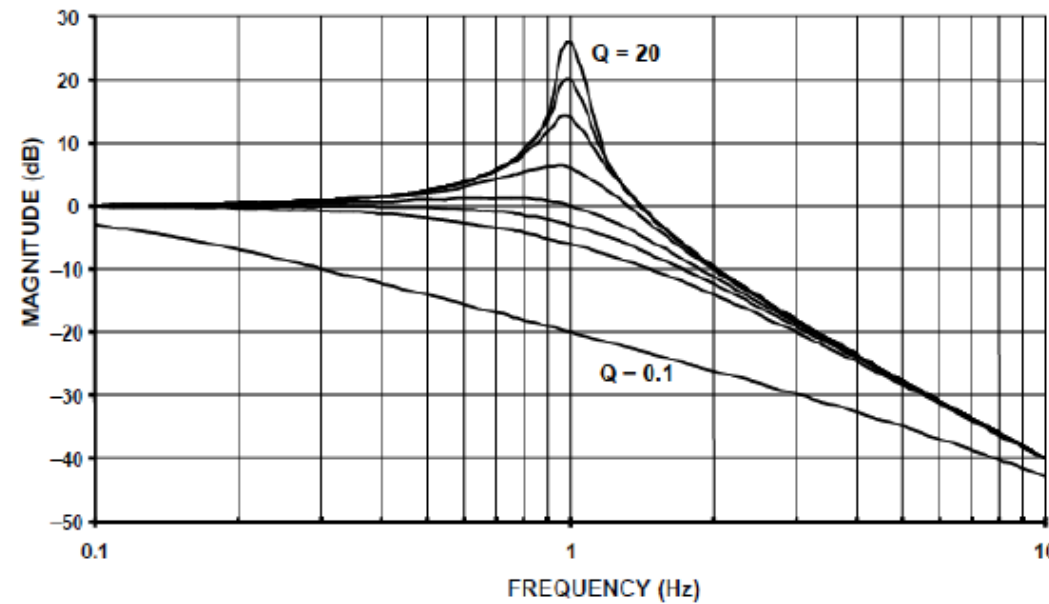
- n : filter order
- First order low-pass filter
- First order high-pass filter

$$H_{lp1}(s) = \frac{H_0 \omega_0}{s + \omega_0}$$

$$H_{hp1}(s) = \frac{H_0 s}{s + \omega_0}$$

Transfer function

- Second order filter ($n = 2$)
 - F_0 : cut-off frequency
 - Q : quality factor $Q = 1/2\zeta$



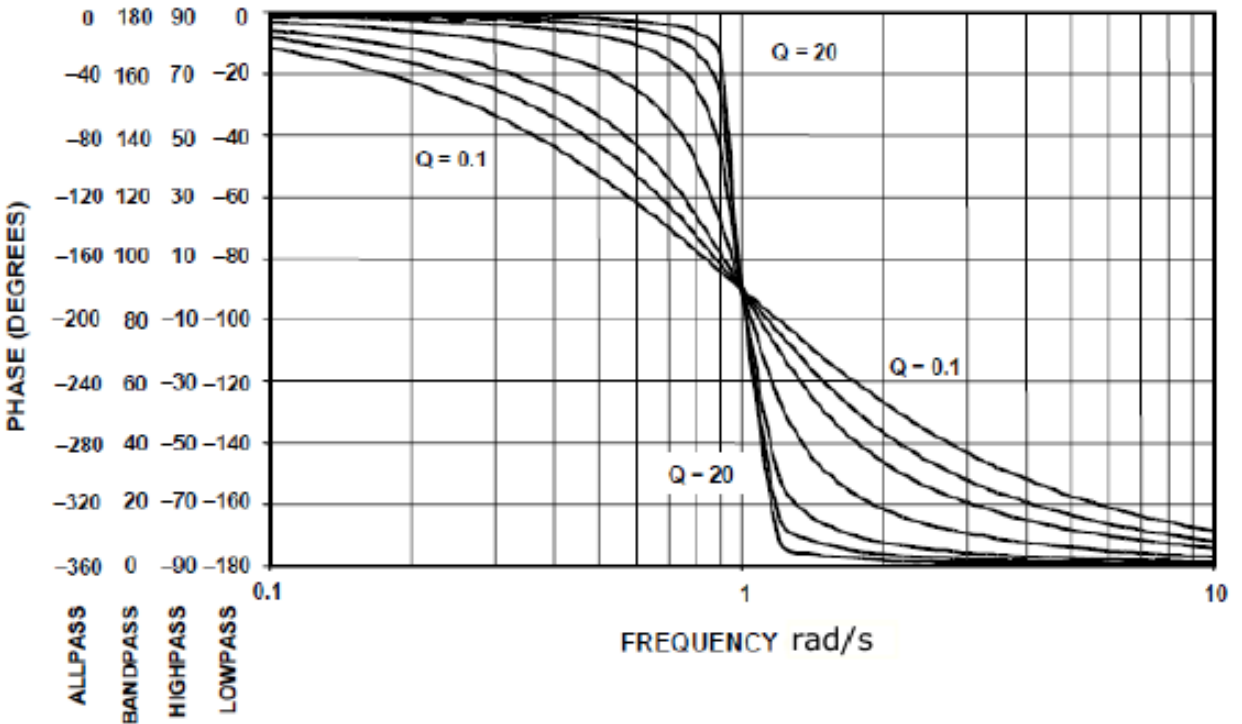
FILTER TYPE	MAGNITUDE	POLE LOCATION	TRANSFER EQUATION
LOWPASS			$\frac{\omega_0^2}{s^2 + \frac{\omega_0}{Q}s + \omega_0^2}$
BANDPASS			$\frac{\frac{\omega_0}{Q}s}{s^2 + \frac{\omega_0}{Q}s + \omega_0^2}$
NOTCH (BANDREJECT)			$\frac{s^2 + \omega_z^2}{s^2 + \frac{\omega_0}{Q}s + \omega_0^2}$
HIGHPASS			$\frac{s^2}{s^2 + \frac{\omega_0}{Q}s + \omega_0^2}$
ALLPASS			$\frac{s^2 - \frac{\omega_0}{Q}s + \omega_0^2}{s^2 + \frac{\omega_0}{Q}s + \omega_0^2}$

Transfer function

- Phase response
- Band-pass filter
 - Selectivity

$$Q = \frac{F_0}{F_H - F_L}$$

$$F_0 = \sqrt{F_H F_L} \quad BW = F_H - F_L$$



Time response of filters

- Design of filters
 - Frequency and time response specifications
 - Impulse, step, sinusoidal input
- The impulse response of a filter, in the time domain, is proportional to the bandwidth of the filter in the frequency domain
- Amplitude discrimination (the ability to distinguish between the desired signal from other, out of band signals and noise) and time response are inversely proportional.

Filter realizations

- Butterworth, Cheybeschev, Bessel and Ellipic filters
- Butterworth: flat pass band and flat stop band
- Cheybeschev: ripple pass-band and flat stop-band
- Ellipic: ripple pass-band and ripple stop-band
- Each filter type have distinct pole positions in the s-plane
- Butterworth (buttap), Bessel (besselap), Chebyschev (cheb1ap, cheb2ap), Elliptic (ellipap)

First order filter

$$H(s) = \frac{V_o(s)}{V_{in}(s)}$$

$$= \left(1 + \frac{R_f}{R_1} \right) \left(\frac{Z_2}{Z_1 + Z_2} \right)$$

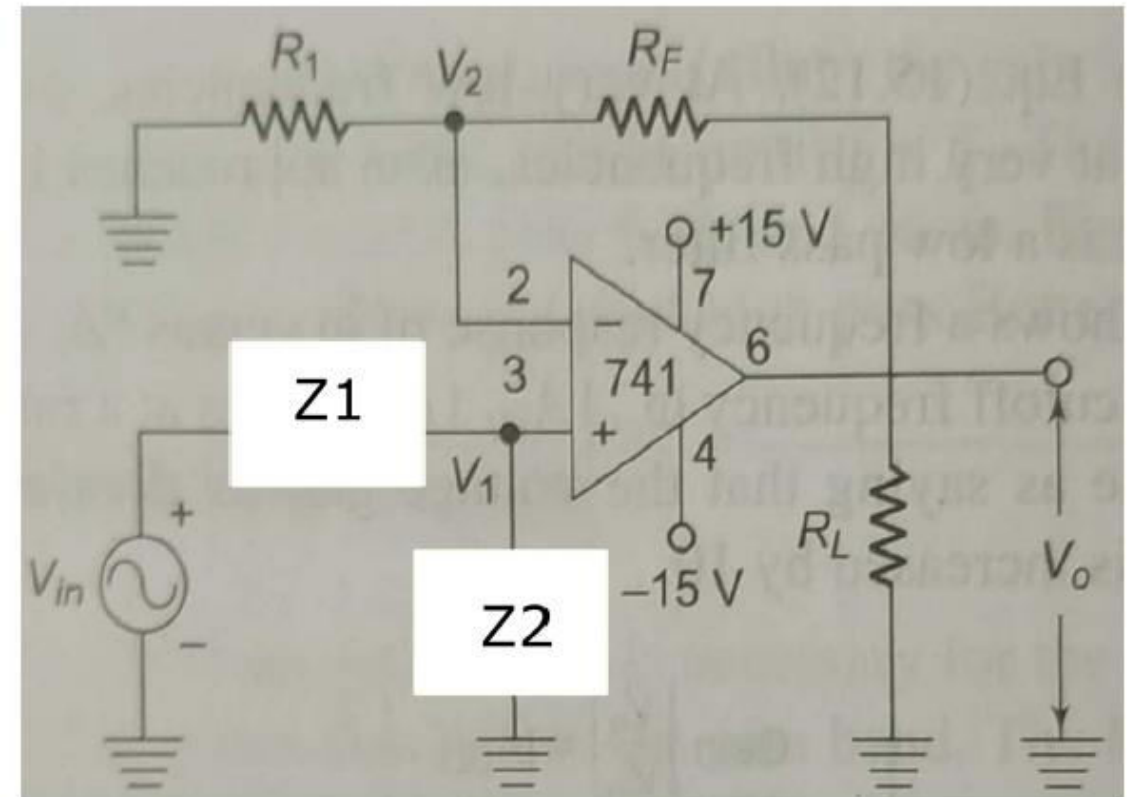
- Low pass and High pass filter

$$Z_1 = R \text{ and } Z_2 = 1/sC$$

$$H(s) = \left(1 + \frac{R_f}{R_1} \right) \left(\frac{1/RC}{s + 1/RC} \right)$$

$$|H| = \frac{H_0}{\sqrt{1 + (\omega/\omega_0)^2}}$$

$$\phi = -\tan^{-1}(\omega/\omega_0)$$



$$Z_1 = 1/sC \text{ and } Z_2 = R$$

$$H(s) = \left(1 + \frac{R_f}{R_1} \right) \left(\frac{s}{s + 1/RC} \right)$$

$$|H| = \frac{H_0(\omega/\omega_0)}{\sqrt{1 + (\omega/\omega_0)^2}}$$

$$\phi = \pi/2 - \tan^{-1}(\omega/\omega_0)$$

Second order filter

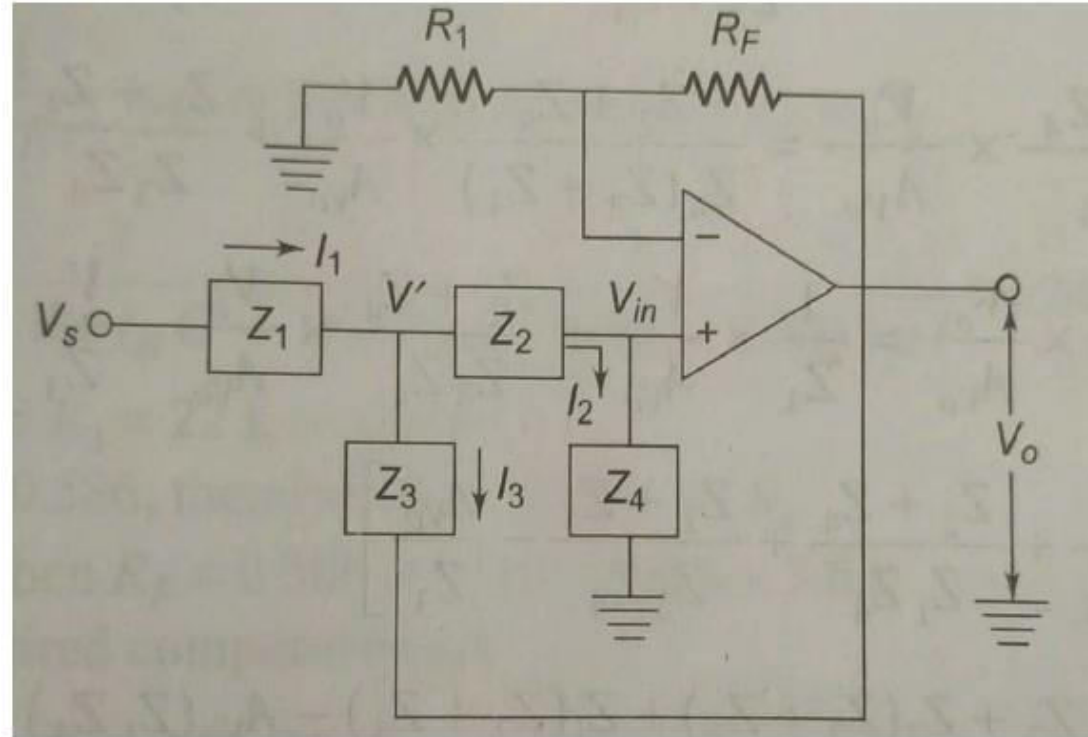
- Transfer function

$$I_1 = I_3 + I_2$$

$$\frac{V_s - V'}{Z_1} = \frac{V' - V_o}{Z_3} + \frac{V'}{Z_2 + Z_4}$$

$$V' = \left(1 + \frac{Z_2}{Z_4}\right) \frac{V_0}{H_0}$$

$$H(s) = \frac{V_o(s)}{V_s(s)} = \frac{H_0 Z_3 Z_4}{(Z_1 + Z_2 + Z_4) Z_3 + (1 - H_0) Z_1 Z_4 + Z_1 Z_2}$$



$$H_{LP2}(s) = \frac{H_0 / R_2 R_3 C_2 C_3}{s^2 + \left[\left(\frac{1}{R_2} + \frac{1}{R_3} \right) \frac{1}{C_2} + \frac{(1-H_0)}{R_3 C_3} \right] s + \frac{1}{R_2 R_3 C_2 C_3}}$$

- Low pass filter: $Z_1 = R_2$ and $Z_2 = R_3$, $Z_3 = 1/sC_2$ and $Z_4 = 1/sC_3$.